UNIVERSITY OF NOVA GORICA
GRADUATE SCHOOL

Characterization of TDP-43, an ALS related protein using *Drosophila melanogaster* model

DISSERTATION

Giulia Romano

Mentor: Fabian M. Feiguin, PhD, MD

Nova Gorica, 2014

UNIVERZA V NOVI GORICI
FAKULTETA ZA PODIPLOMSKI ŠTUDIJ

KARAKTERIZACIJA TDP43, SLA POVEZANI PROTEIN, Z UPORABO DROSOPHILA MELANOGASTER MODELA

DISERTACIJA

Giulia Romano

Mentor: dr. Fabian Feiguin

Nova Gorica, 2014

Abstract

TDP-43 is a 43kDa is a RNA binding protein, ubiquitously expressed that localizes predominantly in the cell nucleus and belongs to the heterogeneous nuclear ribonucleoprotein family (nRNPs). TDP-43 is an evolutionarily highly conserved protein, functionally involved in several molecular processes related to RNA metabolism; such us pre-mRNA splicing, transcription, mRNA stability, microRNA biogenesis, transport and translation. Alterations in the intracellular distribution of TDP-43 were recently found in patients suffering from Amyotrophic Lateral Sclerosis (ALS), a late-onset disorder that predominantly affects motoneurons. Indeed, in affected brains TDP-43 appears inside insoluble protein aggregates distributed predominantly in the cytoplasm outside the cell nucleus, suggesting that these alterations may relate to the pathological symptoms of the disease. However, the physiological functions of TDP-43 *in vivo* or its potential role in the neurodegenerative process behind ALS are not known. In order to address these issues, I genetically suppressed the conserved TDP-43 homologous gene in *Drosophila* (TBPH) and observed that TBPH loss of function alleles in flies presented serious defects in insects' locomotion, dramatic reductions in the life span and structural defects in the organization of motoneuron synapses at the neuromuscular junctions. Interestingly, I found that these phenotypes could be rescued by reintroducing the human TDP-43 protein in motoneurons, indicating that these phenotypes were specific to TDP-43 function and suggesting that similar defects might be expected if TDP-43 function is affected in ALS patients. Considering the intracellular requirements of TDP-43 activity, I found that this is a short-living protein, permanently required in neurons to regulate *Drosophila* motility and synaptic assembly through the direct modulation of different presynaptic molecules like the vesicular protein Syntaxin1A and the microtubule binding protein Futsch/MAP1B. This indicated that synaptic organization and nervous transmission defects may represent clear pathological consequences of TDP-43 dysfunction *in vivo*. Importantly, I could also establish that late

expression of TDP-43 was able to recover the synaptogenesis and locomotion defects in TDP-43 minus adult flies, revealing an unexpected late-stage functional and structural neuronal plasticity. These findings suggest that late therapeutic approaches based on TDP-43 functionality might also be successful in human pathology.

Povzetek

TDP-43 je 43kDa, splošno izražena beljakovina, ki se veže na RNA in ki se pretežno lokalizira v celičnem jedru ter spada v družino heterogenih jedrnih ribosomskih proteinov (nRNPs). TDP-43 je evolucijsko izjemno ohranjena beljakovina, ki funkcijsko sodeluje v več molekularnih postopkih, povezanih s presnovo RNA, kot je povezovanje na nivoju pre-mRNA, transkripcija, stabilnost mRNA, biogeneza mikroRNA, transport in translacija. Pri pacientih, obolelih za amiotrofično lateralno sklerozo (ALS), s starostjo pogojeno motnjo, ki pretežno prizadene motorične nevrone, so nedavno odkrili spremembe intracelularne distribucije TDP-43. V obolelih možganih se TDP-43 pojavi v netopnih beljakovinskih agregatih, ki se pretežno distribuirajo v citoplazmi zunaj celičnega jedra. Kar kaže na to, da so lahko te spremembe povezane s patološkimi simptomi bolezni. Vendar fiziološka funkcija TDP-43 *in vivo* oziroma njena morebitna vloga v nevrodegenerativnem postopku, povezanem z ALS, še ni znana. Za potrebe proučevanja sem pri Drosophili (TBPH) genetsko zavrla ohranjen homologni gen TDP-43 in opazila, da pri mušicah izguba funkcijskih alel TBPH predstavlja resne okvare pri premikanju žuželk, močno skrajša življenjsko dobo in povzroči strukturne okvare pri razporeditvi sinaps motoričnih nevronov na živčno-mišičnih stikih. Zanimivo je odkritje, da lahko te fenotipe pri motoričnih nevronih rešimo s ponovno uvedbo humane beljakovine TDP-43, kar kaže na to, da lahko pri pacientih z ALS v primeru škodljivega vpliva na delovanje TDP-43 pričakujemo podobne okvare. Upoštevajoč intracelularne zahteve aktivnosti TDP-43 sem odkrila, da je to beljakovina s kratko življenjsko dobo, ki mora biti v nevronih nenehno prisotna, da uravnava gibljivost Drosophile in sinaptično sestavo s pomočjo neposrednega prilagajanja različnih presinapričnih molekul, kot je vezikularna beljakovina Syntaxin1A in beljakovina Futsch/MAP1B, ki povezuje mikrotubule, kar kaže na to, da lahko razporeditev sinaps in okvare transmisije živčnih impulzov predstavljajo jasne patološke posledice disfunkcije TDP-43 *in vivo*.

Pomembno je, da sem poleg tega ugotovila, da je lahko pozno izražena TDP-43 obnovila sinaptogenezo in izboljšala gibalne okvare pri odraslih

mušicah s porušeno TDP-43, s čimer je pokazala na nepričakovano funkcionalno in strukturno plastičnost živčevja v poznam stadiju. Ugotovitve kažejo na to, da bi lahko kasnejše zdravljenje, ki bi temeljilo na funkcionalnosti TDP-43, bilo uspešno tudi v humani patologiji.

Ključne besede: ALS , Drosophila , Nevromišična Junction , Syntaxin1A , TDP- 43

Summary

Figures Index

Genotype abbreviations

GS-TB =TBPH$^{\Delta 23}$/TBPH$^{\Delta 23}$,UAS-TBPH;elav-GS GAL4/+

GS-TB$^{F/L}$ = TBPH$^{\Delta 23}$/TBPH$^{\Delta 23}$;elav-GS GAL4/UAS-TBPH$^{F/L150\text{-}152}$

GS-TB+RU = indicates the above genotype was treated with RU486

GS-TB+ET = indicates the above genotype was treated with ethanol

GS-TB+RU+rel24h = indicates the above genotype was treated with RU486and then released from drug for 24 hours;

GS-TB+RU 12hpulse=indicates the above genotype was treated with a RU486 pulse for 12hours;

TT-TBc =tubulin-GAL80^{ts}/+;tubulin-GAL4/+

TT-TBi = tubulin-GAL80^{ts}/+;tubulin-GAL4/TBPH-RNAi

TE-TBc =Dicer(x);TBPH$^{\Delta 23}$,tubulin-GAL80^{ts}/+;elav-GAL4/+

TE-TBi =Dicer(x);TBPH$^{\Delta 23}$,tubulin-GAL80^{ts}/+;elav-GAL4/TBPH-RNAi

TBc =Dicer(x);TBPH$^{\Delta 23}$,elav-GAL4/UAS-GFP;+/+

TBi = Dicer(x);TBPH$^{\Delta 23}$,elav-GAL4/+;TBPH-RNAi

Abbreviations

%	percentage
°C	degrees Celsius
µl	microliter
µm	micrometer
µM	micromolar
nM	nanomolar
ABC	ATP-binding cassette
AEL	after egg laying
AD	Alzheimer's disease
ALS	amyotrophic lateral sclerosis
BSA	bovine serum albumin
CAST	CAZ-associated structural protein
CAZ	cytomatrix at the active zone
CDK	cyclin dependent kinase
CDS	coding DNA sequence
CFTR	cystic fibrosis trans-membrane regulator gene
CJD	Creutzfeldt-Jakob disease
CNS	central nervous system
DNA	deoxyribonucleic acid
dsRBM	double strand RNA binding motif
EMSA	electrophoretic mobility shift assay
ESCRT	endosomal sorting complexes required for transport
FALS	familial amyotrophic lateral sclerosis
FTLD	frontotemporal lobar degeneration
FUS/TLS	fused in sarcoma/translocated in liposarcoma
GRD	glycine rich domain
GSS	Gerstmann-Sträussler-Scheinker syndrome
HD	Huntington's disease
HDAC	histone deacetylase
hNFL	human neurofilament
hnRNP	heterogeneous ribonuclearprotein
HRP	horseradish peroxidase

GFP	green fluorescence protein
GRD	glycine rich domain
GS	gene switch
IP	immunoprecipitation
ISN	inter segmental nerve
MAP	microtubule associated protein
NMDA	N-methyl D-aspartate
MND	motor neuron disease
MT	microtubule
n	number of replicates
NES	nuclear exportation signal
NLS	nuclear localization signal
NMJ	neuromuscular junction
NS	nervous system
NSF	N-ethylmaleimide sensitive factor
PAS	polyA site
PD	Parkinson disease
PDZ	post synaptic density protein 95, disc large tumor suppressor 1, zonula occludens-1 protein
PrP	prion protein
qRT-PCR	quantitative reverse transcriptase polymerase chain reaction
RBD	RNA binding domain
RBPs	RNA binding proteins
RNA	ribonucleic acid
RNPs	ribonucleoproteins
RRM	RNA recognition motifs
TARGET	temporal and regional gene expression targeting system
TN	transverse nerve
SALS	sporadic amyotrophic lateral sclerosis
SD	standard deviation
SEM	standard error of the mean
SMA	spinal muscular atrophy
SMN	survival motor neuron
SN	segmental nerve

SNAP	soluble NSF attachment protein
SNARE	soluble NSF attachment protein receptor
UAS	upstream activating sequence
UBI	polyubiquitinated inclusion
UTR	untranslated region
VAMP	vesicle associated membrane protein

1 Introduction

1.1 The role of RNA binding proteins in mRNA biogenesis and processing

The RNA binding proteins (RBPs) have the capacity to recognize and bind single or double stranded RNA to form ribonucleoprotein particles (RNPs). RBPs are localized both in the cytoplasm and the nucleus, in the nucleus the majority of RBPs exist as complexes of protein and pre-mRNA called heterogeneous ribonucleoproteins (hnRNPs). As soon as RNA is transcribed, RBPs have a central role in several cellular processes like post-transcriptional mRNA splicing and stabilization, RNA editing, transport and localization (Dreyfuss *et al*, 2002) (Figure 1).

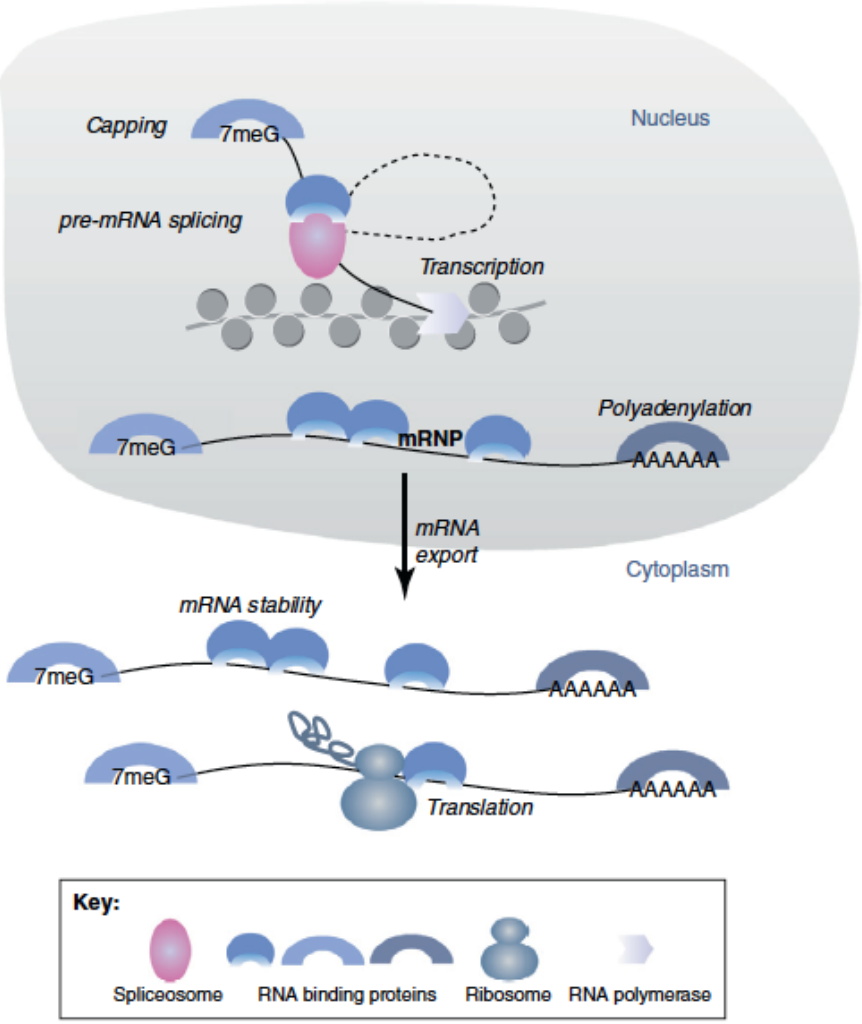

Figure 1 RNA Binding protein involvement in the RNA cycle.

Steps of gene expression in which RBPs play a central role, from (Castello *et al*, 2013).

At the molecular level, the RBPs present different functional domains responsible for their activities, the RNA binding domains (RBDs). Thus, the capacity of these proteins for binding to the RNA is conferred by the combination of specific structural motifs. There are four main RBD families which classified RBPs by structure: the RNA recognition motifs (RRMs), zinc finger domain, hnRNP K homology (KH) domains and the double-stranded RNA binding motifs (dsRBMs) (Cléry & Allain, 2000) (Figure 2).

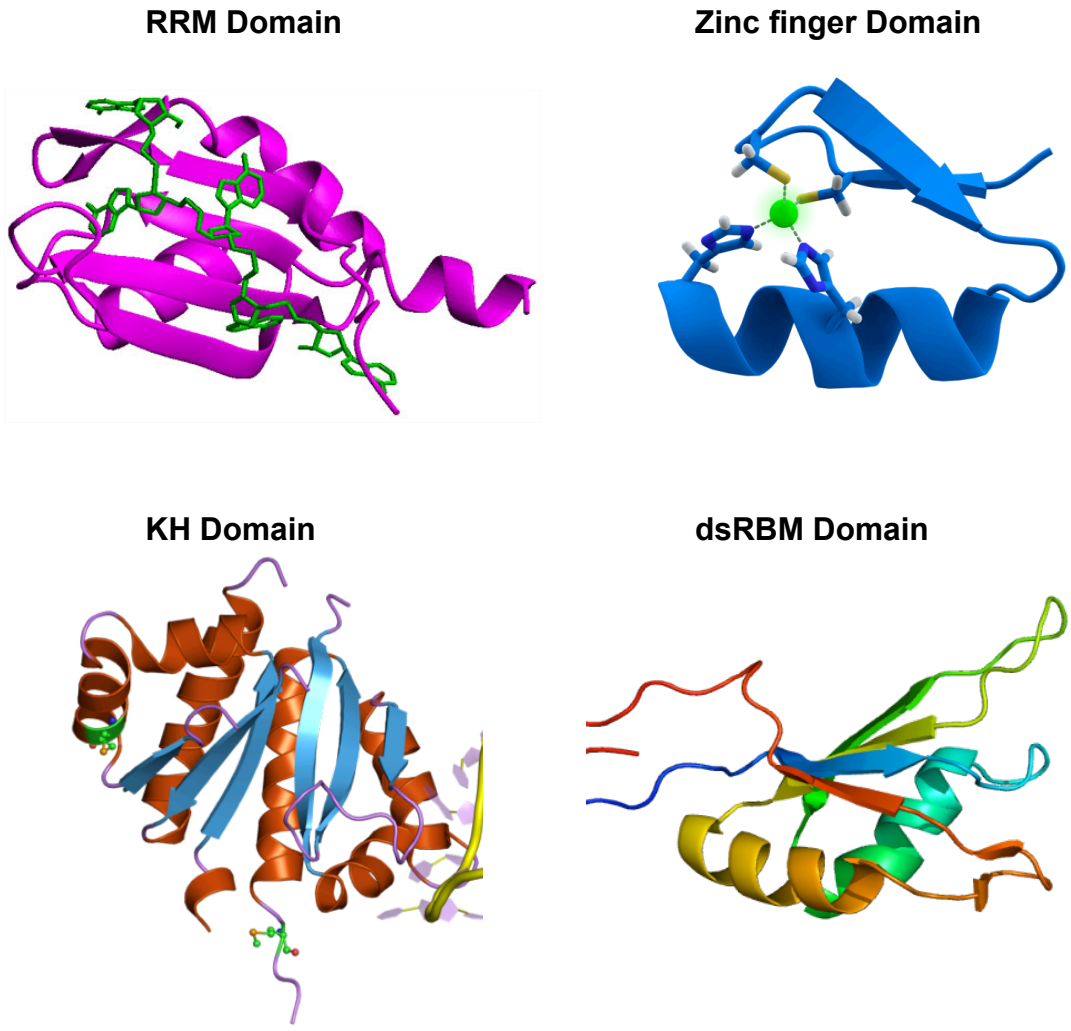

Figure 2 Representation of the most common RNA binding motifs.

From left to right RRM, zinc finger domain, KH domain and dsRBM, adapted from www.wikipedia.com.

The RRM is the most common and better-characterized motif, it is composed by 80 to 90 amino acids and forms a four-stranded β-sheet packed against two α-helices. This constitutes a very complex structural organization that guarantees the specificity in the RNA interaction and recognition. The four-

stranded β-sheet structure interacts with the RNA molecule through the recognition of two or three nucleotides present in the RNA sequence in a very specific manner. The functional role of these domains, were associated with the post-transcriptional activation of gene expression (Maris *et al*, 2005).
Zinc finger (ZnF) is another domain found in RBPs. ZnF is composed by 30 amino acids and exhibits a ββα topology where a β-harpin and a α-helix are joined together through a zinc ion. Initially ZnF was found interacting with dsDNA and only recently has its ability to bind RNA molecules been demonstrated. The ZnF β-strands are not involved in RNA interaction like in most RRMs, but rather are involved the protein loops and α-helices (Teplova & Patel, 2008).
The hnRNP K homology (KH) domain is composed by 70 amino acids. Two structures of KH has been reported, the type I and the type II. Type I is βααββα topology, composed of three antiparallel β-strands packed against three α-helices. Type II differs from type I by a αββααβ topology. KH motifs are able to interact with RNA or ssDNA targets forming a binding cleft that usually accommodates four bases (Grishin, 2001).
The dsRBM instead is composed by 70 to 75 amino acids that are responsible in recognizing and binding double stranded sequences of RNA specifically. Although the structural organization of these domains is less characterized than RRM, they appear to form a αβββα topology. These motifs are often found in multiple copies (e.g., up to five in Staufen protein in *Drosophila*) and are involved in several processes such as: RNA interference, processing, localization, editing and translational control (Chang & Ramos, 2005). Commonly dsRBMs use residues from the α1-helix and β1-β2 loops to contact the minor grooves and α2-helix and loop4 to contact the major grooves.

Alterations in RBPs-RNA interactions were found to be at the core of several degenerative diseases (Cooper *et al*, 2009), revealing the important role that these proteins have in the cellular homeostasis. Nevertheless, only few RBPs have been studied in detail. Based on these, it has been shown that RBPs preferentially interact with the 3'UTR untranslated regions (UTRs) of

the mRNA molecules where the transcription and splicing of these messengers is regulated (Wang *et al*, 2008; Mayr & Bartel, 2009; Danckwardt *et al*, 2011).

Recent studies demonstrated a strong association between mutations in RBPs and different human hereditary diseases (Lukong *et al*, 2008; Darnell, 2010). The spectrum of disorders include several diseases originating from defects in the Nervous System (NS) like spinal muscular atrophy (SMA), amyotrophic lateral sclerosis (ALS), frontotemporal lobar degeneration (FTLD) or Alzheimer's and Huntington's disease (AD and HD) (King *et al*, 2012). On the contrary, molecular analysis performed in affected patients revealed the presence of pathologically modified RBP proteins, abnormally localized inside insoluble protein aggregates. In agreement with that, the ribonuclear protein TDP-43 was found to be present in the pathological inclusions observed in the brains of patients suffering with ALS (Neumann *et al*, 2006). Similar defects in the RBP protein FUS were detected in ALS patients (Kwiatkowski *et al*, 2009; Vance *et al*, 2009), demonstrating the relevant role of this protein in preserving neuronal activity.

Defects in RBPs function were also detected in diseases related to the correct functioning of the survival motor neuron (SMN) gene, which has a critical incidence in the pathological modifications observed in SMA and, although SMN is not a RBP, it has been demonstrated that the SMN complex plays an essential role in the biogenesis and assembly of the small nuclear ribonucleic particles (snRNPs), a type of RBPs (Gabanella *et al*, 2007; Neuenkirchen *et al*, 2008), suggesting that modifications in the metabolism of these proteins may affect the cellular survival. Based on these aspects, the hexanucleotide RNA repeat expansions detected in the non coding region of the C9orf72 gene found in ALS and FTD patients and also observed in the expansion of trinucleotide RNA repeats, indicated that the presence of these abnormal sequences may induce the formation of RNA foci followed by the sequestration of specific RBPs like the hnRNP (Stepto *et al*, 2014).

Another example that involves RBPs with neurodegenerative disorders is the evidence that a consistent number of RBPs contain a prion like domain. Prion diseases, as Creutzfeldt-Jakob disease (CJD) or Gerstmann-Straussler-Scheinker syndrome (GSS), are fatal neurodegenerative disorders

characterized by accumulation of misfolded isoform of the prion protein (PrP) (Imran & Mahmood, 2011).

Another crucial aspect of RBPs relates to their interactions. In fact it seems that several RBPs are required to guarantee their functional regulation on RNA molecules. Several studies have compared different RBPs and their targets, providing evidence that in most of the cases the same RNA can be bound by multiple factors and not exclusively by one (Hogan *et al*, 2008; Ankö *et al*, 2010). Evidence of the cooperation between RBPs has also been found in our laboratory, Romano M. and colleagues (2014) demonstrated that Hrp38 (the *Drosophila* ortholog of human hnRNP A1/A2) can bind very efficiently with human TDP-43 protein and TBPH (*Drosophila* TDP-43 homolog). Moreover it has been demonstrated that Hrp38 and TBPH genetically interact to prevent locomotion defects and reduce life span in a *Drosophila* model of ALS, strongly supporting the hypothesis of a functional interaction between TBPH/Hrp38 and TDP-43/hnRNP A/B (Romano *et al*, 2014).

This evidence revealed that RBPs are emerging as key proteins in several neurodegenerative diseases. In order to truly define the pathogenesis of these diseases and efficiently develop new therapeutic strategies the exact pathways that involve RBPs have to be better understood.

1.2 TDP-43

TDP-43 is a very well conserved protein that belongs to the family of heterogeneous ribonucleoprotein (hnRNP) and, according to that, orthologous genes of TDP-43 were found in different species from higher eukaryotes like mice and rats to *Drosophila melanogaster*, *Xenopus laevis* or *Caenorhabditis elegans* (Ayala *et al*, 2005; Wang *et al*, 2004). This high degree of sequence conservation suggests that TDP-43 may play a fundamental role in the regulation of basic cellular mechanisms. The distribution of this protein inside these organisms, TDP-43 is expressed in different tissues including brain, heart, pancreas, spleen, testis, ovary, lung, placenta and kidney (Buratti & Baralle, 2001). In physiological conditions, the

protein predominantly localizes in the cell nucleus with some traces in cytoplasm due to its continuously shuttling between nucleus and cytoplasm (Ayala *et al*, 2008b).

Although the molecular organization of the TDP-43 locus suggests that this coding gene may transcribe for eleven different isoforms of the protein, Western blot and immunoprecipitation analysis performed on a variety of human tissues or cultured cell lines detected the presence of a unique, major, protein of 43 kDa (Wang *et al*, 2004). Nevertheless, complex post-translational modifications as hyperphosphorylations, abnormal ubiquitinations or protein cleavages were described in pathological conditions indicating that these alterations may affect TDP-43 metabolism or function (Arai *et al*, 2006; Buratti *et al*, 2001; Neumann *et al*, 2006).

1.3 TDP-43 structure

The N-terminal part of this protein contains two highly conserved RNA Recognition Motifs known as RRM1 (from residue 104 to 200) and RRM2 (from residue 191 to 262). This region also contains two nuclear localization signals (NLS1, amino acids K82/R83/K84 and NLS2, amino acids K95/K97/R98) as well as two nuclear export signs located at the end of the RRM2 domain (source: http://prosite.expasy.org).

The C-terminal domain of TDP-43 presents a glycine rich area (GRD) followed by a low complexity region that presents a more variable amino acid composition compared with other species (Figure 3) (Buratti & Baralle, 2008).

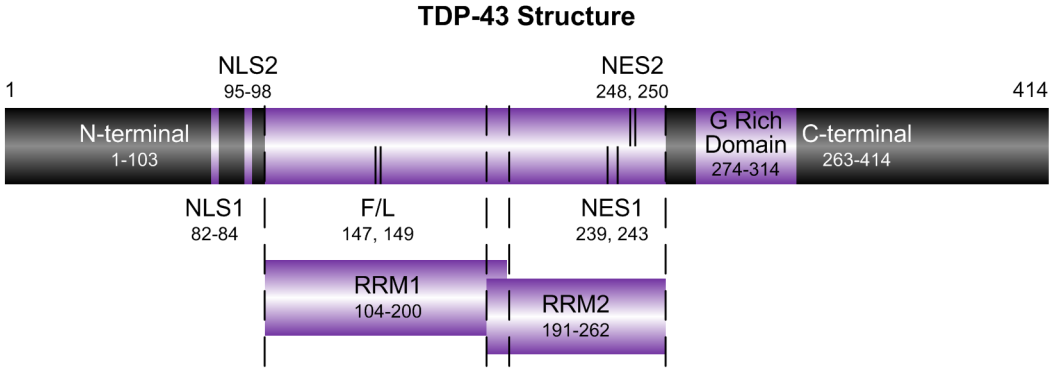

Figure 3 Schematic representation of the TDP-43 structure.

The image shows the different domains present in the protein. Nuclear Localization Signal, NLS; RNA Recognition Motifs, RRM; Phenylalanine, F; Leucine, L; Nuclear Exportation Signal, NES; Glycine, G.

The highly conserved RRMs domains of TDP-43 are essential for the functional interactions of this protein with the RNA molecules (Ayala *et al*, 2005) and it was demonstrated that they can bind with high affinity single stranded TG dinucleotide stretches (Buratti & Baralle, 2001). These domains are the most conserved portion of the protein through the species, in fact the amino acid identity of RRM domains between human TDP-43 and the Drosophila homolog is 79% (Ayala *et al*, 2005). Experimental evidence using Electrophoretic Mobility Shift Assay (EMSA) has shown that RRM1 domain is necessary and sufficient for the binding to the RNA. In support of this observation, it was demonstrated that two point mutations resulting in an amino acid changing (Phenylalanine 147 in Leucine and Phenylalanine 149 in Leucine, F147L and F149L) in the RRM1 region, provoked the inability of the molecule to interact with RNA molecules. Similar amino acid substitutions or the complete deletion of the RRM2 domain, did not affect the capacity of TDP-43 to interact with the RNA molecules (Buratti *et al*, 2001). The C-terminal tail of TDP-43 is less conserved and presents a glycine rich domain responsible for the protein/protein interactions with other hnRNP family members, especially hnRNP A2/B1 and hnRNP A1 (Buratti *et al*, 2005; D'Ambrogio *et al*, 2009). The importance of the C-terminal part of TDP-43 was highlighted by the observations indicating that 2-3% of patients affected by sporadic and familial forms of ALS carry specific missense mutations in this region (Banks *et al*, 2008; Van Deerlin *et al*, 2008; Sreedharan *et al*, 2008).

1.4 TDP-43 function

TDP-43 is involved in several biological processes through its interactions with the DNA and RNA.

1.4.1 TDP-43 and DNA interaction

The first report describing TDP-43 comes from 1995 when this protein was identified as a transcriptional repressor able to bind the a regulatory element in the human immunodeficiency virus type 1 (HIV-1) long terminal repeat (known as TAR) DNA sequence (Ou *et al*, 1995). TAR is critical for the activation of gene expression. Using EMSA (Electrophoretic Mobility Shift Assay) TDP-43 was found to interact with the polypyrimidine-rich region of TAR DNA element. It was also observed that this interaction inhibits the transcription of the viral genome, affecting the life cycle of the virus (Figure 4).

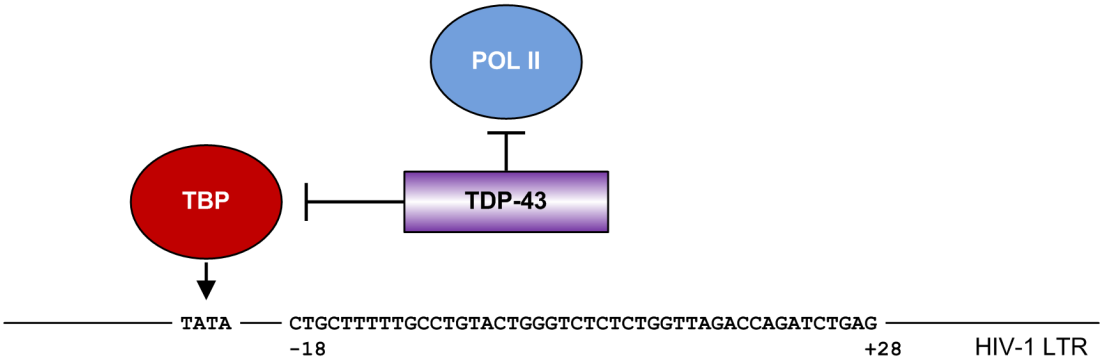

Figure 4 TDP-43 and HIV-1 transcription regulation.

TDP-43 inhibits the assembly of TBP (TATA-Binding-Protein) to HIV-1 LTR (Long Terminal Repeat), this interaction blocks the transcription of the viral genome.

Another evidence of the interaction of TDP-43 with the DNA involved the promoter of the *acrv1* gene that codes for the acrosomal protein SP-10 in mouse (Figure 5) (Abhyankar *et al*, 2007; Reddi *et al*, 1999).

Figure 5 TDP-43 and mouse *acrv1* promoter regulation.

The mouse *acvr1* gene, which codes for the sperm acrosomal protein SP-10, contains in its promoter region two GTGTGT motifs (at -172 and -160 position on antisense strand). TDP-43 binds this region in a GTGTGT dependent manner, actin as a transcriptional repressor of *acrv1* gene during spermatogenesis.

1.4.2 TDP-43 and RNA interactions: role in mRNA splicing

One of the best-characterized aspects of TDP-43 function is the role played by this protein in the regulation of mRNA splicing. Thus, it was described that TDP-43 is able to recognize and bind to the GU rich sequences present in the 3' splice sites of different transcripts, to inhibit the molecular process that lead to exon recognition (Buratti *et al*, 2001). Parallel studies indicated that TDP-43 forms part of the splicing machinery encharged of the mRNA processing of several mRNAs, like the cystic fibrosis trans-membrane regulator gene (CFTR) (Buratti *et al*, 2001; Pagani *et al*, 2000), the apolipoprotein AII (ApoII) messenger (Mercado *et al*, 2005) and the survival motor neuron (SMN) transcripts (Bose *et al*, 2008). The CFTR protein belongs to the ABC class of ion channel transporters (ATP-binding cassette transporters) that carriages chloride and ions across epithelial cell membranes (Childers *et al*, 2007). Mutations of the CFTR gene, affect the functioning of the chloride ion channels in the affected cell membranes, leading to the development of cystic fibrosis. The pathological mechanism behind these mutations resides in the abnormal skipping of the exon 9 followed by the formation of a non functional protein, that is unable to maintain the ionic balance in the affected tissues (Delaney *et al*, 1993), (Figure 6).

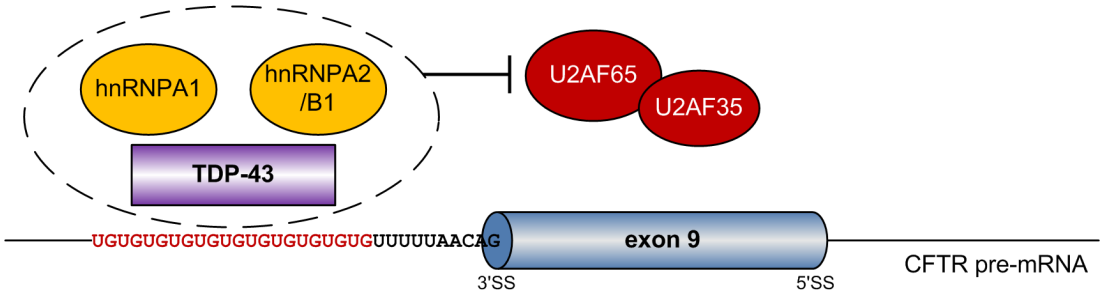

Figure 6 TDP-43 and the interaction with CFTR pre-mRNA.

TDP-43 binds the UG long repeats upstream exon 9 of pre-mRNA of CFTR, causing the skipping of the exon 9 and consequently the production of an aberrant protein.

At the molecular level, it was demonstrated that TDP-43 recognizes the series of TG repeats present in the pre-mRNA of CFTR, inhibiting the recognition of the adjacent exon and causing the alternative skipping of the

exon 9 (Buratti & Baralle, 2001). The lack of exon 9 provokes the translation of a not functional protein (Strong *et al*, 1993) and, in agreement with this view, it was reported that patients suffering of cystic fibrosis present a higher number of TG repeats compared to controls (Ayala *et al*, 2006).

TDP-43 also regulates the alternative splicing of the exon 3 in the Apo AII gene by the direct binding of this protein to the series of TG repeats present in the 3' splice site of the messenger RNA. In this case, however, the Apo AII exon 3 is always constitutively included in the mature RNA and no disease modifications were associated with the skipping of this exon, indicating the presence of supplementary elements in the regulation of TDP-43-mediated alternative splicing. In agreement with this hypothesis, it was observed that the recruitment of different proteins like SC35, SF2/ASF, SRp40 and SRp55 on the spliceosomes were able to neutralize inhibitory activity of TDP-43 on exon 3 recognition (Mercado *et al*, 2005), (Figure 7).

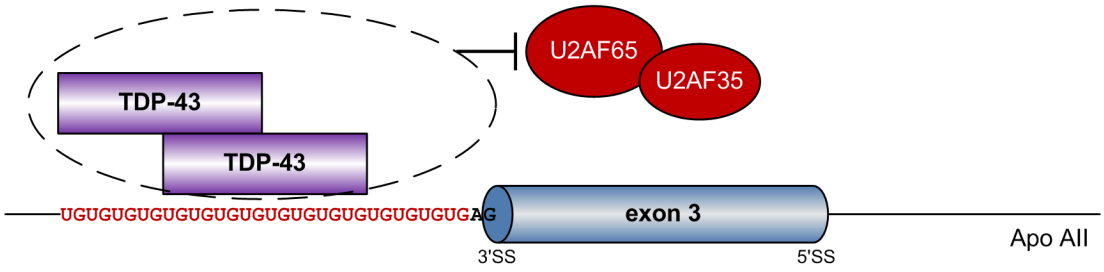

Figure 7 Interaction of TDP-43 with Apo AII mRNA.

TDP-43 binds the UG repeats at the 3' splicing site (3'SS) of Apo AII exon, inhibiting exon 3 inclusion, however other splicing factors counterbalance this effect, causing finally an inclusion of the exon.

Alterations in TDP-43 function, were also related with the splicing processes that involve the inclusion of the exon 7 in the mRNA of the survival motor neuron protein (SMN), in association with the splicing defects observed in the spinal muscular atrophy (SMA) (Bose *et al*, 2008).

1.4.3 TDP-43 and mRNA stability

The RNA binding ability of TDP-43, was also associated with the stabilization of the human neurofilament (hNFL) mRNA transcripts (Campos-Melo *et al*, 2013; Strong *et al*, 2007). The hNFL protein is one of the main structural

components of neuronal cytoskeleton and, together with actin and microtubules, is responsible for neuronal integrity, shape and organelle motility (Mukhopadhyay *et al*, 2004). Regarding to that, co-immunoprecipitation experiments have shown that TDP-43 is able to interact with 3' UTR region (nucleotides 135 and 185 after the stop codon) of the hNFL transcripts to stabilize them and prevent their degradation (Figure 8) (Strong *et al*, 2007).

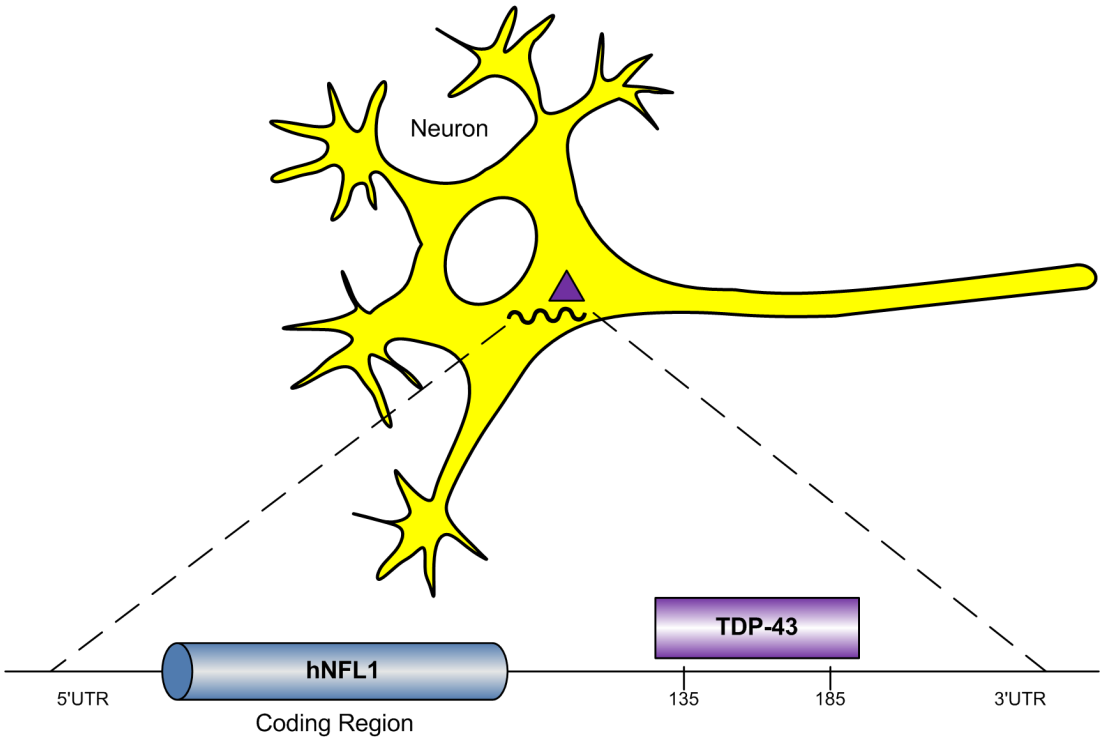

Figure 8 hNFL1 transcript stabilized by TDP-43 binding.

TDP-43 interacts with the 3'UTR of hNFL1, stabilizing the transcript and preventing its degradation.

1.4.4 TDP-43 and its auto-regulation

More recently, it was demonstrated that TDP-43 can binds to its own mRNA to regulate its intracellular levels (Avendaño-Vázquez *et al*, 2012). TDP-43 overexpression activates a 3'UTR intron, inducing the excision of the proximal polyA site (PAS) pA1. That causes the activation of a cryptic PAS that prevent TDP-43 expression (Figure 9). This self-regulation mechanism is tightly controlled and is particularly significant in proteins associated with subcellular toxicity (Ayala *et al*, 2011).

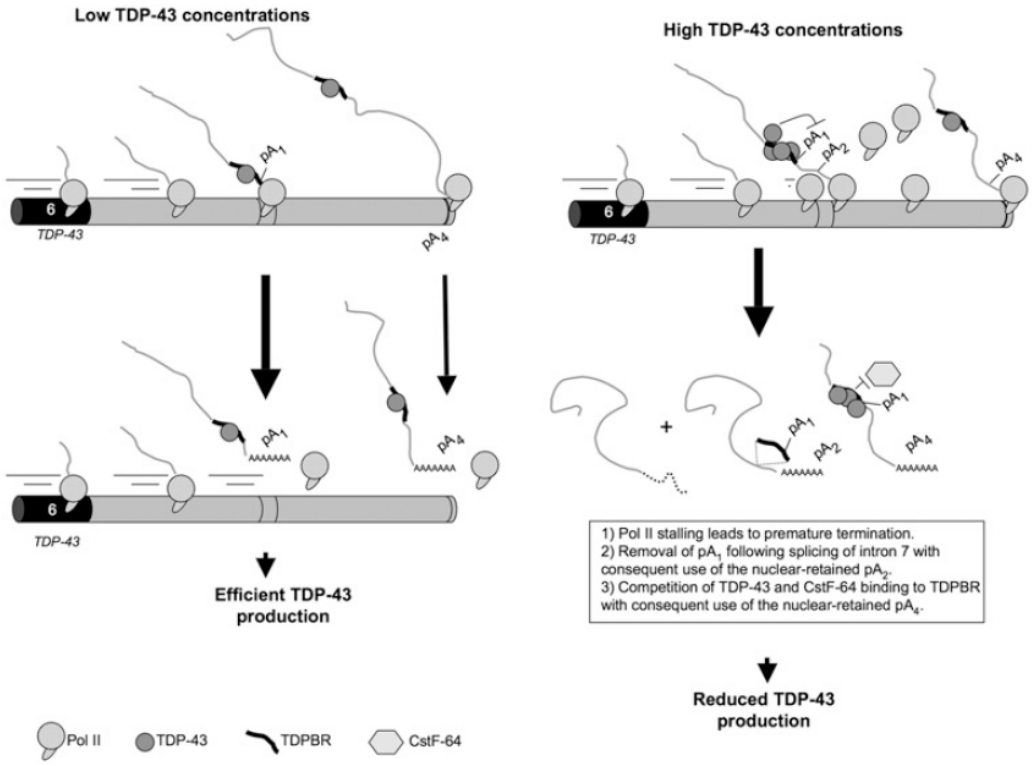

Figure 9 Model of TDP-43 auto-regulatory mechanism.

Normally Pol II synthesized two main isoforms of TDP-43 mRNA using pA1 or pA4. When TDP-43 protein levels are high there is an increase in TDP-43 binding to mRNA, causing intron 7 splicing with the abolishment of pA1 signal. From (Avendaño-Vázquez *et al*, 2012).

Defects in TDP-43 self-regulation may explain some of the possible mechanisms behind those TDP-43 proteinopathies characterized by the aberrant accumulation of this protein in the neuronal cytoplasm. In agreement with that, several recent studies performed on different animal models (*Caenorhabditis elegans*, mouse, and *Drosophila*) demonstrated that TDP-43 overexpression is sufficient to induce neurodegeneration (Ash *et al*, 2010; Li *et al*, 2010; Tsai *et al*, 2010; Wils *et al*, 2010; Xu *et al*, 2010).

1.4.5 TDP-43 and other processes

TDP-43 is involved also in other different processes, which have not been fully investigated. For example it is known that TDP-43 interacts with Drosha complex, an RNAse III endonuclease, protagonist of miRNA processing by cleaving both strands of the pri-microRNA to generate a 60-70 base pair stem-loop intermediate called pre-microRNA. Some miRNA involved in neuronal development are regulated by TDP-43 (Gregory *et al*, 2004; Buratti *et al*, 2010; Kawahara & Mieda-Sato, 2012). TDP-43 has been demonstrated to participate at the regulation of retinoblastoma (pRb) protein phosphorylation, through the repression of a cyclin-dependent kinase (CDK6) (Ayala *et al*, 2008a). Control of CDK6 expression by TDP-43 is mediated by TG repeats present in abundance both in the introns and in the 3' UTR of the CDK6 transcript. The CDK6 of chicken contains no TG repeats; indeed it is not affected when TDP-43 is knocked-down in DF-1 chicken cells. Up-regulation of CDK-6 leads to an increased phosphorylation of the retinoblastoma protein and the pRb related protein 2 (pRb2/p130). The nuclear dimorphism and the increase in the apoptotic events that follow TDP-43 knock down, seem to be pRB pathway dependent considering the fact that in Saos- 2 cells (Human Osteosarcoma cell line) there is no nuclear abnormalities and no increased programmed cell death, since pRb pathway is disrupted.

More recently TDP-43 has been linked with expression of histone deacetylase 6 (HDAC6) (Fiesel *et al*, 2010). A silencing of TDP-43 protein in human embryonic kidney HEK293E and in neuronal SH-SY5Y cells, through RNAi strategy, has been performed to identify relevant targets of TDP-43. In this way has been discovered that the mRNA and the protein levels of HDAC was down regulated. In addition, has been demonstrated an accumulation of acetyl-tubulin which is the major HDAC6 substrate. Using *Drosophila melanogaster* fly model has been performed an *in vivo* validation that has confirmed these observations (Fiesel *et al*, 2010).

1.5 TDP-43 and neurodegeneration

Defects in the intracellular distribution of TDP-43 were recently demonstrated to be associated with the alterations observed in different neurodegenerative diseases. In particular TDP-43 was related with the locomotive defects present in patients suffering of amyotrophic lateral sclerosis (ALS) and with the intellectual disability described in patients affected by frontotemporal lobar degeneration (FTLD) (Arai *et al*, 2006; Neumann *et al*, 2006). FTLD, after Alzheimer and Lewy Body disease, is the third major cause of cortical dementia. ALS instead, is a motor neuron disease with an incidence of 1 in 100,000 individuals, characterized by the progressive loss of brain stem and spinal motor neurons that lead to painless weakness and muscle atrophy with no sensory symptoms. Parallel studies utilizing different approaches revealed that TDP-43 was also altered in other neurodegenerative diseases including Alzheimer disease (AD) and Parkinson disease (PD) (Geser *et al*, 2009).

Histological studies performed in post-mortem brain tissue of ALS and FTLD patients revealed the presence of insoluble cytoplasmic aggregates of TDP-43 aberrantly accumulated in the hippocampus, neocortex and spinal cord areas (Forman *et al*, 2007; Igaz *et al*, 2009). Interestingly, it was observed that the TDP-43 protein present inside these aggregates appeared highly phosphorylated and ubiquitinated. Moreover, small C-terminal fragments produced after the cleavage of full length protein were also detected inside these insoluble clusters (Hasegawa *et al*, 2008, 2010; Mackenzie, 2007). Regarding to these modifications, the primary sequence of TDP-43 has potential phosphorylation sites as serine (41), threonine (15) and tyrosine (8) and aberrant phosphorylation patterns which was first observed by Neumann *et al*, 2006. Neumann and colleagues (2006) noted the presence of a 45 kDa band corresponding to TDP-43 in addition to the 43 kDa band corresponding to the expected molecular weight of the protein, in their study also showed that the presence of this 45 kDa band was abolished after the dephosphorylation of the urea-extracted protein fractions from FTLD-U brains. Concerning the presence of small fragments of TDP-43 (approximately 25 kDa) inside the cytoplasmic inclusions, it is believed that

they may have generated after the enzymatic degradation of the N-terminal region of the protein that present specific cleavage sites for caspases (Rohn & Head, 2009). Nevertheless, these studies were not able to define whether these modifications in the aggregation status of TDP-43 initiated the neurotoxic mechanisms of the disease or they represented the secondary consequences of a previously established neurodegenerative process.

A possible answer to these questions was obtained through the genetic analysis and the identification of mutations in TDP-43 associated with familial cases of ALS (Pesiridis *et al*, 2009). These mutations were predominantly localized in the C-terminal part of the protein and mainly represented missense mutations with only one exception in which the changes introduced in the amino-acid sequence generated the early formation of a stop codon (Figure 10). Thus, the genetic analysis contributed to indicate that defects in TDP-43 might have a primary role in the development of the disease, opening the door to more specific studies to define the physiological function of this protein in normal conditions and/or pathological situations. Regarding to the disease is very well known that the formation or the accumulation of insoluble protein clusters is a common characteristic of many neurological disorders, however, the pathological meaning of these modifications is a matter of a continuous debate. In the specific case of TDP-43, one hypothesis assumes that the formation of these pathologic aggregates inside the cytoplasm may provoke a depletion of the protein from the cell nucleus causing a potential loss of function of TDP-43 in the nucleus. Alternatively, the formation and accumulations of these aggregates might be the direct cause of the neurotoxic effect observed in the disease (Amador-Ortiz *et al*, 2007; Ayala *et al*, 2008b; Filimonenko *et al*, 2007; Sanelli *et al*, 2007; van der Zee *et al*, 2007). In any case, direct answers to these questions would indicate the pathological mechanisms behind the neurodegeneration observed in these patients.

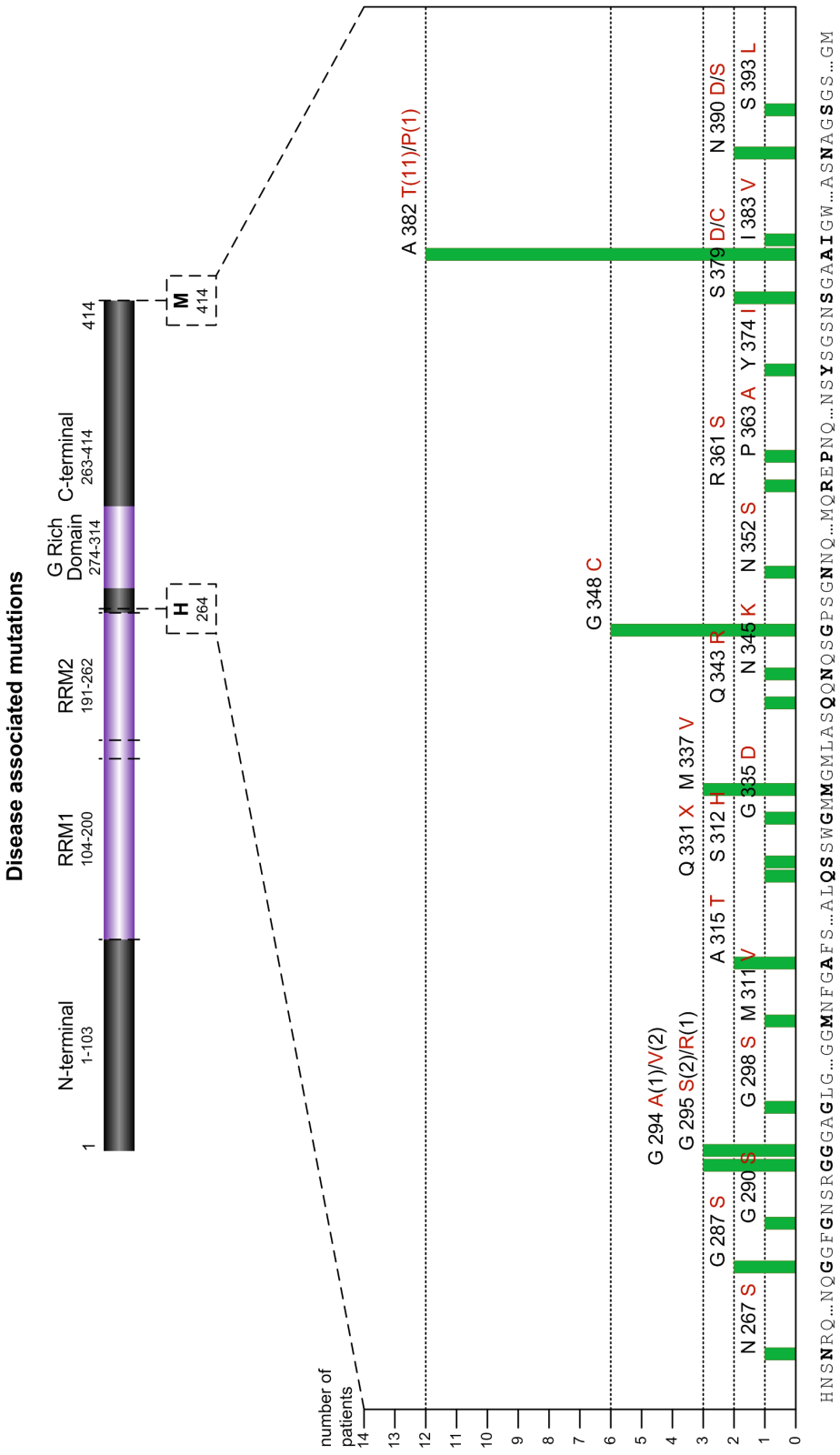

Figure 10 Schematic representation of mutations ALS associated in TDP-43 protein.

Incidence of ALS associated mutation in TDP-43 protein. Adapted from (Buratti & Baralle, 2009).

Besides TDP-43, a similar RNA-binding protein called Fused in Sarcoma/Translocated in Liposarcoma (FUS/TLS) was similarly found in the neuronal tissue of patients affected by FTLD and ALS (Budini *et al*, 2011; Huey *et al*, 2012; Murayama, 2010; Kwiatkowski *et al*, 2009; Vance *et al*, 2009). The FUS/TLS protein, was described to play several roles in many aspects of the RNA metabolism, especially transcriptional regulation, mRNA processing and micro RNA biogenesis (Fiesel & Kahle, 2011). TDP-43 and FUS present similar physiological aspects: both proteins are predominantly localized in the nucleus and contained RNA recognition motifs. The involvement of these two proteins in ALS and FTLD strongly suggested that defects in RNA processing might be the principal clinical manifestation of these disorders. An outline of TDP-43 and FUS involvement in ALS and FTLD is reported in (Figure 11).

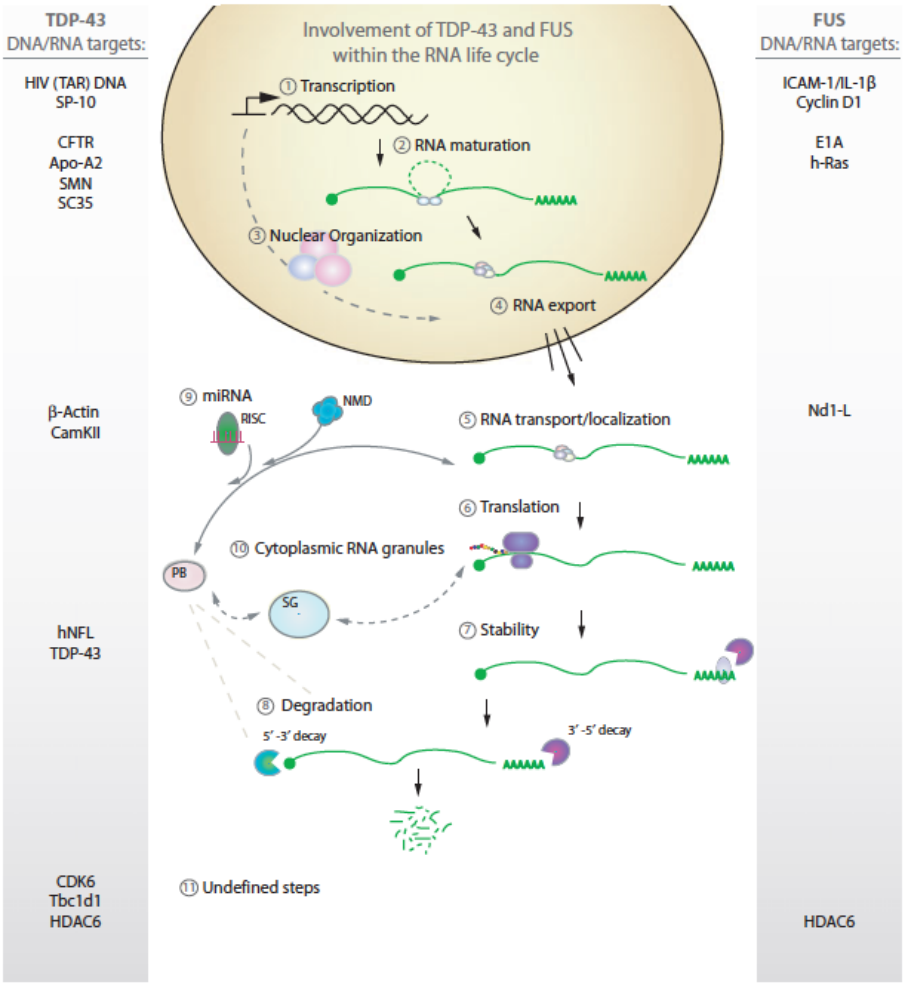

Figure 11 TDP-43 and FUS in mRNA lifecycle.

DNA/RNA targets of TDP-43 (left) and FUS (right) are reported at each step of the RNA lifecycle. Taken from (Fiesel & Kahle, 2011).

In agreement with this hypothesis, recent studies also found that a significant portion of patients affected by ALS or FTLD exhibited an abnormal expansion of the non-coding (GGGGCC) hexanucleotide repeats present in the proximal regulatory region of the *C9orf72* gene sited on the chromosome 9, a condition commonly referred to as c9FTD/ALS (Murray *et al*, 2011). These repeats, in non-affected individuals extend from 1 to 25 copies, whereas in affected patients the repeats motifs reach from 500 to 4,000 copies (DeJesus-Hernandez *et al*, 2011) and represent the most prevalent genetic cause of familial ALS and FTD (34.2% and 25.9% of the cases respectively). The close association between the clinical symptoms related with these expansions repeats and the capacity of TDP-43, FUS and C9orf72 to interact with these aberrant sequences, strongly suggest that these alterations might be correlated (van Blitterswijk *et al*, 2012). Nevertheless, disease mechanisms associated with repeat expansion disorders, including haploinsufficiency (diploid organism with only one single functional copy of a gene), RNA toxicity, and abnormal translation of expanded repeat sequences, are beginning to emerge.

1.6 Amyotrophic lateral sclerosis

Amyotrophic lateral sclerosis (ALS), also termed as Lou Gehrig or Charcot disease, is a rapidly progressive and fatal neurodegenerative disorder without cure available with an incidence of 1 in 100,000 people and a prevalence of 6-8 in 100,000 people per year. The disease mainly damages motor neurons: upper and lower motor neurons become affected causing a rapidly progressive weakness followed by muscle atrophy and fasciculation, spasticity, dysarthria, dysphagia and dyspnea (Figure 12) (Pasinelli & Brown, 2006; Shaw *et al*, 2001).

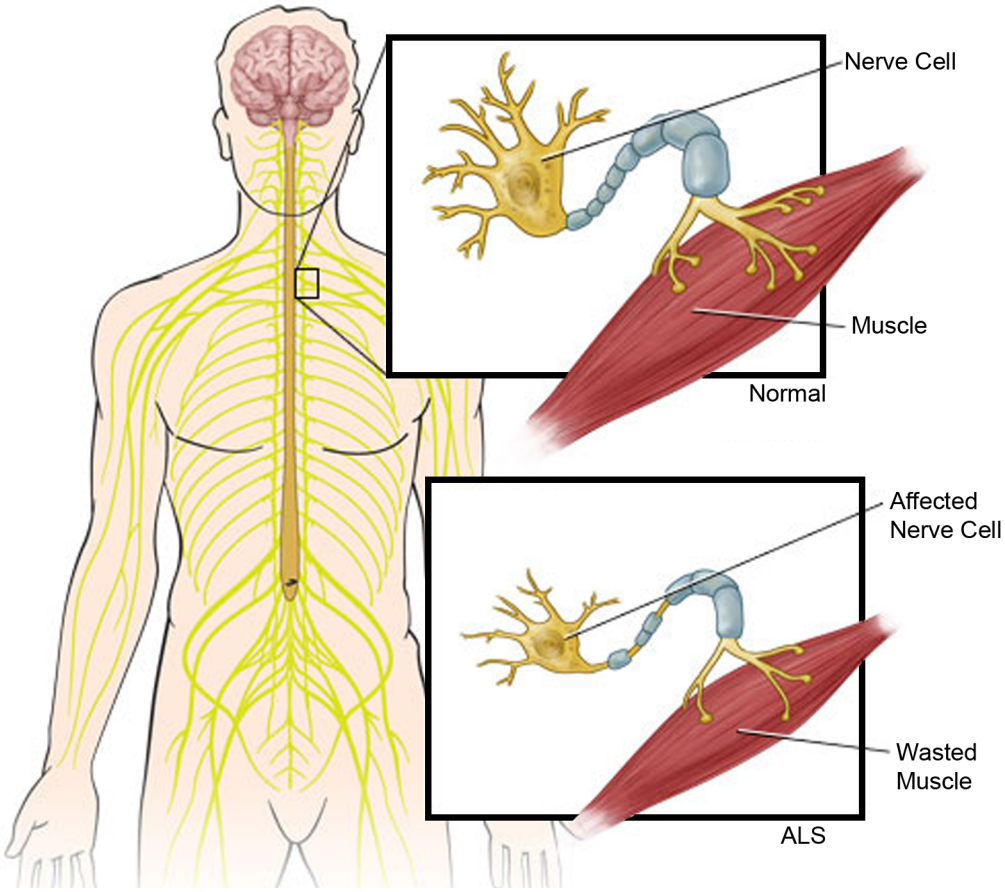

Figure 12 ALS main features.

Healthy neuromuscular junction is schematized in the upper section of the figure, on the contrary in the bottom section is schematized an affected neuromuscular junction. The nervous fiber is subjected to a progressive demyelination and subsequent atrophy and loss of connection with the muscle fiber. Adapted from *http://health.ucsd.edu/specialties/neuro/specialty-programs/als-clinic/Pages/patient-care.aspx.*

Sensory nerves, involuntary nervous system and cognitive function are in most of the cases unaffected. Cases presenting dementia or cognitive dysfunction are less frequent (Phukan *et al*, 2007; Strong & Yang, 2011). Nevertheless, experts of the field suggest that the involvement of cognitive dysfunction is underestimated due to the difficulty of the diagnosis. The ALS onset is around 45-60 years, however exceptional cases with younger and older patients are documented. Initial studies indicated a small prevalence for ALS in male, however, more recent analysis suggested an equal ratio between genders may exist (Worms, 2001; Zoccolella *et al*, 2008). There are no effective cures for ALS, although the riluzole (2-amino-6-trifluoromethoxy

benzothiazole) shows a slowdown in the progression of the disease, prolonging the survival rate by three months (Rowland & Shneider, 2001).

In relation with others neurodegenerative diseases, ALS is classified in two predominant forms: familial ALS (FALS) and sporadic ALS (SALS). SALS cases are the 90% of ALS forms, while FALS forms concern the remaining 10% of the total patients and originate from the inheritance of an autosomal dominant mutation. The first gene discovered in relation with the ALS was the superoxide dismutase 1 (SOD1) in 1993 (Rosen, 1993) nowadays, thanks to the advances of the technology, new genes associated with this disease have been discovered like TDP-43 or TAR DNA-binding protein (TARDBP), fused in sarcoma (FUS), optineurin (OPTN), valosin-containing protein (VCP), hexanucleotide repeat expansion in the C9ORF72 gene, ubiquilin 2 (UBQLN2), sequestosome 1 (SQSTM1), profiling 1 (PFN1) among others. Nevertheless, the most frequent alterations were observed in the following molecules:

SOD1

SOD1 mutations covered about the 20% of familial cases and the 3% of the sporadic cases of ALS (Rosen, 1993; Shaw *et al*, 2001). The gene coding for the SOD1 protein is located on chromosome 21 and several mutations localized in this locus have been characterized. Experimental evidences about the involvement of SOD1 with the pathogenesis of ALS were obtained through a series of studies performed on transgenic mice, where the induction of human SOD1 caused the selective degeneration of motor neurons (Gurney, 1994).

Further analysis of familial forms has also revealed other genetic locus closely linked to the disease, such as the one on chromosome 18q (Hadano *et al*, 2001), 16q (Ruddy *et al*, 2003) and 20p (Sapp *et al*, 2003), expanding the possible causes of this disease.

TDP-43

Neumann and colleagues (2006) discovered that TDP-43 was the major component of the ubiquitin-positive neuronal inclusions present in ALS and FTLD patients. Mutations in TDP-43 covered about the 4% of FALS cases

and a smaller percentage of SALS cases (Chiò *et al*, 2012). The presence of polyubiquitinated inclusions (UBIs) in affected tissues is a common marker of ALS and the presence of these inclusions may constitute an indirect evidence of the cellular failure in the recirculation of damaged proteins, normally performed by the proteasome apparatus (Leigh *et al*, 1991). The UBIs are commonly present in ALS patients with dementia and Tau-negative inclusions and, at the moment, the only connection between these two pathological forms are these modifications in TDP-43 (Arai *et al*, 2006; Neumann *et al*, 2006).

FUS

Shortly after the discovery of TDP43, FUS was identified in association with FALS carrying mutations in the chromosome 16p (Lagier-Tourenne *et al*, 2012). Although familial mutations in FUS comprise the 4% of the cases, the functional affinity of this protein with TDP-43 enhanced the relevance of this discovery.

OPTN

OPTN regulates several cellular processes such as vesicle trafficking, protein secretion, cell division and host defence. Mutations of OPTN has been described for the first time in a cause of FALS by (Maruyama *et al*, 2010).

VCP

In 2010 another protein involved in FALS has been discovered: VCP (Johnson *et al*, 2010). Recently it has been demonstrated that mutations of VCP cause mitochondrial uncoupling, determining a significant decrease of ATP production.

C9ORF72

In 2011 an expansion of hexanucleotide repeats in C9ORF72 has been described as cause of FALS and FTD (DeJesus-Hernandez *et al*, 2011). Pathogenic repeats are present in 40% of FALS cases and 7% of SALS (Majounie *et al*, 2012).

1.6.1 TDP-43 function in animal models

During the last years, the interest to understand the function of TDP-43 has increased exponentially. Taking advantage of the high degree of conservation of this protein among different species, in particular the functional domain of TDP-43 that binds to the RNA, a high number of different animal models have been generated to investigate the physiological role of TDP-43 *in vivo* and its involvement in the neurodegenerative processes.

In mouse, the knockdown of TDP-43 provoked lethality during embryonic development, indicating that the function of this protein is essential for embryos survival.

The study of Wegorzewska and colleagues (2009) found that mice expressing ALS mutant forms of human TDP-43 develop a progressive and fatal neurodegenerative disease that recapitulates some of the common traits found in both ALS and FTLD. Surprisingly, cytoplasmic TDP-43 aggregates were not present in these animals, suggesting that the formation of protein aggregates is not required to induce neurodegeneration. Instead, this study suggest that alterations in the DNA/RNA-binding capacity of the TDP-43 is fundamental to induce neurodegeneration (Wegorzewska *et al*, 2009).

In a more recent study, Wils and colleagues (2010) generated transgenic mouse lines, one line in homozygous and another one in hemizygous for wild type human TDP-43. They showed a TDP-43 dose-dependent degeneration of cortical and spinal motoneurons and the development of spastic quadriplegia. Moreover they have observed a TDP-43 dose-dependent degeneration in non-motor cortical and subcortical neurons. In the affected spinal cord and brain regions of mice expressing transgenic TDP-43 have been found ubiquitinated and phosphorylated aggregates both in nucleus and in cytoplasm. Besides, the characteristic 25kDa C-terminal fragments (CTFs) were also recovered from mice brains. (Wils *et al*, 2010).

Using *Caenorhabditis elegans*, Ash and colleagues (2010) generated an *in vivo* model of TDP-43, expressing human TDP-43 protein. In order to obtain and to study TDP-43 physiological function and the steps that lead to neurotoxicity, TDP-43 was expressed under the control of a pan-neuronal

driver in worms. Transgenic worms expressing human TDP-43 protein in neuronal cells showed a uncoordinated movements and anomalies in motoneuron synapses (Ash *et al*, 2010). The neuronal overexpression of the endogenous *C.elegans* TDP protein (TDP-1) also confirmed the data obtained with the human protein. Genetic deletion of the TDP-1 gene did not affect movement or motoneuron synapses. Deletion of both RNA recognition domains (RRM1 or RRM2) blocked neurotoxic effects, as well as the deletion of the C-terminal region. TDP-43 variants were found to accumulate in the nucleus of these animals, although their subnuclear distribution was altered.

In the literature it is also present a zebrafish (*Danio rerio*) ALS model. In this model, the effect of expression of three different mutated forms of human TDP-43 (A315T, G348C and A382T) linked with ALS pathology has been tested. The overexpression of these ALS mutant variants caused a motor phenotype in embryos. These animals exhibited short motoneuron axons, premature and excessive branching and severe swimming defects. The knockdown of TDP-43 led to a similar phenotype, which can be rescued by expressing back TDP-43 wild type but not expressing the ALS mutant forms of TDP-43 (Kabashi *et al*, 2010).

Finally, in *Drosophila melanogaster* have been also generated loss of function alleles in order to test the physiological function of TDP-43 *in vivo*. TBPH knockdown (homolog of TDP-43 in *Drosophila*) has been described to present uncoordinated movements and progressive paralysis (Diaper *et al*, 2013; Feiguin *et al*, 2009; Hazelett *et al*, 2012; Lin *et al*, 2011). At the molecular level, these functional alterations were accompanied by modifications in the organization of the synaptic microtubules inside the terminals buttons (Godena *et al*, 2011).

1.7 TBPH: the homolog of TDP-43 in *Drosophila melanogaster*

Human TDP-43 presents a high conservation in *Drosophila* despite the enormous phylogenetic distance between these two species. In flies the homolog protein is called TBPH and is coded by a gene located on the second chromosome (2R:19746589-19750104). According to Fly Base (*www.flybase.org*), six annotated transcripts were reported that codify for six different protein isoforms after alternative splicing of the mRNA (Figure 13).

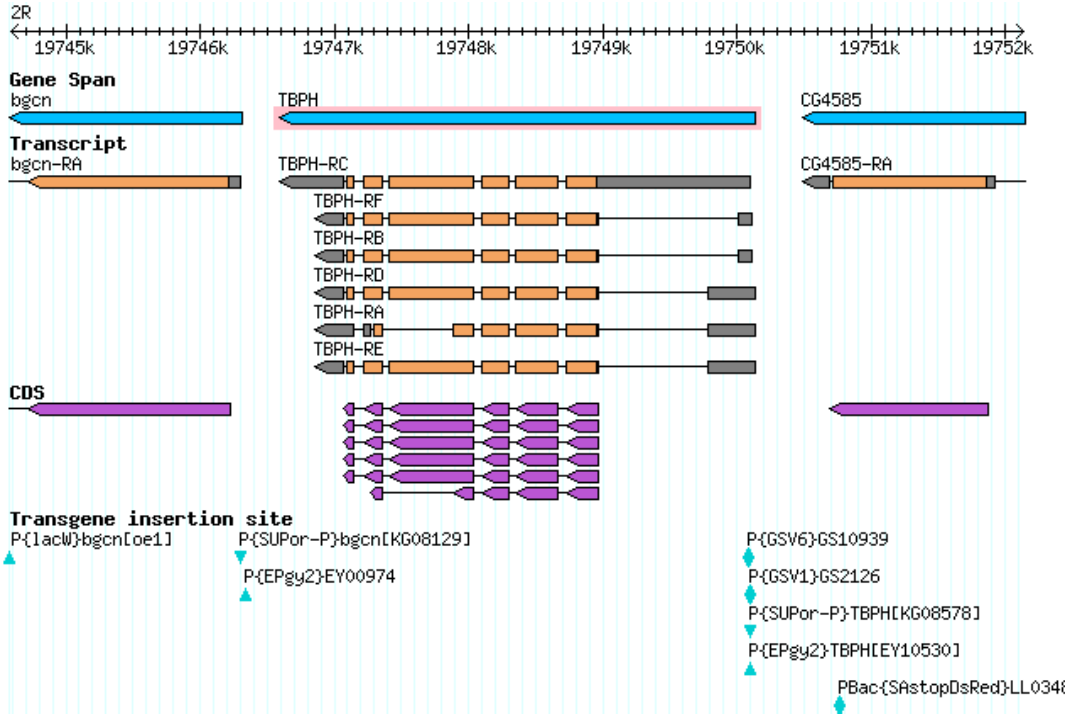

Figure 13 Chromosomal location of TBPH gene, and representation of its transcripts and the relative CDS.

Adapted from *www.flybase.org*.

The overall homology between the fly and the human proteins is 11.8% while the identity is 34.4% that becomes higher in the N-terminal region where the two main RNA-binding functional domains (RRM1 and RRM2) reside (75% of identity) (Figure 14). Less conservation was found in the C-terminal region of the protein that in *Drosophila* is a longer compared with the human but, in both cases, they present similar glycine rich domains.

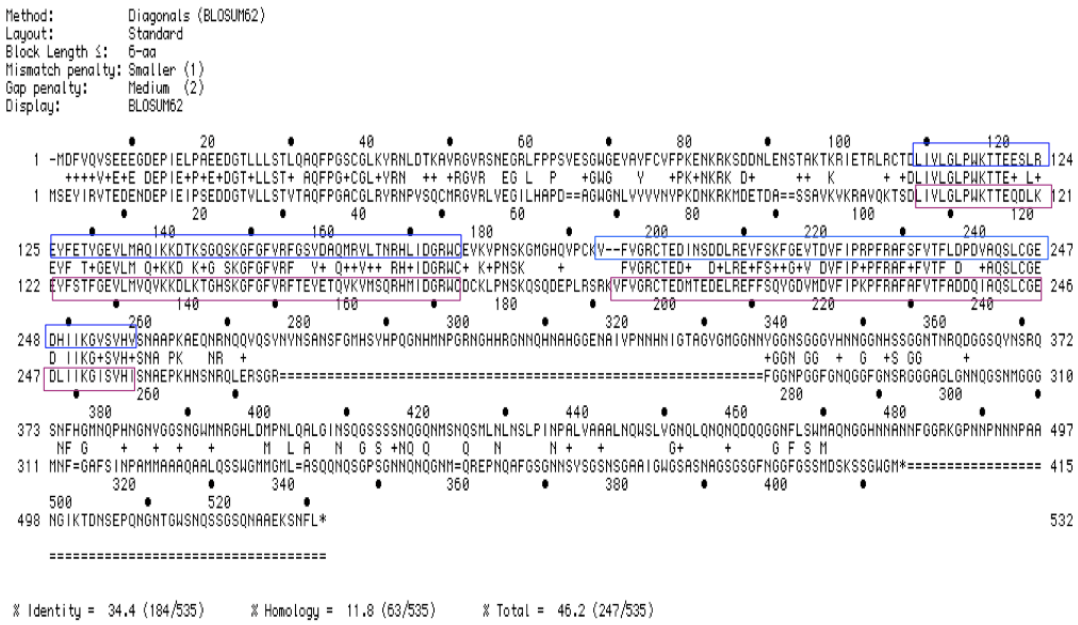

Figure 14 hTDP-43 versus TBPH.

Parallel between human TDP-43 amino acidic sequence (bottom line) and TBPH *Drosophila* amino acidic sequence (top line). In boxes are reported the RRMs domains.

The degree of conservation between the *Drosophila* and the human proteins does not only concern the sequence but also includes the functional properties. Human TDP-43 is able to inhibit exon 9 CFTR inclusion in HeLa cells (Buratti *et al*, 2001) and this function can be replaced by expressing TBPH (Ayala et al, 2005), indicating that these proteins similarly regulate exon splicing and suggesting that they may share comparable functions during the regulation of the RNA metabolism.

1.8 *Drosophila melanogaster*

Drosophila melanogaster is a Diptera that belongs to the family of *Drosophilidae*. This specie is commonly known as the fruit fly or the vinegar fly and is one of the most common models used in biology and neurobiology. Historically, Thomas Hunt Morgan introduced these insects to the laboratory and together with his students at the Columbia University identified the first genetic mutations in flies at the early 1900s. These initial studies, together with the series of studies performed by his group, established the basis of the modern genetics.

1.8.1 *Drosophila* life cycle

The development of *Drosophila* is simple and depends on the temperature. At 25°C, the life cycle is of 9-10days (Figure 15). The embryogenesis in *Drosophila* starts with the deposition of eggs. These embryos usually hatch between 18 to 22 hours after egg laying (AEL) and become 1st instar larvae at 24 hours AEL followed by the second and the third instar larval stages after 48 and 72 hours AEL respectively. The larvae become pupae and take 4.5 days to complete their metamorphosis, after which, the adult fly eclosed out by breaking the pupal shall case. Newly hatched flies can easily be recognized for the wings still closed and the clear body pigmentation. Few hours of after birth the wings result perfectly opened and the body acquires the normal pigmentation.

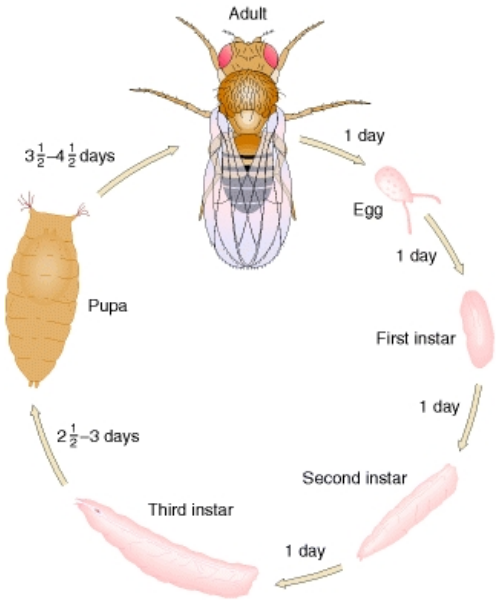

Figure 15 Schematic representation of the *Drosophila* life cycle.

Starting from embryo there are three different larval stages, a pupa period and finally the eclosion to adult fly.

The females begin to be sexually receptive about 12 hours after birth. Wild type *Drosophila* has red eyes and the body is segmented with transversal black rings across the abdomen. They exhibit sexual dimorphism then male and female flies can be easily distinguishable. Only male flies have a sex comb, a row of dark bristles on forelegs. Female flies have a long abdomen composed of seven segments pointed towards the anus, tip of the abdomen is dark black and round in male flies and the body size is smaller than in females with only five segments in the abdomen.

1.8.2 *Drosophila* in biology

In some cases, observations in cell lines are not sufficient to explain complex process in the context of an intact organism. Regarding to that, mammalian model systems offer several *in vivo* opportunities and extensive similarity to the human brain, however, the time required to perform experiments in these models sometimes can be prohibitive. *Drosophila melanogaster*, on the other hand, is a model with a rapid generation time and large progeny numbers produced in a single cross. *Drosophila* also posses a small annotated genome devoid of problems linked to genetic redundancy, they also posses

much simpler genetics with four pairs of chromosomes compared to 23 in humans and 12,000 genes compared to 25,000 in humans.

The conservation with vertebrates is very high, a comparative genome analysis reveals that approximately 75% of the human genes involved in single diseases have a *Drosophila* orthologous (Fortini *et al*, 2000) allowing, consequently, the analysis *in vivo* of the mechanisms behind complex human pathologies like neurological disorders, cancer or similar developmental and metabolic diseases like obesity, cardiovascular diseases and immune systems deficits (Bier, 2005).

Regarding the neurodegenerative diseases, the nervous system of *Drosophila* is much simpler compared to the human brain (~200,000 neurons compared to 1 billion neurons in humans) nonetheless, flies are able to perform complex motor behaviours like flying, walking or climbing (Ambegaokar *et al*, 2010). Moreover, the fly brain is organised into different areas that perform specialized functions, for example, there are defined zones for learning, memory, vision and olfaction. The formation and assembly of the synaptic connections during the development of the nervous system is also well and extensively characterized in *Drosophila* making possible the analysis of the modifications produced by pathological alterations. The sophisticated genetic and molecular tools available in flies give the opportunity to produce specific manipulations in individual neurons and determine the potential role of different molecules in neuronal homeostasis.

1.8.3 Models of human diseases in *Drosophila*

Different genetic approaches can be utilized to study the molecular function of genes involved in human diseases using *Drosophila melanogaster*.

One possibility is to express in flies human genes carrying specific mutations, associated with the disease, and determine whether these modifications alter the functionality of this protein *in vivo* (forward-genetics).

Alternatively, it is possible to study in *Drosophila* the function of endogenous proteins that present strong homology with conserved genes implied in human diseases (reverse genetics).

Thus, interesting phenotypes can emerge by reducing or eliminating the gene expression or by overexpressing the gene product. In that respect, nearly all of the current fly models of neurodegenerative diseases were made using the GAL4/UAS (upstream activating sequence) system, which allows the ectopic expression of a transgene in a specific tissue (Brand & Perrimon, 1993a). With this system, a human disease-related transgene can be placed under the control of the yeast transcriptional activator GAL4 protein. In the absence of GAL4, the transgene is inactive but when these flies are crossed with GAL4 expressing flies in a specific tissue pattern, the transgenic protein can be expressed and the phenotypes generated easily analysed (Figure 16).

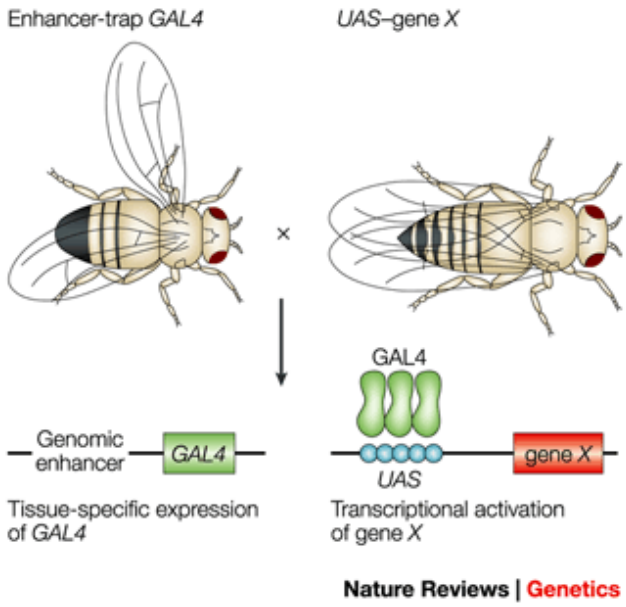

Figure 16 GAL4 system.

In the GAL4-UAS system, two transgenic fly lines are created. In the first (UAS–transgene fly), the transgene is placed downstream of a UAS activation domain that consists of GAL4-binding sites. The second fly line contained the GAL4, which is a yeast transcriptional activator. In the absence of GAL4, the transgene is transcriptionally inactive; on the contrary in presence of GAL4 the transgene is transcriptionally active. Adapted from Nature Reviews.

A similar scheme can be adapted to induce the expression of in interference RNAs (RNAi) against specific genes to create hypomorphic alleles. Once *Drosophila* models of neurodegenerative disease reproduced specific phenotypes related with the disease, the system allows to perform genome

wide screening to identify potential modifiers of these phenotypes. Another approach consists in a genetic screen to interrogate the genome for mutations that modify a neurodegenerative phenotype. Random mutations are produced by chemical or insertional mutagenesis, and the ability of these mutations to suppress or enhance the phenotype of interest is tested. The unbiased approach has the potential to identify new proteins, or to implicate previously defined cellular pathways that were not suspected to be important in neurodegenerative disease (Muqit & Feany, 2002).

1.8.4 *Drosophila* NMJ

The *Drosophila* neuromuscular junctions (NMJs) has been used as model system to study synaptic formation and function since the mid 1970's, (Jan & Jan, 1976; Magazanik & Vyskocil, 1979). The NMJs can be easily analysed morphologically and electro physiologically and are one of the most powerful models used to understand the processes that govern the communications between the pre and the postsynaptic membranes in neurons. *Drosophila* NMJs, posses a high degree of similarity with the mammalian neuromuscular plaques and the other central synapses of the nervous system that utilize glutamate as a neurotransmitter (Koh *et al*, 2000). This system was also widely used to characterize synaptic development and neurotransmission control (Keshishian *et al*, 1996).

The NMJs in the *Drosophila* larval bodies are organized in individual segments (A1-A7) that present a series of different muscles arranged in a specific pattern, identically repeated in every segment. These segments are composed by 30 different muscles, innervated by specific motoneurons, specifically targeted to individual muscle fiber (Gramates & Budnik, 1999; Keshishian & Chiba, 1993). The small number of neurons and muscles and their unique identity gives the possibility to study in details and with high reproducibility the interactions between muscles and neurons. There are a total of 32 motoneurons that innervate specific muscle through the formation of and average of six nerve branches (Hoang & Chiba, 2001), (Figure 17).

The nerve branches are: ISN (inter segmental nerve branch), SNa (segmental nerve branch a), SNb (segmental nerve branch b), SNc

(segmental nerve c), SNd (segmental nerve branches d) and TN (transverse nerve).

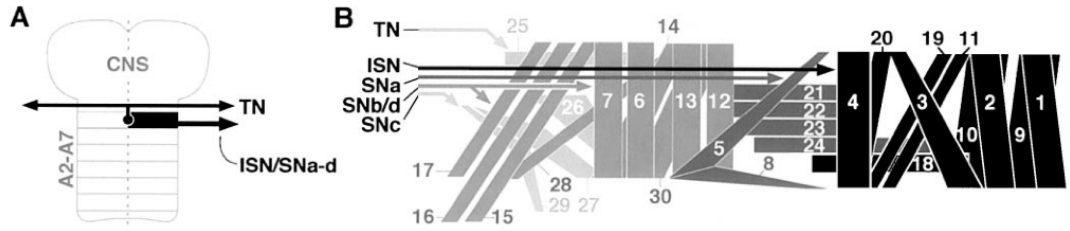

Figure 17 *Drosophila* NMJ structure.

(A) Each segment is bilaterally symmetric from abdominal segment 2 to segment 7. In (B) is schematized one hemi segment of larval body wall. It is represented the disposition of the muscle and the entrance of the nerve branches. Adapted from Hoang and Chiba, 2001.

The axons of the motoneurons reach the surface of the muscles to form specialized connections called neuromuscular synapses through the differentiation of synaptic boutons. These structures are well characterized and, based on their dimensions, can be classified in four major categories:

- type 1b are the largest boutons (3-6μm), are found in all muscle and are glutamatergic (Johansen *et al*, 1989);
- type 1s are smaller that 1b (2-4μm), are present in all muscle and are glutamatergic (Johansen et al., 1989);
- type II are the smallest boutons (1-2μm), have very elaborated branches and are not present on all muscle, these synaptic boutons used as neurotransmitter glutamate and octopamine (Monastirioti *et al*, 1995);
- type III has medium size (2-3μm), are present only on muscle 12 and contain glutamate and insulin, as putative hormone neurotransmitter (Gorczyca *et al*, 1993).

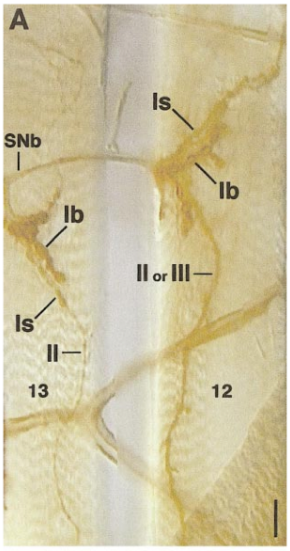

Figure 18 Boutons classification.

Through the innervation pattern on muscle 12 and 13 it is possible an overview of all species of synaptic boutons: 1b, 1s, II and III. Adapted from Hoang and Chiba, 2001.

The synaptic transmission between the motoneurons and the muscles requires the precise structural and functional assembly of the pre and the postsynaptic terminals. The presynaptic terminal boutons contain a high number of synaptic vesicles filled with the neurotransmitter and ready to be released. Though the perfect temporal correlation of the events that initiate the synaptic transmission are not well known, is believed that the Ca^{++} flux through voltage channels promotes the docking of the presynaptic vesicles with the structural protein Bruchpilot (Brp), homolog to the vertebrate CAST (cytoskeletal matrix associated with the active zone (CAZ) associated structural protein) (Ziff, 1997). Bruchpilot forms part of the characteristic T-bar structures, required for the release of the neurotransmitter in the synaptic cleft. The presence of the neurotransmitter promotes the activation of the glutamate receptors localized in the postsynaptic membranes (Dresbach *et al*, 2001). The Glutamate receptors exhibit five subunits: GluRIIA, GluRIIB, GluRIIC, GluRIID and GluRIIE coded by different genes (Schmid *et al*, 2006), at the protein level the receptors are organized in functional complexes made out two subunits that combine the GluRIIA or GluRIIB units together with the different subunits GluRIIC, GluRIID and GluRIIE. The glutamate receptors are present in the postsynaptic membranes before the formation of the

synapses, however, the functional clusters exclusively form after the stimulus provided by the presynaptic activity (Broadie & Bate, 1993).

Drosophila postsynaptic membranes also present non-NMDA (N-methyl D-aspartate) receptors, homologous to vertebrate non-NMDA ionotropic receptors, in charged of the fast excitatory transmission (DiAntonio *et al*, 1999; Schuster *et al*, 1991).

1.8.5 *Drosophila* synaptic vesicle cycle

The release of neurotransmitters at the synaptic zone of *Drosophila* nerve terminals is mediated by the regulated exocytosis of synaptic vesicles. This process shares many characteristics and molecular components with the less specialized membrane fusion events that normally occur during the cells life. Thus, it was observed that the proteins involve in the membrane fusion machinery such as, the soluble *N*-ethylmaleimide-sensitive factor attachment protein receptors (SNAREs), the ATPase *N*-ethylmaleimide-sensitive factor and the Rabs GTPase are highly conserved from yeast to human and similarly required for synaptic activity or vesicular trafficking (Rothman, 1994).

Similarly, the continuous formation and fusion of synaptic vesicles are essential to support the rapid and repeated rounds of neurotransmitters release and, consequently, neurotransmission. This process is initiated in response to the presynaptic Ca^{2+} influx and involves the activation of the SNARE protein complex. These proteins are present on the surface of both membranes (presynaptic membrane and synaptic vesicles membrane) and are responsible for the fusion of lipid bilayers (Chen & Scheller, 2001; Jahn *et al*, 2003), (Figure 19). The SNARE proteins were initially classified as v-SNARE and t-SNARE according on their localization on the vesicles or in the target membranes. More recently, these proteins have been reclassified as R-SNARE and Q-SNARE based to the conserved arginine or glutamine residues present in their core SNARE motifs (Fasshauer *et al*, 1998).

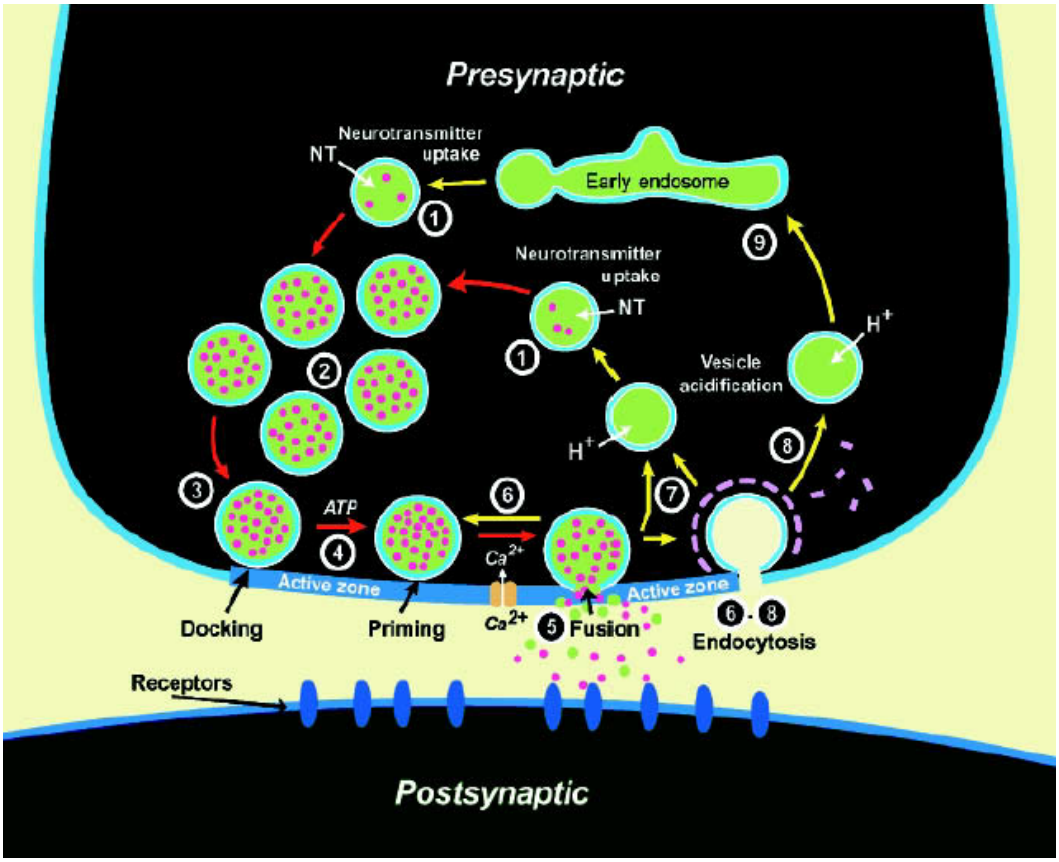

Figure 19 Synaptic vesicle cycle.

(1) The synaptic vesicles are filled with neurotransmitters and formed (2) a ready synaptic vesicles pool. (3) Vesicles dock at the active zone and undergo a priming reaction (4). Ca^{++} triggered the fusion and the opening of the pore (5). After the neurotransmitters release, the vesicles undergo endocytosis to recycle the vesicles; a local reuse (6), a fast recycling without endosomal intermediate (7), clathrin mediated endocytosis (8) or a endocytosis mediated via endosomes (9). Adapted from (Sudhof, 2004).

The synaptic cycle of vesicular of exocytosis and endocytosis in *Drosophila* is basically mediated by three different SNARE proteins: Synaptobrevin (which is a membrane protein associated with the presynaptic vesicles), Syntaxin 1A (which is localized in the plasma membrane of the synaptic terminals) and Synaptosomal-associated protein 25 (SNAP-25, which is involved in the formation of a tight complex to bring together synaptic vesicle and plasma membranes) (Sudhof, 2004). The docking of synaptic vesicles at the active zones depend on the formation of a "synaptic core complex" formed by the interaction of Synaptobrevin (through its R-SNARE motif) with the Q-SNARE motif of Syntaxin 1 and SNAP-25 (McMahon & Gallop, 2005).

The protein complex assembly, described above, leads to the fusion of the synaptic vesicles with the presynaptic membranes.

The recycling process of the fused vesicles, instead, is performed through endocytosis that may occur across different regulatory pathways. The most frequent and better-characterized process of vesicular recycling is the clathrin-mediated endocytosis. In this process, adaptor proteins (APs) recruit clathrin to the plasma membrane and induce membrane invaginations allowing the recycling of the vesicles (Richmond & Broadie, 2002). Endocytotic pathways independent of clathrin to recycle synaptic vesicles are less characterized (Gupta *et al*, 2009) and implicate the transport of synaptic vesicles via the specialized endosomes (Hoopmann *et al*, 2010). Newly internalized vesicles are routed to recycling endosomes where the constitutive proteins are sorted for a new synaptic cycle or internalized into the multi-vesicular bodies (MVB), through the ESCRT (endosomal sorting complexes required for transport) machinery, for protein degradation (Raiborg & Stenmark, 2009). The events described above including the intracellular trafficking of the synaptic vesicles are tightly regulated by the Rab GTPase family (Mahoney *et al*, 2006). This family of small GTPase are able to regulate the endosomal trafficking of the membrane proteins through their capacity to regulate the specific tethering of the synaptic vesicles with the endosomes (Baetz & Goldenring, 2013; Christoforidis *et al*, 1999; Simonsen *et al*, 1998), to interact with SNARE proteins (Luzio *et al*, 2010; Sørensen *et al*, 2006) and the interactions of the endosomes with the microtubules (Horgan & McCaffrey, 2011; Ishida *et al*, 2012).

2 Research aims

The TDP-43 protein is widely described to be involved in the neurodegenerative process behind ALS and FTD, although the physiological role of TDP-43/TBPH *in vivo* and the events that lead to pathological condition are still not clearly known.

The purpose of this study is to characterize and define the physiological role of TDP-43/TBPH in the central nervous system of a complete organism utilizing Drosophila melanogaster to better understand the alterations that may occur in pathological conditions.

In order to achieve this objective, I defined the following, specific aims:

1. To characterize of the physiological role of the *Drosophila* TDP-43 protein (TBPH) *in vivo*.
2. To identify the molecular mechanisms and metabolic pathways regulated by TBPH *in vivo*.
3. To determine the chronological requirement of TBPH function during neuronal development.
4. To determine the functional requirements of TBPH in fully differentiated neurons.
5. To establish the initial molecular modifications behind TBPH dysfunction and to evaluate the regenerative capacity of the affected neurons *in vivo*.

3 Materials and methods

3.1 Generation of constructs

In this work two plasmids were used: pKS69 and pUASTattB.

Vector pKS69 is 13Kb long (Figure 20) and derives by modification of the plasmid pP {Casper-LacZ}. The plasmid contains the sequence for the P element that mediates recombination of the gene of interest into the genome of the fruit fly.

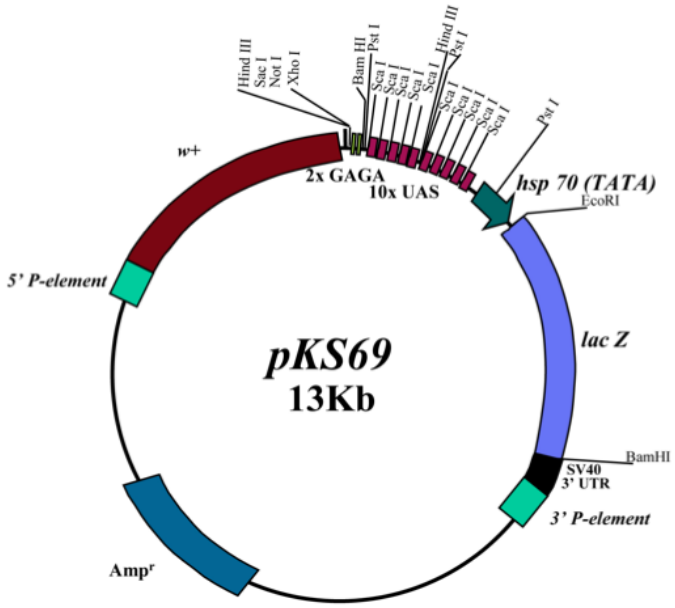

Figure 20 pKS69 vector map.

The plasmid contains a white gene (w+), a genetic marker that codes for the colour of the eye and allows identifying the flies in which the recombination of transgene has occurred. In the vector are present 10 tandem arrayed optimized Gal4 binding sites, the UAS sequences, followed by hsp70 TATA box and transcriptional start, a poly linker containing unique restriction sites and the SV40 terminator site with the polyadenylation site. In the vector, it is also present the ampicillin resistance for the selection of colonies in *E. coli*.

The plasmid pUASTattB (Figure 21) is 8.4 Kb long (Gene Bank accession number EF362409), contains the gene w^+ coding for eye pigmentation of the fly, a region with 5 UAS binding sites in front of hsp70 promoter Gal4, loxP sequences, an MCS, the sequence attB and a region for resistance to ampicillin. The attB site allows site-specific integration of the transgene of interest in the attP landing platform created in flies, taking advantages of the phage ΦC31 integrase system (Bischof *et al*, 2007; Groth *et al*, 2004).

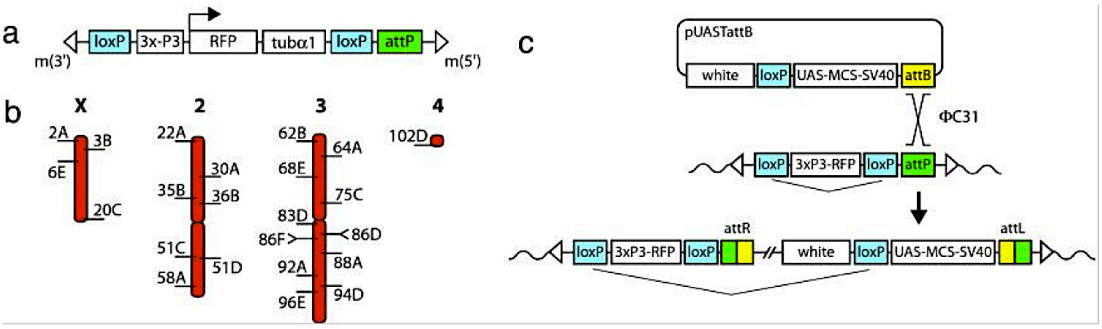

Figure 21 pUAST-attB vector map.

Taken from (Bischof *et al*, 2007).

The cDNA of the human TDP-43, *Drosophila* TBPH and TBPH$^{F/L150/152}$ were cloned in vectors.

3.2 RNA extraction from wild-type flies

Flies were transferred in Ambion TRI Reagent® solution (30µl x flies) and squeezed with a pestle. After a centrifugation step of 12,000 x g for 10 minutes at 6°C to remove debris, the supernatant was recovered and the RNA was extracted using phenol-chloroform method. Finally RNA was dissolved in 50µl of RNase free water. After quantification with Quant-it RNA Assay Kit, RNA was checked stored at -80°C.

3.3 cDNA synthesis: RT-PCR

The RNA (1µg) was treated with DNAse (Promega RQ1#M610A) and subsequently retro transcribed with Superscript III First-Strand Synthesis for RT-PCR (Invitrogen #1808-051) as follows:

DNase Treatment	
Component	Volume/ 10µl reaction
RNA (1µg)	1-8µl
10X buffer	1µl
DNase enzyme	1µl

H_2O	add to 10µl

The mixture was incubated at 37°C for 30 minutes, then DNase Stop solution was added and incubated at 65°C for 10 minutes to inactivate DNase enzyme.

Reverse Transcriptase Reaction	
MIX 1 Component	Volume/ 10µl reaction
RNA (DNase treated)	8µl
OligodT (50mM)	1µl
dNTPs (10mM)	1µl

The mixture was incubated at 65°C for 5 minutes then immediately put on ice at least for 2 minutes.

Reverse Transcriptase Reaction	
MIX 2 Component	Volume/ 10µl reaction
10X RT buffer	2µl
$MgCl_2$ (25mM)	4µl
0.1 M DTT	2µl
RNase OUT	1µl
SuperScript III RT	1µl

The mixture 2 was mixed with mixture 1 and then incubated at 25°C for 10 minutes, then 50°C for 50 minutes to allow cDNA synthesis. The reaction terminated at 85°C for 5 minutes to inactivate the enzyme.

3.4 Cloning

The cDNA Flag tagged of the human TDP-43, Drosophila TBPH and $TBPH^{F/L150/152}$ were cloned into vectors, using the primer sequences reported below:

hTDP-43
fw 5' cggaattcatggactacaaagacgatgacgacaagtctgaatatattcgggtaaccg 3'
re 5' gctctagactacattccccagccagaagac 3'

TBPH
fw 5' cggaattcatggatttcgttcaagtgtcg 3'
re *5'* gctctagattaaagaaagtttgacttctccgcggcgtt 3'

$TBPH^{F/L150/152}$
fw 5' cggaattcatggatttcgttcaagtgtcg 3'
re *5'* gctctagattaaagaaagtttgacttctccgcggcgtt 3'
F150/152
fw 5' tccaagggcttaggtttagtgcgcttc3'
re 5' gaagcgcactaaacctaagcccttgga 3'

3.5 High fidelity PCR

For cloning was used the high fidelity PCR following the protocol described here:

High Fidelity PCR	
Component (Initial concentration)	Final concentration
cDNA	100ng
10X Pfx Buffer	1X
10mM dNTPs	0.3mM
50mM $MgSO_4$	1mM

Forward	0.3µM
Reverse	0.3µM
Platinum Pfx polymerase	1U
H_2O	add to 50µl

PCR cycle Program		
Cycle step	Temperature	Time
Initial denaturation	94°C	2 minutes
Denaturation	94°C	15 second
Annealing	according to Tm	30 seconds
Extension	68°C	1 min/ 1Kb
Final extension	68°C	10 minutes

3.6 Agarose DNA gel electrophoresis

DNA samples were size fractionated by electrophoresis in agarose gels ranging in concentrations from 0.8 % w/v (large fragments) to 2 % w/v (small fragments). The gels contained ethidium bromide (0.5µg /ml) and 1X Tris/Borate/EDTA (TBE 5X: 104g Tris, 27.5g boric acid, 10ml of 0.5M EDTA pH8 in 1 liter of water). The gels were electrophoresed at 50-80mA in 1X TBE running buffer. DNA was visualized by UV transillumination and the result recorded by digital photography.

3.7 DNA extraction from agarose gel

The DNA fragments obtained by restriction enzyme may be separated and isolated with an electrophoretic run of preparative type. DNA fragments were eluted from agarose gel with Wizard PCR purification kit (Promega).

3.8 Restriction reaction

The plasmids and PCRs of the fragments were digested with *EcoRI* and *XbaI* enzymes (NEB) in the following reactions:

Restriction Reaction	
Component	Volume/ 150 µl reaction
DNA (1.5-2 µg)	--µl
EcoRI (10U/ µl)	2µl
XbaI (10U/ µl)	2µl
10X ligation buffer	15µl
H_2O	add to 150µl

Mixed products were incubated at 37°C for one hour and successively incubated at 65°C for 20 minutes for the inactivation of the enzymes. The products were separated by electrophoresis through a 1% agarose gel. The bands corresponding to the PCRs fragments were cut from the gel and purified using the QIAquick Gel Extraction Kit (Qiagen). Purified DNA products were eluted in 10µl of elution buffer and ligated as follow described.

3.9 Ligation

The fragment was added in excess to the mixture for the ligation reaction as described below:

Ligation Reaction	
Component	Volume/ 10µl reaction
Purified pUASTattB plasmid	1µl (20ng)
Purified fragment	3µl (100ng)
2X Rapid Ligation Buffer (Promega)	5µl
T4 DNA Ligase (Promega)	1µl

The mixture was incubated for 15 minutes at room temperature.

3.10 Preparation of competent cells

A single colony of *E. coli* DH5α was inoculated into 5ml of liquid Luria-Bertani medium [LB medium: 10g/l bacto-tryptone, 5g/l yeast extract, 10g/l sodium chloride (NaCl), pH 7.5] and grown at 37°C shaking over night. 200ml of LB are inoculated with the stationary culture to obtain an $O.D._{600}$ of

approximately 0.05. Cells were centrifuged at 1,000x g for 15 minutes at 4°C and were re-suspended in 10ml of RF1 frozen buffer (100mM RbCl, 50mM $MgCl_2$, 30mM CH_3COOK, 10mM $CaCl_2$, 15% glycerol, pH 5.8). After 20 minutes of incubation, the cell suspension was centrifuged again for a period of 15 minutes and cells were re-suspended in 2ml of buffer iced RF2 (10mM MOPS, 10mM RbCl, 75mM $CaCl_2$, 15% glycerol). Aliquots of competent cells were directly transformed or stored for further processing at -80°C.

3.11 Transformation

Half of ligation mixture was added to 50µl of competent cells for transformation and placed on ice for 1 hour and half, followed by an heat shock treatment at 42°C for 45 seconds. And brief incubation on ice. Finally 200µl of LB medium was added to the cells which were incubated at 37°C shaker for 1 hour. Transformed bacteria were plated on LB agar plate with ampicillin (100µg/ml) and incubated at 37°C for 18 hours. The positive clones ampicillin resistant were grown in LB-ampicillin medium. Plasmid DNA, successively purified by minipreparation protocol, was tested by restriction analysis to confirm proper insertion.

3.12 Sequencing of clones

Three positive clones of each construct were sequenced to confirm the presence of the specific cDNA fragment inserted in the vector. The clones were sent to Eurofins MWG Operon (Germany) for sequencing.

3.13 Small-scale plasmid DNA extraction (Miniprep)

Minipreps of plasmid were performed with a commercial kit (Wizard Plus Minipreps® DNA Purification System, PROMEGA). The protocol is based on the lysis of bacteria followed by the attachment of plasmid DNA to silica column. Washes were performing with a buffer containing ethanol, and then the plasmidic DNA was eluted with water or 10mM TRIS pH 8.

3.14 Culturing S2 cells

The S2 cell was derived from a primary culture of late stage (20-24 hours old) *Drosophila melanogaster* embryos (Schneider, 1972). S2 cells formed a semi-adherent monolayer when grown in culture flasks at room temperature, without CO_2. The Insect Express medium (Lonza #BE12-730F) was supplemented with 10% heat-inactivated fetal bovine serum (FBS) and 1X antibiotic-antimycotic (SIGMA A5955).

3.15 S2 cells transfection

Before sending the constructs to BEST gene company for the generation of transgenic flies, the expression level of the cloned genes were tested in S2 cells.

Transfection was performed using the Effectene transfection reagent kit (Qiagen) a non-liposomal lipid reagent for DNA transfection. S2 cells were harvested by centrifugation and after removing the supernatant were washed in 10ml of PBS. They were then placed in a petri dish at a concentration of $3x10^6$/ml with 4ml of Insect Express containing 10% heat-inactivated FBS, 50U/ml penicillin and 50µg/ml streptomycin.

The transfection reaction was prepared as follows: 4µl of DNA plasmid (0.25µg/ml) containing the fragment of interest 1µg of plasmid harbouring Gal4 factor and 8µl of Enhancer were added to the condensation buffer (Condensation Buffer, CE) up to a total volume of 150µl and incubated at room temperature for 5 minutes. The mixture was subsequently added of 25µl of Effectene reagent, was mixed by vortexing and incubated at room temperature for 10 minutes to allow transfection complex formation. The transfection complex was added of 1ml of medium then was transferred in petri dish. The cells were incubated at 25°C for at least 48 hours in order to obtain the expression of the protein encoded by the transfected genes.

3.16 Generation of transgenic flies

After the protein expression evaluation in S2 cells, the constructs were sent to Best Gene Company to generate transgenic flies. Different transformant lines were obtained for each transgene. The integration of constructs was

directed, through PhiC31 integrase-mediated transgenesis systems, on estimated cytosite 86F located on the fly third chromosome.

3.17 Biochemical techniques

3.17.1 Protein extraction

The S2 transfected cells were transferred in 1.5ml tubes and washed with PBS, collected by centrifugation at 16,000 x g and re-suspended in 100µl of Lysis buffer (50mM Tris HCl pH 7.6, 750mM NaCl, 1% Triton X-100 and complete mini EDTA-free protease inhibitors commercially available from ROCHE).

Regarding the flies, total protein was extracted from entire flies or specific districts, such as heads, thorax or abdomen. Whole flies were frozen in liquid nitrogen and then vortexed to separate heads from the bodies. The material (8-10ul /head or fly) was transferred into 1.5 ml tubes containing lysis buffer 1X (1.5X Lysis buffer solution: 225mM NaCl, 15mM Tris, 7.5mM EDTA, 15% glycerol, 7.5mM EGTA, 75mM NaF, 6M Urea, 7.5mM DTT and protease inhibitors).

The material in lysis buffer was manually homogenized, followed by centrifugation at 0.5 x g for 5-10 minutes at 6°C. Finally supernatants were collected and stored at -80°C. The quantification of the proteins was performed with Quant-iT™ Protein Assay Kit (INVITROGEN), following the recommended procedure.

3.17.2 Protein extraction for Futsch

To detect Futsch protein a protocol in agreement with (Zou *et al*, 2008) was followed. Twenty fly heads were homogenized in ice cold lysis buffer containing 1% CHAPS, 20mM Tris/HCl (pH 7.5), 10mM EDTA, 120mM NaCl, 50mM KCl, 2mM DTT and protease inhibitors (Roche, Complete Mini EDTA free). The homogenization step was followed by incubation on ice for 5-10 minutes and centrifugation at 9,000 x g for 10 minutes at 4°C. Supernatants were collected and processed for the loading on acrylamide gel.

3.17.3 SDS-PAGE

Sodium dodecyl sulphate polyacrylamide gel electrophoresis (SDS-PAGE) is a method used to separate proteins according to their size. Protein samples were diluted in 1X Laemmli buffer (composition of 5X: 0.3M Tris-Cl pH6.8, 50% glycerol, 10% SDS, 25% ß-mercaptoethanol, 0.05% bromophenol blue) and then boiled at 95°C for 5 minutes. Gels were prepared as follows:

Gel Preparation		
Components	Resolving gel	Stacking gel
Acrylamide M-BIS 40%	4%-10% (v/v)	5% (v/v)
Tris-HCl pH 8.8	0.37M	-
Tris-HCl pH 6.8	-	0.125M
Ammonium persulphate	0.1% (w/v)	0.1% (w/v)
SDS	0.1% (w/v)	0.1% (w/v)
TEMED	0.02% (v/v)	0.02% (v/v)

The amperage applied for running electrophoresis was 20mA in 1X running buffer (Running buffer 10X: 30.28g Tris, 114.13g Glycine, 10g SDS in 1 liter of water).

3.17.4 Western blotting

After electrophoresis, proteins were transferred from the gel to a nitrocellulose membrane (Amersham Biosciences). Blotting lasted 1 hour at 350mA in transfer buffer 1X with 20% methanol (Transfer buffer 10X: 30g Tris, 144g glycine in 1 liter of water).

The membrane was blocked with a solution of 5% milk or 5% bovine serum albumin (BSA, SIGMA) in TBS 0.01% Tween (TBS-T) for 30 minutes at room temperature on shaking platform (TBS buffer 10X: 24.2g Tris, 80g NaCl in 1 liter of water, the solution had pH 7.6). The membrane was then incubated with primary antibody diluted to the appropriate concentration in TBS-T and 5% milk or 5% BSA at 4°C over night.

After five washes in TBS-T, the membrane was incubated with the secondary antibody diluted to the appropriate concentration in TBS-T for 1 hour at room

temperature. The protein detection was performed with SuperSignal®West Femto Maximum Sensitivity Substrate (Thermo).

A list of antibodies used in this work was reported below:

Primary Antibodies		
Name/Supplier	Host	Dilution
Anti Flag M5/Sigma	mouse	1: 1,000
Anti TBPH/house	rabbit	1: 2,000
Anti Syn 3C11c/DSHB	mouse	1: 4,000
Anti Syx 8C3 s/DSHB	mouse	1: 2,500
Anti CSP2c/DSHB	mouse	1: 9,000
Anti BRPs/ DSHB	mouse	1: 2,000
Anti Futsch 22C10s/ DSHB	mouse	1: 200
Anti Dlg 4F3c/ DSHB	mouse	1: 15,000
Anti Tubulin/Calbiochem	mouse	1: 4,000
Anti Actin/Sigma	rabbit	1:1,000

Secondary Antibodies		
Name/Supplier	Host	Dilution
Anti mouse-HRP/Pierce	goat	1: 50,000
Anti rabbit-HRP/Pierce	goat	1: 50,000

3.18 Real-time PCR (qPCR)

RNA samples (3 experimental and 3 control preparations for heads) were used to prepare independent cDNA samples with the Superscript 1st Strand Synthesis Kit (Invitrogen). The cDNA preparations were diluted 1:15 and 1.5µl was used in each reaction for qPCR using the SYBR Green PCR Mastermix (Applied Biosystems). Reactions were performed in the ABI7700

or ABI7500 Fast Real-time PCR system using the default run parameters. For each plate, a melting curve analysis was performed at the end of each run to test for primer specificity Tm. Each plate also contained reactions to test for amplification specificity in the presence or absence of template. RpL11 and Rpl-52 primers were used for control amplification reactions. The primers used for qPCR are listed below.

futsch
fw 5' ctcgccaaagcccacatcacc 3'
re 5'gtcaccctcacactcagctcc 3'
hdac-6
fw 5' cgagcggctgaaggagac 3'
re 5' accagatggtccaccaattcg 3'
rpl-52
fw 5'gaaaataacaaagatctgcttggcc 3'
re 5'aagtggcccttgggcttcag 3'
rpl11
fw 5' ccatcggtatctatggtctgga 3'
re 5' catcgtatttctgctggaacca 3'
synapsin
fw 5' accagaccatcgtactcac 3'
re 5' ccgaaaatcatatcggcatcc 3'
syntaxin
fw 5' tgttcacgcagggcatcatc 3'
re 5' gccgtctgcacatagtccatag 3'
csp
fw 5' ccgataagaacccggacaatg 3'
re 5' tcacggcacagcagataac 3'

3.19 *Drosophila* techniques

3.19.1 *Drosophila* stock handling

Drosophila stocks were purchased from the Bloomington stock centre (Indiana; http://flystocks.bio.indiana.edu/), the *Drosophila* Genetic Resource

Centre (Kyoto; http://www.dgrc.kit.ac.jp/) and *Drosophila* stock centre (Vienna; http://stockcenter.vdrc.at/). Additional stocks were kindly provided by colleagues and other laboratories or were generated as part of this investigation. Stocks were stored at 25°C or 18°C, and were transferred to fresh fly medium every 2 and 4 weeks, respectively. At 25°C, the fly life cycle is completed in 10 days (from egg to adult), whereas at 18°C the life cycle is approximately doubled. Experimental crosses were maintained in a humidified chamber (60%) at 25°C on 12 hours light and 12 hours dark cycles.

3.19.2 Maintaining medium for flies

Flies were cultured in small tubes containing a specific type of growth food composed of corn flavour (700g), water (24l), sugar (1kg), agar (150g), brewer's yeast (1.5kg) and propionic acid (100ml).

3.19.3 *Drosophila* anaesthetisation

The flies were anaesthetised on a gas porous pad using carbon dioxide (CO_2). A constant CO_2 flow provided immediate and continuous anaesthetisation.

3.19.4 RU486 feeding procedure

In *Drosophila* are available various inducible gene expression system, the most used is the GAL4 system (Brand & Perrimon, 1993b). In this system the temporal regulation is absent, to have also a temporal control of the transgene expression the GeneSwitch system is necessary, in which it is possible a spatial as well a temporal control of the transgene expression (Poirier *et al*, 2008).

Larval feeding

Crosses were placed in normal food for one day, to promote adaptation and mating. The next day crosses were transferred on fly food containing RU486 at the molar concentration desired. 3-4 hours were left to lay eggs, parental were removed and the larvae obtained from the culture used for experiments. A stock solution of 10mg/ml RU486 (mifepristone, Sigma) in 80% ethanol

was added during fly food preparation to achieve the required concentration. Control larvae were grown in food supplemented with ethanol only (Osterwalder *et al*, 2001).

Adult feeding

To induce the GeneSwitch system in adult flies a different procedure for feeding flies has been followed. A stock solution of 10 mg/ml RU486 in 80% ethanol was diluted in a 2% sucrose solution to achieve the required concentration. The solution obtained was directly added on the surface of normal fly food. The food with the drug solution was allowed to dry under a hood and then the flies were transferred inside for the analysis. Control larvae were grown in food with a superficial addition of a solution 2% sucrose and ethanol, (Roman *et al*, 2001; Wigby *et al*, 2011).

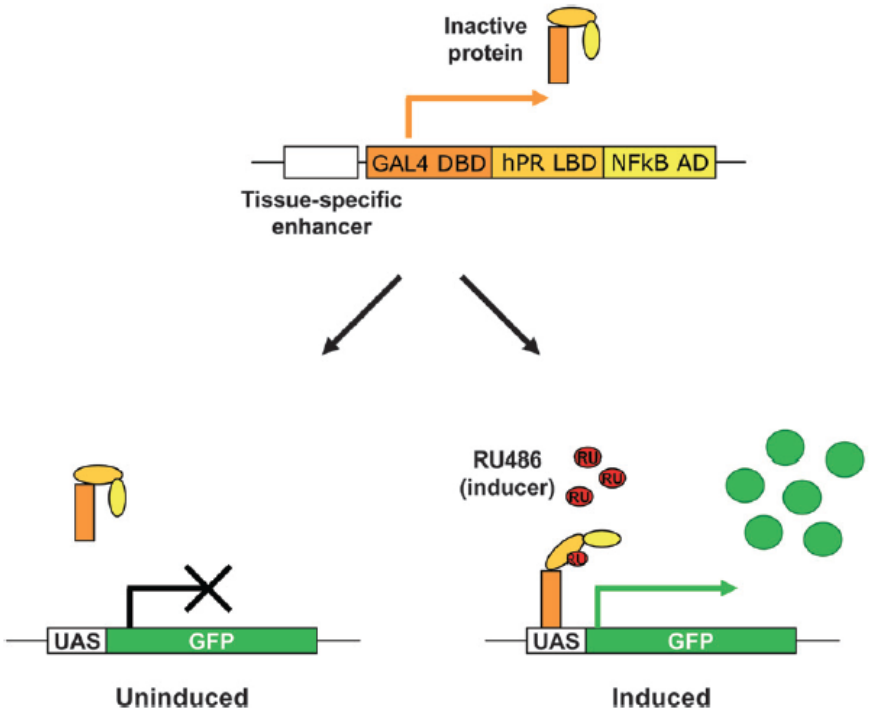

Figure 22 GeneSwitch GAL4 system.

In absence of the RU486 (inducer) the GAL4 protein was expressed but remain transcriptionally inactive. If the inducer was administrated GAL4 become transcriptionally active. Adapted from (Nicholson *et al*, 2008).

3.19.5 TARGET system procedure

Another inducible system used in *Drosophila* is TARGET system (temporal and regional gene expression targeting). This technique is based on the ubiquitous expression of the temperature sensitive version of the GAL80 protein, a strong GAL4 repressor. GAL80 repressed GAL4 transcriptional activity at permissive temperature, with a temperature shift it become inactive and allow GAL4 activity (McGuire *et al*, 2004, 2004)(McGuire *et al*, 2004, 2004)(McGuire *et al*, 2004).

Crosses were maintain in normal food at a controlled temperature of 18°C, to induce GAL4 inactivating GAL80 molecules tubes containing flies were shift at a higher temperature (29°C-31°C). In these experiments a group of control flies were subjected to the same treatments of he other group.

3.20 Phenotypic analysis in *Drosophila*

3.20.1 Climbing assay

The negative geotaxis (movement against the gravity) is an innate characteristic of *Drosophila* (Benzer, 1967; Kazemi-Esfarjani & Benzer, 2000). The key point of this assay is that *Drosophila* flies respond rapidly to light stimulus (photo taxis) (Benzer, 1967). Thus the flies were admitted in the cylinder, a distal lamp was put to provide the stimulus and the flies' capability to reach the end of the tube was measured within fifteen seconds. This behaviour is stable during the first three weeks of adult life, but progressively declines with age, thus the activity has been measured at 7, 14 and 21 days of fly's life (Kazemi-Esfarjani & Benzer, 2000).

In details, 50ml glass cylinder was divided into three parts as bottom, middle and top (5cm each part). Flies were carefully transferred in the cylinder without anaesthesia and dropped to the bottom. After period of adaptation of 30 seconds, climbing ability has been scored counting the flies that reach the top of the cylinder in 15 seconds. Flies were assessed in batches of 20, with a portion of male and female 1:1. Three trials were performed on each day of the test (7th-14th-21st day) and the average was considered as a climbing final score. A minimum of 100 flies was tested for each genotype.

3.20.2 Survival rate

Adult flies were collected during two, three days from the hatch and then were used for lifespan experiment. They were transferred to fresh tubes at a density of 20 individuals per vials with a proportion of male and female 1:1. The lifespan trials were conducted in humidity and temperature controlled condition with a light and dark cycle of 12 and 12 hours. Every second day, without anaesthetization the flies were transferred to new tubes containing fresh medium and deaths were scored (Bass et al., 2007). Approximately 200 flies were tested for each genotype.

3.20.3 Larval movement

Drosophila larvae show natural peristaltic movements, a kind of muscle contraction that create a wave which starts at the end of the larvae passing to body and ends at the mouth. This movement allows moving one step forward. In physiological condition this movement is interrupted by pausing, turning and head swinging (typically to explore a new place), (Rodriguez Moncalvo & Campos, 2009). During each wave the larval hook (mouth) makes an anchor point to advance. Evaluation of the peristaltic waves has been done testing the movements of third instar larvae. 100mm agar plates (1%) have been used for the test, larvae carefully transferred into the agar plate were allowed to adapt for 30 second and then recorded for 2 minutes. Minimum 20-30 larvae per each genotype were counted individually and average has been taken. Separate agar plate was used for each genotype.

3.20.4 Walking assay

Young flies with 3-4 days aged were used to test the walking ability. A 145mm Petri plate has been used, creating grid lines of 1x1cm squares in the bottom, to measure the distance travelled. Fly was placed individually in the centre of the petri plate and, after a period at least of 30 seconds for environment, tested for 30 seconds, counting the number of 1x1 grids crossed by walking. Minimum 50 flies were tested individually from each genotype.

3.21 Immunohistochemistry studies

3.21.1 Dissection of the larval fly brain

Larval brain dissection was performed referring to the protocol published on Nature Protocol (Wu & Luo, 2006). Larvae at the instar of interest were taken from the tube of culture and quickly washed with some water and transferred on a glass slide in a drop of PBT buffer (PB supplemented with 0.3% Triton X100). The brains were removed and placed into a 0.5 ml tube containing a solution of PBT containing 4% paraformaldehyde and kept on ice. The collected brains were placed on a nutator mixer and left to fix for 20 minutes in 4% paraformaldehyde. After fixation, the paraformaldehyde was removed and two quick washes followed by three washes of 20 minutes in PBT buffer were done. Tissue were blocked in 5% NGS blocking solution for 30 minutes and subsequently incubated with primary antibody in PBT overnight at 4°C. After primary antibody incubation larval brains were washed in PBT (3 x 20 minutes) followed by secondary antibody incubation in PBS-T for 2 h at RT. After the incubation the previously described washing cycle was repeated and Slowfade®Gold antifade was added. Brains were allowed to settle in Slowfade®Gold antifade at 4°C for one night. The day after brains were mounted on a glass slide to be afterward analysed at confocal microscope.

Reagent and Solutions

PBT buffer: PBT 1X (100mM NaHPO4/NaH2PO4, pH7.2) 0.3% Triton-100.

4% paraformaldehyde fixing solution: 16%PFA and PBT buffer in a ratio of 1:3.

Blocking solution: 5% NGS (Normal Goat Serum, Chemicon) in PBT buffer.

Alexa Fluor® Secondary antibodies, (Life Technologies).

Slowfade®Gold antifade, (Life Technologies).

3.21.2 Neuromuscular junction dissection

Neuromuscular junctions were performed during third larval stage. Selected larvae were quickly washed with some water and transferred on a Sylgard dish for dissection. Larvae were pinned at both ends with minute pins (Austerlic Insect Pins 0.1 mm diameter, Fine Science Tools, Germany).

Larval body wall muscle was carefully opened at the dorsal side using Spring scissors (Fine Science tools, Germany). The muscle walls were pinned out and the internal organs were removed and carefully washed with dissection solution. Larvae were fixed for 20 minutes using 4% paraformaldehyde in PBS followed by washes (3 x 5 minutes) in PBS-T (PBS supplemented with 0.1% (v/v) Tween) and by blocking in 5% Normal Goat serum NGS) solution. Larvae were incubated in in primary antibody diluted in PBS-T over night at 4°C. After primary antibody incubation larvae were washed in PBS-T (3 x 10 minutes) followed by secondary antibody incubation in PBS-T for 2 at RT. The excess of secondary antibody was removed by washes (3 x 15 minutes) in PBS-T. Finally the Slowfade®Gold antifade reagent was added and the samples were allowed at 4°C for one night. The day after the larvae were mounted on a glass slide. Fluorescence was detected using confocal microscope (Carl Zeiss LSM 510).

Reagent and Solutions

Dissection Solution: 128mM NaCl, 2mM KCl, 4mM MgCl2, 0.1mM CaCl2 (freshly prepared), 35.5mM Sucrose and 5mM Hepes (pH 7.2).

PBST: PBS 1X 0.1% Tween20.

4% paraformaldehyde fixing solution: 16%PFA, PBS buffer and water in a proportion of 1/4,1/4 and 1/2.

Blocking solution: 5% NGS (Normal Goat Serum, Chemicon) in PBST buffer.

Alexa Fluor® Secondary antibodies, (Life Technologies).

Slowfade®Gold antifade (Life Technologies).

A table of antibodies used in immunofluorescence was reported below:

Primary Antibodies		
Name/Supplier	Host	Dilution
Anti Flag M5/Sigma	mouse	1:200
Anti TBPH/ house	mouse	1: 200
Anti GFP/ Invitrogen	rabbit	1:200
Anti Syn 3C11c/ DSHB	mouse	1: 15
Anti Syx 8C3s/ DSHB	mouse	1: 15

Anti CSP2c/ DSHB	mouse	1: 50
Anti BRPs/ DSHB	mouse	1: 50
Anti Futsch 22C10s/DSHB	mouse	1: 50
Anti Dlg 4F3c/DSHB	mouse	1:250
Anti Elav/DSHB	rat	1:250
Anti Elav/DSHB	mouse	1:250
Anti HRP/Jackson	rabbit	1:150

Secondary Antibodies		
Name	Host	Dilution
Alexa Fluor® 555 phalloidin	-	1:25
Alexa Fluor® 488 (mouse, rabbit)	goat	1:500
Alexa Fluor® 555 (mouse, rabbit, rat)	goat	1:500
Alexa Fluor® 647 (rat)	chicken	1:500

3.21.3 Bouton shape

The boutons with a round and smooth surface, with also an equal diameter on both axes, were considered as “Regular” boutons. On the contrary deformed boutons with a fusiform appearance were considered as “Irregular” boutons. Graph has been generated reporting the percentage of regular and irregular boutons on the total number of these. Boutons were stained with anti HRP that recognize neuronal tissue in Drosophila. HRP staining has been a great tool for the analysis of NMJ morphology since it is specific for the presynaptic compartment (Jan & Jan, 1982).

3.21.4 Quantification of Futsch staining

Larvae used for these analyses were processed simultaneously for immunohistochemistry and confocal images were acquired under identical condition. Quantification were done following a previous study with some readjustment (Packard *et al*, 2002). The bounded appearance of Futsch in the proximal boutons in general occupies the whole bouton area more then 75% was considered as “Full” bouton. The boutons in which Futsch

appeared fragmented and occupied less than 75% of the area are classified as “Diffuse”. Finally boutons without Futsch staining are considered as “Empty” boutons.

3.21.5 Quantification of pre and postsynaptic markers

Larvae used for these analyses were processed simultaneously for immunohistochemistry and confocal images were acquired under identical condition. Synaptic boutons from muscle 6 and 7 (segment A2) were used for quantitative analysis. Samples were double labelled with anti-HRP and the markers chosen and the ratio of mean intensity of marker/HRP has been measured. To quantify the cluster volume of Bruchpilot and Glutamate Receptor IIA a ratio between volume occupied by the marker inside a single bouton per total volume of the analysed bouton. Adapted from (Diaper *et al*, 2013; Thomas *et al*, 1997). Images were processed with ImageJ, and then statistically analysed using Prism.

3.22 Data analysis and statistic

Confocal images were acquired at the same fluorescence intensity using Zeiss LSM510 confocal microscope. Statistics were performed using GraphPad Prism software. One way ANOVA was performed using Bonferroni’s multiple comparison test to compare three or more independent groups. T-test was performed to compare two independent samples. Log-rank test was used to analyse survival curves. The significance between variables was shown in each image following this conversion of p value: * if $p<0.05$; ** if $p<0.01$; ***if $p<0.001$.

4 Results

4.1 A fly model of ALS pathology

A fly model of ALS pathology was generated through the knock out of the TBPH gene, the *Drosophila* homolog of human TDP-43. P-element technology (EY10530) was then used to generate chromosomal deletions in the TBPH locus. Two mutants lines were isolated, $TBPH^{\Delta 23}$ and $TBPH^{\Delta 142}$, showing genomic deletions of 1.6 and 0.8 kb respectively. The $TBPH^{\Delta 23}$ deletion occurred as a a result of the complete elimination of the P-element, while the $TBPH^{\Delta 142}$ deletion retained a fragment of the original EY10530 due to the imprecise excision of the P-element (Feiguin *et al*, 2009).

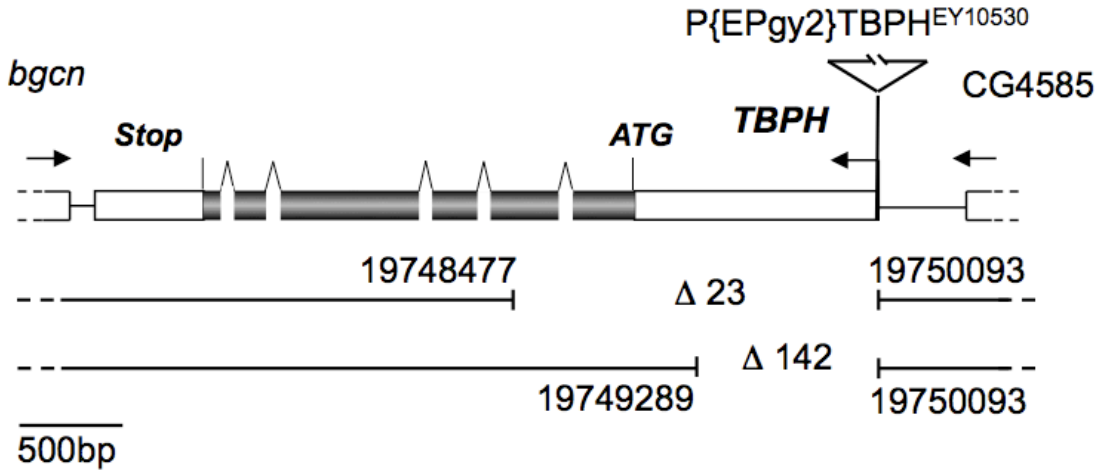

Figure 23 TBPH mutant alleles.

Schematic representation of TBPH mutant alleles. CG4585 and *bgcn* are the two adjacent genes present towards 5' and 3' strand of TBPH respectively. In the coding region (in gray) the start of translation (ATG) and the ends with stop codon (Stop) are indicated. The insertion site of the P-element $P\{EPgy2\}TBPH^{EY10530}$ used for mutants construction is indicated and the extent of the deletions of the two generated mutants, $TBPH^{\Delta 23}$ and $TBPH^{\Delta 142}$, are outlined by the broken lines.

In order to determine whether the TBPH protein was still present in these alleles after the genomic deletions, a TBPH protein fragment from amino acid 1-268 was utilized to immunize rabbits and generate specific polyclonal antibodies. With this tool in hands a western blot analysis on adult fly heads was performed that confirmed the total abolishment of TBPH protein in both

mutants, with wild type flies (W1118) having been used as a positive control (Figure 24).

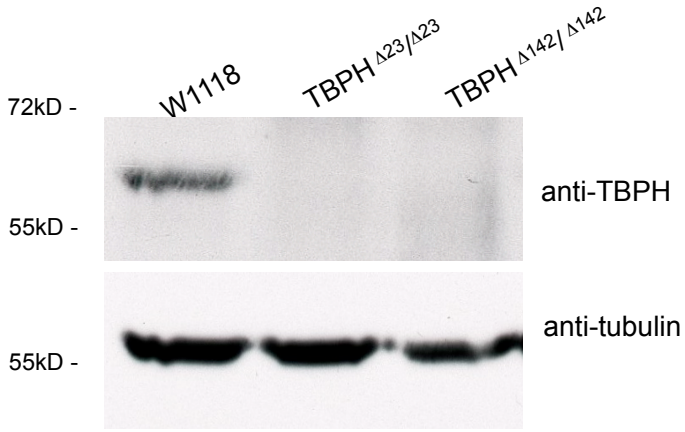

Figure 24 Western blot analysis of TBPH protein in mutants.
Western blot analysis, stained with polyclonal anti-TBPH antibody, detected no endogenous protein in mutant fly heads compared to the TBPH protein signal in wild type flies (W1118). Tubulin was used as a loading control.

4.1.1 Characterization of TBPH loss of function *in vivo*

A quantitative analysis of TBPH mutant flies from embryonic stages to adulthood was performed to characterize possible defects during development. TBPH knockout flies successfully survived during embryogenesis as indicated by the analysis of first instar larvae formation that showed a segregation of the alleles in perfect agreement with the Mendelian Inheritance Laws of Genetics (Figure 25).

Genotype	GFP +	GFP-	n
$TBPH^{\Delta 23}$/CyOGFP	1640 (67%)	811 (33%)	2451
$TBPH^{\Delta 142}$/CyOGFP	967 (67%)	483 (33%)	1450

Figure 25 Alleles segregation at L1 stage in TBPH mutants.

The analysis of first instar larvae showed the segregation of the mutant alleles to the progeny with the expected frequency (33%) and without signs of embryonic lethality. GFP+ were larvae carrying the mutation in heterozygosis and GFP- were larvae carrying both mutated alleles.

The absence of embryonic lethality in *Drosophila* TBPH mutant is in contrast with the evidence obtained in other TDP-43 animal models, such as the mouse where TDP-43 knockout did cause embryonic lethality (Kraemer *et al*, 2010; Sephton *et al*, 2010; Wu *et al*, 2010). A possible explanation for these differences could be the presence of the maternal protein in the *Drosophila* embryos coming from the oocyte. Further analysis is necessary to confirm this hypothesis.

Continuing with the analysis, it was observed that more than 60% of the first instar larvae arrived at pupal stages. A high percentage of these flies then died at pupal eclosion stages or remained trapped inside their pupal case (Figure 26).

Genotypes	1st Instar larvae (28 h) N	Pupa		Eclosed flies		Trapped flies		Motility defects (%)
$TBPH^{\Delta 23}/CyO^{GFP}$	1127	734	65%	586	52%	26	2%	0
$TBPH^{\Delta 142}/CyO^{GFP}$	1056	616	58%	446	42%	42	4%	0
$TBPH^{\Delta 23}/TBPH^{\Delta 23}$	930	591	64%	197	21%	295	32%	100
$TBPH^{\Delta 142}/TBPH^{\Delta 142}$	539	327	61%	86	16%	172	32%	100
OregonR	758	628	83%	543	72%	15	2%	0

Figure 26 Developmental viability analysis of TBPH mutant flies.

The developmental viability analysis indicates low larval and pupal lethality. On the contrary, adult flies present severe defects during eclosion and adulthood. Next to the genotype the number of 1st instar larvae analysed is reported, followed by the number of animals reaching the subsequent stage and the relevant percentage.

Eclosed mutant flies, appeared morphologically identical to wild type controls apart from the fact that they showed a dramatic reduction of life span (Figure 27) and presented severe locomotive defects both during larval stages and adulthood.

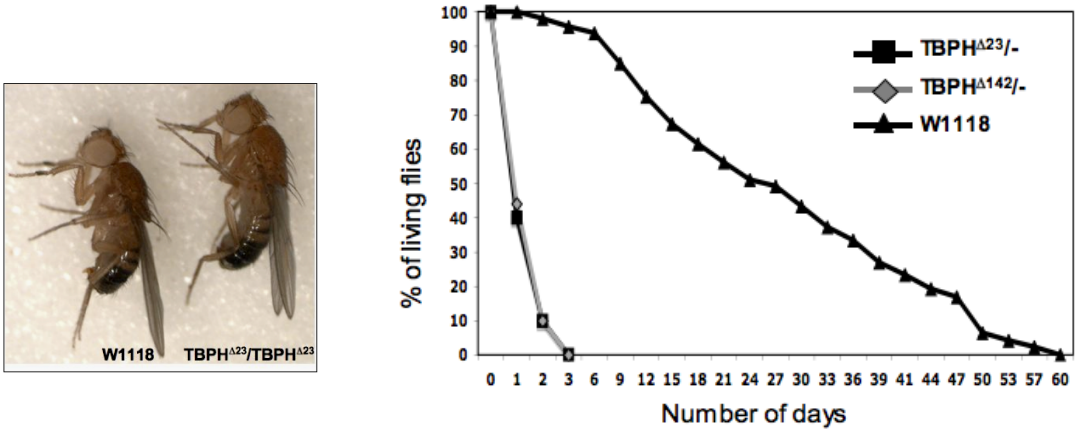

Figure 27 Appearance and life span of TBPH mutant flies.

The picture showed the identical external appearance of mutant $TBPH^{\Delta 23/-}$ (right fly) and wild type W1118 flies (left fly). The chart depicts the life span analysis of these animals. Wild type flies in standard condition survived approximately 60 days, while

the two mutants showed a much reduced life span. TBPH mutant flies survived a maximum of 3 days; a very severe phenotype.

The movements of the mutant adult flies were spastic and uncoordinated, moreover, these flies were unable to walk normally (Feiguin *et al*, 2009). In addition, TBPH had been suppressed by the expression of an RNA interference (RNAi) (Dietzl *et al*, 2007), exclusively in neural tissues (see $TBPH^{\Delta 23/+}$; elav>RNAi3v) using the pan-neuronal driver elav-GAL4. I observed that these flies also presented locomotive defects in climbing assays, indicating that the suppression of the TBPH function exclusively in neuronal tissues is sufficient to produce locomotive defects (Figure 28A and B). To determine whether these phenotypes were specifically due to the lack of the TBPH protein, TBPH minus flies were rescued by reintroducing the human protein (hTDP-43) or the endogenous protein TBPH in the CNS. The expression of the TDP-43 or the TBPH transgenes by elav-GAL4 (pan neuronal driver), (Antic & Keene, 1997) or D42-GAL4 (motoneuron specific driver), (Sanyal, 2009), was sufficient to rescue any locomotive defects and life span of TBPH null flies (Figure 28).

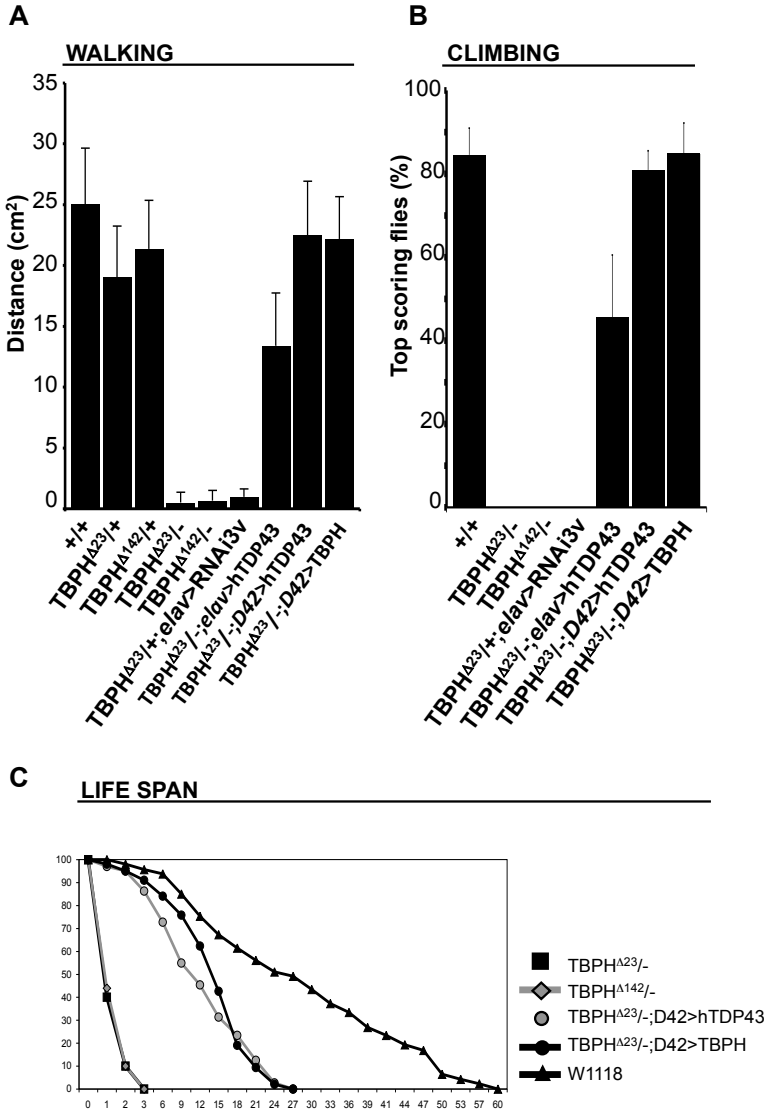

Figure 28 Presynaptic TBPH function regulates flies locomotion.

(A) Walking and (B) climbing assay on adult flies are reported in the figure. TBPH homozygous alleles ($TBPH^{\Delta 23/-}$ and $TBPH^{\Delta 142/-}$) and heterozygous alleles treated with elav>TBPH RNAi ($TBPH^{\Delta 23/+}$;elav>RNi3v) presented impaired spontaneous walking and climbing abilities compared with W1118 (+/+), $TBPH^{\Delta 23}$ heterozygote ($TBPH^{\Delta 23/+}$) and $TBPH^{\Delta 142}$ heterozygote ($TBPH^{\Delta 142/+}$). These defects became recovered by expressing hTDP-43 or TBPH with elav-GAL4 (pan neuronal) or D42-GAL4 (motorneuron) drivers. (C) Life span reduction in TBPH mutant flies can be rescued by the expression of either *Drosophila* or human TDP-43 transgene in D42-GAL4 expressing neurons. n=50 for walking assay; n=100 for climbing assay; n=250 for life span. $p<0.0001$ by ANOVA. Error bars SD.

In order to uncover the origin of the locomotive defects, I decided to investigate whether the organization of the motoneuron synaptic terminals was affected in *Drosophila* TBPH mutants. For these experiments I analysed

the neuromuscular junctions (NMJ) of third instar larvae and found that the knockout of TBPH produced deep alterations in the formation of motor neuron presynaptic terminals with a reduced number of synaptic branches and synaptic buttons as shown in (Figure 29 and Figure 30). Moreover, I found that these phenotypes were followed by defects in larval motility and were rescued by the reintroduction of either the human or the endogenous transgene (Figure 29E).

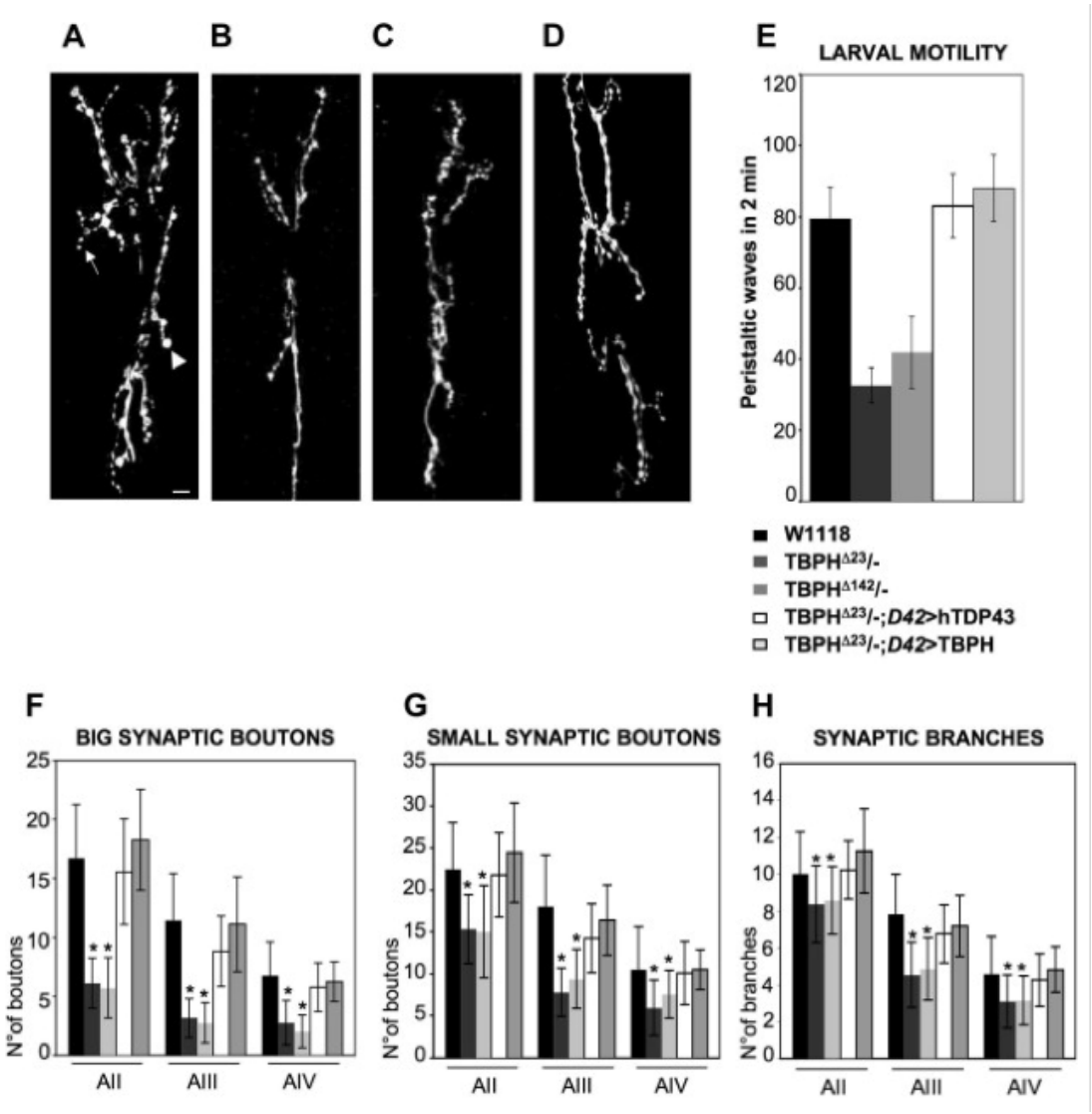

Figure 29 Morphological defects at neuromuscular synapses in TBPH mutants.

(A-D) Confocal images of NMJs on muscle 6 and 7 (abdominal segment III) at L3 larval stage, stained with anti-HRP antibody of (A) wild type, (B) TBPH$^{\Delta 23/-}$, (C) TBPH$^{\Delta 142/-}$ and (D) rescue (TBPH$^{\Delta 23/-}$;D42>hTDP43). Scale bar 10µm. (E) Larval motility analysis showed a reduction of peristaltic wave movements in the two mutants (Δ23 in dark grey and Δ142 in mild grey), compared to wild type (in black). This condition is rescued by introducing hTDP-43 (in white) and endogenous TBPH (in light grey) under D42-GAL4 driver (motor neuron specific). n=20 for each

genotype. (F) Number of 1b synaptic boutons was significantly reduced in TBPH mutant alleles compared with wild type larvae, which are further recovered by the expression of hTDP-43 in motor neurons. (G and H) Small synaptic boutons and synaptic branches were also reduced in $TBPH^{\Delta 23/-}$ and $TBPH^{\Delta 142/-}$alleles. Three abdominal segments were represented with AII, AIII, AIV. n=15 *p<0.0001. (E) Error bars SD.

The mechanisms behind the phenotypes described above, could be due to defects in synaptic growth, with defects in the formation of new synaptic buttons or alterations in the stabilization of the already formed structures. To explore these possibilities, I analysed the organization of NMJs from 38 hours after egg laying (AEL) at first instar larvae stage (L1) to 62 hours AEL second instar stage (L2), and 110 hours AEL stage (L3). The analysis of these NMJ terminals showed no significant incremental differences during first instar larval stages (L1) between the control and the TBPH mutants. On the contrary, growing differences started to be evident during the second instar larvae stage (L2) and became even more pronounced at third instar larval stage (L3) (Figure 30A-D). The presynaptic ramification in TBPH mutants appeared to be affected as reflected by the strong reduction in the complexity of presynaptic terminals. In TBPH mutant larvae, the number of axonal branches and synaptic boutons appeared smaller and very few additions of synaptic buttons were detected in TBPH mutant flies compared with wild type controls. (Figure 29G,H). This data indicates that TBPH is required to maintain and sustain synaptic growth during larval development. All these pathological traits could be rescued by the expression of TBPH or hTDP-43 under the neuronal driver (Figure 29D,E).

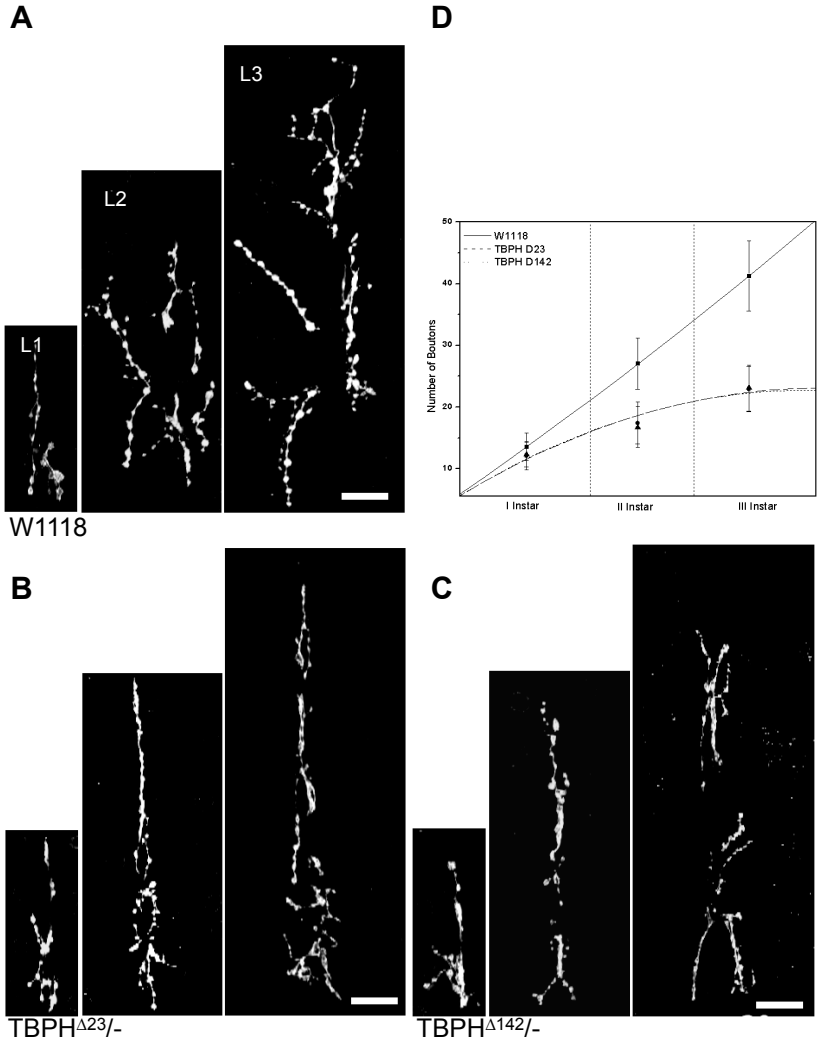

Figure 30 Loss of TBPH function affects synaptic growth.

Confocal images of (A) wild type, (B) TBPH$^{\Delta 23/-}$ and (C) TBPH$^{\Delta 142/-}$ NMJs on muscle 6 and 7 (abdominal segment II) in precise moments of larval stages: L1 (38h AEL), L2 (62h AEL) and L3 (110 AEL), using anti-HRP antibody. Scale bar 20µm. (D) Quantification of the number of the big boutons (1b) showed a linear growth in wild type during larval development, while in the two mutant lines growth defects are evident, starting from L2 stage. n=15.

4.1.2 Bouton shape in TBPH mutant NMJs

The defects described in TBPH mutants were frequently associated with alterations in synaptic bouton shape; therefore the analysis of bouton morphology was investigated. The characterization of the axon terminals in these flies confirmed the presence of defects in the shape of the synaptic terminal buttons. Normally, wild type synaptic boutons are well-rounded and show a well-defined smooth external surface, with a rather uniform and regular distribution along the presynaptic terminals that resemble the beads

on a string (Johansen *et al*, 1989). Mutant synaptic boutons instead appeared very deformed and irregularly distributed, with several fusiform-shaped structures with a clear loss of their round and smooth surface (Figure 31).

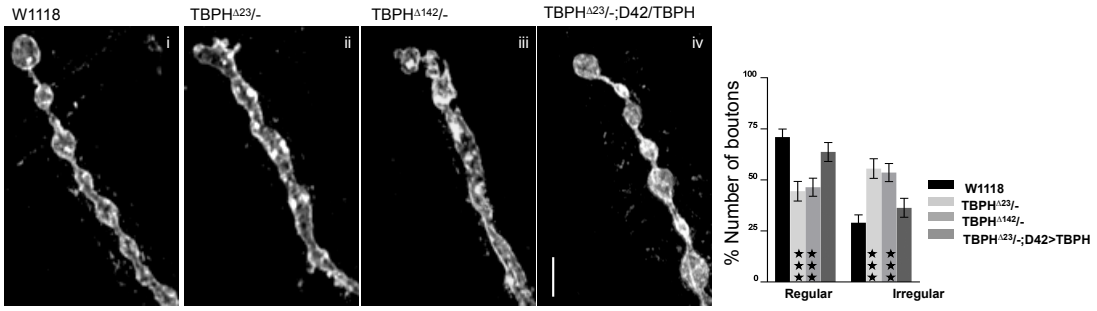

Figure 31 Boutons shape in TBPH mutants.

Confocal image of synaptic terminal boutons in third instar NMJs, muscle 6/7 on II abdominal segment. The pictures depict: regular round boutons of wild type (i), fused irregular boutons of the two mutants (Δ23, ii; Δ142, iii) and the rescue of the phenotype with expression of TBPH transgenic protein exclusively in motoneurons ($TBPH^{\Delta 23/-}$;D42>TBPH, iv). The graph depicts the quantification of round and regular boutons compared to irregular boutons. n=200 boutons ***p<0.0001 ANOVA. Scale bar 5μm. Error bars SEM.

4.1.3 TBPH mutants do not affect motoneuron formation and survival

In order to know whether the TBPH loss of function defects were restricted to synaptic terminals or whether they also affect the formation and differentiation of motoneurons in the *Drosophila* brain, the transmembrane GFP protein (UAS-mCD8-GFP) was expressed using D42-GAL4, to label motoneurons (Lee & Luo, 1999). In wild type and in TBPH mutant L3 larvae the number of GFP positive motoneurons was analysed in a targeted area of the brain, specifically in the dorsal plan of the ventral nerve cord (Figure 32). The count of GFP positive cells showed that the number of motoneurons was not altered, proving that defects in TBPH did not affect motoneuron survival.

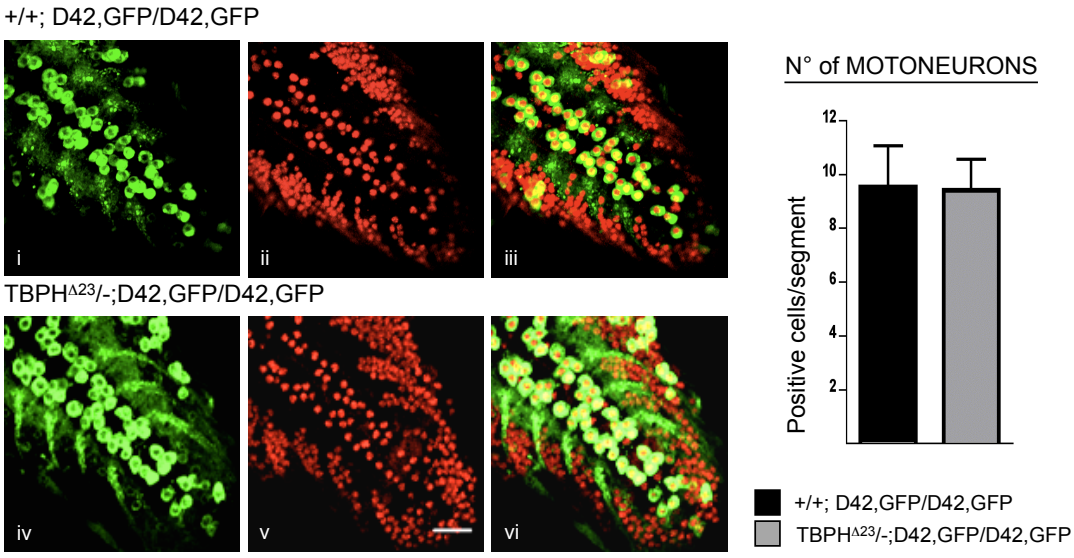

Figure 32 GFP expression in motoneurons.

Confocal images of third instar larval brain (ventral ganglia). D42-GAL4 drove expression of mCD8-GFP protein in dorsal medial clusters of motoneurons in wild type (i-iii) and in TBPH$^{\Delta 23/-}$ background (iv-vi). The green area shows GFP transgenic protein, the red, Elav (neuronal specific endogenous nuclear protein). Quantification has been done by counting the number of GFP positive motor neurons in terminal abdominal segments (a4, a5, a6 and a7) of dorsal clusters of the ventral nerve cord. No differences have been found. n=7 brains. Scale bar 20µm. Error bars SEM.

4.1.4 Characterization of postsynaptic membranes in TBPH mutant larvae

Despite the fact that the experiments described above indicate that the synaptic defects observed in the NMJs of the TBPH mutant larvae were mainly generated by defects in synaptic growth, it is still possible that they may reflect problems in the stabilization of the synapses. To ascertain this, I first analysed muscle condition in TBPH minus larvae. No obvious defects were found in muscle size, indicating that TBPH minus phenotype in synaptogenesis was not due to developmental problems in muscle growth or differentiation (Figure 33).

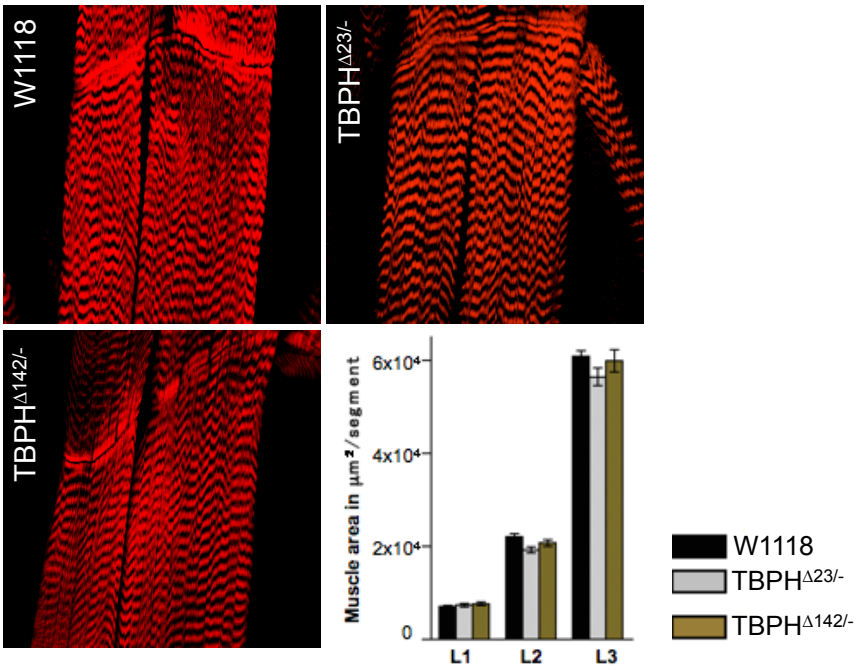

Figure 33 Analysis of muscles in TBPH mutants.

Confocal Image of third instar larval body wall muscles (muscle 6/7) stained with phalloidin in wild type, $TBPH^{\Delta 23/-}$ and $TBPH^{\Delta 142/-}$. Quantification of muscle area showed no significant difference between the wild type and TBPH mutants during larval development. n=15.

In order to evaluate the presence of presynaptic retraction *in vivo*, L3 NMJs were stained with Disc Large (Dlg), a muscular resident protein associated with the postsynaptic membranes. In *Drosophila* NMJs the presynaptic membrane forms synaptic boutons that become enveloped within the muscle cell (Collins & DiAntonio, 2007). The muscle membrane that surrounds individual synaptic boutons is composed of extensive muscle-membrane folds that create a postsynaptic structure termed the sub-synaptic reticulum (SSR), (Budnik *et al*, 1996). The SSR can be labelled with antibodies directed against scaffolding proteins like Discs Large (Dlg). The formation of SSR and the clustering of postsynaptic proteins requires the innervation of the motor neuron terminal (Featherstone *et al*, 2002; Saitoe *et al*, 2001). The presence of well-organized postsynaptic Dlg as opposed to a presynaptic terminal identifies places where the presynaptic terminal resided. Synaptic footprints have been explained as being the traces of mature synaptic contacts that have been formed and then retracted (Eaton *et al*, 2002; Graf *et*

al, 2011). The count of footprints is commonly used to study retraction events, a similar assay is used routinely with the vertebrate NMJ as a measure of synapse elimination (Wernig *et al*, 1980). Thus, to quantify synaptic retraction events Dlg and anti-HRP labelled presynaptic membrane terminals have been used (Chen & Featherstone, 2005). Double-labelled NMJs of third instar larvae were analysed and no significant differences in the number of footprints were found in the TBPH mutant flies compared to wild type controls (Figure 34). These results suggested that the defects of TBPH mutant flies were due to a failure of synaptic bouton formation rather than a presynaptic retraction phenomenon.

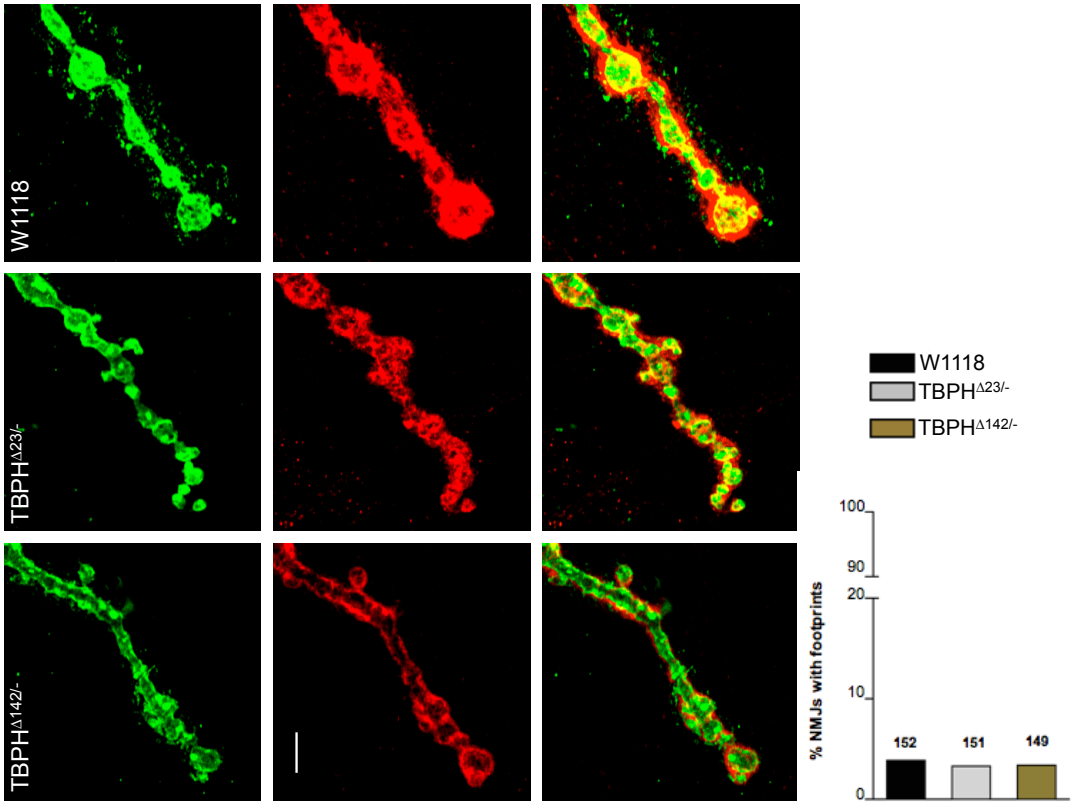

Figure 34 Analysis of footprints in TBPH mutants.

Confocal image of third instar larval pre and postsynaptic terminals (muscle 6/7) stained with HRP (in green) and Dlg (in red) in wild type, TBPH$^{\Delta 23/-}$ and TBPH$^{\Delta 142/-}$. Quantification of footprints showed no differences between wild type and the two mutants. n=150 boutons. Scale bar 5µm.

4.2 TBPH is required for microtubule organization at synaptic terminals

This initial characterization of TBPH mutant flies showed that TDP-43 plays a role in the formation and maintenance of the synaptic terminal morphology with growth defects and failings in the addition of new synaptic boutons. In relation to that, the alterations observed in the shape of the synaptic boutons, are often linked to defects in the cytoskeletal apparatus. Formation of new boutons at the synaptic terminals is mainly achieved in two ways. One is the addition of new synaptic boutons to the existing ones by *de novo* pathway (Casadio *et al*, 1999) while the second mechanism is based on the division of pre-existing boutons to generate two (Zito *et al*, 1999). In both cases, a regulated microtubule organization is essential for controlling the process (Roos *et al*, 2000). Cytoskeletal elements are an essential prerequisite for axonal outgrowth and synapse formation. Once synapses have been formed, the neuronal cytoskeleton supports their maintenance and further maturation (Goellner & Aberle, 2012). The microtubule-associated protein Futsch is necessary for the organization of synaptic microtubules in *Drosophila* and is the homolog of the human microtubule-associated protein MAP1B. The central domain of this protein is full of repetitive sequences similar to neurofilament proteins (Hummel *et al*, 2000). Functional analysis confirmed the central role played by Futsch in dendritic and axonal growth. Mutant flies for Futsch showed a reduced number of synaptic boutons with increased bouton size and altered microtubule organization that could be rescued by the expression of the MAP1B homology domain (Roos *et al*, 2000). I, therefore, hypothesized that in TBPH mutant flies, an altered microtubule (MT) organization could be the molecular mechanism behind the defects observed in NMJs growth. To test this hypothesis, I analysed the distribution of Futsch and the MT organization in the TBPH minus L3 flies (Miech *et al*, 2008). The staining of Futsch was performed using the anti-22C10 specific monoclonal antibody (Hybridoma Bank) and I found that in wild type NMJs the Futsch labelling occupied the main part of the synaptic boutons filling the most proximal part of these structures almost completely. In the newly formed or distally located synaptic boutons, Futsch staining instead became

fainter, fragmented and more diffuse (Packard *et al*, 2002). Based on this, to quantify the presynaptic organization and protein levels of Futsch, the staining pattern of this antigen at each synaptic bouton was scored as a percentage of the number of boutons in which Futsch immunostaining appeared full, diffuse or absent (Godena *et al*, 2011).

For these experiments, third instar larvae were dissected and analysed. I observed that in TBPH mutant terminals the staining pattern of Futsch was dramatically modified, with an increased number of synaptic boutons presenting strongly reduced, diffuse or empty Futsch staining patterns compared to control NMJs. These phenotypes could be rescued by expressing back the TBPH transgene in the motoneurons, demonstrating that these alterations were specific of the TBPH function (Figure 35A and B). In agreement with these results, Western blot studies indicated that the protein levels of Futsch were reduced in $TBPH^{\Delta 23/-}$ and $TBPH^{\Delta 142/-}$ heads compared with wild type flies (Figure 35C).

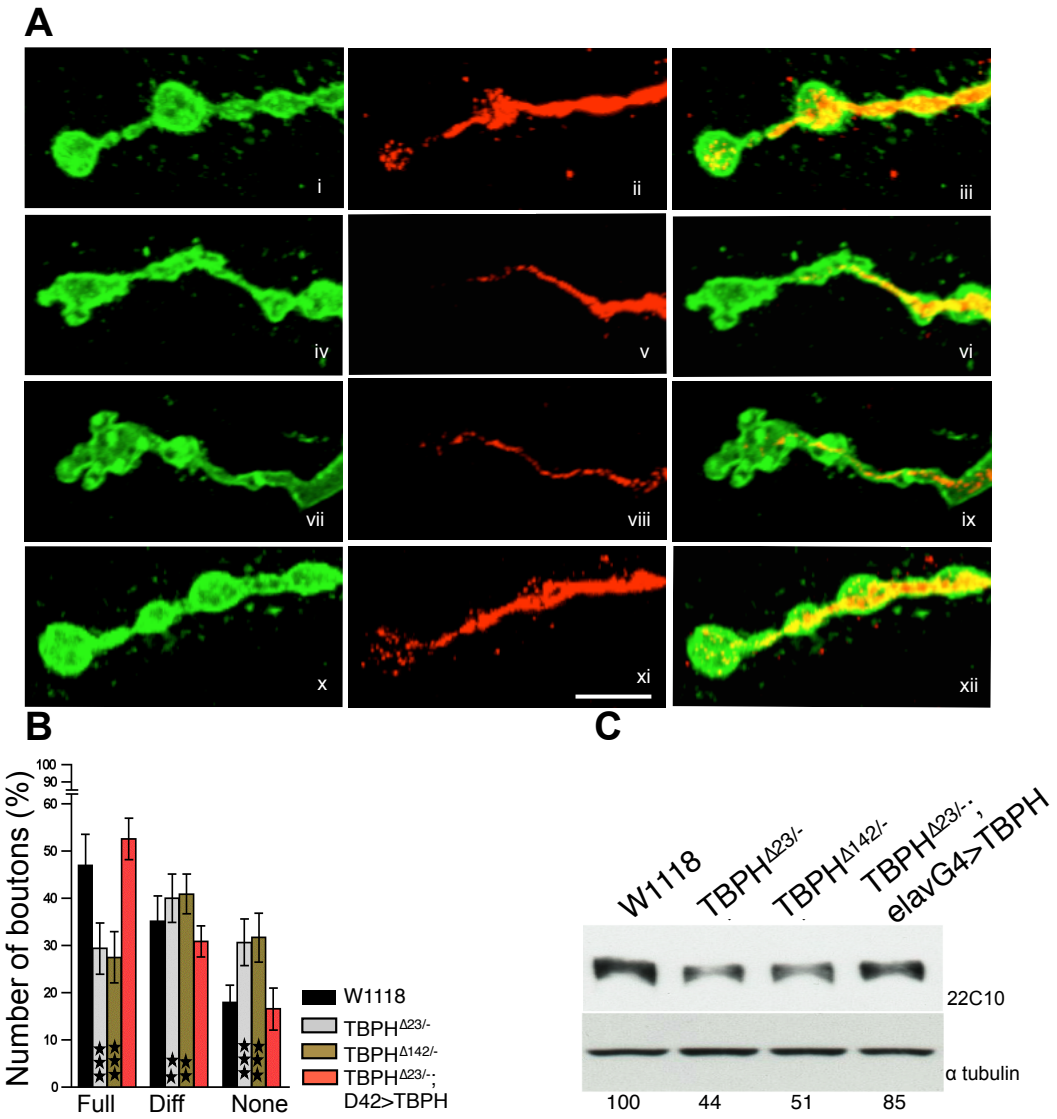

Figure 35 MT organization in TBPH mutants.

(A) Confocal images showed Futsch staining in wild type (i-iii), TBPH$^{\Delta 23/-}$ (iv-vi), TBPH$^{\Delta 142/-}$ (vii-ix) and in TBPH$^{\Delta 23/-}$;elav-GAL4/TBPH (x-xii), the green area shows HRP and the red area depicts the Futsch protein. Complete absence of Futsch staining (red) is observed in the terminal boutons of the two mutants. Futsch staining is restored by elav-GAL4 driven expression of TBPH transgene in mutant background. (B) Quantification of Futsch staining for each genotype. **p<0.001, ***p<0.0001, ANOVA analysis; n=16 larvae. Error bars SEM. (C) Western blot analysis on adult heads showed a reduce expression level of Futsch in TBPH minus alleles when compared to wild type and rescue. Quantification of normalized protein amount was reported below each lane (mean ± SEM: 100 ± 1; 44 ± 2; 51 ± 1.9; 85 ± 1.2). n=4.

4.3 TBPH RNA-binding capacity is essential for its function *in vivo*

I found that the neuronal expression of the TBPH transgene by either elav-GAL4 or D42-GAL4 was able to rescue the synaptic morphology, MTs distribution, locomotive impairments and life span of TBPH$^{\Delta 23}$ homozygous flies, indicating that the TBPH controls all these aspects through its function. Next, I decided to test whether the functional activity of the protein depended on its ability to bind RNA. To address this question, I generated a mutant isoform of TBPH unable to bind to RNA due to the exchange of the two conserved phenylalanines located in the RNA recognition motif 1 (RRM1), amino acids 150 and 152, into leucines (Figure 36) (Ayala *et al*, 2005; Buratti & Baralle, 2001).

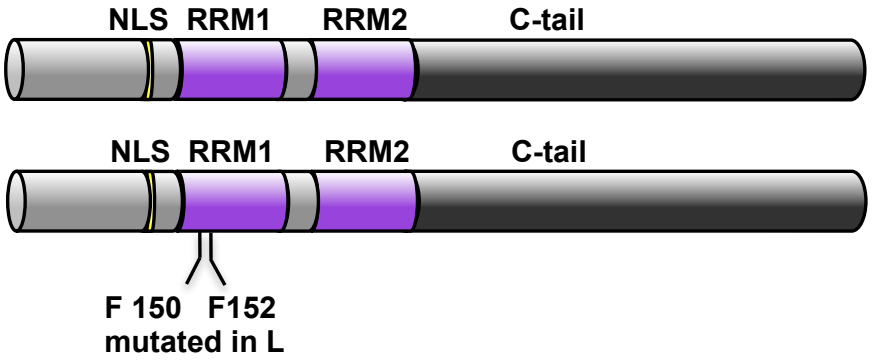

Figure 36 Schematic representation of TBPH wild type and TBPH$^{F/L}$ mutant constructs.

Schematic representation of two TBPH forms. On the top there is the wild type full-length form of TBPH, on the bottom there is the TBPH $^{F/L150-152}$ mutant version. The two constructs are totally identical, except for two amino acidic mutations: two phenylalanine residues in leucine at the position 150 and 152, which are located in the RRM 1 motif.

Similar amino acids are conserved in the human protein at the position 147 and 149, respectively.

The TBPH $^{F/L150-152}$ transgene was then inserted in the *Drosophila* genome, using the site-specific recombination integrase of phage PhiC31 (Groth *et al*, 2004) and the expression levels of the TBPH $^{F/L150-152}$ transgene was compared with the wild type protein via Western blot (Figure 37A). Subsequently, L3 larval brains were stained with anti-TBPH specific

antibodies to compare the intracellular localization of the transgenic proteins in neuronal cells. The result showed that both proteins similarly localize in the nucleus of the motoneurons present in the dorsal area of the ventral ganglia in *Drosophila* brains (Figure 37B).

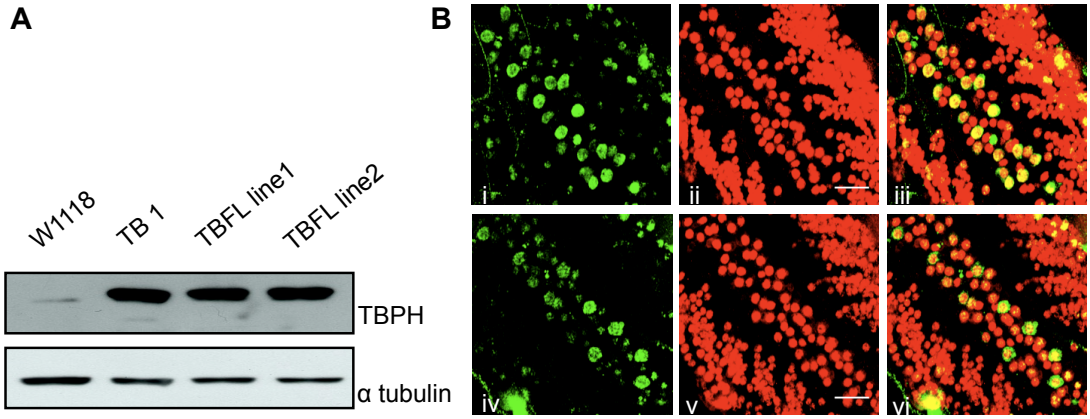

Figure 37 Comparison analysis of expression level and localization of TBPH and TBPH$^{F/L150-152}$ transgenes.

(A) Western blot analysis on adult heads of transgenic flies. The expression under GMR-GAL4 (glass multiple reporter) of the different TBPH transgenes (TBPH wild type=TB1; and two insertions of TBPH $^{F/L150-152}$ mutants=TBFL line1 and line2) showed a comparable protein level among different transgenic flies. In the lower panel tubulin has been used as loading control. Quantification of the normalized protein amounts was reported below each lane. n=3. (B) Confocal images of the dorsal section of larval brain of TBPH (i-iii) and of TBPH $^{F/L150-152}$ (iv-vi) transgenes expressed under elav-GAL4 driver. The green area depicts anti-Flag and red is anti-Elav staining (endogenous nuclear protein specific for neurons). n=10. Scale bar 10μm.

Subsequently, the two transgenes were separately expressed in the CNS of the TBPH mutant flies, and the capacity of these constructs to rescue the phenotypes observed in TBPH minus insects was evaluated. I observed that the TBPH$^{F/L150-152}$ variant was not able to recover the locomotive effects observed in TBPH mutant larvae or adult flies compared to insects expressing the wild type form of TBPH (Figure 38), indicating that the RNA-binding activity of the TBPH RRM1 domain is essential for its function *in vivo*. However, the TBPH mutant flies expressing TBPH $^{F/L150-152}$ showed some degree of activity compared to TBPH mutant flies rescued with GFP (negative control), suggesting that a residual protein activity may reside in the second RNA-binding domain (RRM2) although this function is not sufficient to supply the lack of the RRM1 activity.

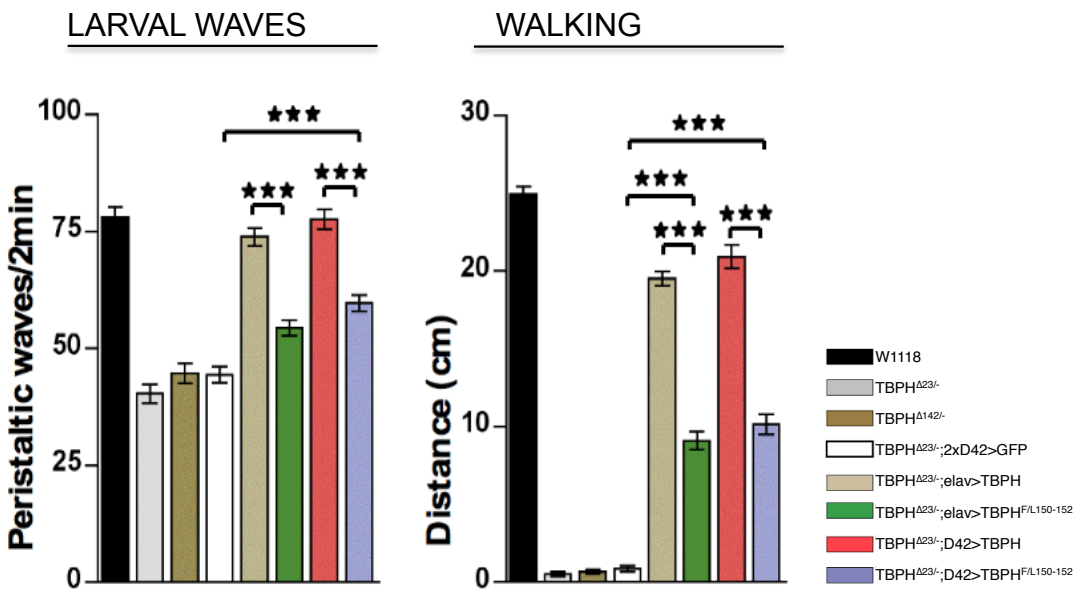

Figure 38 Rescue of motility using TBPH wild type versus TBPH$^{F/L150-152}$.

Larval movement (left panel) and walking assay (right panel) on adult flies showed that TBPH$^{F/L150-152}$ variant was not able to recover mutant phenotype (TBPH$^{\Delta 23/-}$). Only in the adult flies there was an improved effect compared to mutants or to GFP rescue (TBPH$^{\Delta 23/-}$; D42>GFP), but still not sufficient to reach the rescue obtained with the TBPH transgene. The analysis has been performed under the control of two different drivers (elav-GAL4 which is pan neuronal and D42-GAL4 which is motoneuron specific). n=40 larvae, n=50 flies, ***p<0.001 ANOVA. Error bars SEM.

In addition to the functional analysis, I observed that the expression of the TBPH$^{F/L150-152}$ transgene in motoneurons (D42-GAL4) of TBPH$^{\Delta 23/-}$ homozygous flies failed to recover the anatomical defects observed in mutant animals regarding to the number of synaptic boutons, synaptic branches and MTs organization compared to wild type rescue controls (Figure 39A,B-E). Moreover, I found that the biochemical levels of Futsch protein in TBPH$^{F/L150-152}$ rescue fly heads were not recovered (Figure 39F), although the transgenic expression levels were even higher than the endogenous TBPH protein (Figure 37A). Nonetheless, based on these results I can conclude that the RNA-binding activity of TBPH, through the RRM-1 domain is definitively essential for the molecular regulatory functions of TBPH *in vivo*.

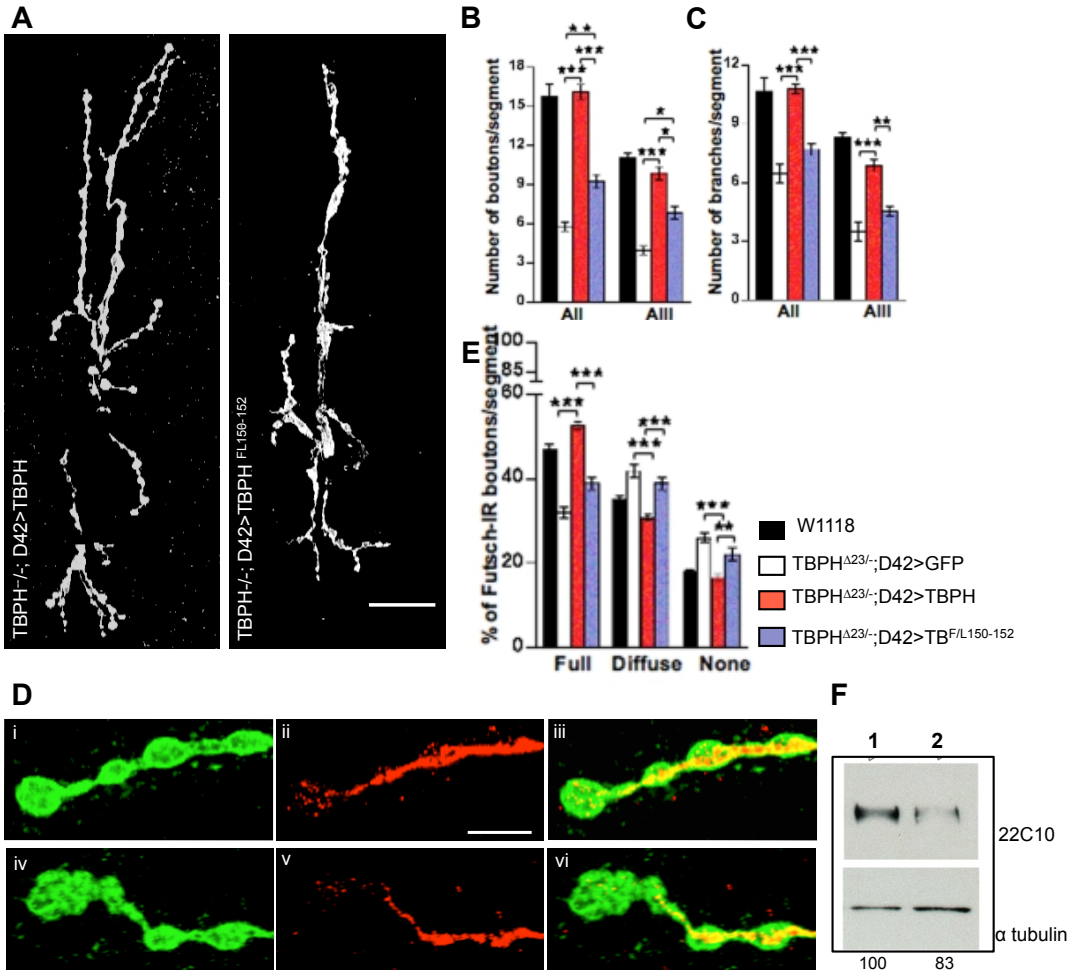

Figure 39 NMJ phenotype in TBPH$^{F/L150-152}$ rescue.

(A) Confocal images showed presynaptic terminals in muscle 6/7 (abdominal segment II). TBPH rescue (TBPH$^{\Delta 23/-}$;D42>TBPH) and TBPH$^{F/L150-152}$ rescue (TBPH$^{\Delta 23/-}$;D42>TBPH$^{F/L150-152}$) showed the different degree of recovery between the two transgenes. It was evident that the TBPH$^{F/L150-152}$ fly was not able to rescue, the complexity of the terminal as well as TBPH wild type. The quantifications of the phenomena are reported in (B), number of boutons per segment and in (C), number of branches per segment. n=12 larvae. Scale bar 20µm. (D) Confocal images showed Futsch (in red) and HRP staining (in green) in the terminal boutons of L3 TBPH (i-iii) and TBPH$^{F/L150-152}$ (iv-vi) rescue. n=12 larvae. Scale bar 5µm. (E) Futsch staining quantification *p<0.01, p<0.001, p<0.0001, one-way ANOVA. (F) Western blot analysis showed a reduction of Futsch protein levels in TBPH$^{F/L150-152}$ rescue (line 2, TBPH$^{\Delta 23/-}$;elav>TBPH$^{F/L150-152}$) compared with TBPH wild type rescue (line 1, TBPH$^{\Delta 23/-}$;elav>TBPH), (upper panel). Tubulin was used as a loading control (bottom panel). Quantification of normalized protein amount was reported below each lane (mean ± SEM: 100 ± 1; 83 ± 5.4). n=3. Error bars SEM.

4.4 Constitutive TBPH transgenic expression in mutant CNS at physiological level

The results described above showed that *Drosophila* TBPH minus presented uncoordinated movements and progressive paralysis that lead to a premature death. These functional alterations were accompanied by molecular modifications in the organization of the microtubules in the synaptic terminals. Alongside these phenotypes, a fundamental question must be asked, namely when these alterations originate or, in other words, what the temporal requirements of the TBPH function in motoneurons are.

In order to address this question, the Gene-Switch (GS) RU486-inducible GAL4 system was used. This system is the most widely used for generating spatially restricted transgene expression and is based on the GAL4-UAS principle. Thus, to promote the temporal and spatial control of the TBPH expression, the neuronal specific elav-GS GAL4 fused with the progesterone receptor was utilized, following that, the transcriptional activation was induced through the addition of the specific ligand RU486 (mifepristone) (Roman *et al*, 2001). The TBPH protein expression *in vivo* could be detected 5 hours after the systemic application of RU486 in either the fly food or in solution like “larval bathing”. Furthermore, this system allowed a very fine modulation of the protein expression levels by changing the concentration of RU486 in the fly food.

For these experiments I generated flies carrying elav-GS GAL-4 (neuronal specific driver) in the TBPH minus background (GS-TB: TBPHΔ23/-;elav-GS GAL4/UAS-TBPH). Wild type flies and GS-TB were treated with different concentration of RU486 (0.05 to 0.25μM) dissolved in fly food immediately after embryogenesis throughout the different larval stages. Brains of third instar larvae were dissected and analysed via Western blot (Figure 40A). I found that a 0.1μM dose of RU486 induced transgenic expression of the TBPH at a level comparable to the endogenous level. In the second line of Western blot flies not fed with the drug food were loaded and no signal was detected, proving the proper efficiency of the GS system. A lower concentration of RU486 (0.05μM) was not able to produce a protein level

similar to the wild type TBPH endogenous levels as showed in the quantification in (Figure 40B).

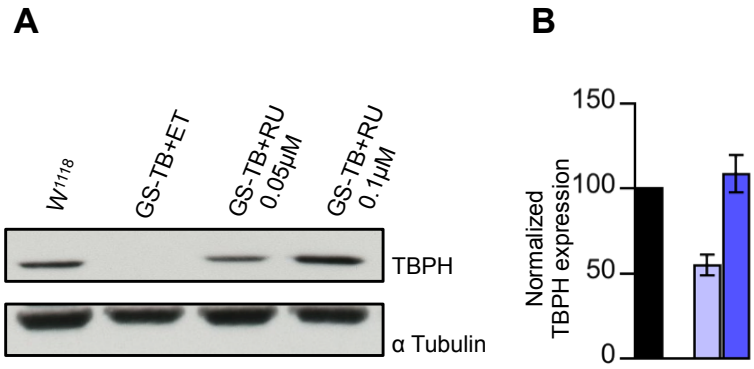

Figure 40 Constitutive TBPH expression at physiological level through Gene Switch system.

(A) Western blot analysis on L3 larval brains probed for TBPH and alpha-tubulin showed that 0.1µM of RU486 (blue column) was able to induce a transgenic TBPH expression similar to endogenous level in wild type W1118 L3 brains (black column). The light blue and white columns refer to 0.05µM dose and ethanol only treatments respectively. Genotypes: $TBPH^{\Delta 23/-}$;elav-GS GAL4/UAS-TBPH (GS-TB); ET=ethanol treated; RU=RU486 treated. n=3. Error bars SEM.

The 0.1µM dose of RU486 was sufficient to rescue larval motility (Figure 41), compared with flies treated with different doses (0.05 and 0.25µM), ethanol (no TBPH transgenic induction: GS-TB+ET) or flies expressing $TBPH^{F/L150-152}$ ($TB^{F/L}$), the RNA-binding defective version of TBPH (Figure 41).

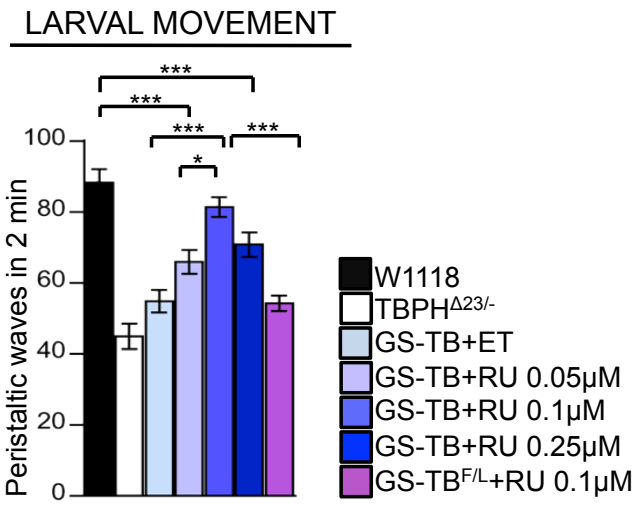

Figure 41 Constitutive TBPH expression at physiological level recovers wild type motility.

Analysis of peristaltic waves in third instar larvae showed a complete larval movement recovery using 0.1µM dose administration; on the other hand a lower dose (0.05µM) was not sufficient for the recovery. A higher dose (0.25µM) showed a toxic effect. Equivalent expression of the RNA binding defective isoform of TBPH (GS-TB$^{F/L}$) was unable to rescue the phenotypes. n=30 larvae *p<0.05 **p<0.01 and ***p<0.001 calculated by one-way ANOVA. Error bars SEM.

The other defects previously described in TBPH mutant were analysed in these flies. The NMJs growth (Figure 42) and MAP1B-Futsch organization in synaptic terminal boutons (Figure 43) were rescued in flies treated with the 0.1µM dose (GS-TB+RU). On the contrary, GS-TB+ET and GS-TB$^{F/L}$ flies were not able to recovery neither NMJs growth, nor Futsch organization inside synaptic boutons compared to the wild type.

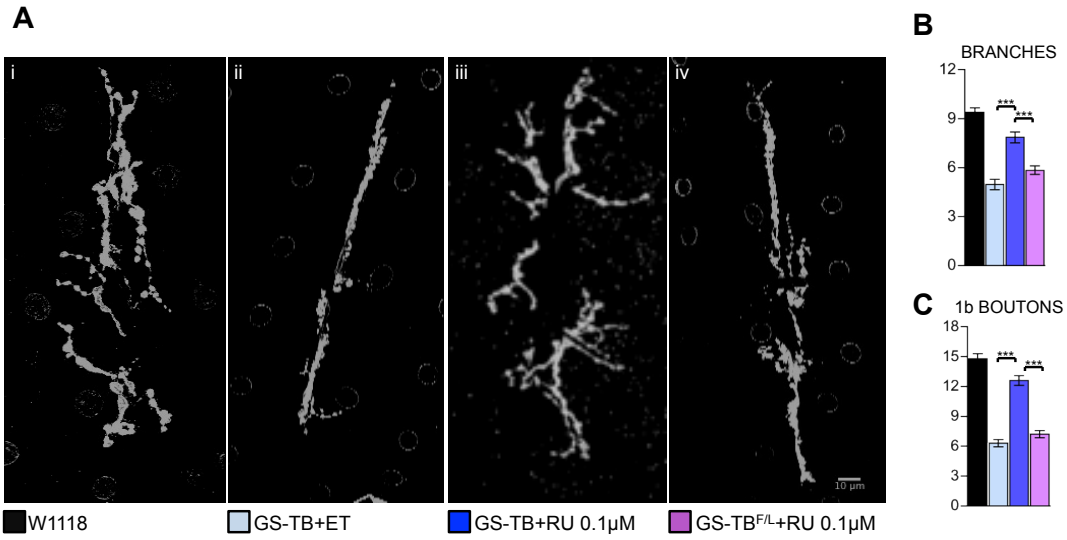

Figure 42 Constitutive TBPH expression at physiological level recovered wild type morphology at the NMJs level.

(A) Confocal images of NMJ morphology in muscle 6/7 abdominal segment II of (i) W^{1118}, (ii) GS-TB+ET, (iii) GS-TB+RU 0.1µM and (iv) GS-TB$^{F/L}$+RU 0.1µM probed with neuronal marker hrp. (B,C) were quantification of branches and 1b boutons. A significant rescue of mutant phenotype expressing transgenic TBPH under the pan neuronal driver (elav-GS GAL4) was observed. No rescue was observed in animals expressing the mutant form TBPH$^{F/L}$ or in animals treated with the vehicle media only (ethanol). *p<0.05 **p<0.01 and ***p<0.001 calculated by one-way ANOVA. Scale bar 10µm. Error bars SEM.

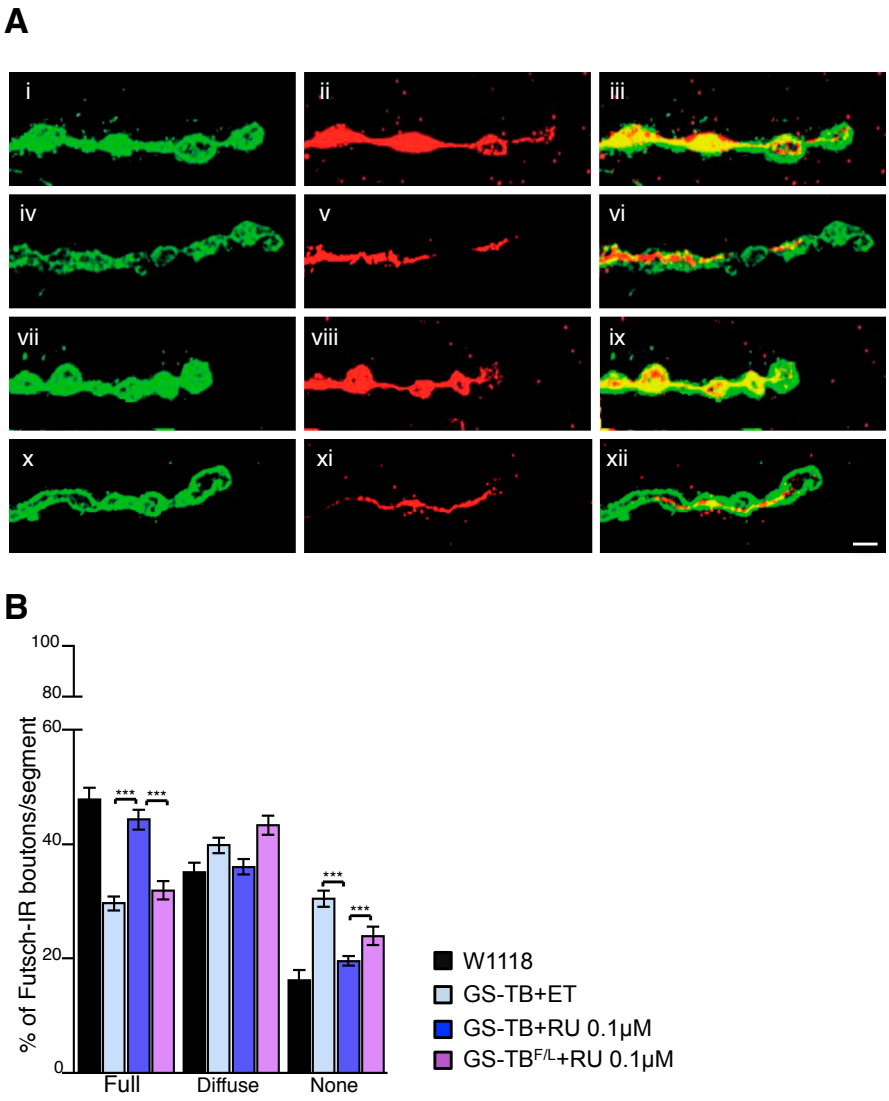

Figure 43 Constitutive TBPH expression at physiological level recovers wild type synaptic microtubules organization (Futsch).

(A) Confocal images of NMJs in third instar larvae. Muscles 6/7 of II abdominal segment were stained for Futsch (in red) and for HRP (in green). (i-iii) W^{1118}, (iv-vi) GS-TB+ET, (vii-ix) GS-TB+RU 0.1µM and (x-xii) GS-$TB^{F/L}$+RU 0.1µM. (B) Quantification of Futsch staining showed absence of Futsch protein at the most distal, newly formed, boutons in GS-TB+ET and GS-$TB^{F/L}$+RU 0.1µM. Instead expression of the TBPH protein by elav-GS GAL4 rescued Futsch staining. n=15 larvae. **p<0.01 and ***p<0.001 calculated by one-way ANOVA. Scale bar 5µm. Error bars SEM.

4.5 Temporal analysis of TBPH requirements in the *Drosophila* nervous system

After the validation of the GS system and its reliability as a system to rescue the functional and morphological defects observed in TBPH minus phenotype, I used the GS system to define the temporal requirements of TBPH for the regulation of locomotion and NMJs formation *in vivo*. The availability of proteins is a fundamental tool for an organism to regulate its growth, differentiation, development and survival. Indication about the turn over of a protein gives indirect evidence of the grade of necessity and importance of that protein. The aim of these experiments was to test whether the TBPH protein was necessary during all larval stages or if it had a limited role in a specific period of the development. For this experiment, I induced TBPH expression in CNS of TBPH mutants flies at specific periods of time during the development of larvae as schematically represented in (Figure 44).

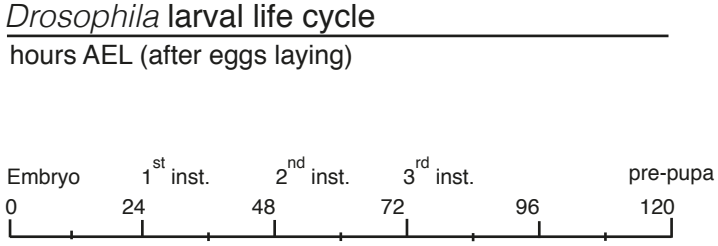

Figure 44 Scheme of *Drosophila* larval cycle.

The scheme represents the division of the larval life cycle into three different main stages. Embryogenesis lasts 22-24 hours. The first instar larvae last 24 hours as do the second instar. The third instar lasts 48 hours and following that, the pre-pupal and pupal stages start. This data refers to standard conditions at 25°C.

Several periods of transgene activation were set with a correspondent period of release, of 48 hours after egg laying (AEL) (L1 stage), 72 hours AEL (L1 and L2 stages), 80 hours AEL (L1, L2 and early L3 stages) and a constitutive activation of 96 hours AEL (L1, L2 and L3 stages) respectively, as showed in (Figure 45A).

The rescue of locomotive capacity obtained after the different TBPH induction periods was analysed at the end of stage L3 (Figure 45B). The motility analysis revealed that activations during L1 (24hours activation+48hours release, GS-TB+RU+rel48h) or L1 plus L2 (48hours activation+24hours release, GS-TB+RU+rel24h) were not sufficient to rescue larval locomotion. Only an activation of 80 hours (80hours activation+12hours release, GS-TB+RU+rel12h) showed a rescue of motility phenotype similar to the constitutive rescue (GS-TB+RU) (Figure 45B).

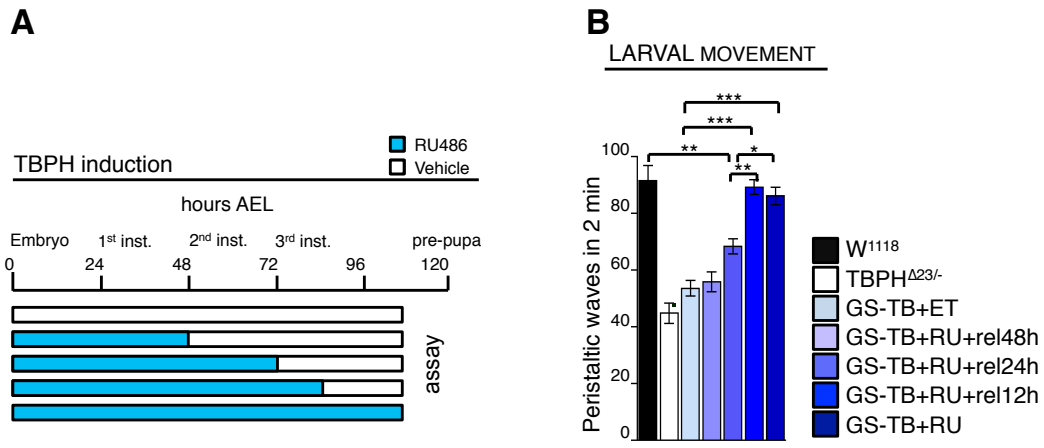

Figure 45 Schematic representation of the experimental procedure and larval motility assay.

(A) Schematic time line designed for TBPH transgenic induction in the nervous system. RU486 is required for the activation of transgene induction by gene switch (GS) GAL4. Embryos were grown in vehicle media or in RU486-containing media for different time periods. Different release times were analysed to evaluate the lasting effect of the TBPH protein. (B) Evaluation of peristaltic waves in the third instar larval stage (96-100hs AEL) in response to the temporal expression of the TBPH protein, indicates that constitutive expression of the protein or a minimum of 12 hours drug release during L3 stages guarantees a complete recovery of motility behaviour. n= 30 larvae. * $p<0.05$, ** $p<0.01$ and *** $p<0.001$ calculated by one-way ANOVA. Error bars SEM.

I also analysed the levels of TBPH protein expression at the end each drug treatment, and at the end of the larval period at L3 stage (96-100 hours AEL) (Figure 46). The results obtained showed that the TBPH protein was effectively induced immediately after RU486 treatments, but disappeared from L3 brains at the end of the third instar larval stage. The induced protein remained detectable up to a release of 12 hours, after longer release time, no protein was detectable via Western blot. Upon measuring protein levels

found 24, 12 and 6 hours of RU486 release respectively comparing these to the constitutive TBPH expressing fly, I found a gradual reduction of TBPH protein levels. The quantitative analysis of the normalized TBPH/Actin intensity values demonstrated that the half-life of the TBPH protein was of about 12 hours (Figure 46B). This data taken together with the motility results suggests that TBPH has a relatively short half-life and that the protein is permanently required in the nervous system during the development.

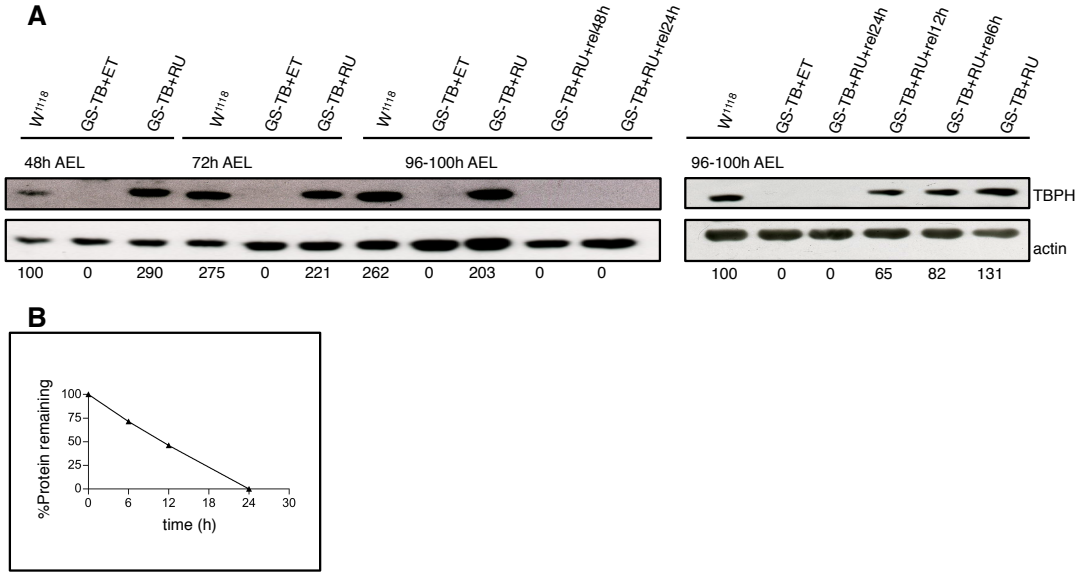

Figure 46 Western blot analysis to evaluate TBPH half-life.

(A) Western blot analysis of larval brains probed for TBPH and Actin. Brains were taken at different larval stages and the analysis showed the effective induction of transgene protein at a comparable amount of the endogenous protein. The releases point analysis showed that transgenic TBPH levels appeared progressively reduced after 6 or 12 hours post-treatment and definitely undetectable 24 hours post-treatment. (B) TBPH protein levels, normalized on tubulin, at different RU486 release time points were plotted on the graph and the half-life of the TBPH protein estimated at around 12 hours. Prism software was used for the data analysis. n=3, analysis performed with ImageJ.

The NMJs morphology of these larvae was also analysed at the end of L3 larvae stage. This analysis confirmed previous results obtained with the motility assay in L3 larvae. The TBPH protein was permanently required in CNS to regulate the functional organization of motoneuron synaptic connections (Figure 47).

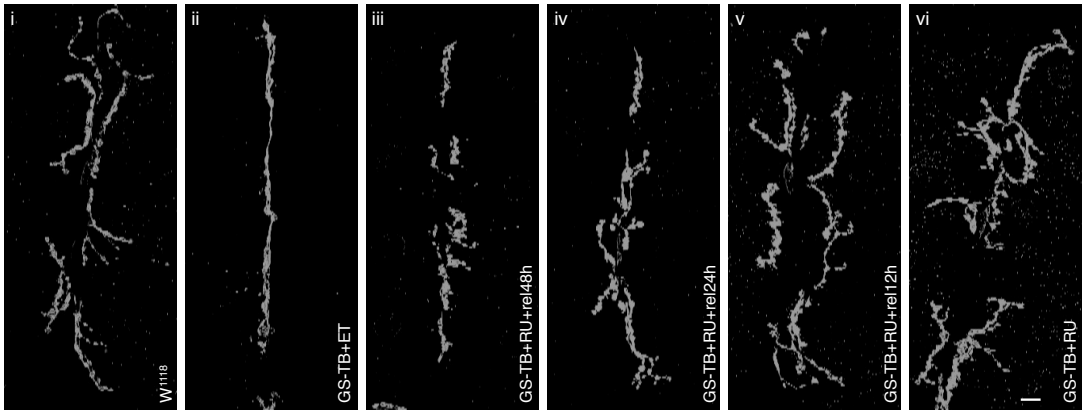

Figure 47 Functional evaluation of TBPH requirement.

Analysis of NMJs morphology in L3 larvae (96-100 hours AEL) stained with anti-HRP. Transgenic expression of TBPH during 48 or 72 hours after AEL was not able to rescue motoneuron synaptic terminals. On the contrary, flies constitutively treated with RU486 (vi, GS-TB+RU) or at 12 hours post treatment (v, GS-TB+RUrel12h) were able to completely recover their presynaptic architecture. n=10 larvae. Scale bar 10μm. Error bars SEM.

4.6 Acute suppression of TBPH induces an early neurodegeneration in adult neurons.

Neurological symptoms observed in ALS patients and in TBPH minus flies indicated that the assemble of neuronal circuits that control locomotive behaviours may be similarly affected (Feiguin et al. 2009; Godena et al. 2011). Nevertheless, it is not known whether these phenotypes originate from defects that occurred during motoneuron differentiation or later in a tissue where neurons were already fully differentiated.

The results described above suggest that temporary defects in TBPH function might be sufficient to induce neurological defects in the *Drosophila* model. This possibility is particularly relevant in the case of sporadic forms of ALS (sALS), the most frequent manifestation of the disease (90-95%). In sALS the etiopathogenesis started in already differentiated tissues during adulthood, apparently without any defects in the early stages. To test this hypothesis, I blocked TBPH expression in healthy adult flies. For these experiments I used a GS analogous system called the TARGET system (temporal and regional gene expression targeting system), (McGuire *et al*, 2003). In the TARGET technique a temperature sensitive version of the GAL80 protein ($GAL80^{ts}$) is expressed ubiquitously under the control of the tubulin 1-alpha promoter (Matsumoto *et al*, 1978). GAL80 is a yeast protein

which binds the transactivation domain of GAL4, preventing the activation of transcription in yeast (Lue *et al*, 1987; Wu *et al*, 1996). GAL80 repression of GAL4 is alleviated by a simple temperature shift. Crucially, the TARGET system is fully compatible with the vast array of GAL4 lines already established. With this system it is possible to create an excellent temporal control of the GAL4 system, antagonizing GAL4 with the GAL80 repressor.
TARGET flies containing TubulinGAL4, TubulinGAL80^{ts}, UAS-TBPH RNAi and UAS-Dicer (called TT-TBi) and control flies containing TubulinGAL4, TubulinGAL80^{ts} and UAS-Dicer (called TT-TBc) were generated. The UAS-Dicer was used to improve RNAi efficiency (Dietzl *et al*, 2007). Flies were grown at 18°C to maintain the repressive effect of GAL80 on TubulinGAL4. Immediately after the adult flies eclosion, the animals were divided into three groups: one control group was maintained at 18°C, the other two groups were transferred at 29°C and 31°C respectively, in order to abolish GAL80 repression activity and allow GAL4 to induce transcription of the TBPH RNAi (Figure 48).

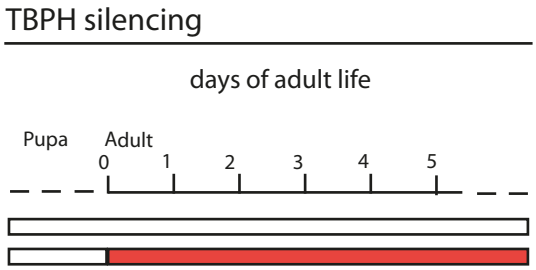

Figure 48 Schematic representation of TBPH adult silencing.

The strategy was to maintain a stable physiological condition during the embryogenesis, larval and pupal periods. From the first day of adult life, the TBPH RNAi was activated through a controlled temperature shift. A group of flies were shifted (red bar) to a temperature of 29°C and another group to a temperature of 31°C, a milder and a stronger RNAi TBPH activation respectively. A control group was maintained at 18°C (white bar).

I observed that TT-TBi flies eclosed at 18°C presented similar levels of TBPH protein in head extracts as wild type control flies (TT-TBc) indicating that the RNAi against TBPH was not activated and therefore confirming the proper functionality of the TARGET system. On the contrary, adult flies switched to 31°C immediately after adult eclosion, showed strong reductions in the TBPH protein levels, indicating that the TARGET system was able to efficiently

reduce TBPH protein expression levels in already differentiated adult tissues (Figure 49A). More interestingly, flies eclosed at 18°C and shifted to 29°C, after a few days would closely reproduce the neurological phenotypes observed in TBPH minus flies (Figure 49B, C). TT-TBi flies showed evident locomotor problems in climbing assays immediately following 7 days at 29°C. These phenotypes became more evident after 14 days of uninterrupted TBPH-RNAi expression, compared to control flies or flies maintained at restrictive temperatures (18°C). Flies shifted to 31°C showed a further worsening of the phenotype, both in climbing capacity and in life span (Figure 49B, D). The worsening of the RNAi induced phenotype was due to a temperature-mediated dose effect. At 31°C GAL80 is inactivated to a higher degree than at 29°C. This data demonstrates that the life span and locomotive behaviours appeared seriously compromised in flies expressing TBPH-RNAi (TT-TBi) compared with controls (TT-TBc). This suggests that abrupt reductions in TBPH functional levels were sufficient to provoke early neurological defects and degeneration in adult flies.

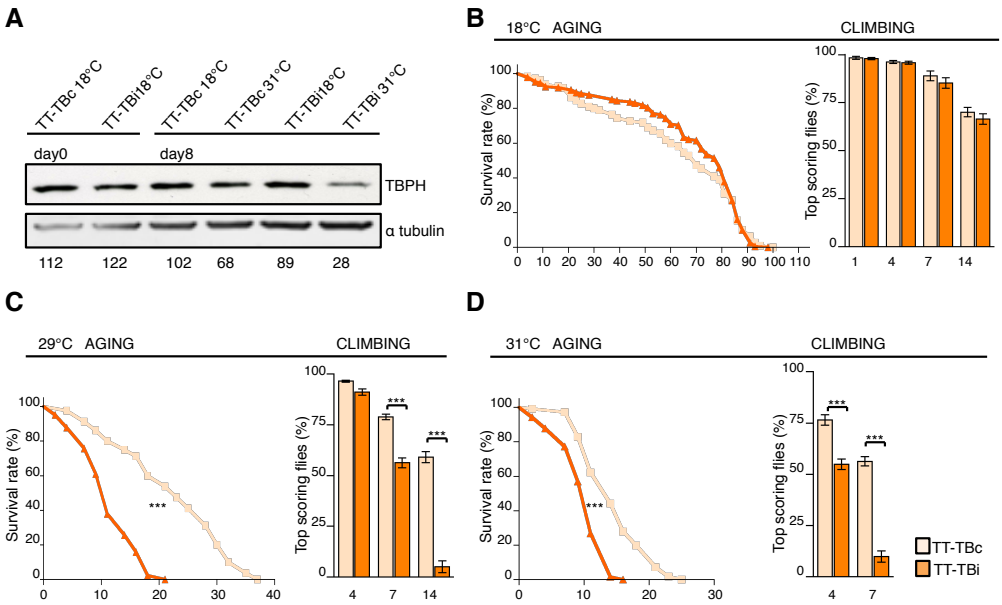

Figure 49 Acute TBPH suppression in adult flies.

(A) Western blot analysis of *Drosophila* adult heads probed for TBPH and alpha-tubulin showed a reduction of TBPH protein levels after 8 days of TARGET mediated RNAi expression in adult flies at permissive temperature of 31°C. No reduction is detectable in control flies maintained at restrictive temperature of 18°C. Genotypes: UAS-Dicer; tubulin-GAL80^{TS}/+; tubulin-GAL4/+ (TT-TBc) and UAS-Dicer; tubulin-GAL80^{TS}/+; tubulin-GAL4/TBPH RNAi (TT-TBi). n=3. (B-D) Life span analysis and climbing assay was performed on TT-TBc flies and on TT-TBi. (B) Life span and climbing assay performed in flies maintained at the restrictive temperature

(18°C) showed no differences in these traits. (C and D) Life span and climbing assays performed in flies shifted to the two different permissive temperatures (29°C and 31°C) immediately after adult eclosion showed serious neurological alterations in locomotive behaviours with an important reduction in their life span. n=200 flies each group ***p<0.001 calculated by one-way ANOVA, ***p<0.001 calculated by log-rank test. Error bars SEM.

4.7 TBPH minus phenotype can be reverted by late expression of transgenic protein in CNS tissue

The adult brain has long been viewed as a collection of neuronal networks that maintain a fixed configuration of synaptic connections. The neuroplasticity of the nervous system is to the possibility of experiencing structural and functional changes in response to physiological events, environmental stimuli or pathological events. Many recent studies have reinforced the idea of a plastic brain in old age. These studies suggest that a training after a brain injury or targeted therapy can activate the tissue and trigger a process to stimulate functional recovery (Holtmaat *et al*, 2013; Maya-Vetencourt, 2013). This suggests that the brain, has the possibility of compensating defects, even in adulthood.

A fundamental questions for patients affected by ALS is to know whether a late correction of the TDP-43 function can revert or improve the neurological symptoms of the disease. Having already described the temporal role of TDP-43 in the regulation of larval locomotive behaviours and synaptic architecture, I have subsequently analysed whether the reintroduction of TDP-43 in mature animals could rescue neurological defects caused by the absence of TBPH. To perform these experiments, I utilized the Gene-Switch system, previously described, to induce late expression of transgenic TBPH protein in TBPH minus neurons *in vivo*. GS-TB flies ($TBPH^{\Delta 23/-}$; *elav*-GS GAL4/UAS-TBPH) were treated with either RU486 or ethanol during 12 or 24 hours at mature third instar (L3) larval stage until the end of the larval period (96-102 hours AEL), as reported in (Figure 50).

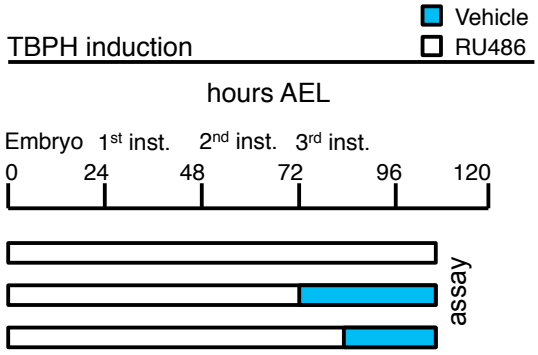

Figure 50 Schematic representation of the experimental procedure to induce late transgenic TBPH expression in L3.

Schematic time line of TBPH induction. Synchronised larvae were grown in vehicle media and transferred during L3 stage in RU486 media for 24 and 12 hours to promote TBPH expression. The control group was maintained in vehicle media. After the period of transgene activation the larvae were assessed.

A Western blot analysis was performed to verify the efficiency of transgene activation after the drug treatment and confirmed the efficiency and functionality of the system (Figure 51A). If transgenic TBPH expression was not induced, no differences were observed in larval motility compared with mutants alone. Similar results were obtained when transgenic rescue was performed expressing the TBPH isoform unable to bind RNA (GS-TB$^{F/L}$), (Figure 51B). When TBPH expression was induced during 24 hours after L3 larval formation (72hs AEL) or exclusively for 12 hours in older (86 hours AEL) third instar flies, a motility recovery was observed. In these animals, most of the pathological defects, such as larval locomotion, structural re-elaboration of motor neurons presynaptic terminals, formation of new synaptic branches, addition of new synaptic boutons and recovery of Futsch-positive cytoskeletal loops were consistently recovered to levels indistinguishable from controls (Figure 51C-F).

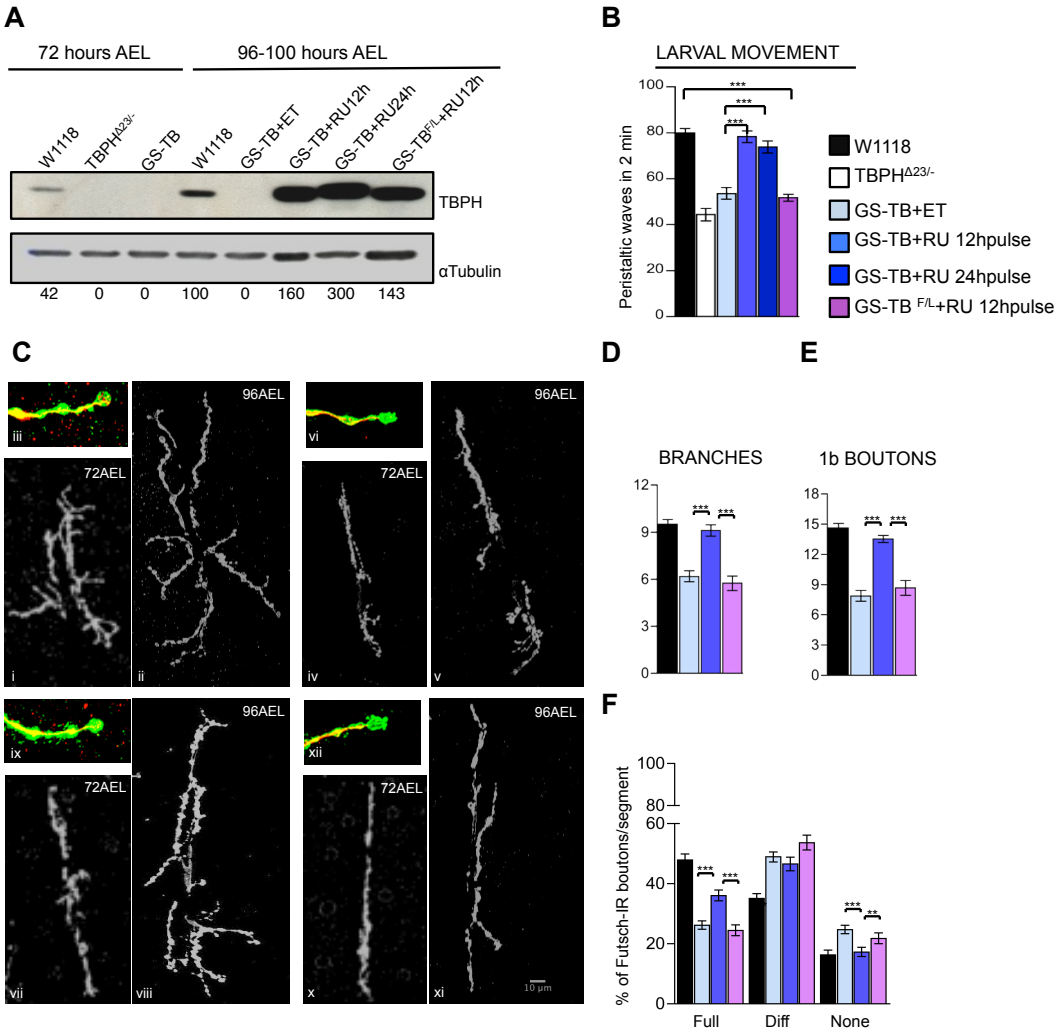

Figure 51 TBPH minus phenotype could be reverted by late expression of transgenic protein in larval CNS.

(A) Western blot of L3 brains before RU486 induction (72h AEL) and after the drug addition (96-100h AEL). Before drug administration no transgenic protein was detectable, after 12 or 24 hours of drug addition, induction of the transgenic protein was clearly observed. Quantification amounts of normalized protein were reported below each lane. n=3. (B) Evaluation of peristaltic waves in L3 larvae after 24 and 12 hours of TBPH induction showed a significant increase in larval motility compared to similar treatment using $TB^{F/L}$ isoform. n=30 ***p<0.001 calculated by one-way ANOVA. (C) Confocal images of NMJ terminals in muscles 6/7, abdominal segments II probed for HRP and Futsch (square green and red) showed a robust presynaptic growth in W1118 L3 larvae from 72 to 96 hours AEL through the addition of newly formed, round shaped and Futsch positive (red in detail) synaptic boutons (i-iii). GS-TB+ET larvae presented reduced synaptic bouton formation and Futsch levels (iv-vi). After 24 hours of TBPH induction, in GS-TB+RU flies, a vigorous regrowth of the synaptic structures was observed (vii-ix), compared to GS-$TB^{F/L}$+RU treated flies (x-xii). Scale bar 10µm. (D) Quantification of NMJs terminal branches, (E) 1b boutons and (F) Futsch intracellular distribution (cytoskeleton). n=15 larvae **p<0.01 and ***p<0.001 calculated by one-way ANOVA. Error bars SEM.

Even if the nervous system of L3 larvae is composed of mature and differentiated neurons, I still decided to determine whether the recovery observed in late larvae was also possible in adult flies. For these experiments, I treated immediately eclosed GS-TB adult flies with RU486, as schematised in (Figure 52).

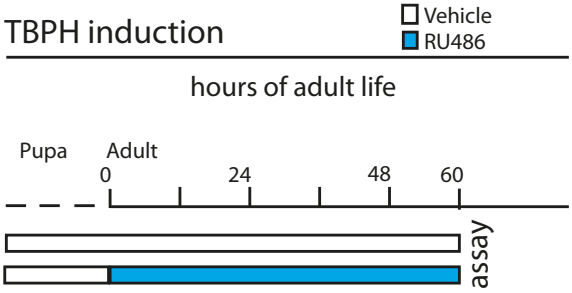

Figure 52 Schematic representation of experimental procedures.

Schematic time line of TBPH induction. Larvae were grown in normal conditions; just born adult flies were transferred in RU486 media (light blue bar), in order to activate the TBPH transgene. The control population was maintained in vehicle media (white bar).

For these experiments, immediately eclosed GS-TBPH adult flies were treated with different doses of RU486 (2mM and 5mM) and then tested. A strong recovery of locomotive behaviours was found after 60 hours of transgenic TBPH induction (Figure 53A and B). A control expressing UAS-GFP transgene was used to exclude possible toxic effects due to the higher RU486 concentration. A western blot was performed to verify the effective transgene activation. These results established that late functional recovery of neuronal activity was possible in TBPH-minus flies, suggesting that they do not have persistent defects in motoneurons function or motor circuit assemble.

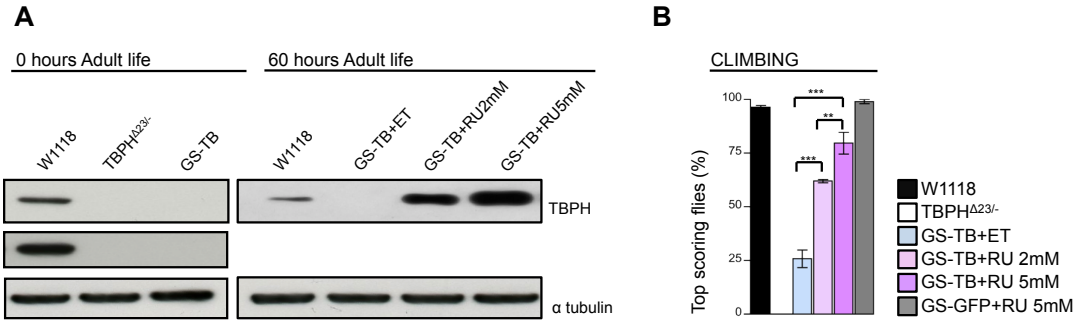

Figure 53 TBPH minus phenotype can be rescued by late expression of the transgenic TBPH protein in adult CNS.

(A) Western blot of adult heads probed for TBPH and alpha tubulin before RU486 induction (left panel) and after 60 hours of TBPH induction (right panel). The quantification of normalized protein amount was reported below each lane. n=3. (B) Climbing assay of late rescued adults showed a significant, dose dependent, recovery of locomotive abilities 60 hours after TBPH activation. n=200 **p<0.01 and ***p<0.001 calculated by one-way ANOVA. Error bars SEM.

4.8 Functional analysis of early events after TBPH dysfunction

The *Drosophila* neuromuscular junction has attracted widespread attention as an excellent model system for studying the cellular and molecular mechanisms of synaptic development and neurotransmission. Axon growth, target selection and synaptogenesis have been well and accurately characterised. The combination between NMJ investigation and the molecular genetic approaches, has lead to the identification of many genes involved in these processes (Gramates & Budnik, 1999; Halpern *et al*, 1991). Recent studies showed that TDP-43 is involved in the expression level regulation and alternative splicing processes of a high number of genes (Hazelett *et al*, 2012; Narayanan *et al*, 2013). To determine the early events that occurred after TBPH dysfunction, I studied the initial alterations in the *Drosophila* motoneuron synaptic terminals in L3 larvae after the acute silencing of TBPH function *in vivo*.

Taking advantage of the TARGET system, I generated flies containing elav-GAL4, TubulinGAL80^{ts}, UAS-TBPH RNAi and UAS-Dicer (called TE-TBi) and control flies containing elav-GAL4, TubulinGAL80^{ts} and UAS-Dicer (called TE-TBc). The experiment was performed maintaining a wild type condition during the early phases of the developmental period, followed by TBPH RNAi treatment commencing immediately after these flies reached the L3 larval stage (Figure 54).

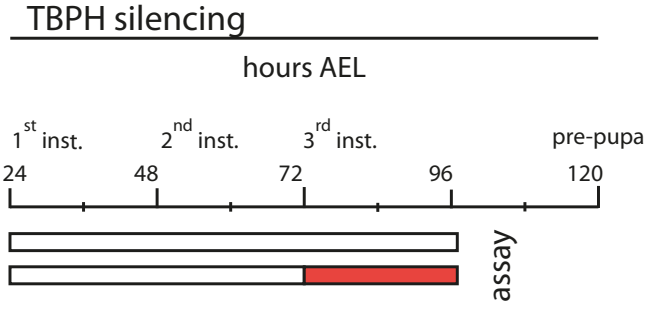

Figure 54 Schematic representation of the experimental procedure of acute TBPH silencing.

Schematic time line of TBPH RNAi induction Larvae were grown at 18°C, then transferred for the final stage of L3 at 29°C (red bar). The control population was maintained at 18°C (white bar).

TE-TBi L3 larvae cultured at 18°C did not present differences in the brain levels of TBPH protein compared with TE-TBc controls, confirming the proper functionality of the TARGET system. On the other hand, TE-TBi larvae after 24 hours of temperature switch showed a strong reduction in the neuronal levels of the endogenous TBPH, compared to controls (Figure 55A). This reduction in protein levels was sufficient to induce locomotive defects in TE-TBi larvae compared to control (Figure 55B).

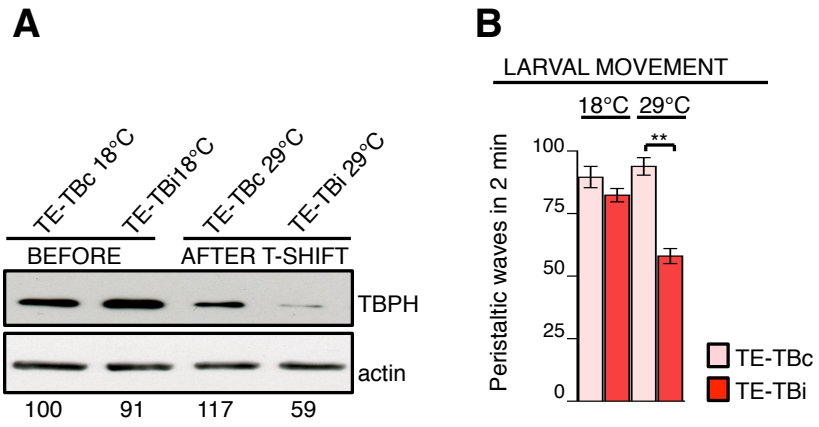

Figure 55 Western blot analysis and larval movement assay after acute TBPH suppression in CNS of mature larvae.

(A) Western blot analysis on larval brains probed for TBPH and actin, showed a reduction in endogenous TBPH protein after 24 hours of RNAi activation in third instar larval neurons using the TARGET system (Genotypes: TE-TBc= UAS-*Dicer;* TBPH$^{\Delta 23}$,*tubulin*-GAL80^{TS}/+*; elav*-GAL4/+ and TE-TBi+24hs = UAS-*Dicer;* TBPH $^{\Delta 23}$,*tubulin*-GAL80^{TS}/+*; elav*-GAL4/TBPH-RNAi). The quantification of normalized protein amount was reported below each lane. n=3. (B) Acute suppression of TBPH by RNAi expression in L3 larval neurons during 24 hours induced a drastic reduction in larval motility. n=30 **p<0.01 calculated by one-way ANOVA. Error bars SEM.

The NMJs anatomy of these larvae was analysed, in order to find a possible perturbation in this system. In contrast with TBPH mutants L3 larvae, the alterations in larvae motility of TE-TBi larvae were not associated with anatomical modifications in the number of synaptic boutons or motoneuron terminal branches at NMJs. I only found the presence of subtle alterations in

the morphology of the synaptic bouton shape in TE-TBi larvae compared to controls (Figure 56B-D), suggesting that functional alterations in synaptic transmission may precede the anatomical defects described in TBPH null flies. The analysis of the cytoskeleton showed defects in Futsch protein distribution at the presynaptic terminals. Compared to the controls, an increment in the number of Futsch empty boutons and a decrease in the number of full boutons in acute silencing larvae was observed (Figure 56E), its quantification is reported in (Figure 56F).

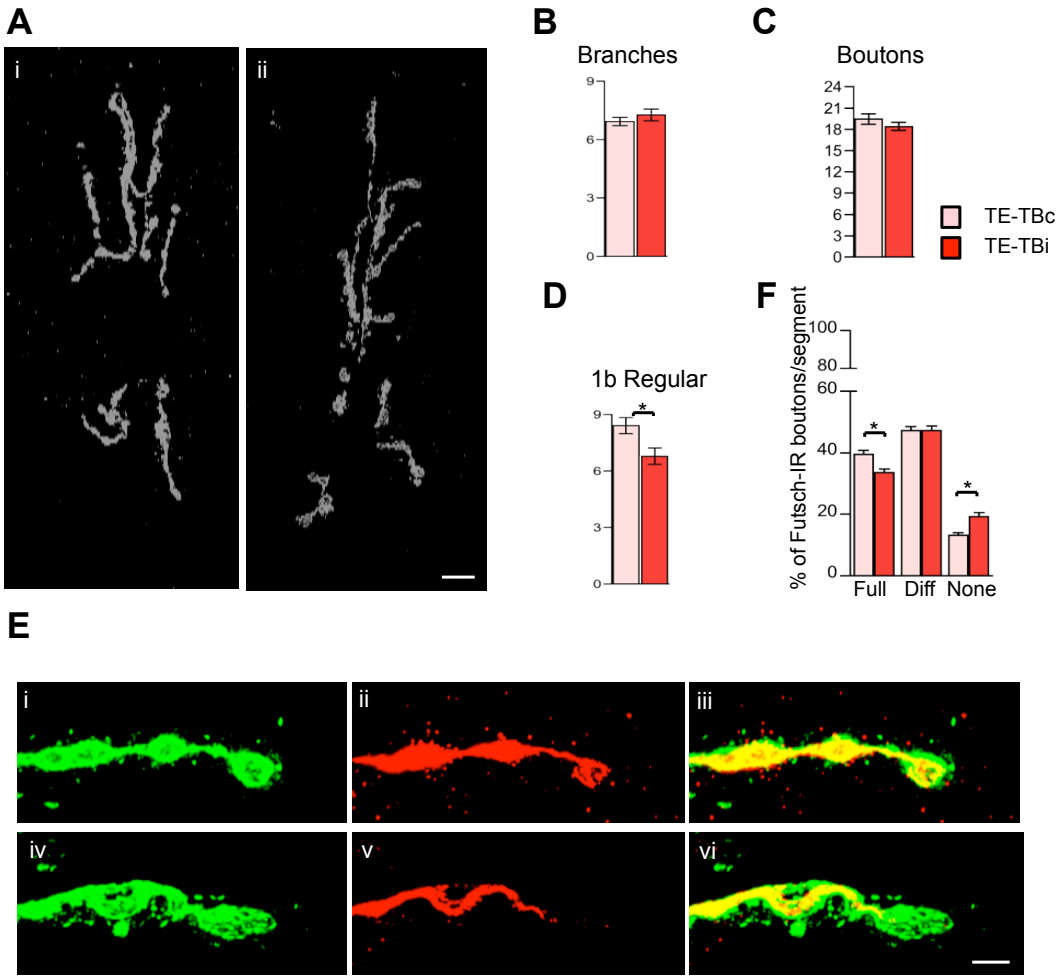

Figure 56 NMJs morphology and cytoskeleton organization after acute TBPH suppression in CNS of mature larvae.

(A) Analysis of NMJs morphology in L3 larvae (96-100hs AEL) stained with anti-HRP. Images showed that acute silencing of TBPH (24 hours) in neurons did not alter the morphology of number of branches, and number of boutons, quantification shown respectively in (B) and (C). Only a mild significant alteration of bouton shape was detected, quantification in (D). n=15 larvae *p<0.05 calculated by T-test. Scale bar 10µm. (E) Confocal images showed anti-Futsch (in red) and anti-HRP (in green) staining at the terminal synaptic boutons of (i–iii) wild type TE-TBc and (iv–vi) acute silencing TE-TBi. (F) Quantification of Futsch staining pattern in muscle 6–7 abdominal segment II showed a decreased number of full Futsch boutons in TE-TBi

compared to TE-TBc. n=15 larvae *p<0.05 calculated by one-way ANOVA. Scale bar 5μm. Error bars SEM.

4.9 Downregulation of presynaptic vesicular proteins are early events after acute TBPH silencing.

Starting from the hypothesis that functional alterations in synaptic transmission may precede the anatomical defects described in TBPH null flies, I analysed whether short time suppression of TBPH in presynaptic neurons affected the expression and/or distribution of molecules involved in synaptic transmission at *Drosophila* NMJs (Keshishian *et al*, 1996; Majumder & Krishnan, 2010). The TE-TBi flies, described in the previous chapter, were used to analyse the NMJs after 24 hours of acute TBPH RNAi induction. The essential components of the secretory machinery like Syntaxin1A (Wu *et al*, 1999), Synapsin (Hilfiker *et al*, 1999) appeared significantly down-regulated after 24 hours of neuronal suppression of TBPH (Figure 57A-C). While similar experimental conditions induced less impressive modifications in the presynaptic levels of Cysteine string protein (Csp) (Dawson-Scully *et al*, 2007), (Figure 57A and D). Interestingly, the acute suppression of presynaptic TBPH did not affect the expression of proteins involved in the structural organization of the synapses like Bruchpilot (Brp) (Wagh *et al*, 2006; Wichmann *et al*, 2008), (Figure 57A and E), a protein required in the organization of active zones at *Drosophila* synaptic terminals. Specifically, neither the distribution nor protein intensity levels were modified in the synaptic terminals of short TBPH suppressed larvae, although more subtle morphological changes at the level of the T-bars level could not be excluded.

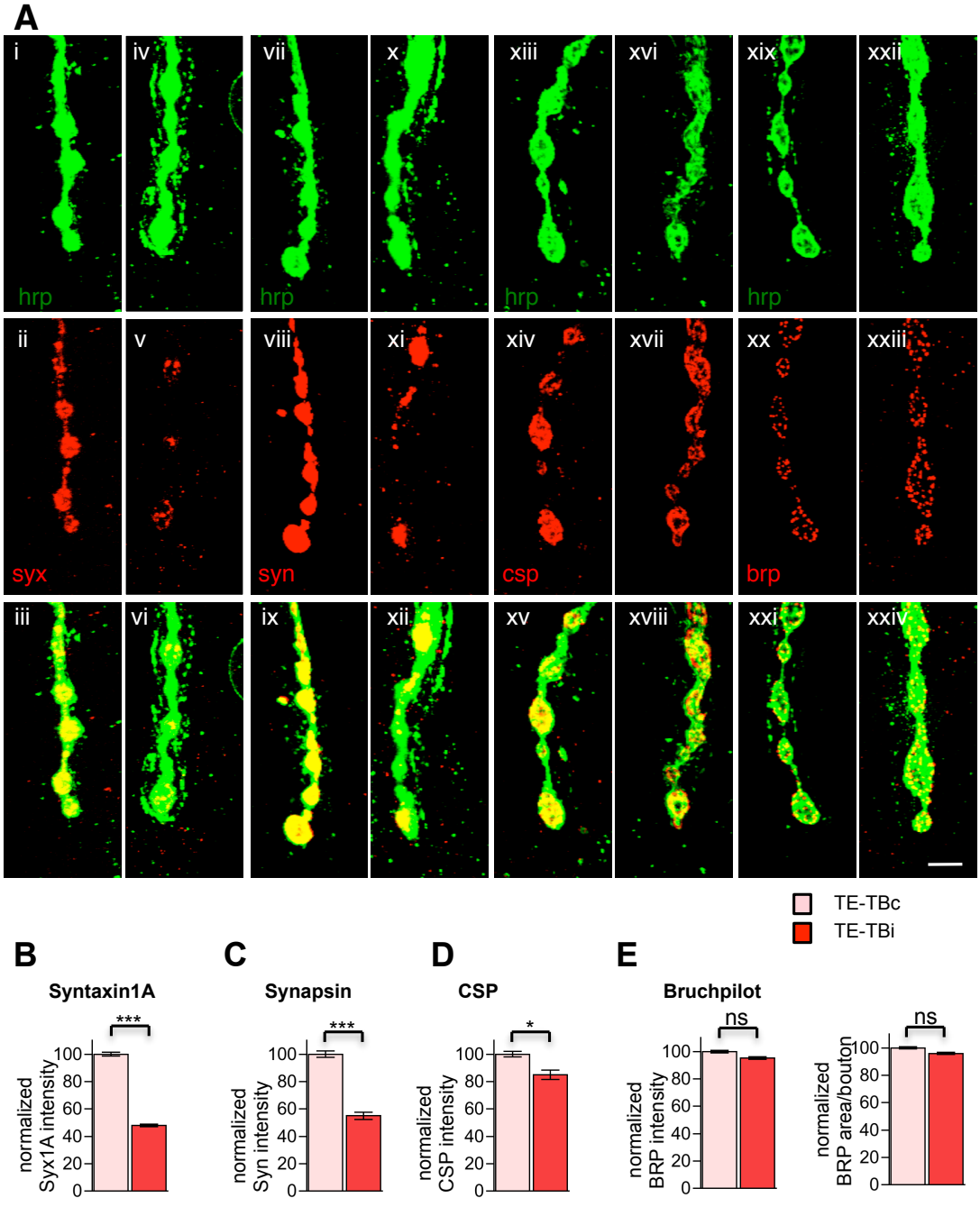

Figure 57 Early events at the presynaptic level after acute TBPH silencing in mature larvae.

(A) Confocal image of NMJs presynaptic boutons in muscle 6/7, II segment compares control third instar TE-TBc larvae (i-iii) stained with anti-HRP (green) to anti-Syntaxin1A (red) with acute silenced TBPH L3 larvae TE-TBi (iv-vi) where Syntaxin1A appears strongly reduced from the synaptic terminals, the differences were quantified in (B). Similarly, control TE-TBc larvae (vii-ix) stained with anti-HRP (green) and anti-Synapsin (red) presented a significant reduction in Synapsin levels compared to TE-TBi larvae (x-xii) and quantified in (C). A mild decrease in Csp staining was observed between TE-TBc controls (xiii-xv) and TE-TBi (xvi-xvii) acute silenced larvae (D). No differences instead were found in the intracellular levels or presynaptic distribution of Brp (xix-xxi) in control neurons versus (xxii-xxiv) acute silenced flies. (E) Depicts the quantification of Brp intensity pattern (left graph) and

receptor area (right graph). n=250/300 boutons *p<0.05 ***p<0.001 calculated by T-test. Scale bar 5µm.

The down-regulation of these synaptic markers was progressive and highly dependent on TBPH function, as the constitutive expression of the TBPH RNAi during complete larval development (TBi flies) exacerbated these phenotypes. Interestingly Bruchpilot even with a constitutive silencing appeared unaltered.

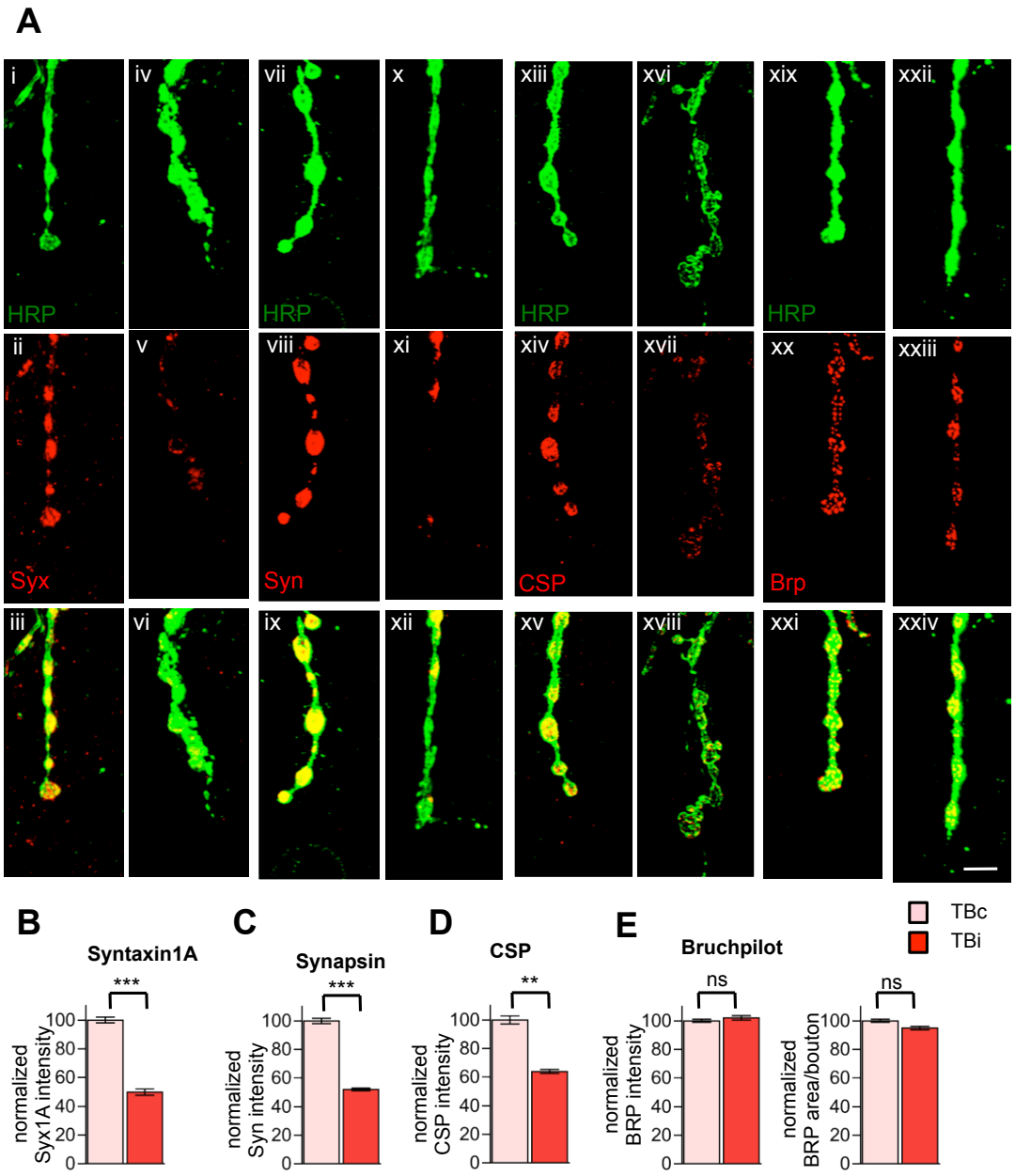

Figure 58 Pre synaptic analysis in constitutive TBPH silencing.

(A) Confocal images of NMJs pre-synaptic boutons in muscle 6/7, II segment compared with control L3 TBc larvae (i-iii) stained with anti-HRP (green) and anti-Syntaxin (red) with constitutive silenced TBi larvae (iv-vi). Genotypes: TBc=UAS-

Dicer; TBPH$^{\Delta 23}$, *elav*-GAL4/UAS-GFP and TBi= UAS-*Dicer;* TBPH $^{\Delta 23}$, *elav*-GAL4/+; TBPH-RNAi/+. Syntaxin appeared strongly reduced from synaptic terminals when TBPH was silenced in neurons, quantification reported in (B). Control (vii-ix) larvae stained with anti-HRP (green) and anti Synapsin (red) showed a similar reduction in silenced larvae (x-xii), quantification reported in (C). A milder decrease in Csp staining was also confirmed between control TBc (xiii-xv) and constitutive silencing TBi (xvi-xviii), quantification reported in (D). No differences were found in levels of Bruchpilot in controls (xix-xxi) versus constitutive silencing (xxii-xxiv), quantification reported in (E), on the left intensity pattern while on right clusters area have been graphed. n=250/300 boutons **p<0.01 ***p<0.001 calculated by T-test. Scale bar 5μm. Error bars indicate SEM.

4.10 The presynaptic function of TBPH is required for the differentiation and maintenance of the postsynaptic structures.

For the formation of neuromuscular junctions, presynaptic neuron activity is required to induce the differentiation of postsynaptic structures on the surface of the subjacent muscles (Bloch & Pumplin, 1988). This suggests that the alterations, earlier described in presynaptic motoneurons, may lead to defects in the formation of postsynaptic structures and muscle denervation problems in acutely RNAi treated larvae.

To test this hypothesis, I used the previously described TE-TBi flies and analysed the distribution of different postsynaptic markers in L3 larval NMJs after 24 hours of presynaptic TBPH suppression. Immunocytochemistry was used to study the distribution of the PDZ domain protein Dlg, a scaffold molecule important to postsynaptic localization of numerous proteins including glutamate receptors (GluRs) (Chen & Featherstone, 2005).

In wild type NMJs, Dlg concentrated around the presynaptic terminals in the postsynaptic zone, surrounding the individual boutons and established well defined structures in the muscular surface (Koh *et al*, 1999). I found that the acute suppression of presynaptic TBPH protein induced dramatic modifications in the localization of Dlg which appeared strongly reduced and abnormally distributed, unable to define single synaptic structures, surrounding large groups of boutons, and even absent from big areas of the presynaptic surface (Figure 59A and B). These early defects in Dlg distribution became progressively stronger in flies expressing anti-TBPH RNAi from the beginning of their neuronal development (Figure 60A and B),

indicating that these modifications are highly dependent of presynaptic TBPH levels.

Similarly, the distribution of the postsynaptic receptor GluRIIA was analysed after 24 hours of presynaptic TBPH-RNAi treatments. In wild type controls (TE-TBc) the GluRIIA was localized in well-defined spots that presented a ring-shaped outline (Figure 59A and C) while in L3 larvae treated with TBPH-RNAi for 24 hours (TE-TBi), the pattern of GluRIIA staining became more diffuse and irregular with significantly less ring-shaped spots. Identical results were found in TBPH-RNAi constitutively treated neurons (Figure 60A and C), indicating that TBPH function is permanently required in presynaptic motoneurons to maintain the differentiation of postsynaptic structures.

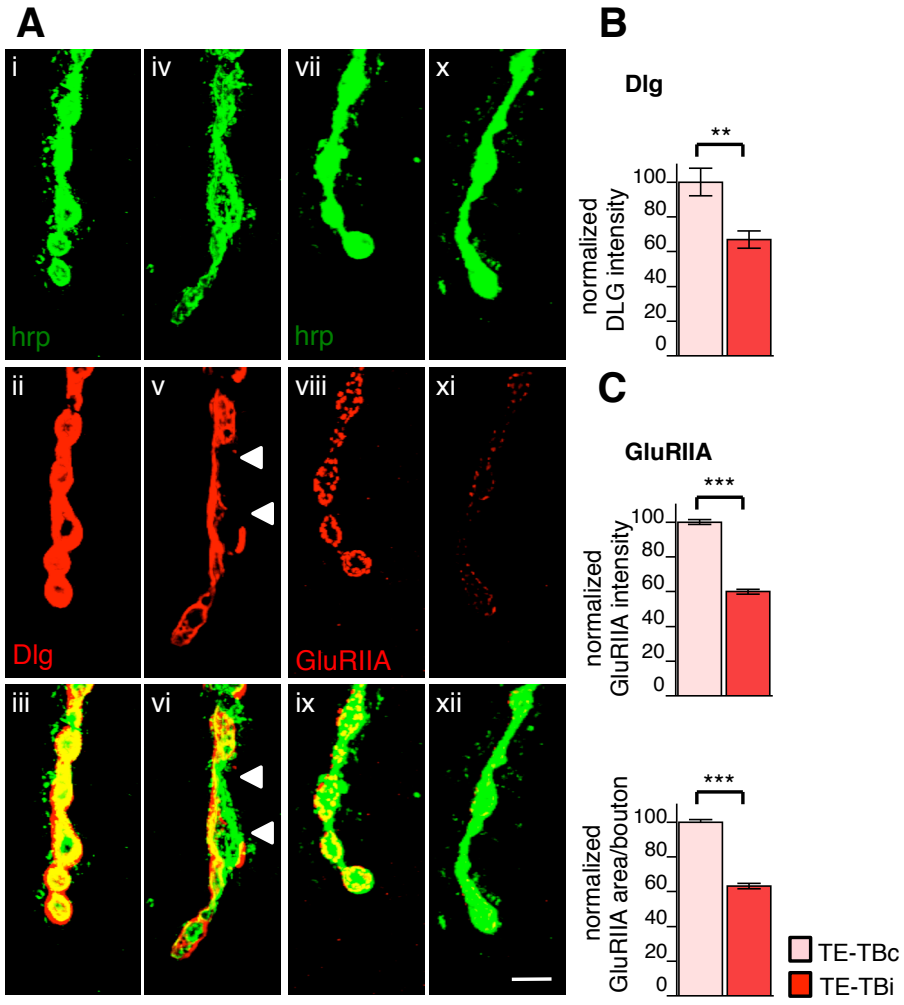

Figure 59 Early events at the postsynaptic level after acute TBPH silencing in mature larvae.

(A) Confocal images of synaptic terminal boutons stained with anti-HRP (presynaptic membrane) in green and with anti-Dlg in red, in control (i-iii, TE-TBc) and in acute 24h silenced TBPH (iv-vi, TE-TBi), showed a strong reduction in Dlg intensity with empty areas in the side of the synaptic boutons. The quantification is reported in the graph (B). Equivalent alterations were also found in the distribution of the glutamate receptor IIA between controls (vii-ix) and acute silenced TBPH (x-xii), the quantification is reported in the graph (C). n=250/300 boutons **p<0.01 ***p<0.001 calculated by T-test. Scale bar 5µm. Error bars SEM.

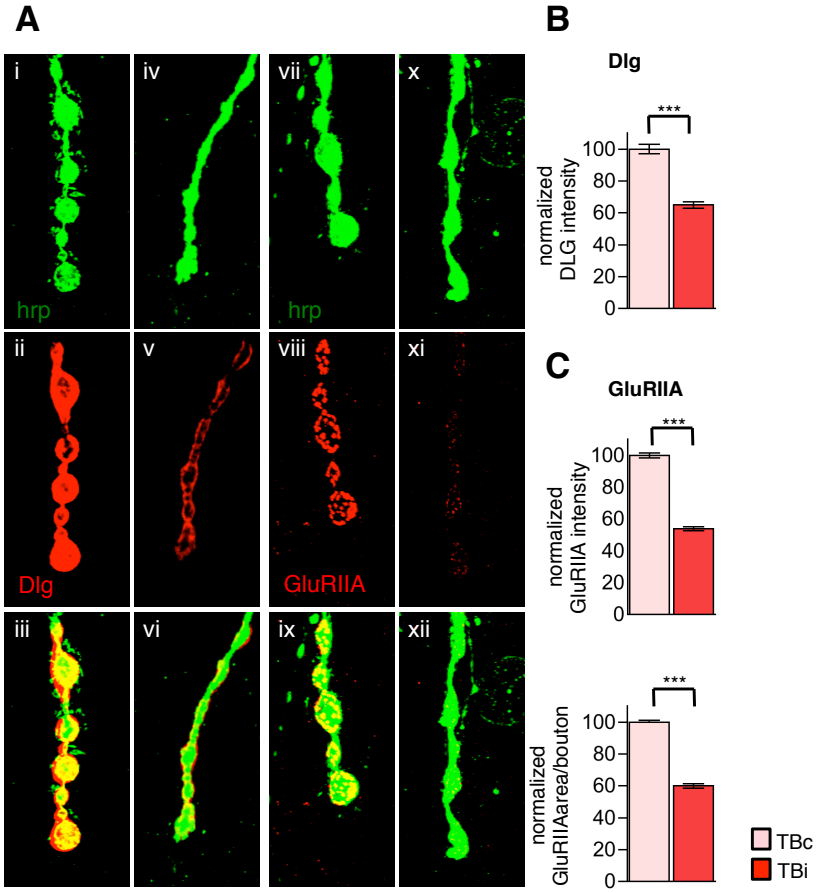

Figure 60 Postsynaptic analysis in constitutive TBPH silencing.

(A) Confocal images of NMJs in muscle 6/7, II segment compares control L3 TBc larvae (i-iii) stained with anti-hrp (green, pre-synaptic membrane) and anti-Dlg (red, post-synaptic membrane) with constitutive silenced TBi larvae (iv-vi). Quantification reported in (B) showed a reduction in Dlg intensity with presence of gaps in post-synaptic borders. Similar alterations were found in distribution of glutamate receptor IIA, between control TBc (vii-ix) and constitutive silencing TBi (x-xii). (C) Quantification of GluRIIA intensity (upper panel) and area (lower panel). n=250/300 boutons **p<0.01 ***p<0.001 calculated by T-test. Scale bar 5µm. Error bars indicate SEM.

4.11 The pre and postsynaptic markers down-regulated after the acute silencing of TBPH are recovered after the expression of the transgenic protein in CNS

To support the previous findings, I performed a series of genetic rescue experiments to check if transgenic TBPH protein expression in TBPH minus flies was able to re-establish the wild type levels of the down-regulated synaptic markers. For this purpose, I performed a Western blot analysis on adult brain tissues of the following genotypes: a control (W1118), $TBPH^{\Delta 23/-}$, $TBPH^{\Delta 142/-}$ and TBPH rescue ($TBPH^{\Delta 23/-;}$elav-GAL4>TBPH). The analysis confirmed the down-regulation of the synaptic markers in both TBPH mutant alleles for Syntaxin1A, Synapsin, Csp, Futsch and Dlg but not for Brp and the recovery of these markers when the TBPH protein was reintroduced back in CNS (Figure 61).

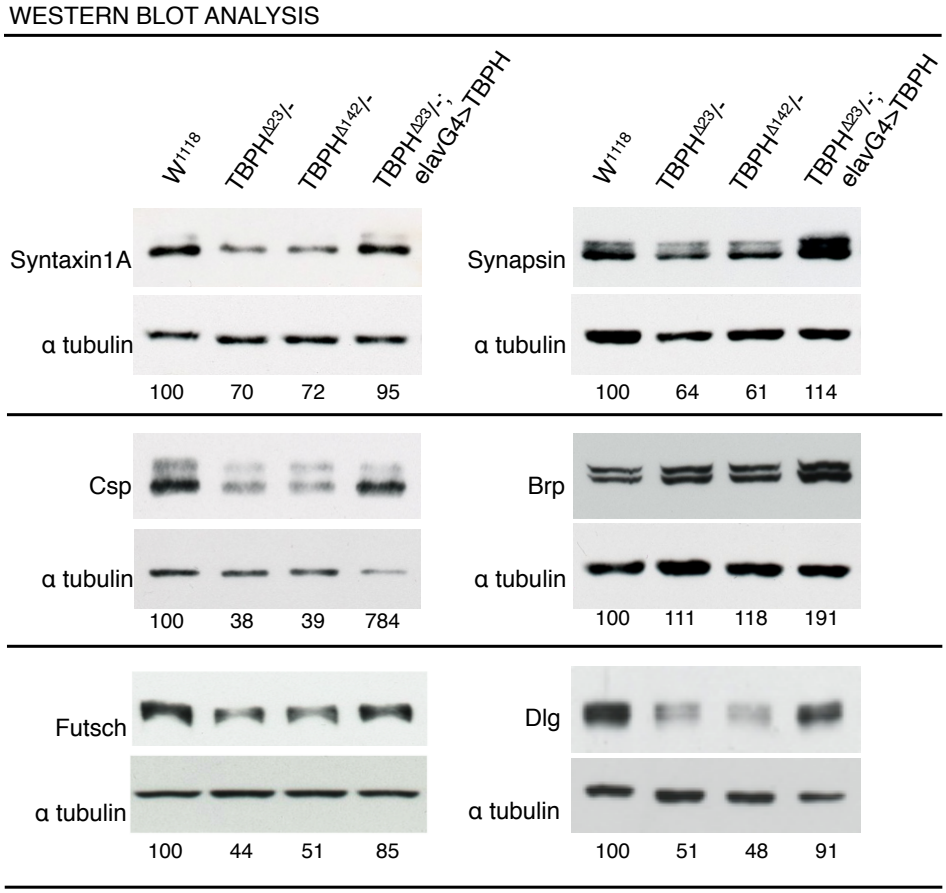

Figure 61 Western blot analysis of pre and post synaptic markers in mutants and in TBPH rescue.

A western blot analysis on adult heads stained with anti-Syx (upper left), anti-Syn (upper right), anti-Csp (middle left), anti-Brp (middle right), anti-Futsch (bottom left), anti-Dlg (bottom right) and anti-alpha tubulin as a loading control, independently confirmed the specific reduction of pre and postsynaptic markers in TBPH minus flies ($TBPH^{\Delta 23/-}$ and $TBPH^{\Delta 142/-}$) compared to wild type and TBPH rescued neurons ($TBPH^{\Delta 23/-}$;elavG4>TBPH). On the contrary, no changes in protein levels were observed for the structural protein Brp. Quantification of normalized protein amount was reported below each lane (mean ± SEM: Syx 100 ± 1; 70 ± 2.2; 72 ± 1; 85 ± 2.6; Syn 100 ± 1; 64 ± 1.2; 61 ± 1.1; 114 ±3.4; Csp 100 ± 1; 38 ± 2.3; 39 ± 2.2; 784 ± 3.1; Brp 100 ± 1; 111 ± 1.5; 118 ± 1; 191 ± 3.4; Futsch 100 ± 1; 44 ± 2; 51 ± 1.9; 85 ± 1.2; Dlg 100 ± 1; 51 ± 2; 48 ± 3; 91 ± 2.7). n=3.

Finally, I also checked if the postsynaptic defects were recovered in TBPH rescued flies. For these experiments, the NMJs of wild type larvae (W1118), $TBPH^{\Delta 23/-}$, $TBPH^{\Delta 23/-}$; elavGAL4>TBPH and $TBPH^{\Delta 23/-}$; elavGAL4>$TBPH^{F/L}$ were dissected and labelled with antibodies against postsynaptic markers. TBPH expression exclusively in neurons was sufficient to recover the postsynaptic defects observed in the distribution of Dlg and GluRIIA found in TBPH loss of function mutants. On the contrary, no recovery was obtained when rescuing with the variant $TBPH^{F/L}$, unable to bind the RNA (Figure 62).

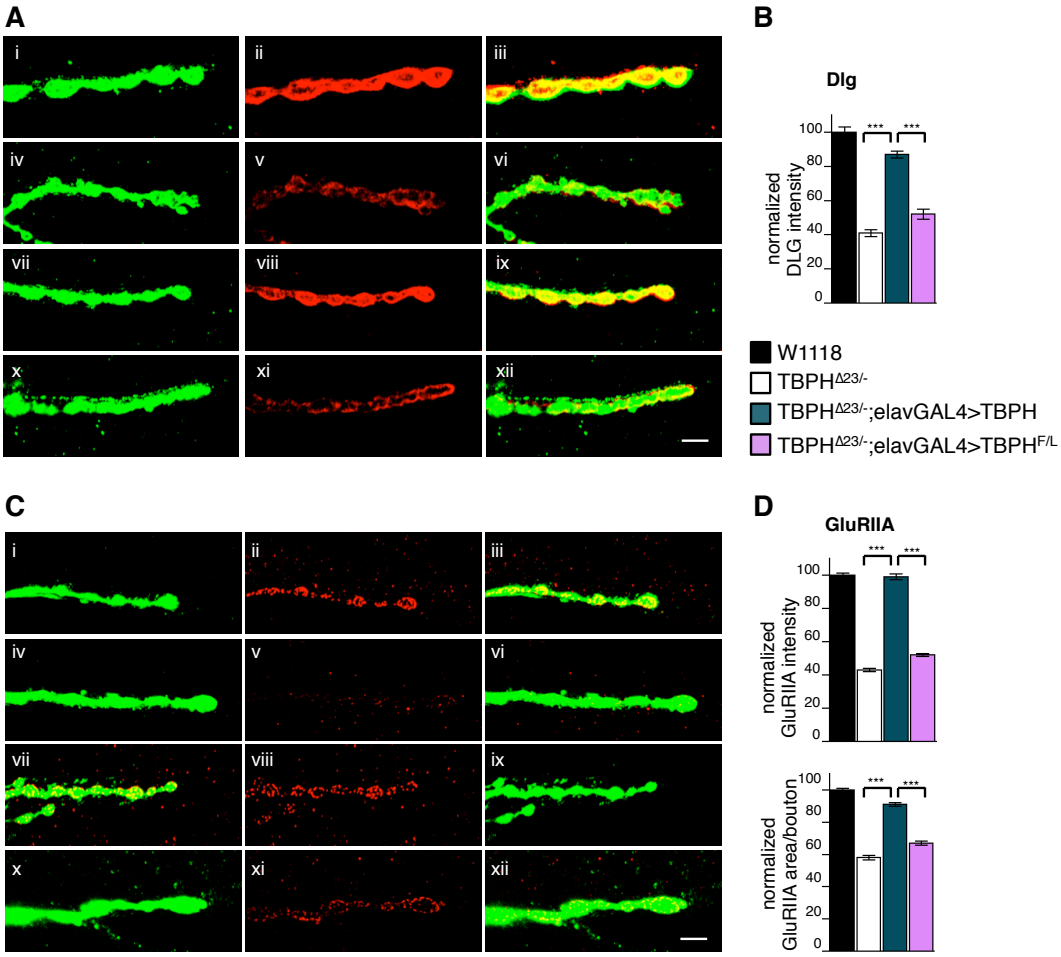

Figure 62 Constitutive neuronal TBPH transgene expression rescues the postsynaptic defects in TBPH minus larvae.

(A) Confocal images of NMJs in muscle 6/7, II segment stained with anti-HRP (green) and anti-Dlg (red). Images showed post-synaptic distribution of Dlg protein in control W1118 (i-iii), TBPH$^{\Delta 23/-}$ (iv-vi), TBPH $^{\Delta 23/-}$; elav-GAL4>UAS-TBPH (vii-ix) and TBPH $^{\Delta 23}$/$^{-}$; *elav*-GAL4>UAS-TBPH$^{F/L}$ (x-xii). (B) Quantification of Dlg intensity showed a significantly reduction in TBPH mutant compared to wild type. The mutant phenotype was rescued with the expression of the TBPH transgene in neurons; no rescue was obtained expressing the mutant variant of TBPH (TBPH$^{F/L}$). (C) Confocal images of NMJs in muscle 6/7, II segment stained with anti-HRP (green) and anti-GluRIIA (red). Images showed post-synaptic distribution of GluRIIA protein in control W^{1118} (i-iii), TBPH $^{\Delta 23/-}$ (iv-vi), TBPH $^{\Delta 23/-}$; elav-GAL4>UAS-TBPH/ *tbph*$^{\Delta 23}$, *elav*-GAL4 (vii-ix) and TBPH$^{\Delta 23/-}$; *elav*-GAL4>UAS-TBPH$^{F/L}$ (x-xii). (D) Quantification of GluRIIA intensity (upper panel) and area (lower panel) showed a significant reduction in TBPH mutant compared to wild type, both for intensity and area. The mutant phenotype was rescued with the expression of TBPH transgene in neurons; no rescue was obtained expressing the mutant variant of TBPH (TBPH$^{F/L}$). n=200/250 boutons ***p<0.001 calculated by one-way ANOVA. Scale bar 5µm. Error bars indicate SEM.

4.12 Analysis of mRNA-TBPH physical interactions by immunoprecipitations *in vivo*

The majority of the functional properties of TDP-43 described up to now were found to be mainly linked to the RNA binding ability of this protein (Buratti & Baralle, 2010). Hence, to gain further comprehension into the mechanisms of TBPH action, I investigated any potential physical interactions between the TBPH protein and the mRNAs of the synaptic proteins found to be perturbed in TBPH mutants. For these experiments, flies expressing Flag-tagged TBPH, Flag-tagged TBPH$^{F/L150-152}$ or the unrelated protein Flag-tagged REEP1 were expressed under the control of the elav-GAL4 pan-neuronal driver and utilized for immunoprecipitation assays. Fly heads were homogenized and TBPH was immunoprecipitated by anti-Flag M2 monoclonal antibody (Sigma). Western blot was performed to confirm TBPH immunoprecipitation (Figure 63).

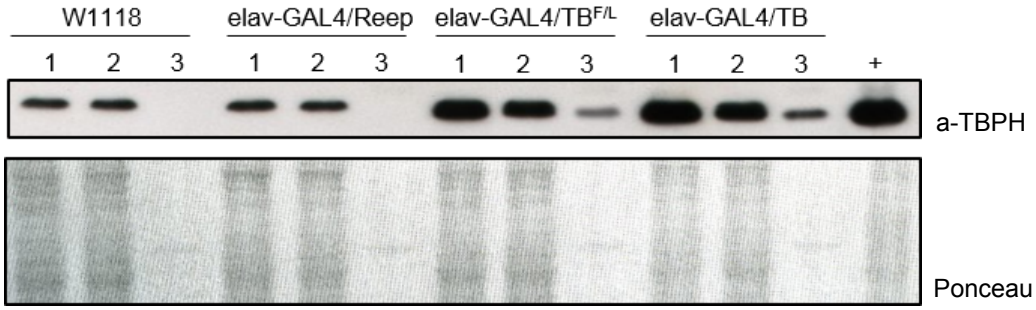

Figure 63 Western blot analysis of immunoprecipitation assay.

Western blot analysis on adult heads of the immunoprecipitation assay, stained with the anti-TBPH antibody. In lines (1) the input material for each genotype is loaded. The input is the head extract obtained after the mechanical squeezing of the tissues. In lines (2) the depleted material is loaded. The depleted material is the head extract after the period of incubation with Flag-functionalized beads. In lines (3) the immunoprecipitated material is loaded. Ponceau staining was used as a control for the loading.

In W1118 and elav-GAL4>REEP no differences in TBPH amounts was detected neither in the input and depleted fraction, nor in the immunoprecipitation, indicating absence of aspecific TBPH binding to the beads. In elav-GAL4>TB^{FL}, a depletion of TBPH protein was notable (lane 2) if compared to the input signal (lane 1), which was present in the immunoprecipitated material (lane 3). In elav-GAL4/TB the depletion of

TBPH protein after incubation with the beads was evident, and moreover a good level of TBPH protein immunoprecipitation was also noticeable (lane3). Ponceau staining of the membrane was reported as the loading control.

4.13 TBPH physically interacts with *syntaxin* and *futsch* mRNA *in vivo*

The RNA bound to the Flag-tagged immunoprecipitated proteins was TRIZOL extracted, retrotranscribed and analyzed through real time quantitative PCR (qRT-PCR).

Interestingly, I observed an enrichment of *futsch* and *syx* mRNA in the TBPH immunoprecipitated samples (10.8 and 2.5 folds respectively) compared to *syn, csp* or the housekeeping genes *rpl-52* and *rpl-11* (Figure 64), indicating that TBPH may preferentially interact with *futsch* and syx mRNA but not with the messengers of *syn* or *csp*. In agreement with this view, I observed that TBPH-*syx* or *futsch* mRNA interactions get lost when similar immunoprecipitations were performed utilizing the RNA-binding defective form of $TBPH^{F/L150\text{-}152}$. This demonstrates that these physical interactions are rather specific. Based on these results, it is interesting to note the presence of different clusters of putative TBPH binding sequences (TG)n both within the 5'UTR and the coding sequence of the *futsch* and *syx* gene (Colombrita *et al*, 2012). These indications would strongly suggest that the function of TBPH may contribute to stabilize subcellular levels of these mRNA and/or to possibly promote their translation.

As expected, I found a high level of enrichment for the putative TBPH binding poly UG repeats, UGs RNA was added to head extracts in order to control the efficiency of mRNA enrichment. As positive controls, I found that the immunoprecipitated TBPH protein complex contained the *hdac-6* mRNA (4.5 folds), in agreement with a previous publication (Fiesel *et al*, 2010).

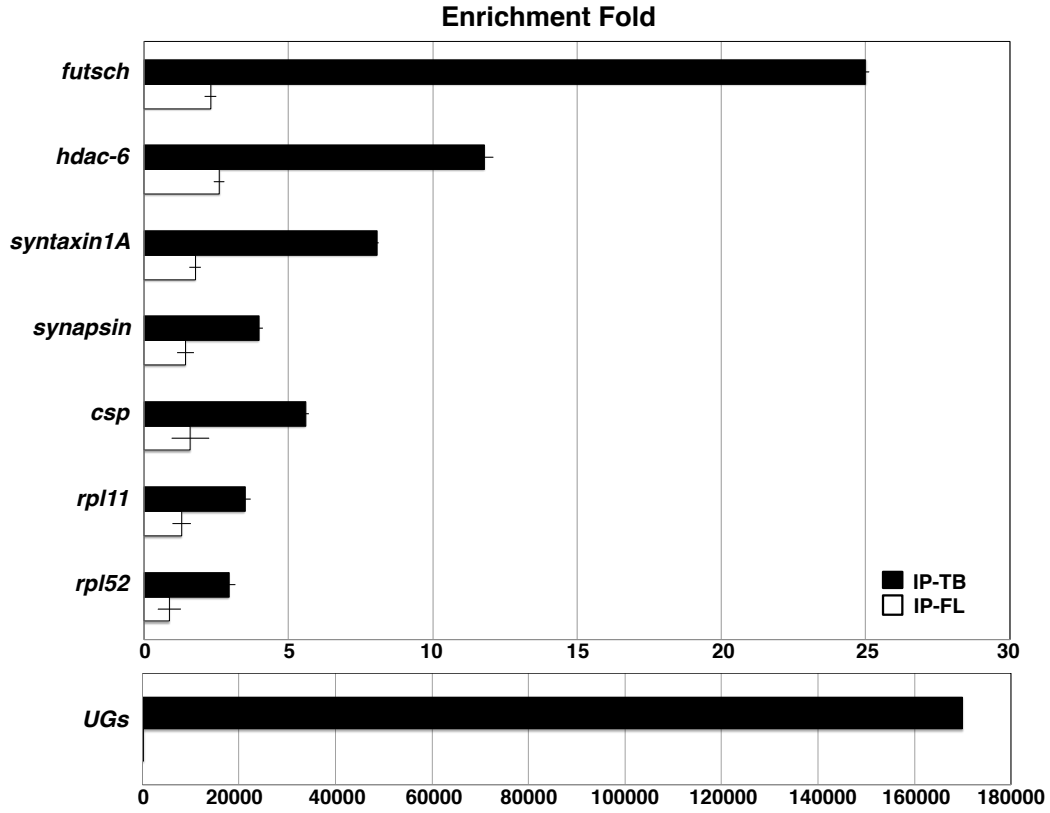

Figure 64 qRT-PCR of immunoprecipitated mRNAs reveals *futsch* and *syntaxin1A* enrichment.

qRT-PCR analysis of mRNAs immunoprecipitated by Flag-tagged TBPH (IP-TB) and its mutant variants TBPH $^{F/L}$ (IP-FL). Real time quantitative PCR was used for quantification of the fold-enrichment above the control (Reep) for TBPH and TBPH$^{F/L}$. Syntaxin1A resulted enriched 2.5 folds in IP-TB if compared to IP-FL, also *futsch* showed a significantly enrichment (10.8 folds) when compared to IP-FL. Significant levels of enrichment were observed for *hdac-6* mRNA and $(UG)_9$ RNA were used as positive controls. The mRNAs of control (ribosomal protein *rpl52* and *rpl11*) were not enriched significantly, as for *csp* and *synapsin*. n=3. Error bars indicate SD.

Taken together, this data demonstrated that TBPH interacted with the *futsch* mRNA and *syntaxin1A* mRNA in a highly specific manner. Defective phenotypes observed in TBPH mutant flies might be influenced directly by the down-regulation of Futsch and/or Syntaxin1A level *in vivo*.

4.14 Human Tau protein induces pre-synaptic terminal rescue in TBPH mutant

One of the main roles of Futsch is to stabilize microtubules at the synaptic boutons. A stabilization of microtubules in mutant flies should be sufficient to rescue anatomical defects observed in mutant flies. Previous work in this field demonstrated that expression of mammalian Tau protein was able to rescue Futsch mutant phenotype in *Drosophila* neurons (Hummel *et al*, 2000; Roos *et al*, 2000). I generated flies expressing human Tau transgene in neurons of TBPH mutant flies. The analysis of NMJs proved that the expression of Tau protein managed to rescue the anatomical defects of TBPH mutant. The synaptic boutons recovered to a normal shape and regained the complexity of their terminals through an increase of terminal branches (Figure 65).

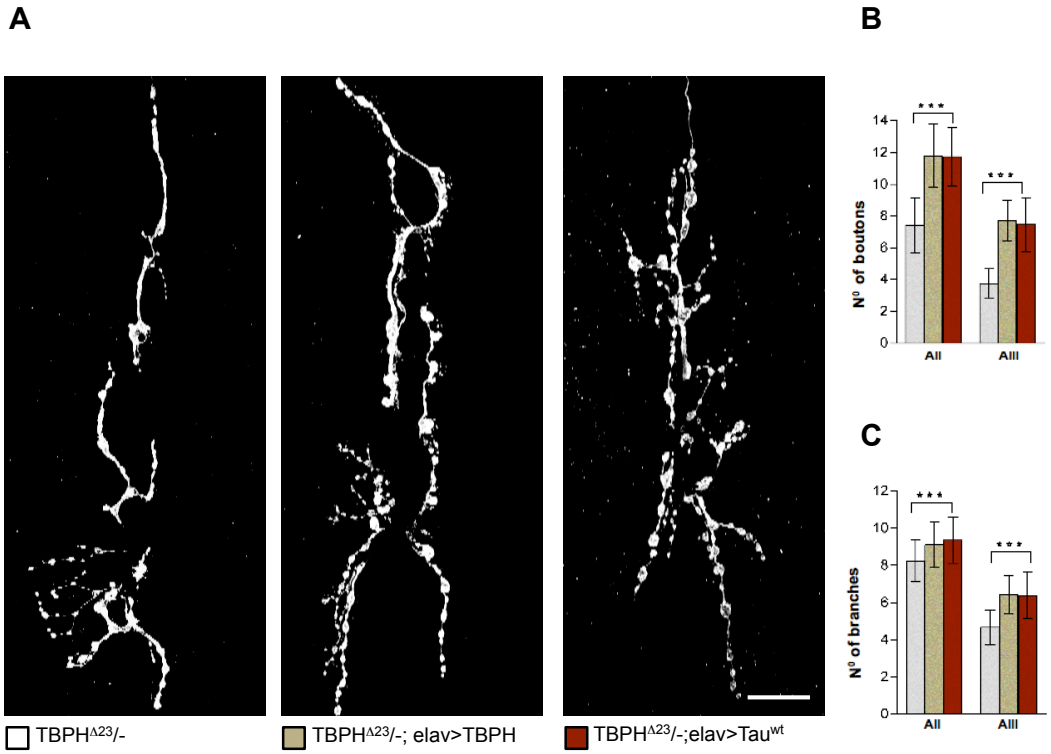

Figure 65 Tau recovered anatomical NMJs defects present in mutant flies.

(A) Confocal images of third instar larvae stained with anti-HRP on muscle 6/7 abdominal segment II of TBPH mutant ($TBPH^{\Delta 23/-}$ left panel), TBPH rescue ($TBPH^{\Delta 23/-}$;elav>TBPH central panel) and Tau rescue ($TBPH^{\Delta 23/-}$;elav>Tau right panel). In (B) and (C) are reported the quantifications of the number of boutons and branches respectively. The quantification was performed on abdominal segment II and abdominal segment III of the larval body muscle wall.

These results demonstrated that the morphological defects observed in TBPH mutant flies were rescued by Tau protein; the Tau rescue was comparable to the rescue obtained with the expression of the endogenous TBPH protein (Figure 65A, central panel). To investigate whether a functional recovery was also achieved by expressing Tau protein, the movement behaviour of mutant larvae expressing Tau protein exclusively in neurons was analysed. Functional recovery of motility was not obtained, indicating that besides the stabilization of microtubules, TBPH may regulate additional functions in motoneurons, probably more linked to the synaptic vesicle pathway, in which other proteins including Syntaxin1A are involved (Figure 66).

4.15 Syntaxin1A rescues TBPH mutant: in locomotive phenotype and in functionality of NMJs

Syntaxin 1A (Syx1A) is a member of SNARE complex family (an acronym derived from "SNAP, Soluble NSF Attachment Protein REceptor). The primary role of SNARE proteins is to mediate vesicle fusion with the cell membrane or with a target compartment (such as a lysosome). Syntaxin1A plays a critical role in several secretory processes, including cuticle secretion and neurotransmitter release, and assists in neuronal membrane maturation (Cerezo *et al*, 1995; Lagow *et al*, 2007; Littleton, 2000).

Previously, I demonstrated that in TBPH mutant flies, Syntaxin1A protein became down-regulated and its mRNA was directly bound by TBPH protein. All these evidences taken together, lead to wonder, whether restoring Syntaxin1A levels may lead to a recovery of the mutant condition. Thus, I generated flies expressing the Syntaxin1A transgene exclusively in CNS (elav-GAL4) in TBPH minus background. The motility capacity of these larvae was assessed, comparing these animals with TBPH mutants who resulted strong impaired. In Syntaxin1A rescue, as well as in TBPH rescue, a recovery of larval motility was found. No recovery was achieved by expressing other markers, such as Futsch/Tau (as already discussed above, in the previous paragraph), Synaptobrevin or by expressing unrelated protein as GFP (Figure 66).

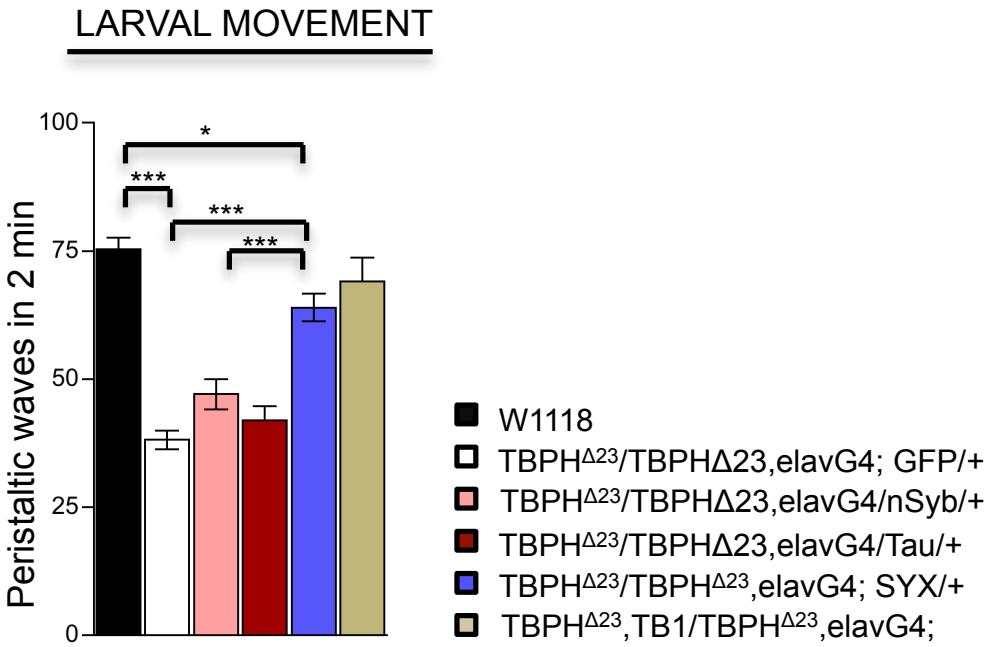

Figure 66 Syntaxin1A rescued mutant phenotype in larval motility.

Peristaltic waves of third instar larvae. The transgenic expression of Syntaxin1A protein in CNS ameliorated significantly motility phenotype, as well as the normal rescue with TBPH. No effect was observed expressing an unrelated protein as GFP or another presynaptic markers as Tau or Synaptobrevin (nSyb). n=30 *p<0.05 ***p<0.001 calculated by one-way ANOVA. Error bars SEM.

Intriguingly, the rescue of Synataxin1A levels with elav-GAL4 was not sufficient to recover the pupal lethality associated with TBPH loss of function (Feiguin *et al*, 2009). To rescue adult flies with Syntaxin1A a milder phenotype than TBPH loss of function was used. In order to do this, TBPH hypomorphic alleles flies were generated by the induction of anti-TBPH RNAi expression in neurons. These flies showed a decreased level of TBPH protein and had a clear defective phenotype in climbing capacity (Figure 67). However, this phenotype obtained through RNAi strategy, was milder than the TBPH mutant phenotype and might offer the possibility to have a less dramatic phenotype to rescue, but was valid to prove the genetic interaction.

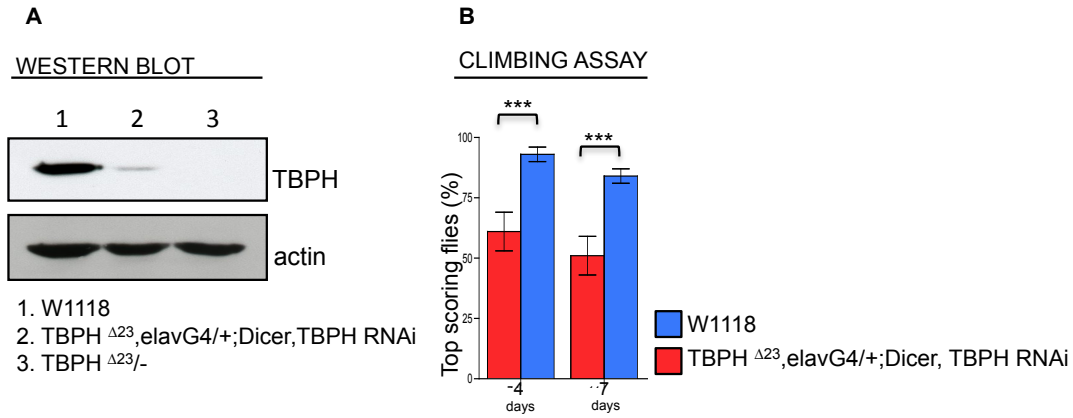

Figure 67 TBPH hypomorphic alleles to perform genetic interaction analysis.

(A) Western blot analysis of adult heads probed for TBPH and actin. In line 1 the control (W1118) was loaded, in the second line the fly with TBPH hypomorphic alleles was loaded and in the final line the TBPH mutant fly was loaded. The biochemical analysis showed the effective reduction of TBPH protein in hypomorphic alleles flies compared to wild type. Actin was used as loading control. (B) Climbing assay on TBPH hypomorphic alleles compared to wild type showed impairment in locomotive behaviour in these flies. n=250, ***p<0.001 t-test was used. Error bars SEM.

Syntaxin1A transgene was expressed in TBPH hypomorphic alleles flies and was able to significantly recuperate the locomotive capacity of these flies in climbing assays compared to GFP expressing controls (Figure 68).

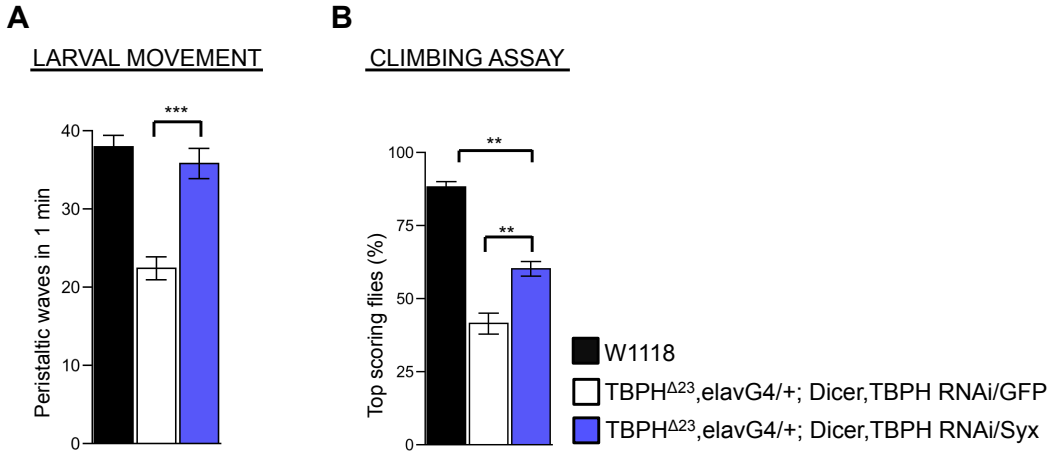

Figure 68 Genetic interactions between TBPH and Syntaxin1A.

(A) Quantification of peristaltic waves of third instar larvae expressing Syntaxin transgene in TBPH hypomorphic alleles flies (TBPH$^{\Delta 23}$,elavG4/+;Dicer,TBPH RNAi/Syx in blue) compare to TBPH hypomorphic alleles model flies expressing an

unrelated protein (GFP) (TBPH$^{\Delta 23}$,elavG4/+;Dicer,TBPH RNAi/GFP in white) and to wild type, in black. Expression of Syntaxin1A transgene showed an improvement in motility performance. The experiment was performed on third instar larvae, grown on normal food at a temperature of 29°C. n=25. (B) The climbing analysis revealed the same results observed in larvae. GFP did not improve the phenotype of TBPH hypomorphic alleles model; on the contrary the improvement obtained expressing Syntaxin1A was clear. The experiment was performed on adult flies at day 4, grown on normal food at a temperature of 25°C. n=100 *p<0.05 **p<0.01 ***p<0.001 calculated by one-way ANOVA. Error bars SEM.

This data suggested that in TBPH mutant a deficit in synaptic transmission occurred, in particular a deficit in neurotransmitter release in the synaptic cleft. In agreement with this hypothesis, I found that Syntaxin1A rescue of TBPH mutant larvae recovered the non-autonomous distribution of the postsynaptic membrane markers Dlg (Figure 69) and GluRIIA (Figure 70) suggesting that proper communication between pre and post zones was restored.

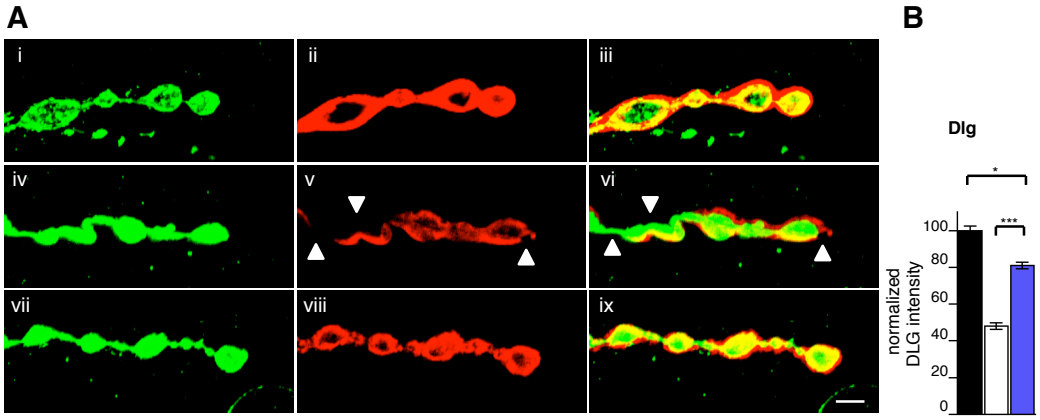

Figure 69 Syntaxin1A transgene restored Dlg in mutant background.

(A) Confocal image of synaptic terminal boutons stained with anti-HRP (pre-synaptic membrane) in green and with anti-Dlg in red. (i-iii, black column) wild type, (iv-vi, white column) TBPH$^{\Delta 23/-}$;elav-GAL4>UAS-GFP, (vii-ix, blue column) TBPH$^{\Delta 23/-}$;elav-GAL4>UAS-Syntaxin1A. A recovery of normal Dlg levels and distribution was observed in Syntaxin1A rescue, no evidence of recovery in GFP (unrelated protein), quantification was observed in (B). n=300/350 boutons *p<0.05 ***p<0.001 calculated by one-way ANOVA. Scale bar 5µm. Error bars SEM.

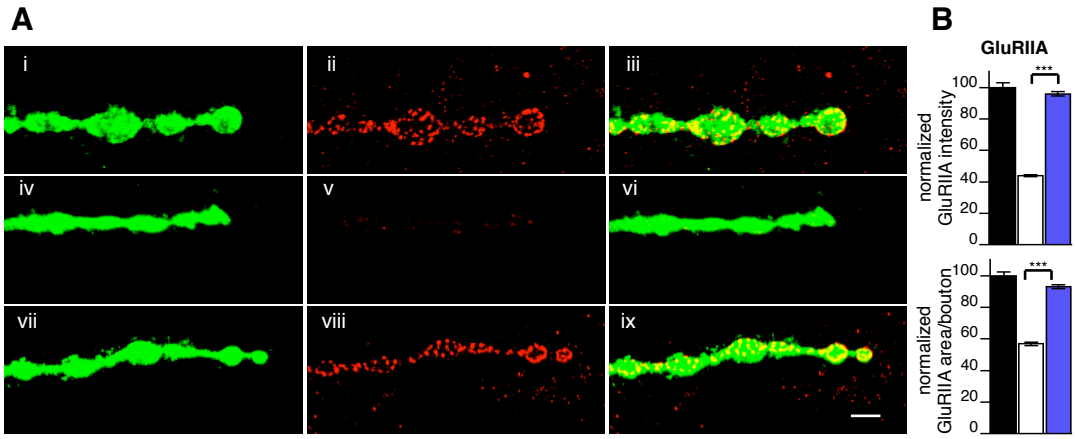

Figure 70 Syntaxin1A transgene restored GluRIIA in mutant background.

(A) Confocal image of synaptic terminal boutons stained with anti-HRP (pre-synaptic membrane) in green and with anti-GluRIIA in red. (i-iii, black column) wild type, (iv-vi, white column) $TBPH^{\Delta 23/-}$;elav-GAL4>UAS-GFP (vii-ix, blue column) $TBPH^{\Delta 23/-}$;elav-GAL4>UAS-Syntaxin1A. A recovery of normal glutamate receptor levels and distribution was observed in Syntaxin1A, no evidence of recovery in GFP (unrelated protein), quantification showed in (B). n=300/350 boutons **p<0.01 ***p<0.001 calculated by one-way ANOVA. Scale bar 5μm. Error bars SEM.

5 Discussion and conclusions

Alterations in TDP-43 protein are commonly found in patients suffering from amyotrophic lateral sclerosis (ALS) and in frontotemporal lobar degeneration (FTLD). TDP-43 is a RNA binding protein, highly conserved across species, involved in mRNA metabolism (transcription, splicing, mRNA stabilization, microRNA biogenesis, transport and stabilization), (Buratti & Baralle, 2009). Thus, the involvement of RNA metabolism in neurodegenerative diseases is starting to appear increasingly important. Therefore, determining the physiological role of the TDP-43 *in vivo* and understanding how defects in this protein function lead to motoneuron degeneration, constituted the main objectives of these studies.

5.1 Characterization of the physiological role of TDP-43 *in vivo*

To characterize the physiological role of TDP-43 protein *in vivo*, I generated genetic deletions in the TDP-43 homolog protein, TBPH, in *Drosophila* and confirmed that these interventions completely suppressed the expression of the endogenous protein in different TBPH minus alleles. Interestingly, I observed that the TBPH mutant phenotypes recapitulated the major traits of ALS pathology, thus, loss of *Drosophila* TDP-43 caused severe defects in locomotion (with spastic and uncoordinated movements that ended in paralysis), weakness and premature death. Moreover, these phenotypes were rescued by reintroducing the TBPH gene exclusively in the CNS and the same results were obtained using the human protein, demonstrating that the TDP-43 function is conserved evolutionarily.

In order to better understand the origin of these motility defects, I decided to analyse the morphology of the TBPH minus motoneuron presynaptic terminals at neuromuscular junctions (NMJs) and observed that, in TBPH minus larvae, the morphology of the presynaptic terminals was seriously affected. I found a reduced number of axonal branches and misshapen synaptic boutons in the terminal synapses of the motoneurons at the NMJ,

indicating that either the formation or the maintenance of these structures was compromised.

Similar morphological analysis of the synaptic terminals performed at different stages of the larval development, revealed no differences between wild type and TBPH mutants during the first larval stage (L1). The defects, however, became significantly evident in the larval stages (L2) and (L3), indicating that TBPH is necessary to promote and sustain synaptic growth during larval development. The analysis of footprints showed no evidence of synaptic retraction, supporting the hypothesis that defects in the growth and addition of new synaptic boutons rather than an increased retraction of already established boutons, represented the principal alterations behind these phenotypes. Expression of TBPH rescued these anatomical defects, indicating the direct and specific role of TBPH in the growth and maintenance of the synaptic terminals at NMJ.

The growth of NMJs occurs by the addition of new synaptic boutons that originate through the budding of their parent boutons. This entire process is mainly sustained by cytoskeletal factors, which I hypothesize, might be affected in TBPH mutants. Based on this, I found that the protein levels of the *Drosophila* specific microtubule binding protein Futsch, homolog to the mammalian MAP1B, were reduced in TBPH minus NMJs. A recovery of these phenotypes was possible by reintroducing the endogenous protein TBPH or the human protein TDP-43 in motoneurons, demonstrating that these alterations were specific to the TBPH function. In addition to this evidence, I also proved that the recovery of the neurological defects was dependent on the RNA binding capacity of TBPH, since the mutant form of TBPH (TBPH $^{F/L\text{-}150/152}$), unable to bind RNA, (Buratti & Baralle, 2001; Voigt *et al*, 2010) was not able to rescue the mutant phenotypes (Godena *et al*, 2011). Considering that Futsch plays a central role during the NMJs expansion process, these findings indicated that defects in the regulation of the protein levels of Futsch might be at the base of the morphological defects observed by the lack of TBPH function.

5.2 TBPH chronological requirements and neurological plasticity

A common characteristic of many neurodegenerative diseases is the late onset of pathological symptoms during adult life. The question regarding whether these neurological alterations occurred during neuronal development or later on, in already differentiated neurons, remains open. Clarifying these aspects might give an important contribution to better understanding ALS pathogenesis or prognosis, and may improve the knowledge required to find original therapeutic strategies. For these reasons, I moved on to analyse the chronological requirements of TBPH during different phases of the *Drosophila* life cycle. The results suggested there is a necessity for a continuous presence of the TBPH protein to guarantee proper locomotion of these flies and proper maintenance of NMJ terminals. The *in vivo* TBPH half-life was calculated to be about 12 hours, extremely similar to the life span recently determined for the human TDP-43 protein in vitro (12.6 hours) (Watanabe *et al*, 2013). These results highlight the similarities between the fly and human homologues and support the idea that TBPH function must be permanently required during neuronal development. To understand whether similar requirements for TBPH function were necessary in adult flies, we tested the effects of TBPH suppression in adult tissues through the expression of an RNAi against the protein. Interestingly, we observed that the acute suppression of TBPH in adult flies induced a rapid decrease in the climbing abilities of these insects and an abrupt collapse of their life span. These phenotypes, very similar to the symptoms described in ALS pathology, indicating that similar situations might be expected in individuals with sporadic defects in TDP-43 function.

A fundamental issue revolving around neurological disorders is to determine whether the affected neurons are able to recover from these pathological situations. Based on this, I evaluated the possibility of recovering TBPH mutant phenotypes in flies with already well differentiated neurons in which the pathological signs were clearly manifested. I observed that the late provision of TBPH in mature mutant L3 larvae provoked a rapid improvement of larval locomotion together with the regrowth and reassembly

of the motoneuron synaptic terminals. I also found that a similar late induction of TBPH in adult neurons was able to reactivate locomotive behaviours in otherwise paralyzed flies, demonstrating long lasting neuronal plasticity in TBPH minus flies. These results also suggest that affected neurons are still alive and able to recover their synaptic activity.

5.3 Early events of TBPH dysfunction *in vivo*

Recent studies have identified a huge number of potential TDP-43 targets, most of them belonging to proteins involved in synaptic activity pathways (Arnold *et al*, 2013; Hazelett *et al*, 2012). For example, one study on mouse adult brains performed a massive parallel sequencing and splicing sensitive junction arrays in which genes with very long introns encoding for proteins implicated in synaptic activity appeared highly modified (Polymenidou *et al*, 2011). Another study, through RIP-sequencing analysis found target genes for TDP-43 involved in RNA metabolism, neuronal development and synaptic function (Sephton *et al*, 2011).

I therefore decided to analyse the events that occurred immediately after TBPH dysfunction and found that 24 hours after reducing TBPH an immediate decrease in L3 larval locomotion occurred.

These motility defects correlated with a strong decrease in the synaptic levels of vesicular membrane proteins such as Syntaxin1A, Synapsin and Csp that was also observed in flies constitutively expressing the anti-TBPH RNAi during the complete larval development or in adult flies carrying TBPH loss of function mutations. Interestingly, I observed that structural proteins of the synaptic terminals like Bruchpilot were not affected after similar treatments, indicating that these synaptic alterations were rather specific and suggesting that vesicular membrane pathways like exo-endocytosis or synaptic transmission might be directly affected upon TBPH dysfunction. Defects in this process could imply the presence of alterations at nerve-muscle contact level. In this regard, I tested the molecular organization of the postsynaptic membranes after the acute TBPH suppression and found alterations in the distribution of Dlg protein, a scaffold molecule crucial to the postsynaptic localization of numerous proteins including the glutamate

receptors. Dlg appeared strongly reduced and abnormally distributed, unable to define single synaptic structures, surrounding large groups of boutons, and even absent from big areas of the presynaptic surface. I also observed a decreased in Glutamate receptor IIA, the pattern of GluRIIA staining became more diffuse and irregular with significantly less ring-shaped spots typically found in wild type. These early defects in Dlg and GluRIIA became progressively increased in flies expressing anti-TBPH RNAi from the beginning of the neuronal development, indicating that these modifications are highly dependent of presynaptic TBPH levels. In support of these observations, I found that transgenic expression of TBPH exclusively in neurons was sufficient to rescue the postsynaptic defects in Dlg and GluRIIA distribution observed in TBPH minus NMJs, confirming that early defects in motoneuron neurotransmission may lead to muscle denervation in *Drosophila*.

5.4 TBPH directly interacts with *syntaxin1A* and *futsch* mRNA

Previous studies have demonstrated that the functional properties of TDP-43 strongly depend on its RNA binding ability (Buratti & Baralle, 2010). Therefore to gain further comprehension of the mechanisms of TBPH functionality, I tested for a possible direct interaction between the TBPH protein and the mRNAs of the perturbed markers found to be down-regulated after the acute suppression of TBPH. The co-immunoprecipitation assay *in vivo* of TBPH protein revealed a significant mRNA enrichment for *futsch* and *syntaxin1A*, proving direct evidences of physical interactions between these mRNAs and the TBPH protein *in vivo*. Moreover, to test the functional relevance of these protein-mRNA interactions, I analysed whether the prevention of Futsch or Syntaxin1A down-regulation in TBPH mutant flies was able to recover the neurological phenotypes described above.

Previous data demonstrated that neuronal expression of mammalian Tau protein was able to rescue Futsch loss of function phenotype in *Drosophila* neurons (Bettencourt da Cruz *et al*, 2005). Thus I expressed Tau protein in TBPH mutant flies found a rescue of the morphological defects described in the TBPH mutant NMJs, however the functional rescue was not achieved

indicating that TBPH has a role in the stabilization of microtubules but also regulates other additional functions, not through Futsch interaction. On the other hand, the expression of Syntaxin1A transgene in the TBPH mutant, was able to rescue the locomotive defects of the mutant phenotype and moreover it also appeared to rescue the structural defects observed in the distribution and localization of the postsynaptic membrane proteins, Dlg and GluRIIA at the NMJs level. This evidence demonstrated that regulation of Syntaxin1A levels through the direct interaction with TBPH was fundamental to promote the formation and differentiation of the motoneuron synaptic terminals. Intriguingly, I observed that the rescue of Synataxin levels with Elav-Gal4 was not sufficient to recover pupal lethality associated with TBPH loss of function (Feiguin *et al*, 2009). Nevertheless, I observed that Syntaxin expression in adult TBPH hypomorphic alleles, generated by the induction of anti-TBPH RNAi expression in neurons, was able to significantly recuperate the locomotive capacity of these flies in climbing assays compared to GFP expressing controls, confirming the relevance of these regulatory interactions in adult flies.

5.5 Possible mechanism of TBPH dysfunction

The transmission of electro-chemical signals from neurons to muscles is essential to induce and maintain, the formation of postsynaptic structures in muscle surfaces. Consequently, it was described that defects in synaptic transmission affected the intracellular distribution of different postsynaptic proteins like Dlg and the Glutamate Receptor from the muscle surface (Budnik *et al*, 1996; Chen & Featherstone, 2005; Lee *et al*, 2009).

Considering that the acute suppression of TBPH in mature larvae provokes the down-regulation of Syntaxin1A, and causes defects in the organization of the postsynaptic proteins Dlg and the Glutamate Receptor at the NMJs, the data strongly indicates that TBPH regulates synaptic transmission. In agreement with that, it was previously described that Syntaxin1A plays a central role in synaptic membrane fusion and recycling events as well as neurotransmitter release (Khuong *et al*, 2013; Kidokoro, 2003).

At the functional level, the connection between all these gene expression steps is usually provided by the assembly in distinct multimeric complexes made by different combinations of nuclear proteins. Among the proteins responsible for creating the «backbone» of these multimeric complexes, the hnRNP class of RNA Binding proteins (RBPs) certainly plays a major role in terms of numbers and quantity. This is especially true in neurons that display an extremely high complexity at the level of differential RNA expression, generated in good part by hnRNP proteins. One expectation of such important role played by hnRNP proteins is that their eventual mis-regulation would certainly be capable of causing neuronal death.

In keeping with this view, one of the major breakthroughs in ALS and other neurodegenerative disease research in recent years has been the discovery that alterations in RNA metabolism may play a major role in the onset and progression of various diseases such as ALS and FTLD. Common causes of these diseases include alterations in the aggregation, sequence and localization status of factors such as TDP-43, FUS/TLS and other FET family proteins (FUS, EWSR1 and TAF15) (Hoell *et al*, 2011). In addition, the presence of hexanucleotide expansions in the C9orf72 gene associated with disease has also raised the possibility that the effect of pathological RNA foci may contribute sequestering additional RBPs, and thus contribute to influence the onset and progression of disease. Recently, it has been shown that mutations in hnRNP A/B protein family can be associated with the development of ALS and multisystem proteinopathy. Nonetheless there is still much to learn regarding the importance of this protein family in neuronal survival (Kim *et al*, 2013). In agreement with this hypothesis, parallel experiments performed in our laboratory detected that the *Drosophila* Hrp38 (homologue to human hnRNP A/B family) physically interacts with TDP-43 and the reduction of the Hrp38 expression in *Drosophila* brains produces significant locomotive alterations with the shortening of the life span (Romano *et al*, 2014), closely resembling the defects observed in TBPH-knockout flies and suggesting that these proteins might be involved in the regulation of common metabolic pathways.

Therefore, I can conclude that TBPH plays a fundamental role in promoting the formation and differentiation of neuromuscular synapses and the correct process of synaptic vesicle dynamics like exocytosis. This function is mediated by the capacity of this protein to interact with the RNA molecules and others RBPs inside multimeric complexes to regulate the cytoplasmic levels of different synaptic proteins, as Futsch or Syntaxin1A through modifications in the metabolism of these messengers.

Subsequently to the TBPH presynaptic dysfunction, alteration in synaptic transmission are expected, followed by secondary defects in the organization of the postsynaptic membranes as the decrease in Glutamate receptor activity and in Dlg protein levels (a simplified scheme of this process is reported in Figure 71).

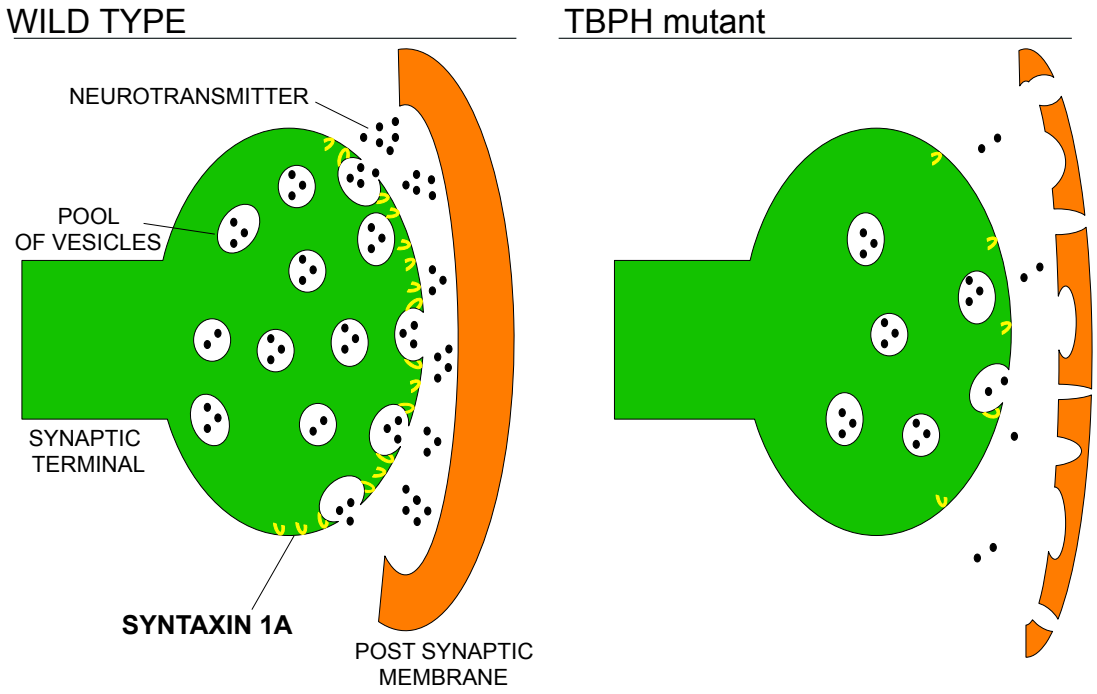

Figure 71 Possible mechanism model in the TBPH mutant.

Schematic representation of synaptic bouton organization in TBPH mutant.

In agreement with this view, I observed that improving Syntaxin1A levels in TBPH mutant phenotypes was sufficient to recover the functional motility defects present in these insects, as well as the structural defects observed in the distribution of the postsynaptic proteins Dlg and GluRIIA, highlighting the

central role of TBPH in the regulation of synaptic function and muscle innervation.

6 Concluding remarks

The main purposes of these studies were to describe the physiological role of the TDP-43 homolog protein in *Drosophila*, known as TBPH, and to identify its functional partners and determine the neurological consequences of the protein dysfunction.

The main conclusions of this thesis can be summarized as follows:

1) TBPH is permanently required in the CNS to regulate locomotive behaviour, life span and the molecular organization of motoneuron presynaptic terminals at NMJs.

2) TBPH directly interacts with *futsch* and *syntaxin1A* mRNA to regulate their intracellular protein levels and synaptic function.

3) Acute defects in TBPH function in neurons provokes a rapid impairment in flies locomotion through the down-regulation of presynaptic vesicular proteins followed by non-autonomous defects in muscles innervation.

4) A late correction of functional TBPH levels in neurons is sufficient to induce the recovery of the neurological phenotypes observed in TBPH mutants and promotes the reassemble of motoneuron synaptic terminals.

Appendix I

Western blot films full size

For each protein analysed via Western blot, a full size film is reported below and a scheme containing the predicted molecular weight of the proteins (obtained from *FlyBase.org*) has been added.

Synapsin

Annotated Polypeptides						
Name	FlyBase ID	Predicted MW (kDa)	Length (aa)	Theoretical pI	RefSeq ID	GenBank protein
Syn-PA	FBpp0088969	57.7	537	9.11	NP_731457	AAN13462
Syn-PD	FBpp0099901	109.4	1041	8.09	NP_731459	AAF54506
Syn-PE	FBpp0099902	64.1	597	9.10	NP_731458	AAN13463
Syn-PF	FBpp0088481	103.0	981	8.10	NP_788628	AAO41538

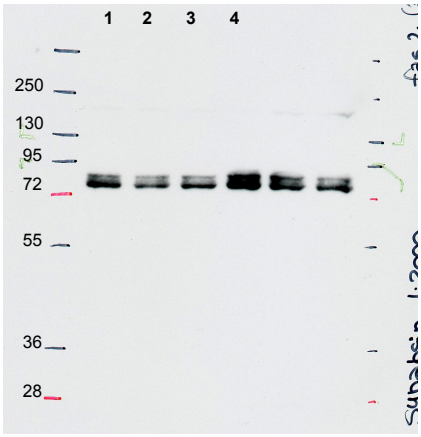

1 W1118
2 TBPH$^{\Delta 23/-}$
3 TBPH$^{\Delta 142/-}$
4 TBPH$^{\Delta 23/-}$;elavG4>TBPH (rescue)

Bruchpilot

Annotated Polypeptides						
Name	FlyBase ID	Predicted MW (kDa)	Length (aa)	Theoretical pI	RefSeq ID	GenBank protein
brp-PD	FBpp0289193	201.7	1740	6.13	NP_724796	AAM71068
brp-PE	FBpp0289194	201.7	1740	6.13	NP_995785	AAS64886
brp-PG	FBpp0289478	206.7	1786	6.25	NP_001097241	ABV53738
brp-PH	FBpp0289769	201.7	1740	6.13	NP_001036535	AAF58930
brp-PI	FBpp0293596	161.7	1397	5.80	NP_001246227	AFH07982
brp-PJ	FBpp0293597	255.3	2238	6.90	NP_001246228	AFH07983
brp-PK	FBpp0293598	197.4	1707	6.27	NP_001246229	AFH07984
brp-PL	FBpp0293599	206.2	1781	6.24	NP_001246230	AFH07985
brp-PM	FBpp0307674	173.5	1498	6.21	NP_001260826	AGB93359

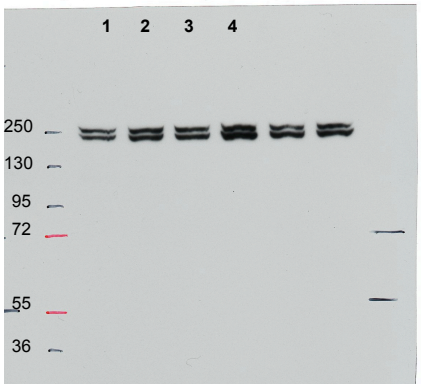

1 W1118
2 TBPH$^{\Delta 23/-}$
3 TBPH$^{\Delta 142/-}$
4 TBPH$^{\Delta 23/-}$;elavG4>TBPH (rescue)

Syntaxin1A

Annotated Polypeptides						
Name	FlyBase ID	Predicted MW (kDa)	Length (aa)	Theoretical pI	RefSeq ID	GenBank protein
Syx1A-PA	FBpp0083973	33.6	291	5.09	NP_524475	AAF56232
Syx1A-PB	FBpp0292260	34.2	296	5.20	NP_001189276	ADV37366

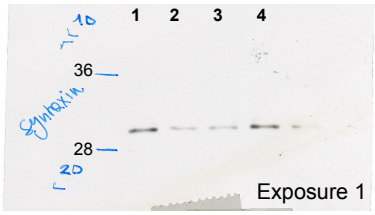

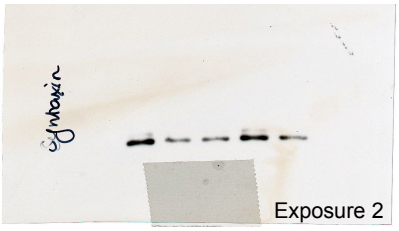

1 W1118
2 TBPH$^{\Delta 23/-}$
3 TBPH$^{\Delta 142/-}$
4 TBPH$^{\Delta 23/-}$;elavG4>TBPH (rescue)

Csp

Annotated Polypeptides						
Name	FlyBase ID	Predicted MW (kDa)	Length (aa)	Theoretical pI	RefSeq ID	GenBank protein
Csp-PA	FBpp0078145	23.8	223	5.03	NP_524213	AAF51817
Csp-PB	FBpp0078146	26.9	249	5.32	NP_730713	AAF51816
Csp-PC	FBpp0078147	24.6	228	5.04	NP_730714	AAN12195
Csp-PD	FBpp0306787	26.2	244	5.30	NP_001262206	AGB94899
Csp-PE	FBpp0306788	26.2	244	5.30	NP_001262207	AGB94900
Csp-PF	FBpp0311238	26.9	249	5.32		

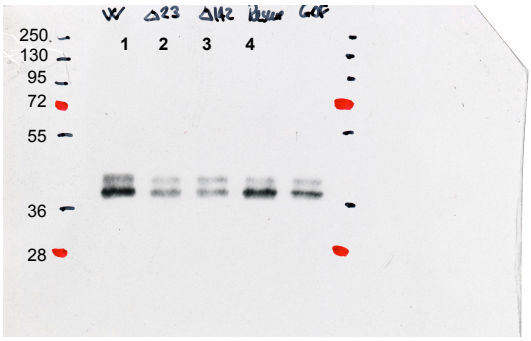

1 W1118
2 TBPH$^{\Delta 23/-}$
3 TBPH$^{\Delta 142/-}$
4 TBPH$^{\Delta 23/-}$;elavG4>TBPH (rescue)

TBPH

Annotated Polypeptides						
Name	FlyBase ID	Predicted MW (kDa)	Length (aa)	Theoretical pI	RefSeq ID	GenBank protein
TBPH-PA	FBpp0088569	37.7	332	6.42	NP_477399	AAF47080
TBPH-PB	FBpp0088567	58.1	531	7.15	NP_477400	AAF47079
TBPH-PC	FBpp0088568	58.1	531	7.15	NP_599145	AAF47078
TBPH-PD	FBpp0088570	58.1	531	7.15	NP_726373	AAM68274
TBPH-PE	FBpp0290857	58.1	531	7.15	NP_001163280	ACZ94552
TBPH-PF	FBpp0290858	58.1	531	7.15	NP_001163281	ACZ94553

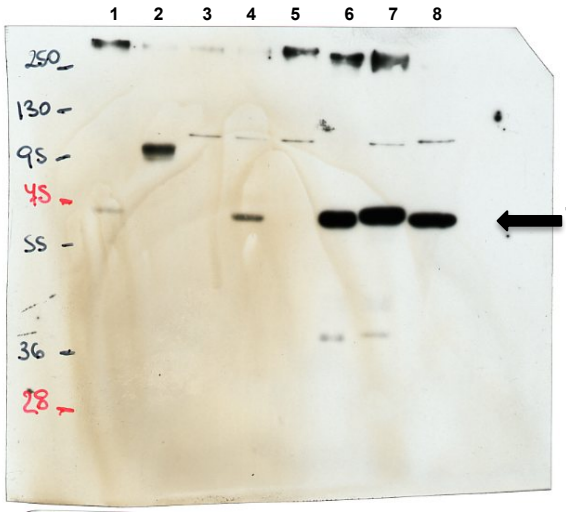

1 W1118
2 TBPH$^{\Delta 23/-}$
3 TBPH$^{\Delta 23/-}$;elavGS G4>TBPH $_{inactivated}$ (inactivated rescue)
4 W1118
5 TBPH$^{\Delta 23/-}$;elavGS G4>TBPH $_{inactivated}$ (inactivated rescue)
6 TBPH$^{\Delta 23/-}$;elavGS G4>TBPH $_{activated}$ (activated rescue)
7 TBPH$^{\Delta 23/-}$;elavGS G4>TBPH $_{activated}$ (inactivated rescue)
8 TBPH$^{\Delta 23/-}$;elavGS G4>TBPH$^{F/L}$ $_{activated}$ (activated rescue)

Futsch

Annotated Polypeptides						
Name	FlyBase ID	Predicted MW (kDa)	Length (aa)	Theoretical pI	RefSeq ID	GenBank protein
futsch-PC	FBpp0111540	592.1	5495	4.61	NP_001096864	ABW09325
futsch-PE	FBpp0300235	592.1	5495	4.61	NP_001162632	AAF45622
futsch-PF	FBpp0300236	592.1	5495	4.61	NP_001245461	AFH07176

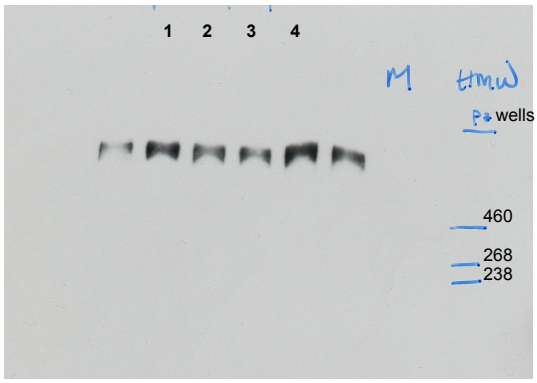

1 TBPH$^{\Delta 23/-}$;elavG4>TBPH (rescue)
2 TBPH$^{\Delta 142/-}$
3 TBPH$^{\Delta 23/-}$
4 W1118

Actin

Annotated Polypeptides						
Name	FlyBase ID	Predicted MW (kDa)	Length (aa)	Theoretical pI	RefSeq ID	GenBank protein
Act5C-PA	FBpp0070787	41.8	376	5.16	NP_727048	AAF46098
Act5C-PB	FBpp0070788	41.8	376	5.16	NP_511052	AAN09154
Act5C-PC	FBpp0100124	41.8	376	5.16	NP_001014726	AAX52479
Act5C-PD	FBpp0100125	41.8	376	5.16	NP_001014725	AAX52480
Act5C-PE	FBpp0311818	41.8	376	5.16		

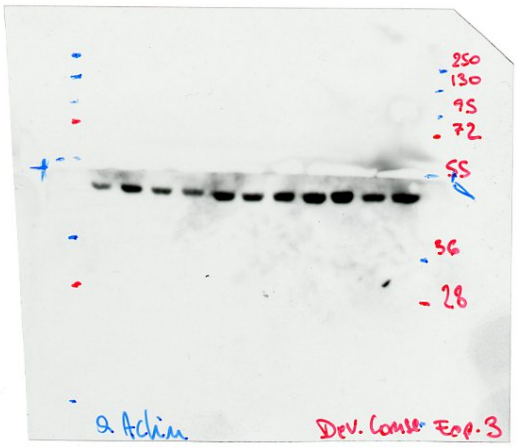

α Tubulin

Annotated Polypeptides						
Name	FlyBase ID	Predicted MW (kDa)	Length (aa)	Theoretical pI	RefSeq ID	GenBank protein
αTub84B-PA	FBpp0081153	49.9	450	4.78	NP_476772	AAF54067

Disc Large

Annotated Polypeptides						
Name	FlyBase ID	Predicted MW (kDa)	Length (aa)	Theoretical pI	RefSeq ID	GenBank protein
dlg1-PA	FBpp0073342	103.2	968	8.49	NP_727520	AAF48038
dlg1-PB	FBpp0089351	106.7	970	6.75	NP_996406	AAS65308
dlg1-PC	FBpp0073339	24.4	208	10.43	NP_727518	AAF48037
dlg1-PD	FBpp0073341	102.4	960	7.87	NP_511120	AAF48039
dlg1-PE	FBpp0089350	102.4	960	7.87	NP_996407	AAS65313
dlg1-PF	FBpp0073340	88.7	816	4.49	NP_727519	AAN09630
dlg1-PG	FBpp0089352	104.0	975	7.15	NP_996405	AAS65312
dlg1-PH	FBpp0089353	100.2	911	6.95	NP_996404	AAS65309
dlg1-PI	FBpp0089348	24.4	208	10.43	NP_996403	AAS65310
dlg1-PJ	FBpp0089349	24.4	208	10.43	NP_996402	AAS65311
dlg1-PK	FBpp0111724	100.5	911	8.77	NP_001096955	ABW09394
dlg1-PL	FBpp0111725	104.3	946	6.61	NP_001096956	ABW09395
dlg1-PM	FBpp0290503	112.5	1030	4.80	NP_001162718	ACZ95253
dlg1-PN	FBpp0290504	102.4	960	7.87	NP_001162719	ACZ95254
dlg1-PO	FBpp0291324	24.2	206	10.43	NP_001162720	ACZ95255
dlg1-PP	FBpp0300431	104.9	983	7.56	NP_001245622	AFH07336
dlg1-PQ	FBpp0300432	104.0	975	7.15	NP_001245623	AFH07337
dlg1-PR	FBpp0303416	106.8	1001	8.95	NP_001259446	AGB95289
dlg1-PS	FBpp0305459	102.4	960	7.87	NP_001259447	AGB95290
dlg1-PT	FBpp0305460	100.6	943	9.06	NP_001259448	AGB95291
dlg1-PU	FBpp0305461	23.3	198	10.43	NP_001259449	AGB95292

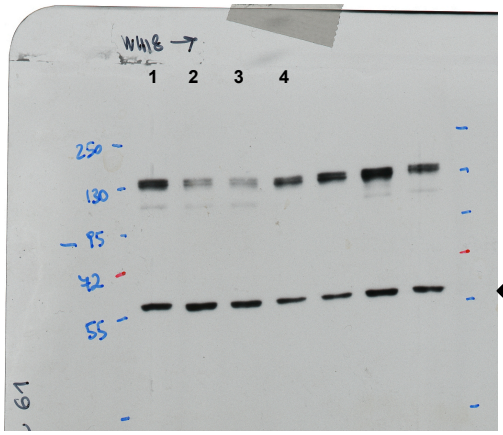

1 W1118
2 TBPH$^{\Delta 23/-}$
3 TBPH$^{\Delta 142/-}$
4 TBPH$^{\Delta 23/-}$;elavG4>TBPH (rescue)

← α tubulin

Appendix II

Candidate's publication

The candidate has published during the PhD period the following articles, on which most of the thesis work is based:

Feiguin F, Godena VK, Romano G, D'Ambrogio A, Klima R, Baralle FE. Depletion of TDP-43 affects Drosophila motoneurons terminal synapsis and locomotive behavior. FEBS Lett. 2009 May 19;583(10):1586-92.

Godena VK*, Romano G*, Romano M, Appocher C, Klima R, Buratti E, Baralle FE, Feiguin F. *(These authors contributed equally to this work). TDP-43 Regulates Drosophila Neuromuscular Junctions Growth by Modulating Futsch/MAP1B Levels and Synaptic Microtubules Organization. PLOS ONE. 2011 Mar 11;6(3):E17808.

Romano M, Buratti E, Romano G, Klima R, Del Bel Belluz L, Stuani C, Baralle FE, Feiguin F. Evolutionarily-conserved hnRNP A/B proteins functionally interact with human and Drosophila TAR DNA-binding protein 43 (TDP-43). J Biol Chem. 2014 Feb 3;jbc.M114.548859.

Romano G, Klima R, Buratti E, Verstreken P, Baralle FE, Feiguin F. Chronological requirements of TDP-43 function in synaptic organization and locomotive control. 2014 Neurobiology of Disease (under 2nd resubmission).

FEBS Letters 583 (2009) 1586–1592

FEBS Letters

journal homepage: www.FEBSLetters.org

Depletion of TDP-43 affects *Drosophila motoneurons* terminal synapsis and locomotive behavior

Fabian Feiguin *, Vinay K. Godena, Giulia Romano, Andrea D'Ambrogio, Raffaella Klima, Francisco E. Baralle *

International Centre for Genetic Engineering and Biotechnology, Padriciano 99, 34012 Trieste, Italy

ARTICLE INFO

Article history:
Received 30 January 2009
Revised 3 April 2009
Accepted 13 April 2009
Available online 19 April 2009

Edited by Jesus Avila

Keywords:
Drosophila
TDP-43
Als
Motoneurons
Synapsis
Locomotion

ABSTRACT

Pathological modifications in the highly conserved and ubiquitously expressed heterogeneous ribonucleoprotein TDP-43 were recently associated to neurodegenerative diseases including amyotrophic lateral sclerosis (ALS), a late-onset disorder that affects predominantly motoneurons [Neumann, M. et al. (2006) Ubiquitinated TDP-43 in frontotemporal lobar degeneration and amyotrophic lateral sclerosis. Science 314, 130–133, Sreedharan, J. et al. (2008) TDP-43 mutations in familial and sporadic amyotrophic lateral sclerosis. Science 319, 1668–1672, Kabashi, E. et al. (2008) TARDBP mutations in individuals with sporadic and familial amyotrophic lateral sclerosis. Nat. Genet. 40, 572–574]. However, the function of TDP-43 in vivo is unknown and a possible direct role in neurodegeneration remains speculative. Here, we report that flies lacking Drosophila TDP-43 appeared externally normal but presented deficient locomotive behaviors, reduced life span and anatomical defects at the neuromuscular junctions. These phenotypes were rescued by expression of the human protein in a restricted group of neurons including motoneurons. Our results demonstrate the role of this protein in vivo and suggest an alternative explanation to ALS pathogenesis that may be more due to the lack of TDP 43 function than to the toxicity of the aggregates.

1. Introduction

TDP-43 is a highly conserved and ubiquitously expressed nuclear protein containing RNA binding motives and reported to be involved in pre-mRNA splicing, transcription, mRNA stability, and mRNA transport [4]. Recently, TDP-43 was identified as the main protein component of the intracellular inclusions observed in affected brain areas of patients suffering from Amyotrophic Lateral Sclerosis (ALS), Frontotemporal Lobar Degeneration with ubiquitinated inclusions (FTLD-U) [1,5,6] and Alzheimer disease (AD) [7–9]. In the brain of these individuals TDP-43 appears depleted from the cell nucleus and abnormally localized inside insoluble protein aggregates throughout the cytoplasm. Moreover, missense mutations in the C-terminal part of TDP-43 were identified in 2–5% of sporadic and familial forms of ALS indicating that a tight correlation between TDP-43 protein function and neurodegenerative diseases may exist [2,3].

Despite the fact that the biochemical and structural properties of TDP-43 were extensively studied, its physiological role in vivo or the possible pathological mechanisms that may lead to neuronal diseases were not determined [10]. Regarding this, considerable attention has been given to the potential toxic effect of the TDP-43 protein aggregates observed in the cytoplasm. However it should also be considered that in those neurons TDP-43 seems to be absent from the nucleus. Therefore, it might be possible that the defects observed in ALS patients reflect a loss of TDP-43 nuclear function rather than a pure toxic effect of its aggregates.

We have previously shown that the Drosophila TDP-43 homolog was able to replace the splicing function of the human protein in vitro and in tissue culture cells [11,12], for that reason we decided to investigate the role of TDP-43 in vivo using Drosophila melanogaster as the animal model.

2. Material and methods

2.1. Generation of TBPH null alleles

TBPH loss-of-function alleles were generated by imprecise mobilization of $TBPH^{EY10530}$ transposon using Δ2–3 transposase. Potential candidates were identified by the loss of w^+ markers and balanced to stock. Genomic DNA from 450 lines was used as polymerase chain reaction templates. Primers flanking the EY10530 insertion were used for mapping (1R:19750253-19750232; 2R:19750667-19750640; 1F:19746555-19746576; 3F:19747048-19747071; 4F:19748563-19748583; 5F:19749069-19749089; 6F:19749727-19749746). $TBPH^{\Delta 23}$ revealed a deletion of 1616 bp with complete elimination of the P-element and break

* Corresponding authors.
E-mail addresses: feiguin@icgeb.org (F. Feiguin), baralle@icgeb.org (F.E. Baralle).

0014-5793/$36.00 © 2009 Federation of European Biochemical Societies. Published by Elsevier B.V. All rights reserved.
doi:10.1016/j.febslet.2009.04.019

points at 19748477–19750093. In the case of TBPH$^{\Delta 142}$, the deletion is from 19749289 to 19750093 including a fragment of EY10530 imprecisely excised (1138 bp).

2.2. Preparation of TBPH antibody

TBPH protein fragment from amino acids 1–268 GST conjugated was expressed and purified from *Escherichia coli* over a GST-resin following supplier protocols (Clontech #635610) and utilized to immunize rabbits according to standard immunization protocols.

2.3. Western blot analysis

Drosophila heads were squeezed in lysis buffer (10 mM Tris–HCl pH 7.4, 150 mM NaCl, 5 mM EDTA, 5 mM EGTA, 10% Glycerol, 50 mM NaF, 5 mM DTT, 4 M Urea, and protease inhibitors (Roche Diagnostic #11836170001). The proteins separated by 8% SDS–PAGE, were transferred to nitrocellulose membranes (GE Healthcare #RPN303E) and probed with primary antibodies: TBPH (1:3000) and tubulin (1:2000; Calbiochem #CP06). Secondary antibodies: (HRP)-labeled anti-mouse or anti-rabbit antibodies (1:10000) (Pierce #31460; #31430)) and developed using ECL (#RPN2109; GE healthcare).

2.4. Immunohistochemistry

Larval body wall muscles were dissected in saline containing 0.1 mM Ca^{+2} and fixed in ice-cold 4% paraformaldehyde for 20 min, washed in PBS/0.1% Tween 20, blocked with 5% Normal Goat Serum (NGS Chemicon #S26-100 ML) 30 min. Primary Anti-HRP antibody (Jackson Immunoresearch laboratories, #323-005-021) (1:100) over night at 4 °C. Secondary anti-rabbit antibody conjugated with Alexa 488 (1:500) (Invitrogen #411008) or Phalloidin TRITC (1:500 dilution) for 2 h.

2.5. NMJ analysis

Wandering third instar larvae were processed as before and the number of terminals branches and type 1b (big) and 1s (small) boutons present in muscle 6/7 from abdominal segments 2 to 4 were quantified. To obtain the images from the synaptic terminals, a 12–15 μm deep Z-series containing the entire NMJ were collected with a confocal laser-scanning microscope.

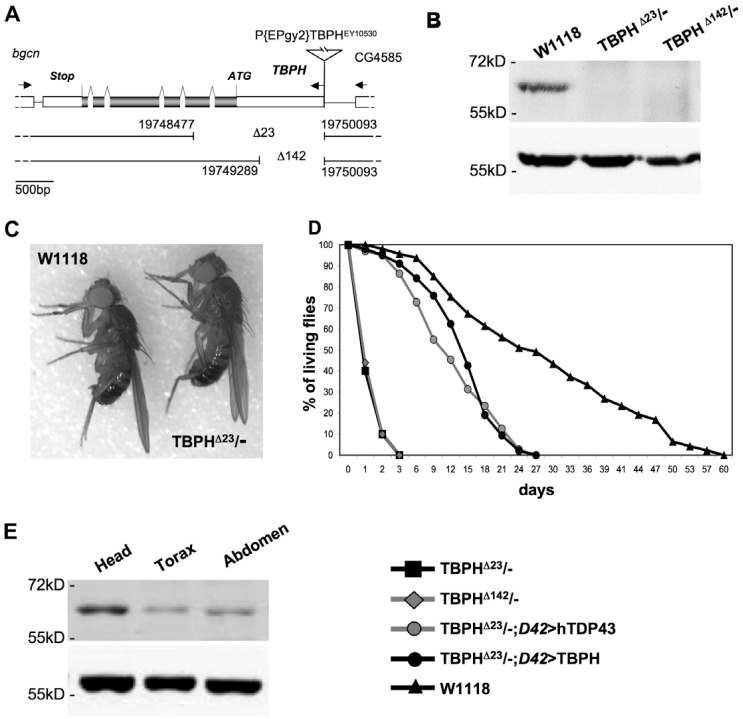

Fig. 1. Depletion of Drosophila TBPH affects locomotive behavior and life span. (A) Schematics of TBPH mutant alleles. (B) Western blot stained with anti-TBPH antibody, detects no endogenous protein in mutant fly heads (upper panel) tubulin was a loading control (bottom panel,). (C) Wild type controls and TBPH mutant flies appear externally identical. (D) Life span reduction in TBPH mutant flies can be rescued by expression of either drosophila or human TDP-43 transgene in *D42*-GAL4 expressing neurons. (E) Western blot analysis shows higher TBPH protein levels in fly heads compared to torax or abdomen (upper panel). Tubulin was a loading control (bottom panel).

2.6. Eclosion analysis

Embryos from TBPH$^{\Delta 23}$/CyoGFP, TBPH$^{\Delta 142}$/CyoGFP and Oregon R flies were collected during two hours at 25°. Homo or heterozygous larvae, identified based on the absence or presence of GFP expression, were selected between 26 and 28 h after egg laying using a fluorescent stereo microscope. Hatched first instar wild type, TBPH homozygous and heterozygous larvae were collected, placed into new vials in batches of 25–30 larvae per vial, and grown at 25°C. Developmental viability was calculated as percentage of hatched first instar larvae that survived to pupae and adulthood.

2.7. Transgenic flies and genetic rescue experiments

Endogenous TBPH and Human TDP-43 cDNAs were Flag tagged and cloned in modified 10 UAS vector (*Eco*RI-*Xba*I) to generate transgenic flies by standard embryo injections (Best Gene Inc.). Insertion lines on the 3rd chromosome were combined with 2nd chromosome TBPH$^{\Delta 23}$ allele using second and third chromosome compound balancer (ST). TBPH$^{\Delta 23}$;UAShTDP-43/ST females were crossed against TBPH$^{\Delta 23}$;*D42*-GAL4/ST or TBPH$^{\Delta 23}$;*elav*-GAL4/ST males and the number of TBPH$^{\Delta 23}$ homozygous flies in the progeny analyzed.

2.8. RNAi treatment in vivo and fly stocks

The double strand RNAi against TBPH were obtained from VDRC Vienna (ID38377 and ID38379) and target the genomic sequence situated in the chromosomal position 19748365–19748665 that corresponds to the TBPH amino acid sequences 81–180. These lines were crossed against *elav*-GAL4 and *1407*-GAL4 in wild type or TBPH$^{\Delta 23}$ heterozygous backgrounds. All crosses were done at 29°C. All the stocks utilized here (*elav*-GAL4, *1407*-GAL4, *D42*-GAL4, Δ2-3-Sb/TM3 transposase and UAScd8GFP), were obtained from Bloomington Drosophila Stock Center.

2.9. Larval movement

One hundred and twenty hours aged larvae were selected individually, washed briefly with distilled water to remove any remaining food and carefully transferred to a LB agar plate under

Table 1
Developmental viability analysis of TBPH mutant flies.

Genotypes	1st Instar larvae (28 h) N	Pupa		Eclosed flies		Trapped flies		Motility defects (%)
TBPH$^{\Delta 23}$/CyO^{GFP}	1127	734	65%	586	52%	26	2%	0
TBPH$^{\Delta 142}$/CyO^{GFP}	1056	616	58%	446	42%	42	4%	0
TBPH$^{\Delta 23}$/TBPH$^{\Delta 23}$	930	591	64%	197	21%	295	32%	100
TBPH$^{\Delta 142}$/TBPH$^{\Delta 142}$	539	327	61%	86	16%	172	32%	100
OregonR	758	628	83%	543	72%	15	2%	0

Quantitative analysis of TBPH minus flies from embryonic stages to adulthood indicates that this mutation induce little larval or pupal, -but not embryonic-, lethality. Nevertheless, homozygous flies present serious motility defects during eclosion and adulthood.

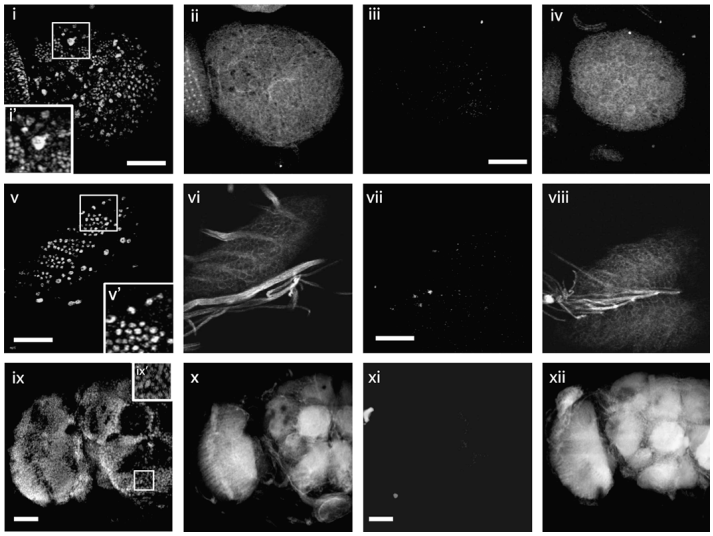

Fig. 2. Endogenous TBPH protein is present in larval and adult brains. Anti-TBPH immunostaining in wild type larval (i, v) and adult (ix) brains show the intracellular localization of the endogenous protein. Squares (i^0, v^0, ix^0) are higher magnifications. Signal disappear in TBPH$^{\Delta 23}$ homozygous brains (iii, vii and xi). ii, vi, x, iv, viii and xii are phalloidin staining. Scale: 50 μm.

stereoscope. Larvae were allowed to adapt for 30 s and the number of peristaltic waves during the period of two minutes time were counted. Around 30 larvae were counted for each genotype and separate LB agar plate was used for each genotype.

2.10. Climbing assay

Newly eclosed males were transferred in batches of 30 to fresh vials and aged for 3–4 days. They were transferred, without anesthesia, to a 15 ml conical tube, tapped to the bottom of the tube, and their subsequent climbing activity quantified as the percentage of flies that reach the top of the tube in 15 s.

2.11. Walking assay

Newly eclosed males were transferred in batches of 15 to fresh vials and aged for 3–4 days. Individual flies were placed in the center of 145 mm Petri dish marked with 1 cm square grid. Locomotion was quantified as the number of grid line crossings during 30 s.

2.12. Life span

Adult flies were collected during two days and transferred to fresh tubes at a density of 20 per vial with a proportion of 10 male

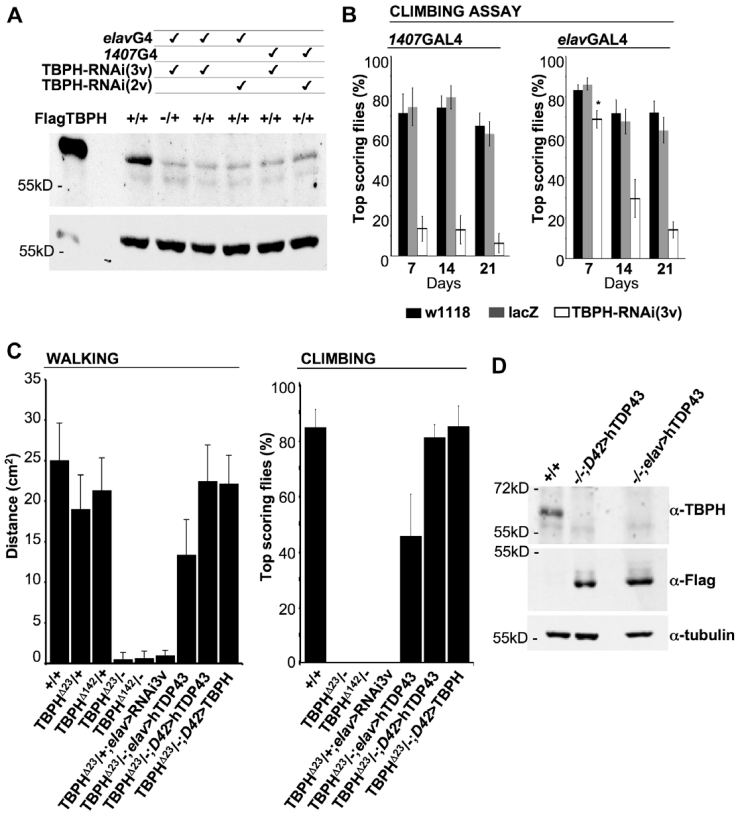

Fig. 3. Presynaptic TBPH function regulates flies locomotion. (A) Expression of two different TBPH RNAi insertions in neurons using *1407*-GAL4 and *elav*-GAL4 reduced endogenous TBPH protein in adult heads (upper blot). First line shows TBPH transfected S2 cell extracts as a positive control. (+/+) states for wild type backgrounds while (/ +) is for $TBPH^{\Delta 23}$ heterozygous flies. Tubulin was internal loading control (lower blot). (B) Climbing defects in TBPH RNAi treated flies during time, *1407*-GAL4 > TBPH-RNAi (left) and *elav*-GAL4>TBPH-RNAi (right), compared to wild type or GAL4 flies expressing UAS-LacZ. $n = 100$ flies for genotype, error bars indicate S.D.; asterisk $P < 0.0001$ by ANOVA single factor. (C) TBPH homozygous or heterozygous alleles treated with *elav*-GAL4 > TBPH RNAi (forth, fifth and sixth lanes of the left graph), present impaired spontaneous walking and climbing activities (second, third and forth lanes of the right graph). These defects become suppressed by expressing hTDP-43 with the pan-neuronal *elav*-GAL4 or the more restricted neuronal driver *D42*-GAL4. Similar rescue was obtained with the endogenous TBPH protein (last three lanes). $n = 50$ flies for each genotype, error bars indicate S.D.; $P < 0.0001$ calculated by ANOVA single factor. (D) Western blot analysis of rescued flies. $TBPH^{\Delta 23}/TBPH^{\Delta 23}$;*D42*-GAL4/UAShTDP-43 and $TBPH^{\Delta 23}/TBPH^{\Delta 23}$;*elav*-GAL4/UAShTDP-43 flies were blotted using antibodies against TBPH (upper blot) and against Flag to label flagged hTDP-43 (middle blot). Observe that Flagged hTDP-43 strains do not express endogenous TBPH. Tubulin was the loading control (lower blot).

and 10 female. All the experiments were conducted in a humidified, temperature controlled incubator at 25 °C and 60% humidity on a 12-h light and 12 h dark cycle. Flies were fed with standard cornmeal (2.9%), sugar (4.2%), yeast (6.3%) fly food. Every third day, flies were transferred to new tubes containing fresh medium and deaths were scored. Survival rate graph was plotted with percentage of survival flies against days. Approximately 260 flies were tested per each genotype.

3. Results and discussion

3.1. Loss of Drosophila TDP-43 affects locomotive behaviors and life span

To suppress the drosophila TDP-43 gene (TBPH-CG10327) we generated chromosomal deletions from TBPH^{EY10530} (see Section 2). Two of these excised lines, TBPH$^{\Delta 23}$ and TBPH$^{\Delta 142}$ showed small 1.6 and 0.8 kb deletions, respectively, that partially removed TBPH coding and regulatory regions (Fig. 1A). These deletions completely abolished endogenous protein expression and were therefore considered null alleles of TBPH (Fig. 1B). Homozygous TBPH$^{\Delta 23}$ or TBPH$^{\Delta 142}$ flies were viable after embryogenesis and more than 60% of them arrived to pupal stages, with the majority (80%) undergoing metamorphosis. Nevertheless, a high percent of TBPH mutant animals were unable to eclose and remained trapped inside their pupal cages (Table 1). Homozygous flies that instead managed to get rid of the external cuticle were morphologically identical to wild type controls (Fig. 1C), however, they presented dramatic locomotive defects with spastic, uncoordinated, movements, incapacity to fly or walk normally and reduced life span (Fig. 1D and Supplementary Movies S1 and S2).

To determine the place of TBPH function, we explored its endogenous distribution and intracellular localization. TBPH protein was present at higher concentrations in head tissues compared with thorax or abdomen in adult flies (Fig. 1E). Similarly, our anti-TBPH antibody could detect the endogenous protein in

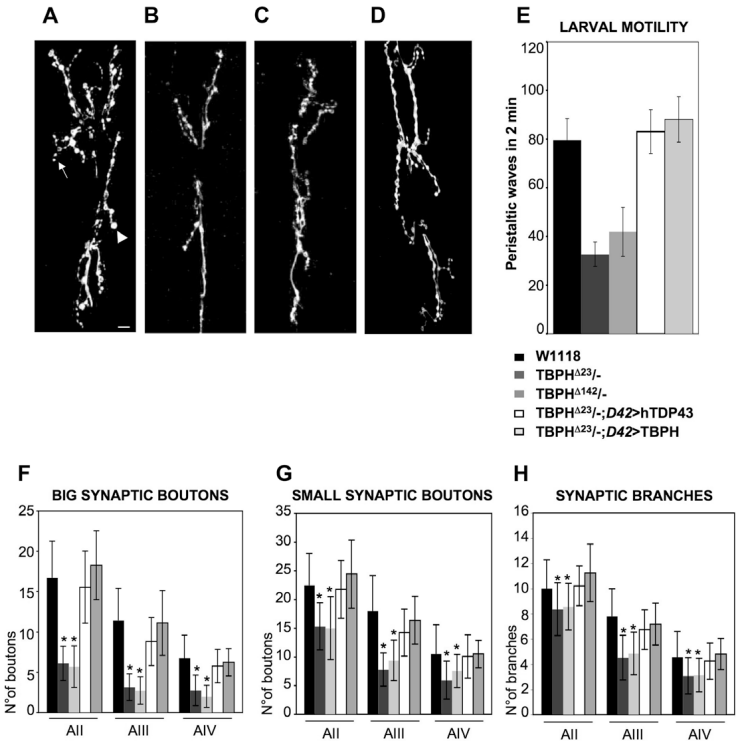

Fig. 4. Morphological defects at neuromuscular synapsis in TBPH mutant flies. (A) Confocal images of motoneurons presynaptic terminals at muscles 6 and 7 (abdominal segment III) in wild type third instar larvae stained with anti-HRP antibodies, reveals the branching pattern and the presence of big (arrowhead) and small (arrow) synaptic boutons. (B) and (C) Similar staining and anatomical position for TBPH$^{\Delta 23}$ and TBPH$^{\Delta 142}$ homozygous larvae respectively, show reduced axonal branching pattern and number of synaptic boutons. (D) TBPH$^{\Delta 23}$ minus third instar larvae rescued by expressing UAShTDP-43 in motoneurons with *D42*-GAL4 shows recovery of presynaptic complexity with increased formation of synaptic boutons and axonal terminal branching. Magnification 63 . (E) Number of peristaltic waves observed during 2 minutes in 120 h third instar larvae. $n = 20$ for each genotype, error bars indicate S.D.; $P < 0.0001$ calculated by ANOVA. (F) Quantification of big synaptic boutons present in consecutives abdominal segments ($n = 20$ animals). (G) Analysis of small synaptic boutons ($n = 20$ animals). (H) Quantification of presynaptic terminals branches in wild type, TBPH minus and hTDP-43/TBPH rescued third instar larva. $n = 20$ animals for each genotype, error bars indicate S.D.; $P < 0.0001$ calculated by ANOVA single factor. Scale: 10 μm.

neuronal cells during larval development and adulthood (Fig. 2). TBPH staining showed very well defined spherical structures that may correspond to the cell nucleus inside neuronal cell bodies present in optic lobes (Fig. 2i and ii) midbrain areas and ventral ganglia of larval (Fig. 2v and vi) and adult brains (Fig. 2ix and x). Identical immunostaining performed in TBPH minus tissues did not detected any particular signal confirming the specificity of the observations described above (Fig. 2iii, iv, vii, viii, xi and xii). These experiments demonstrate that TBPH is highly expressed in neuronal tissues from developmental stages to adulthood and suggest that its loss of function may induce locomotive deficits of neurological origin.

3.2. TDP-43 function in neurons regulates flies locomotion

To test this hypothesis, we decided to suppress TBPH expression by RNA interference (RNAi) exclusively in neural tissues [13]. Expression of TBPH RNAi using two different pan-neuronal drivers *elav*-GAL4 and *1407*-GAL4 [14], consistently reduced endogenous TBPH protein levels in Drosophila heads and induced locomotive defects in climbing assays (Fig. 3A and B). More convincingly, we observed that these phenotypes became enhanced if similar RNAi treatments were applied to TBPH heterozygous flies (see *elav* > RNAi3v; $TBPH^{\Delta 23}$/+ in Fig. 3C and Supplementary Movie S3), indicating that suppression of TBPH activity in post mitotic neurons was the presynaptic activity of sufficient to induce locomotive defects in vivo. To confirm these results we decided to rescue TBPH minus phenotypes by reintroducing the deleted gene. In addition, we decided to test whether the human protein (hTDP-43) was able to replace the endogenous protein in vivo. For these experiments we generated transgenic flies containing flag tagged TBPH and hTDP-43 cDNAs and targeted their expression in TBPH minus backgrounds using the GAL4/UAS system (Fig. 3D). Strikingly, we found that the expression of hTDP-43 by the neuronal post mitotic driver *elav*-GAL4 managed to rescue the motility defects observed in TBPH homozygous flies to a situation similar to wild type (Fig. 3C, and Supplementary Movie S4). Moreover, we found that expression of hTDP-43 in a more restricted population of neurons that include motoneurons by *D42*-GAL4 [15], was sufficient to rescue TBPH null phenotypes. In fact, these flies recovered their locomotive capacities (Fig. 3C, and Supplementary Movie S5) and incremented their life span (Fig. 1D) demonstrating that hTDP-43 function is evolutionary conserved and sufficient in a limited subpopulation of neurons to restore these traits. However, the partial recovery of the life span observed in these *D42*-GAL4 expressing flies indicates that TDP-43 may also be required in other types of neurons or different tissues.

3.3. TDP-43 regulates the formation of motoneurons presynaptic terminals at NMJ

To gain insight into the mechanisms behind these motility defects, we decided to analyze the morphology of motoneurons presynaptic terminals at neuromuscular junctions (NMJ) in TBPH minus flies. To label these structures we used anti horseradish peroxidase antibodies (HRP) that label neuronal membranes [16] and quantified the synaptic pattern of motoneuron axons that innervate muscles 6 and 7 in three different larval abdominal segments (AII, AIII, AIV). These structures present two types of synaptic boutons that can be easily distinguish by their size in 1b (big) and 1s (small) (Fig. 4A) [17]. We observed that in TBPH minus larvae, the complexity of the presynaptic terminals became dramatically affected as reflected by the reduced number of axonal branches and synaptic boutons present inside the muscles (Fig. 4B and C, F–H). In addition, we found that these anatomical defects together with the functional problems in larval motility could be rescued by the expression of hTDP-43 under *D42*-Gal4 (Fig. 4D and E) indicating that the morphological modifications observed at the synaptic terminals are the basis of these behavioral problems and TBPH/hTDP-43 function is required to form and maintain these structures.

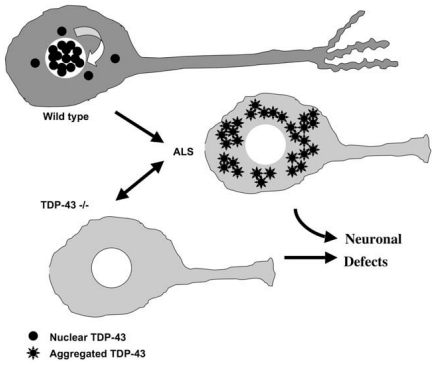

Fig. 5. Possible mechanism of TDP-43 mediated neurological defects in ALS. TDP-43 is a nuclear protein that in wild type situation shuttles to the cytoplasm. In ALS brains instead, it becomes abnormally aggregated in the cytoplasm and depleted from the cell nucleus suggesting that these modifications may be related to the neurological problems observed in these patients. We found that depletion of Drosophila TDP-43 was sufficient to generate atrophic presynaptic terminals and to induce locomotive defects in vivo. Since the human TDP-43 protein was able to assume the role of the endogenous gene in flies, we hypothesize that nuclear loss of TDP-43 function may be related to the locomotion problems observed in the disease. This view provides a new interpretation of the pathological mechanisms in ALS and predicts similar defects at neuromuscular junctions in affected patients.

Thus, our results demonstrate that the activity of TDP-43 in neurons is necessary to regulate locomotive behaviors in vivo and indicates that the neurological problems observed in ALS patients may not be restricted to the formation of insoluble protein fragments of aggregated TDP-43 within the cytosol but also to the loss of TDP-43 function in the nucleus (see model in Fig. 5).

In view that TDP-43 was characterized as RNA binding protein of the heterogeneous nuclear ribonucleoproteins (hnRNP) family with splicing inhibitory capacity [18], it may well be that TDP-43 induce motoneurons defects by affecting spliceosomes activity and/or mRNA transport and localization. Similarly, multiple defects in mRNA processing associated with locomotive deficiencies were recently described for the survival motor neuron protein (SMN) [19], giving a major support to the idea that defects in the mRNA metabolism may play a significant role in motoneuron degeneration. In conclusion our data demonstrate an evolutionary conserved function of TDP-43 in regulating synaptic terminals and locomotive behaviors and provide a new model to understand the mechanisms that lead to TDP-43 mediated neurological diseases in vivo.

Acknowledgments

To Emanuele Buratti and members of the Baralle's lab for useful discussions. To Serena Zacchigna and Chiara Appocher for advice and help. This work was supported by the Ministero dell'Universita' e della Ricerca (Grant No. RBLA03AF28-003), Telethon Onlus Foundation (Grant No. GGP06147) and by a European community grant (EURASNET-LSHG-CT-2005-518238).

Appendix A. Supplementary data

Supplementary data associated with this article can be found, in the online version, at doi:10.1016/j.febslet.2009.04.019.

References

[1] Neumann, M. et al. (2006) Ubiquitinated TDP-43 in frontotemporal lobar degeneration and amyotrophic lateral sclerosis. Science 314, 130–133.
[2] Sreedharan, J. et al. (2008) TDP-43 mutations in familial and sporadic amyotrophic lateral sclerosis. Science 319, 1668–1672.
[3] Kabashi, E. et al. (2008) TARDBP mutations in individuals with sporadic and familial amyotrophic lateral sclerosis. Nat. Genet. 40, 572–574.
[4] Buratti, E. and Baralle, F.E. (2008) Multiple roles of TDP-43 in gene expression, splicing regulation, and human disease. Front. Biosci. 13, 867–878.
[5] Arai, T. et al. (2006) TDP-43 is a component of ubiquitin-positive tau-negative inclusions in frontotemporal lobar degeneration and amyotrophic lateral sclerosis. Biochem. Biophys. Res. Commun. 351, 602–611.
[6] Geser, F. et al. (2009) Clinical and pathological continuum of multisystem TDP-43 proteinopathies. Arch. Neurol. 66, 180–189.
[7] Amador-Ortiz, C. et al. (2007) TDP-43 immunoreactivity in hippocampal sclerosis and Alzheimer's disease. Ann. Neurol. 61, 435–445.
[8] Bigio, E.H. (2008) TAR DNA-binding protein-43 in amyotrophic lateral sclerosis, frontotemporal lobar degeneration, and Alzheimer disease. Acta Neuropathol. 116, 135–140.
[9] Rohn, T.T. (2008) Caspase-cleaved TAR DNA-binding protein-43 is a major pathological finding in Alzheimer's disease. Brain Res. 1228, 189–198.
[10] Kwong, L.K., Neumann, M., Sampathu, D.M., Lee, V.M. and Trojanowski, J.Q. (2007) TDP-43 proteinopathy: the neuropathology underlying major forms of sporadic and familial frontotemporal lobar degeneration and motor neuron disease. Acta Neuropathol. 114, 63–70.
[11] Ayala, Y.M., Pantano, S., D'Ambrogio, A., Buratti, E., Brindisi, A., Marchetti, C., Romano, M. and Baralle, F.E. (2005) Human, Drosophila, and *C. elegans* TDP43: nucleic acid binding properties and splicing regulatory function. J. Mol. Biol. 348, 575–588.
[12] D'Ambrogio, A., Buratti, E., Stuani, C., Guarnaccia, C., Romano, M., Ayala, Y.M. and Baralle, F.E. (2009) Functional mapping of the interaction between TDP-43 and hnRNP A2 in vivo. NAR, in press.
[13] Dietzl, G. et al. (2007) A genome-wide transgenic RNAi library for conditional gene inactivation in Drosophila. Nature 448, 151–156.
[14] Luo, L., Liao, Y.J., Jan, L.Y. and Jan, Y.N. (1994) Distinct morphogenetic functions of similar small GTPases: Drosophila Drac1 is involved in axonal outgrowth and myoblast fusion. Genes Dev. 8, 1787–1802.
[15] Parkes, T.L., Elia, A.J., Dickinson, D., Hilliker, A.J., Phillips, J.P. and Boulianne, G.L. (1998) Extension of Drosophila lifespan by overexpression of human SOD1 in motorneurons. Nat. Genet. 19, 171–174.
[16] Jan, L.Y. and Jan, Y.N. (1982) Antibodies to horseradish peroxidase as specific neuronal markers in Drosophila and in grasshopper embryos. Proc. Natl. Acad. Sci. USA 79, 2700–2704.
[17] Budnik, V., Gorczyca, M. and Prokop, A. (2006) Selected methods for the anatomical study of Drosophila embryonic and larval neuromuscular junctions. Int. Rev. Neurobiol. 75, 323–365.
[18] Buratti, E., Brindisi, A., Giombi, M., Tisminetzky, S., Ayala, Y.M. and Baralle, F.E. (2005) TDP-43 binds heterogeneous nuclear ribonucleoprotein A/B through its C-terminal tail: an important region for the inhibition of cystic fibrosis transmembrane conductance regulator exon 9 splicing. J. Biol. Chem. 280, 37572–37584.
[19] Zhang, Z., Lotti, F., Dittmar, K., Younis, I., Wan, L., Kasim, M. and Dreyfuss, G. (2008) SMN deficiency causes tissue-specific perturbations in the repertoire of snRNAs and widespread defects in splicing. Cell 133, 585–600.

OPEN ACCESS Freely available online

PLoS one

TDP-43 Regulates Drosophila Neuromuscular Junctions Growth by Modulating Futsch/MAP1B Levels and Synaptic Microtubules Organization

Vinay K. Godena[1☯], Giulia Romano[1☯], Maurizio Romano[2], Chiara Appocher[1], Raffaella Klima[1], Emanuele Buratti[1], Francisco E. Baralle[1]*, Fabian Feiguin[1]*

1 International Center for Genetic Engineering and Biotechnology, Trieste, Italy, **2** Department of Life Sciences, University of Trieste, Trieste, Italy

Abstract

TDP-43 is an evolutionarily conserved RNA binding protein recently associated with the pathogenesis of different neurological diseases. At the moment, neither its physiological role *in vivo* nor the mechanisms that may lead to neurodegeneration are well known. Previously, we have shown that TDP-43 mutant flies presented locomotive alterations and structural defects at the neuromuscular junctions. We have now investigated the functional mechanism leading to these phenotypes by screening several factors known to be important for synaptic growth or bouton formation. As a result we found that alterations in the organization of synaptic microtubules correlate with reduced protein levels in the microtubule associated protein *futsch*/MAP1B. Moreover, we observed that TDP-43 physically interacts with *futsch* mRNA and that its RNA binding capacity is required to prevent *futsch* down regulation and synaptic defects.

Citation: Godena VK, Romano G, Romano M, Appocher C, Klima R, et al. (2011) TDP-43 Regulates Drosophila Neuromuscular Junctions Growth by Modulating Futsch/MAP1B Levels and Synaptic Microtubules Organization. PLoS ONE 6(3): e17808. doi:10.1371/journal.pone.0017808

Editor: Jessica Treisman, Skirball Institute of Biomolecular Medicine - New York University Medical Center, United States of America

Received November 10, 2010; **Accepted** February 11, 2011; **Published** March 11, 2011

Funding: The authors have no support or funding to report.

Competing Interests: The authors have declared that no competing interests exist.

* E-mail: baralle@icgeb.org (FEB); feiguin@icgeb.org (FF)

☯ These authors contributed equally to this work.

Introduction

TDP-43 is an RNA binding protein of 43 kDa that belongs to the hnRNP family and plays numerous roles in mRNA metabolism such us transcription, pre-mRNA splicing, mRNA stability, microRNA biogenesis, transport and translation [1,2]. TDP-43 is very well conserved during the evolution, especially with regards to the two RNA-recognition motifs (RRMs), the first (RRM1) being responsible for the binding of TDP-43 with UG rich RNA [3]. In consonance with these described functions, TDP-43 prevalently resides in the cell nucleus where it co-localizes with other members of the RNA processing machinery [4]. Nevertheless, in pathological conditions such as amyotrophic lateral sclerosis (ALS) and frontotemporal lobar degeneration (FTLD), TDP-43 appears in the form of large insoluble protein aggregates redistributed within the cytoplasm [5]. At the moment, however, it is not clear how these alterations may lead to neurodegeneration. In theory, the cytosolic accumulation of TDP-43 may induce a toxic, gain of function effect on motoneurons whilst the exclusion of TDP-43 from the cell nucleus may lead to neurodegeneration due to a loss of function mechanism. At present, several lines of evidence mainly from different cellular and animal models support either view suggesting that both models may be acting to lead the disease condition [6,7]. Recently, to determine the physiological role of TDP-43 *in vivo* we have reported that the flies which lack the TDP-43 homologue (TBPH) closely reproduce many of the phenotypes observed in ALS patients, such as progressive defects in the animal locomotion and reduced life span [8]. Moreover, we have observed that loss of TDP-43 function in *Drosophila* resulted in reduced number of motoneurons terminal branches and synaptic boutons at neuromuscular junctions (NMJs), indicating TDP-43 may regulate the assembly and organization of these structures. In coincidence with that, it should be noted that overexpression of TDP-43 in Drosophila has been reported to increase dendritic branching [9], lead to motor dysfunction and reduced life span [10], axon loss and neuronal death [11], is generally toxic regardless of inclusion formations [12], and at least in part is the cause behind the degeneration associated with TER94 mutations which is the Drosophila homologue of the VCP protein [13]. Taken together, and in consideration that Drosophila TDP-43 (TBPH) can functionally substitute for human TDP-43 in functional splicing assays [14], all these reports confirm that Drosophila may represent a highly suitable animal model to investigate TDP-43 functions both in normal and disease conditions.

Drosophila larval NMJ is a well-characterized system to analyze the cellular and molecular events that are involved in synapse development and plasticity [15]. Synaptic growth during larval development is expanded according to muscle size and is accomplished by the addition of new boutons to the existing presynaptic terminals [16]. Typically, defects in synapse formation and synaptic growth are linked to cytoskeleton abnormalities, since the synaptic boutons and the newly formed buds require the underlying presynaptic microtubules to maintain their structural organization and plasticity inside the innervated muscles. Thus, to determine the physiological role of TDP-43 *in vivo* and the pathological consequences of its altered function, we decided to

analyze in depth the molecular organization of *Drosophila* NMJs during larval development in TDP-43 minus flies.

Results

TDP-43 is Required for Synaptic Growth and Bouton Shape

Growth and formation of motoneurons synaptic terminals at the neuromuscular junctions (NMJs) in *Drosophila melanogaster* entails continuous addition and stabilization of new synaptic boutons to accommodate the rapidly growing larval muscles during development [17]. It was recently described also by us and other researchers that loss of function mutations in TDP-43 induced locomotive defects and influenced the morphological organization of the NMJ [8,18]. However the mechanisms behind these phenotypes, whether they were due to defects in synaptic growth or stabilization, are not known. To explore these possibilities, we now decided to quantify motoneurons terminal branches formation and expansion, together with the number of big synaptic boutons (1b) created on muscles 6 and 7 at different stages of larval development. For these experiments we analyzed NMJs organization from 38 hrs first instar larvae (L1), 62 hrs second instar (L2), to matured 110 hrs third instar larvae (L3), using two different TBPH mutant alleles. The neuronal membrane marker anti-HRP was used to determine whether synaptic terminal defects occur in TBPH minus alleles. No significant differences in the NMJ morphology during first instar larval stages (L1) were detected in two TBPH minus alleles compared to wild type controls (Figure 1A–C L1 and 1D for quantifications, wt = 13.4±0.4 boutons, $TBPH^{D23}$ = 11.8±0.46 boutons, $TBPH^{D142}$ = 12.2±0.38 boutons, n = 16 larvae, p>0.05. We also observed that presynaptic ramifications and muscular insertions appeared normal in L1, TBPH mutant motor axons. In contrast to this, we observed significant abnormalities in L2 TBPH mutants regarding to NMJ morphology (Figure 1A–C L2 and 1D, wt = 27±0.67 boutons, $TBPH^{D23}$ = 17.4±0.58 boutons, $TBPH^{D142}$ = 16.6±0.53 boutons, n = 16 larvae, p<0.001). The synaptic terminal defects were even more evident in third instar larval stage (L3), where a very little addition of new synaptic boutons was detected in TBPH mutant flies (Figure 1A–C L3 and 1D, wt = 41±0.80 boutons, $TBPH^{D23}$ = 22.5±0.87 boutons, $TBPH^{D142}$ = 23±0.87 boutons, n = 17 larvae, p<0.001). Muscle development was normal in TBPH mutant flies since no differences in organ growth, cytoskeleton organization or postsynaptic differentiation were observed regarding to wild type controls (Figure S1A–F and G). Thus, these experiments indicated that TBPH function in motoneurons promotes presynaptic growth and the addition of new synaptic boutons during larval development.

In addition, we analyzed whether synaptic stability was compromised in TBPH minus larvae. For these experiments, we used a previously established assay to quantify presynaptic retraction events in NMJ. This assay is based on the evidence that formation of postsynaptic structures in *Drosophila* muscles depends on the presence of the pre-synaptic terminals [19]. Therefore, postsynaptic resident proteins will only be present at sites where presynaptic terminals are located. Consequently, postsynaptic sites that do not have opposite presynaptic neuronal markers, identify regions of the NMJs where the nerve terminals once were present and retracted leaving their "footprints" [20]. To quantify synaptic retraction events or footprints we used a postsynaptic marker protein Discs-large (Dlg) and anti-HRP staining to label presynaptic terminals [21]. Double-labeled NMJ of third instar larvae were analyzed and no significant differences in the number of footprints were found in TBPH minus flies (Figure S1 Hiv-Hvi $TBPH^{D23}$, Hvii–Hix $TBPH^{D142}$) compared to wild type controls (Figure S1 Hi–Hiii and I for quantifications). These data further suggested that the NMJ defects observed in TBPH mutants were due to a lack of new synaptic bouton formation rather than to increased presynaptic retraction. In order to control that the TBPH loss of function defects at motoneuron synaptic terminals were not due to a more general problem of neuronal degeneration, we determined the viability of these motoneurons by expressing the GFP protein using the *D42*-GAL4 driver in both wild type and TBPH mutant flies. Larval brains were dissected at third instar stage and stained with the neuronal marker *elav* (Figure S2A). The number of GFP positive neurons in the terminal abdominal segment, in particular a4-a5-a6-a7, of the dorsal cluster of the ventral nerve cord was counted [22]. We found that the viability of motoneurons was not affected in TBPH mutant flies (Figure S2B) indicating that the synaptic phenotypes described above were specific for TBPH function.

Defects in synaptic growth as described in TBPH mutants were very often associated with alterations in synaptic bouton shape. We therefore analyzed the morphology of individual big synaptic boutons present on muscles 6 and 7 in L3 wild type and TBPH mutant larvae. Staining with anti-HRP antibodies showed that, wild type 1b boutons were rounded and had a smooth surface with a uniform distribution along the presynaptic terminals that resemble the "beads on a string" (Fig. 1E) [23]. $TBPH^{D23}$ and $TBPH^{D142}$ mutant synaptic boutons appeared deformed and were irregularly spaced along the terminal axons with several fused or elongated silhouettes and clear loss of their characteristic round-smooth shape (Figure 1F–G). Similar alterations were observed in TBPH-RNAi expression in neurons by using the *elav*-GAL4 driver (Figure 1H), implying the neuronal origin of these defects. Although the analysis was centered on muscles 6 and 7, aberrant boutons were detected in almost every body muscle examined. This bouton phenotype was highly penetrant and specific for TBPH gene function since genetic rescues performed in TBPH mutant neurons, obtained by expressing the endogenous TBPH protein with *D42*-GAL4 driver, was able to recover the phenotype (Figure 1I, and 1J for quantifications). Thus, these experiments demonstrated that TBPH function is required in motoneurons to sustain synaptic growth and boutons shape.

Testing for Potential Alterations in Cytoskeletal Factors that Sustain Synaptic growth and Bouton shape

The exponential growth of *Drosophila* NMJ during development occurs by the addition of new boutons. Newly formed boutons originate after budding from their parent boutons and NMJ expansion takes place by extending neural processes and bouton enlargement. This entire process is mainly supported by the underlying presynaptic cytoskeleton and induced us to hypothesize that alterations in the organization of these structures might explain the morphological defects observed in TBPH mutant alleles. In support of this idea, it was previously described that NMJ defects similar to TBPH loss of function were found in several other mutants that induce alterations in the organization of the microtubules (MT) at the synaptic terminals [24,25].

Based on these considerations we therefore decided to test for alterations at the level of important factors known to play a role in synaptic organization at the cytoskeletal level. Regarding to that, the intracellular localization of different presynaptic proteins involved in synaptic function such as Bruchpilot [26] and Synapsin [27] were not affected by the absence of TBPH function (Figure S3A,B). Similarly, we did not find alterations in the expression levels of the adhesion protein Fasciclin II (Figure S3C) [28], type II BMP receptor Wit-C (Figure S3D) [29], Bruchpilot (Figure S3E) and the cytoskeletal protein Spectrin (Figure S3F) [30]. For the

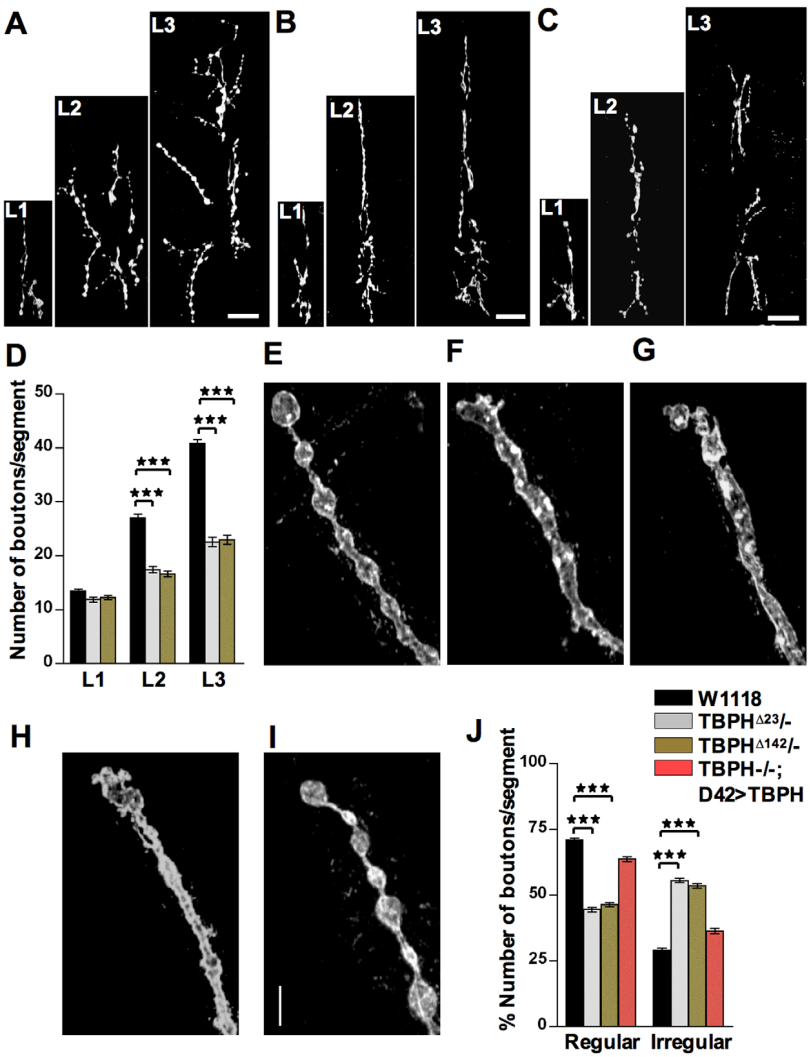

Figure 1. Loss of TBPH function affects synaptic growth and boutons shape. (A) Confocal images of wild type NMJs on muscle 6 and 7, abdominal segment II, at L1 (38 h), L2 (62 h) and L3 (110 h) stages using α-HRP antidody. (B) And (C) Similar α-HRP staining showing NMJ morphology at different stages of larval development in TBPH^{D23} and TBPH^{D142} homozygous larvae. Scale bar 20 μm. (D) Quantifications showing total number of boutons present in the abdominal segment II of wild type and TBPH mutant alleles during larval development. (E) Regular shape and distribution of 1b boutons in wild type NMJs compared to misshapen boutons in (F) TBPH^{D23}/- (G) TBPH^{D142}/- and (H) TBPH^{D23}/+;*elav*>TBPH-RNAi mutants. (I) Bouton shape is rescued by expressing UAS TBPH in motor neurons with *D42*-GAL4. Scale bar 5 μm. (J) Quantifications showing regular and irregular boutons present in the abdominal segment II at third instar larval stages in wild type and mutant alleles. *** Indicates $p<0.001$ calculated by one-way ANOVA. Error bars indicate SEM.
doi:10.1371/journal.pone.0017808.g001

contrary, our experiments detected that the protein levels of *futsch* were consistently reduced in TBPH minus heads (Fig. 2C). This was considered particularly interesting since *futsch* is a neuron-specific microtubule binding protein homolog to human MAP1B responsible for maintaining MT integrity at presynaptic terminals during NMJ expansion [31]. In addition, mutations in *Drosophila* MT binding protein *futsch* reproduce many of the alterations that are observed in TBPH loss of function, such as small NMJ with deformed boutons [32], suggesting that altered MT organization could represent at least part of the molecular mechanism behind the NMJ defects observed in TBPH minus flies.

TDP-43 Activity is Necessary for Microtubule Organization at Presynaptic Terminals

To test this possibility, we then decided to investigate the MT organization by analyzing *futsch* staining, which labels bundled and unbundled MTs and provides a reliable marker for the cytoskeleton at presynaptic terminals [24,33,34]. Anti-*futsch* specific antibody 22c10 was used to stain MTs and big boutons at muscle 6/7 were analyzed. In wild type NMJs, *futsch* labeling highlights bundled MTs and occupies the main part of the presynaptic terminals, filling almost completely the proximal synaptic boutons. In newly formed or distally located synaptic boutons, however, *futsch* staining was fainter, fragmented and more diffuse (Figure 2Ai–Aiii). The *futsch*-staining pattern at each synaptic bouton was scored as percentage of the number of boutons in which *futsch* immunostaining appeared full, diffuse or absent (Figure 2B). Compared with this situation, in TBPH mutant alleles total *futsch* staining was dramatically modified. An increased number of boutons had a diffuse pattern and complete absence of *futsch* was observed at distal terminals (Figure 2Aiv–Avi TBPH^{D23}, Avii–Aix TBPH^{D142} and 2B for quantifications). These pheno-

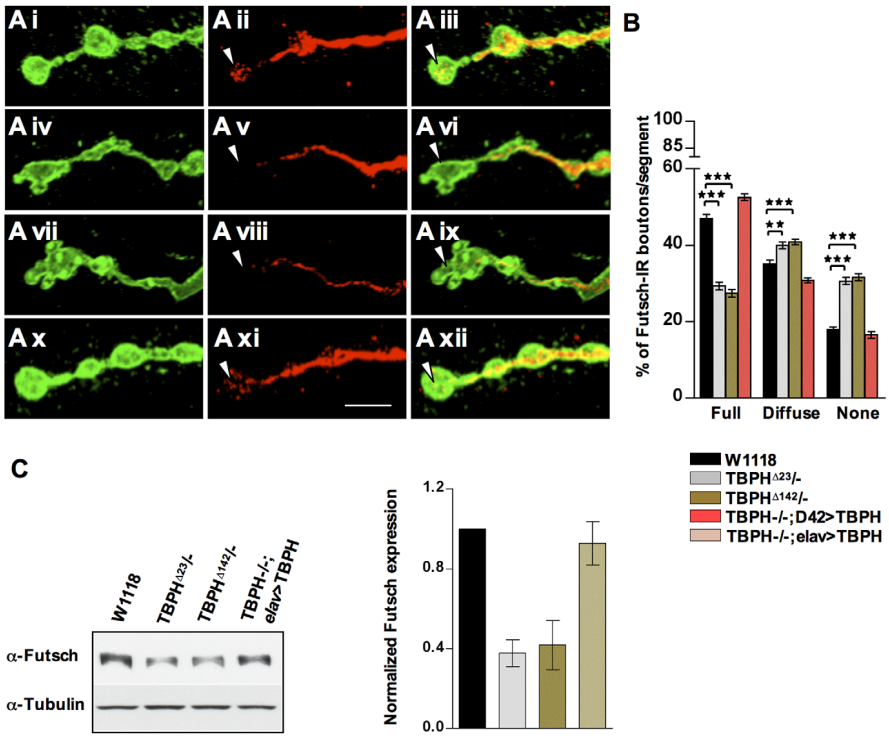

Figure 2. Loss of TBPH interferes with microtubule organization. (A) Confocal images showing *futsch* staining at the terminal synaptic boutons of (Ai–Aiii) wild type, (Aiv–Avi) TBPH^{D23}, (Avii–Aix) TBPH^{D142}. Note the complete absence of *futsch* at the most distal, newly formed, boutons in TBPH mutants (arrow head). (Ax–Axii) Expression of TBPH protein by *D42*-Gal4 rescues *futsch* staining in TBPH mutant larvae. (B) Quantifications of *futsch* staining pattern in muscle 6–7 abdominal segment II showing increased number of diffused *futsch* and *futsch* negative boutons in TBPH mutant alleles compared to wild type. $n = 15$ larvae. **$p<0.01$ and ***$p<0.001$ calculated by one-way ANOVA. (C) Western blot analysis and the respective histogram confirmed the reduced *futsch* expression levels in TBPH mutant fly heads compared to wild type. $n = 4$.
doi:10.1371/journal.pone.0017808.g002

types together with *futsch* protein levels, however, could be rescued by expressing the TBPH protein in motoneurons with *D42*-GAL4 (Figure 2Ax–Axii, 2B and 2C) demonstrating that these alterations were specific of TBPH function and suggesting that MT stability in TBPH mutants might be affected in concomitance with *futsch* down regulations. To test this possibility, we performed double staining of presynaptic terminals with antibodies against acetylated tubulin and HRP. Acetylation of specific lysine residue in α-tubulin is a posttranslational modification that marks stabilized MTs and contributes to the regulation of microtubule dynamics [35]. Moreover, increased α-tubulin acetylation and MT stability was noticed in cells transfected with microtubule-associated proteins such as MAP1B, MAP2 or Tau [36]. In TBPH minus alleles, acetylated MTs are significantly reduced in distal boutons (Figure 3Aiv–vi TBPH^{D23}, Avii–ix TBPH^{D142} arrow head and 3B for quantifications) compared to prominent tubulin acetylation labeling in wild type terminal boutons (Figure 3Ai–iii and 3B). The decrease in acetylated tubulin labeling was rescued by introducing the endogenous protein back in motoneurons using *D42*-GAL4 (Figure 3Ax–xii and 3B).

Reduced *futsch* and Microtubules Stability Cause the Presynaptic Defects Observed in TDP-43 Mutants

Although heterozygous and trans heterozygous combinations between the mutant alleles of *futsch* ^{N94} and TBPH^{D23} did not show major differences in synaptic growth or bouton numbers compared with wild type controls (Figure S4A–B), we observed that the neuronal expression of the TBPH protein in TBPH^{D23} homozygous mutant flies was not able to rescue the presynaptic phenotypes if one copy of *futsch* was removed from the genetic background. Thus, *futsch*^{N94}/+;TBPH^{D23}/TBPH^{D23};*elav*-GAL4> TBPH animals (Figure 4D, F–G) compared to +/+; TBPH^{D23}/TBPH^{D23}; *elav*-GAL4>TBPH flies (Figure 4C, F–G), showed structural defects in the assembled synaptic terminals with reduced number of 1b boutons and terminal branches. At the molecular level, we found that the organization of stable MTs were affected in *futsch*^{N94}/+;TBPH^{D23}/TBPH^{D23}; *elav*-GAL4>TBPH flies (Figure 5Ax–xii) compared to +/+; TBPH^{D23}/TBPH^{D23}; *elav*-GAL4>TBPH flies (Figure 5Avii–ix), indicating that TBPH function may requires *futsch* activity to stabilize MTs during synaptic growth and bouton formation. Likewise, we found that stabilization of MTs at motoneurons synaptic terminals was sufficient to rescue the anatomical defects observed in TBPH mutant flies. For these experiments we took the advantage of previous data demonstrating that the neuronal expression of mammalian Tau was capable of rescuing Futsch loss of function phenotypes in *Drosophila* neurons by replacing the microtubule-binding ability of the endogenous protein [37]. Thus, we used a transgenic fly expressing low levels of human Tau in TBPH^{D23} homozygous neurons using *elav*-GAL4. We found that human Tau expression in TBPH^{D23} mutant larvae rescued the reduced number of synaptic boutons and terminal branches in TBPH mutant alleles (Figure 4E, 4F–G). We also found that the rescued boutons were round with a smooth outline and beaded appearance like wild type controls. Furthermore, we observed that the presence of acetylated MTs in distal presynaptic structures was also rescued by human Tau expression (Figure 5Axiii–xv and 5B for quantifications) demonstrating that defects in MT stability were responsible for the morphological defects observed in TBPH mutant boutons. Although, Tau-induced morphological rescue of presynaptic terminals was almost equivalent to the values obtained with the expression of the endogenous TBPH protein itself (Figure 4F–G and Figure 5B) functional recovery of larval motility was not achieved in Tau-rescued flies (Figure S4C) indicating that

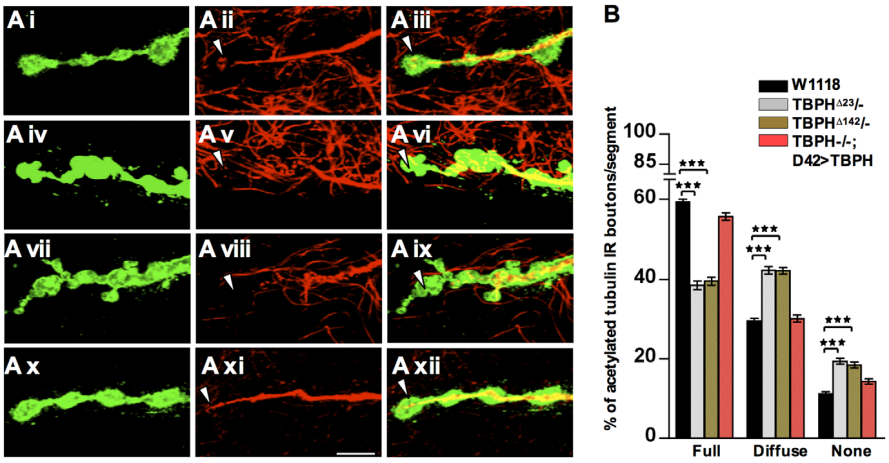

Figure 3. Reduced stable MT and Tubulin acetylation in TBPH mutants. (A) Confocal images showing wild type boutons with stable MT bundles (Ai–Aiii, arrowhead) labeled by acetylated Tubulin. TBPH mutants (Aiv–Avi) TBPH^{D23}/-, (Avii–Aix) TBPH^{D142}/- show the absence of acetylated MTs staining at the distal boutons (arrowhead). (Ax–Axii) *D42*-GAL4 driven TBPH expression rescues the lack of stable MTs in the TBPH loss of function. Scale bar 5 μm. (B) Quantifications of stable MT labeled by acetylated Tubulin in the abdominal segment II showing significant labeling reduction in TBPH mutant alleles compared to wild type larval NMJ. ***p<0.001 calculated by one-way ANOVA. $n = 16$ larvae.
doi:10.1371/journal.pone.0017808.g003

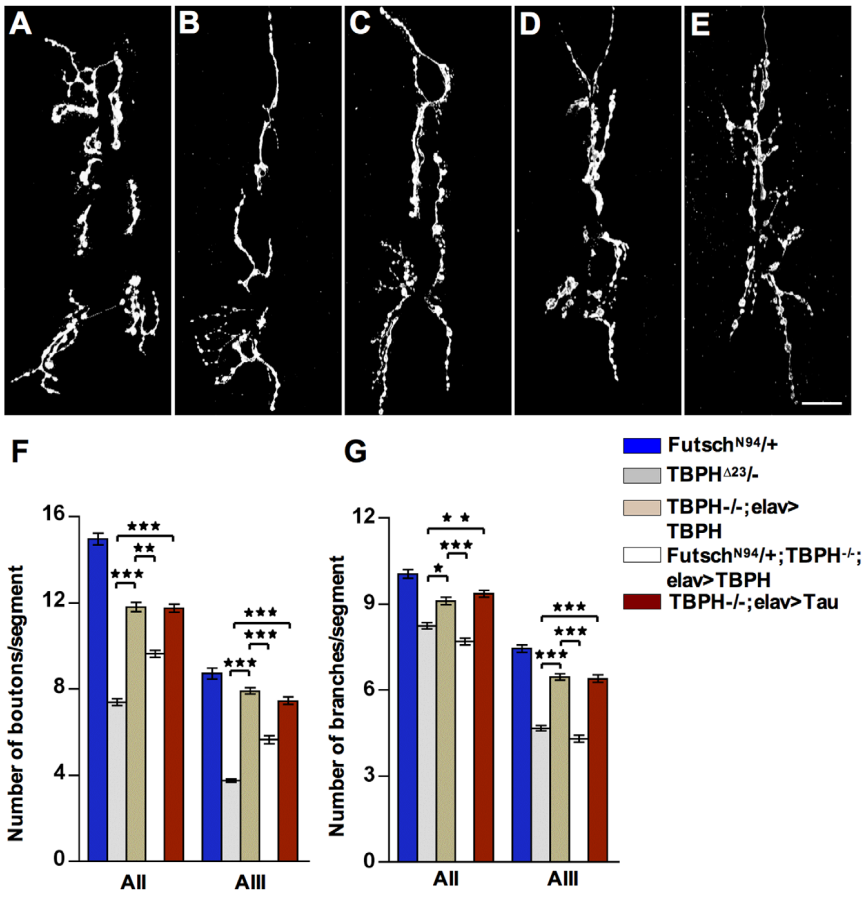

Figure 4. TBPH function requires *futsch* activity to promote NMJ growth. NMJ morphology in muscle 6/7 abdominal segment II of (A) *futsch*^{N94}/+ (B) TBPH^{D23}/- (C) TBPH^{D23}/-;*elav*>TBPH (D) *futsch*^{N94}/+;TBPH^{D23}/-;*elav*>TBPH (E) TBPH^{D23}/-;*elav*>Tau^{wt}, Scale bar 20 µm is valid for all figures. Note the NMJ growing defects in *futsch*^{N94}/+;TBPH^{D23}/-;*elav*>TBPH genotypes compared to TBPH^{D23}/-;*elav*>TBPH. Human Tau protein expression showed the recovery in NMJ growing defects observed in TBPH mutants. (F) Quantifications showing significant reduction in the number of boutons and (G) the number of branches in *futsch*^{N94}/+;TBPH^{D23}/-;*elav*>TBPH genotypes compared to TBPH^{D23}/-;*elav*>TBPH. Tau protein expression recovered the NMJ growing defects observed in TBPH mutants. $n = 13$ larvae.
doi:10.1371/journal.pone.0017808.g004

besides the stabilization of MTs, TBPH may regulates additional functions in motoneurons.

The TBPH Protein Physically Interacts with *futsch* mRNA

Most of the functional properties of TDP-43 described up to now, have been shown to depend very heavily on its RNA binding ability [38]. Therefore, to gain further insights into the mechanisms of TBPH action we first tested for a possible physical interaction between the TBPH protein and *futsch* mRNA (Figure 6). For these experiments we performed immunoprecipitation studies, using a monoclonal anti-Flag antibody, from *Drosophila* heads expressing Flag-tagged TBPH under the control of the *elav*GAL4 promoter (Fig.6A, GOF). Likewise, immunoprecipitation experiments were performed using cells extracts from wild type W1118 flies as well as from flies overexpressing the unrelated Flag-tagged Drosophila protein REEP (Figure 6A, REP) or from flies

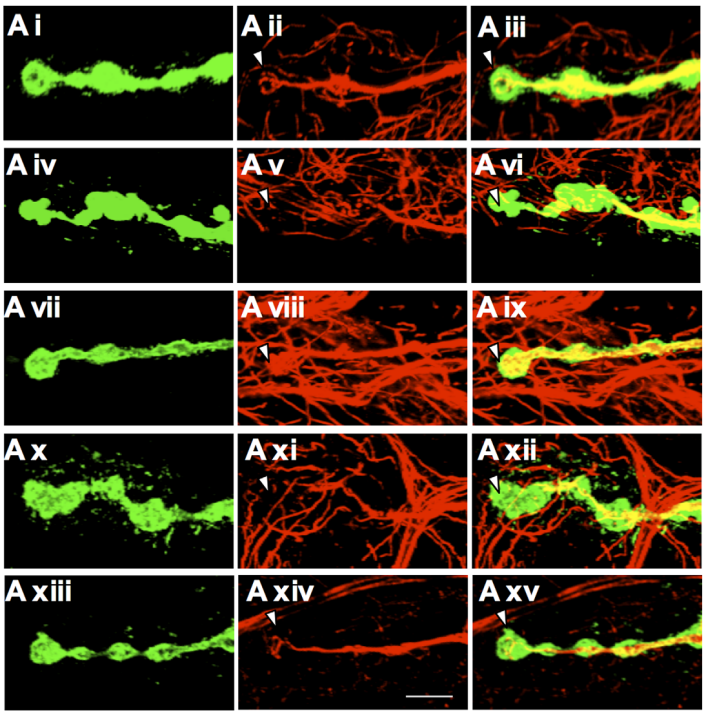
A i
A ii
A iii
A iv
A v
A vi
A vii
A viii
A ix
A x
A xi
A xii
A xiii
A xiv
A xv

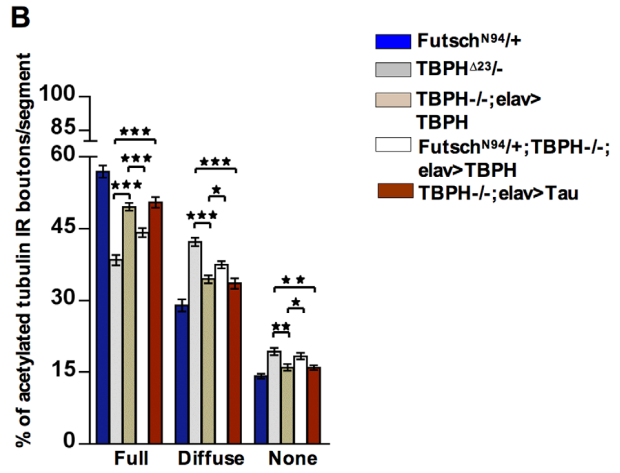
B
% of acetylated tubulin IR boutons/segment
100
85
60
45
30
15
0
Full
Diffuse
None
Futsch^N94/+
TBPH^Δ23/-
TBPH-/-;elav>TBPH
Futsch^N94/+;TBPH-/-;elav>TBPH
TBPH-/-;elav>Tau

Figure 5. TBPH function requires *futsch* activity to stabilize presynaptic MTs. (A) Confocal images showing the distribution of acetylated MTs in distal boutons of (Ai–Aiii) *futsch*^{N94}/+, (Aiv–Avi) TBPH^{D23}/-, (Avii–Aix) TBPH^{D23}/-;*elav*>TBPH, (Ax–Axii) *futsch*^{N94}/+;TBPH^{D23}/-;*elav*>TBPH and (Axiii–Axv) TBPH^{D23}/-;*elav*>Tau. Note that Tubulin acetylation and stable MT reduction was noticed in the distal boutons of Futsch^{N94}/+; TBPH^{D23}/-; *elav*>TBPH compared to similar rescue in the TBPH^{D23} mutant background alone (arrow head). Expression of Tau protein in TBPH mutant alleles was able to rescue the distribution of acetylated MTs at synaptic boutons. Scale bar 5 μm valid for all figures. (B) Quantifications of acetylated stable MTs in muscle 6/7 abdominal segments II $n = 13$ larvae. * $p<0.05$, ** $p<0.01$ and ***$p<0.001$.
doi:10.1371/journal.pone.0017808.g005

overexpressing TBPH F/L150–152 (FL), a variant of TBPH mutated within the RNA binding domain (Figure 6A, FL, and see below). Real Time quantitative PCR was used for quantification of the fold-enrichment above controls (GOF/REP and GOF/FL). As expected, the general level of enrichment was higher for GOF/REP with respect to GOF/FL (for example, for futsch we observe approx. 25X enrichment for GOF/REP and 11X for GOF/FL). This is consistent with the fact that the FL mutant differs from the wild-type protein from just two aminoacid substitutions. As a positive control, we verified by RT-qPCR that the protein complex immunoprecipitated by anti-Flag TBPH contained the *hdac-6* mRNA, in agreement with previous publications [39]. On the other hand, we observed negligible levels of enrichments for rpl-52 mRNA, a ribosomal protein with ubiquitous expression (Figure 6A, rpl-52), as well as for homer, a protein enriched in the nervous system (Figure 6A, homer). No enrichment was also observed for rpl-11 mRNA (data not shown). Also as expected, we observed a higher level of enrichment with the REP protein as opposed to the FL mutant when the putative TBPH binding site (UG)9 was added to head extract samples (Figure 6A). Taken together, these data demonstrate that TBPH interaction with the futsch mRNA is highly specific and supports the hypothesis that the observed effects on futsch protein expression might depend on this direct connection.

The RNA-binding Capacity of TBPH is Essential for its Function *in vivo*

To analyze the functional consequences of this TBPH-*futsch* mRNA physical interaction, we decided to test whether the RNA-binding activity of the protein was responsible for the regulatory roles described above. RNA binding ability of TDP-43 plays an important functional role in alternative splicing and neurodegeneration [40]. In particular, point mutation of two Phenylalanine residues to Leucine (F147L and F149L) in RNP-2 of RRM1 disrupts TDP-43 interaction with RNA, hence describing its importance in RNA recognition [3,41]. Therefore to check for the importance of this RNA binding activity *in vivo* we generated transgenic flies expressing a mutated form of *Drosophila* TDP-43 in which the conserved Phenylalanine residues present at positions 150 and 152, of RNA recognition motif 1 (RRM-1) in TBPH, were replaced with Leucine. Transgenic flies carrying the TBPH$^{F/L150–152}$ construct under UAS sequences were expressed in neurons using *elav*-GAL4 and it was found that TBPH without RNA binding activity was not able to rescue the TBPH loss of function phenotypes compared with endogenous TBPH, although the intracellular localization of these constructs was similar in both the cases (Figure S5A). Thus we found that expression of TBPH$^{F/L150–152}$ using *D42*-GAL4 in TBPH^{D23} homozygous flies failed to recover the anatomical defects observed in mutant animals regarding the number of synaptic boutons, synaptic branches and MTs organization (Figure 6C–G). Moreover, we found that the biochemical levels of *futsch* protein in TBPH$^{F/L150–152}$ rescue fly heads were not recovered (Figure 6H) although the transgenic expression levels were even higher than the endogenous TBPH protein (Figure S5B) indicating that regulation of *futsch* is specific to the RNA binding capacity of TBPH. Finally, we observed that the functional recovery of fly motility in the form of larval movement (Figure S5C), adult flies walking (Figure S5D) and climbing (Figure S5E) was affected in TBPH$^{F/L150–152}$ rescued flies compared to wild type TBPH expressing controls. Interestingly, however, we did observe that the TBPH$^{F/L150–152}$ construct reached some degree of activity compared to TBPH mutant flies rescued with GFP (Fig. 6D, S5C–E), suggesting that some residual protein activity may exist in the other intact domains. Nonetheless, based on these results we can say that the RNA-binding activity of TBPH, through the RRM-1 domain is definitively essential for its function *in vivo*.

Discussion

Evaluating the Potential Functional Connection Between TBPH and *futsch* Expression

Based on the above results, it seems evident that TBPH maintains NMJ growth and MT organization through *futsch* protein action and that TDP-43 RNA binding ability plays a crucial role in this process. Similar to TBPH, other RNA binding protein Fragile X-related (Fxr) gene regulates *futsch* to control synaptic structure and function by directly associating with *futsch* mRNA to alter the expression levels of *futsch* protein. In particular, Fxr acts as a translational repressor of *futsch* to regulate MT dependent synaptic growth and function [34]. Regarding TBPH, therefore, we first of all wanted to determine whether reduced expression of *futsch* protein in our TDP-43 minus flies could be directly related to a reduction in the mRNA levels of these factors. However, quantitative PCR analysis of *futsch* mRNA levels in TDP-43 minus and rescued flies did not show appreciable differences with respect to wild type flies (Fig. S5F). These results suggested that TBPH regulation of *futsch* was not due to differences in RNA stability, transport or translation. In this respect, a visual inspection of the *futsch* gene (FBtr0112628) showed potential UG-repeats in the 5′UTR region near to the ATG codon of the protein that could act as TDP-43 binding site and which could be consistent with a role similar to that of Fxr in affecting mRNA translation. In keeping with this hypothesis, it should be noted that a recent proteomic study performed on the human TDP-43 protein have highlighted its potential interaction with several components of the translational machinery [42], although this has not been confirmed in a subsequent study [43]. Further work, however, will be required to test these hypotheses.

Concluding remarks

In this work, we show that in our TBPH minus *Drosophila* model the changes observed at the level of NMJs and synaptic boutons formation can be explained by defects at the cytoskeleton level, which in turn are mediated by a down regulation of the *futsch* protein (but not mRNA). These results provide additional insight with regards to potential disease mechanisms mediated by TDP-43 and considerably extend our knowledge with regards to defining the basic molecular functions of this protein. Future work will be aimed at better characterizing more in depth the functional mechanism through which TBPH regulates *futsch* protein levels and how these results can be extended to the human disease model.

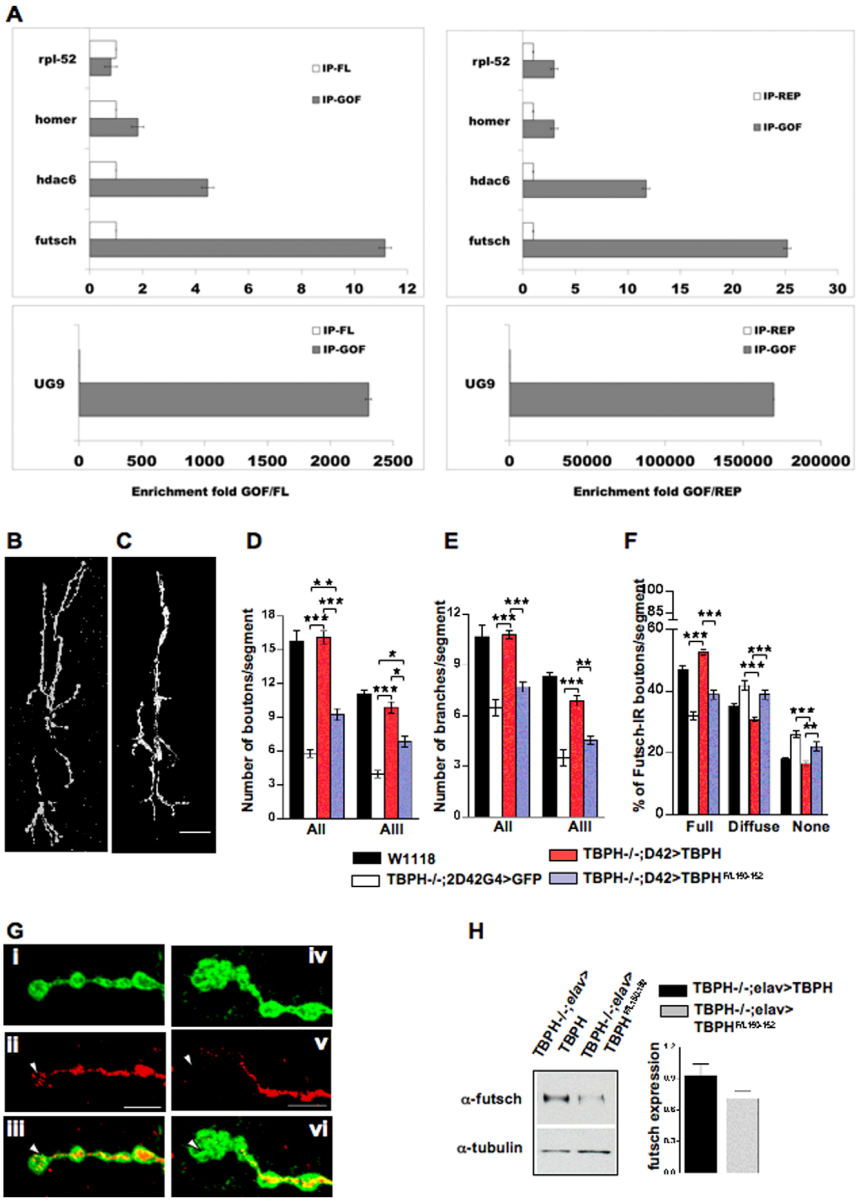
A
rpl-52
homer
hdac6
futsch
IP-FL
IP-GOF
IP-REP
UG9
Enrichment fold GOF/FL
Enrichment fold GOF/REP
B
C
D
E
F
Number of boutons/segment
Number of branches/segment
% of Futsch-IR boutons/segment
AII
AIII
Full
Diffuse
None
W1118
TBPH-/-;2D42G4>GFP
TBPH-/-;D42>TBPH
TBPH-/-;D42>TBPH FL 150-152
G
i
ii
iii
iv
v
vi
H
TBPH-/-;elav>
TBPH
TBPH-/-;elav>
TBPH FL 150-152
α-futsch
α-tubulin
TBPH-/-;elav>TBPH
TBPH-/-;elav>
TBPH FL 150-152
futsch expression

Figure 6. TBPH binding to *futsch* mRNA is required for NMJ growth and MT organization. (A) qPCR analysis of mRNAs immunoprecipitated by Flag-tagged TBPH. The enrichment-fold is referred to an unrelated protein (REP, Right charts) or to the mutant $TBPH^{F/L150-152}$ (FL, Left charts). Significant levels of enrichment were observed for *futsch* mRNA, together with *hdac-6* mRNA and the (UG)9 RNA used as positive controls. The mRNAs of the ribosomal protein *rpl*-52 and homer were not enriched significantively. (B) Wild type TBPH protein expression in $TBPH^{D23}$/-;*D42*>TBPH flies succeed to rescue the synaptic growth compared to (C) TBPH RRM1 mutant isoform in $TBPH^{D23}$/-;*D42*>$TBPH^{F/L150-152}$ larval NMJ, Scale bar 20 μm. (D) Quantifications of big synaptic boutons and (E) terminal branches in muscle 6–7 (abdominal segments II and III) in $TBPH^{F/L150-152}$ and TBPH wild type rescues. (F) Quantifications showing the reduced *futsch* staining in the distal boutons of $TBPH^{F/L150-152}$ rescue NMJs compared to wild type TBPH protein. $n = 12$ larvae. ***$p<0.001$, **$p<0.01$. (G) Confocal images showing reduced *futsch* positive staining in the distal boutons of $TBPH^{F/L150-152}$ rescues (Giv-Gvi see arrowhead) compared to wild type TBPH rescues (Gi-Giii). Scale bar 5 μm. (H) Western blot analysis and the respective histogram showing the reduced levels of *futsch* protein expression in $TBPH^{D23}$/-;elav>$TBPH^{F/L150-152}$ compared with $TBPH^{D23}$/-;elav>TBPH (upper panel) $n = 3$. Tubulin was used as a loading control (bottom panel).
doi:10.1371/journal.pone.0017808.g006

Materials and Methods

Neuromuscular junctions

To quantify the NMJ growth, embryos from all genotypes were collected during 2 hrs in agar plates and staged at 25°C. Homozygous first, second and third instar larvae were selected against GFP expressing chromosome balancers. Body wall muscles were dissected as per the previous protocols [44]. Primary antibodies α-HRP (Jackson immunoresearch laboratory, 1:100), α-Synapsin (DSHB, 1:10), α-Highwire (DSHB, 1:10), α-Bruchpilot (DSHB, 1:10), α-DLG (DSHB, 1:250), α-*futsch* (DSHB, 1:50), α-tubulin (Calbiochem, 1:100) and α-acetylated tubulin (Sigma-Aldrich, 1:2000) and secondary antibodies Alexa 488 Goat-anti rabbit and Alexa 555 Goat-anti mouse IgG (Invitrogen, 1:500) were used.

Quantifications of *futsch* and acetylated Tubulin MT bundles at NMJs: were done as described in [24,45] with minor modifications. The bundled appearance of MTs in the proximal boutons in general occupies >75% of the bouton space was considered as full, while boutons in which MTs are fragmented and occupies <75% of bouton space are classified as diffused. Finally the boutons without MT staining are considered as empty boutons.

Immunostaining

For brains we followed the protocol by Wu et al [46]. Briefly, larval brains were dissected carefully in PB-0.3%Triton-X100 (PBT) buffer and fixed in freshly prepared ice cold 4% paraformaldehyde (PFA) for 30 min. Blocking was done with 5% normal goat serum (NGS) and primary antibodies α-Flag (Sigma, 1:200) and α-elav (DSHB, 1:250) was used. Samples were incubated at 4°C overnight and treated with fluorescent conjugated secondary antibodies Alexa 488 Goat-anti rabbit IgG and Alexa 555 Goat-anti rat IgG (Invitrogen, 1:500) for 2 hrs at room temperature. All primary and secondary antibodies were diluted in PBT-5% NGS. Slow fade gold antifade reagent (Invitrogen) was used as a mounting medium and the samples were analyzed with a confocal laser-scanning microscope.

Larval movement

To evaluate the peristaltic waves of third instar larvae, we followed our previously established protocol [8]. Briefly, Individual larvae were selected and washed carefully with water to remove any remaining food attached to the body. The larvae were carefully transferred with the help of forceps to 0.7% agarose plates (100 mm). Under the stereoscope, larvae were allowed to adopt for 30 sec and start counting the peristaltic waves per 2 min. Minimum 25 larvae per each genotype were counted individually and average has been taken.

Walking Assay

Walking ability of young flies with the age of 3–4 days was performed as described earlier [8]. Briefly, individual fly was placed on transparent 145 mm diameter petri plate whose bottom was marked with 1×1 cm square grid lines. Flies were allowed to adopt for at 30 sec and walking was analyzed by counting the number of 1×1 grids crossed by the fly. Minimum 50 flies were tested individually from each genotype and the average has been taken.

Climbing assay

Climbing ability of different genotypes was performed in an empty transparent Duran 50 ml glass cylinder. The cylinder was divided into three parts as bottom, middle and top. Age matched flies to be tested, were dropped at the bottom of the cylinder carefully and climbing ability was scored based on the flies that are moving onto the top in 15 sec. Three trials was performed on each day and the average was taken as climbing ability. Thirty flies per batch and minimum of 100 flies in each genotype were tested.

Bouton shape

Boutons with round and smooth outline having equal diameter on both the axis were considered as regular boutons, whereas the boutons with deformed shape having rough outline and fusiform appearance are treated as irregular boutons.

Fly stocks

W1118, OregonR, $Futsch^{N94}$, *D42*-GAL4, *elav*-GAL4, UAS-CD8-GFP were obtained from Bloomington Indiana. UAS-Tau^{wt} was gifted by Mel Feany.

Western blot analysis

Protein was extracted using lysis buffer containing 10 mM Tris HCl, pH-7.4, 150 mM NaCl, 5 mM EDTA, 5 mM EGTA, 10% Glycerol, 50 mM NaF, 5 mM DTT, 4 M Urea and protease inhibitors (Complete mini EDTA free from ROCHE). The extracted protein was separated in SDS polyacrylamide gels and blotted on to 0.2 μm nitrocellulose membranes (Sigma-Aldrich). Membranes were blocked and incubated with primary antibodies overnight. Primary antibodies such as α-TBPH (1:3000), α-Wit-C (DSHB, 1:200), α-FasII (DSHB, 1: 100), α-Spectrin (DSHB, 1:3000), α-Bruchpilot (DSHB, 1:300), α-Tubulin (Calbiochem, 1:3000) and α-Actin (Sigma A2066) were used. Goat anti-rabbit/anti-mouse igG HRP conjugated were used as secondary antibodies (1:100000, Pierce). Proteins detection was done with Femto Super Signal substrate (Pierce, 1:10).

Western blots for *futsch* protein levels

Western blot analysis to detect *futsch* protein was done in agreement with Zou. *et al* [47]. Briefly, 20 fly heads were homogenized in ice cold lysis buffer containing 1% CHAPS, 20 mM Tris/HCl (pH 7.5), 10 mM EDTA, 120 mM NaCl, 50 mM KCl, 2 mM DTT and protease inhibitors (Roche, Complete Mini EDTA free). The homogenization step was

followed by incubation in ice and centrifugation at 9000 *g* for 10 min at 4°C. Supernatants were collected and approximately 30 µg of total protein was loaded in pre-cast gradient gels with NuPAGE (Invitrogen NuPAGE® Novex 3–8% Tris-Acetate Gel 1.0 mm, NuPAGE LDS Sample buffer, NuPAGE reducing agent). The upper part of the gel, up to molecular weight 250 kDa, were placed on filters soaked with 1% SDS and transferred to nitrocellulose membrane at 0.12 amp current for 16 hrs in 20 mM Tris and 150 mM Glycine [31]. The lower part of the gel, for tubulin as a loading control, was transferred to nitrocellulose in 20% methanol, 20 mM Tris and 150 mM Glycine for 1 hr, at 350 mA current. Blocking with 5% milk in TBS-T 0.1% Tween20 followed by incubation with primary antibody α-*futsch* (DSHB, 1:400) and α-tubulin (Calbiochem, 1:3000). After extensive washes, membranes were incubated with secondary antibody anti mouse HRP-labeled (Pierce), diluted 1:100000 and developed in Femto Super Signal substrate (Pierce, 1:10).

Quantitative Real-time PCR analysis

Total RNA was extracted from the heads of wild type, TBPH minus alleles and the endogenous rescues (using D42-Gal4 and elav-Gal4) by using Trizol reagent (Invitrogen) as per the manufacturer's protocol. cDNA was synthesized with 1 µg of RNA sample by using M-MLV Reverse transcriptase (Invitrogen) and exameric random primers. Specific primers were designed to amplify *futsch* gene (*futsch*_254s, TTTCGGGATCCAACGGCTTTAAC*; futsch*_349as (96bp), GCGTCCAGTCGGTCTAGG and the gene expression levels was checked by real-time PCR using SYBR green technology. House keeping gene Rpl-11 (Forward, CCATCGGTATCTATGGTCTGGA and reverse, CATCGTATTTCTGCTGGAACCA) was amplified and used to normalize the results. All amplifications were performed on CFX96^{TM}, Real-time PCR detection system (Bio-Rad). The relative expression levels were calculated according to the following equation: $\Delta C_T = C_{T(Target)} - C_{T(normalized)}$.

Immunoprecipitation and RNA identification by RT-PCR

Protein G magnetic beads (Invitrogen) were washed two times with PBS+0.02% tween and coated with anti-FLAG M2 monoclonal antibody (Sigma). Fly heads (W1118, elav>TBPH, elav>FL and elav>REP) were homogenized in a lysis buffer containing 20 mM Hepes, 150 mM NaCl, 0.5 mM EDTA, 10% Glycerol, 0.1% Triton X-100, and 1 mM DTT with a Dounce homogenizer, followed by centrifugation for 5 min at 0.4 g. RNA containing [19]9 repeats, prepared as described by Buratti and collaborators [3], was added to the head extracts in order to control the efficiency of selection between non-specific and specific purification. The pretreated beads and head extracts were mixed and incubated for 30 min at 4°C, followed by washing five times with lysis buffer. Bound RNA transcripts were extracted with DynaMagTM-Spin (Invitrogen). The beads were treated with Trizol (Ambion) and precipitated with glycogen and Isopropanol. First-strand synsthesis was achieved with Superscript^{TM}-III (Invitrogen). Real Time PCRs were carried out with gene specific primers. The used primers are the following:. ***Futsch:*** 5′-CTCGCCAAAGCCCACATCACC-3′ and 5′-GTCACCCTCACACTCAGCTCC-3′. **homer:** 5′-GGTATAAACTGCTGCGGAAG-3′, and 5′-GACACTGATGATGCGGTAC-3′. ***hdac-6:*** 5′-CGAGCGGCTGAAGGAGAC-3′ and 5′-ACCAGATGGTCCACCAATTCG-3′. ***rpl-52:*** 5′-GAAAATAACAAAGATCTGCTTGGCC-3′ and 5′-AAGTGGCCCTTGGGCTTCAG-3′. Specific reverse transcription of [19]9 RNA was carried out with pBSKS 929_950as oligo 5′-AGCGGGCAGTGAGCGCAACGCA-3′. Amplification of [19]9 transcripts was obtained with the following oligos: pBSKS 667_687s 5′-TGGCGGCCGCTCTAGAACTA-3′ and pBSKS 903_924s 5′-ATGTGAGTTAGCTCACTCATTA-3′.

In order to calculate the enrichment fold, initially, all data were normalized to the respective inputs. Then, the signal was represented by how many more fold increase was measured compared to the control signal. To this aim, the enrichment was calculated by subtraction of controls ΔCt (unrelated REP protein (IP-REP) or TBPH$^{F/L150\text{-}152}$ (IP-FL), a variant of TBPH mutated within the RNA binding domain control) from ΔCt of experimental sample overexpressing TBPH-wt (IP-GOF).

The results were derived from three independent immunoprecipitation experiments and error bars represent standard deviations on the normalized ratios.

The statistical significance of differences observed between control- and specific- immunoprecipitation samples was determined by t-test ($p<0.05$).

Data analysis and statistics

Total number of boutons and branches were acquired from longitudinal muscle 6/7 of hemisegments A2 and A3 of all genotypes. Branches were defined as an extension of the presynaptic motor neuron that has not less than two or three boutons. Immunoreactivity of *futsch* and acetylated tubulin was quantified from the images acquired at the same fluorescence intensity using Zeiss LSM510 confocal microscope. Statistics were performed using GraphPad Prism version 4.0b software. One-way ANOVA was performed using Bonferroni's multiple comparison test to compare two or more independent groups. The significance between the variables was showed based on the p-value obtained (*indicates $p<0.05$, ** $p<0.01$ and *** $p<0.001$). All the numbers in the histograms represent mean ± SEM.

Supporting Information

Figure S1 Loss of TBPH does not affect muscles development or synaptic stability. (A, D) Wild type body wall muscles stained with phalloidin and tubulin respectively. Similar stainings in (B, E) TBPH^{D23}/-, (C, F) TBPH^{D142}/- showed no changes in muscle morphology and cytoskeleton organization. (G) Quantifications showing no significant difference between the wild type and the TBPH minus muscles during larval development. (H) Confocal images of postsynaptic DLG protein showing no pre-synaptic retractions in (Hi–Hiii) wild type, (Hiv–Hvi) TBPH^{D23}/- and (Hvii–Hix) TBPH^{D142}/- larval NMJ. Scale 5 µm. (I) Percentage of third instar larvae NMJs presenting footprints showed no significant differences between wild type and TBPH minus alleles. The numbers of NMJs analyzed per each genotype is indicated above the columns.
(TIF)

Figure S2 TBPH loss of function does not affect motoneurons formation and survival. (A) *D42*-GAL4 driven expression of GFP protein in dorsal medial clusters of motoneurons in (Ai–Aiii) wild type background and in (Aiv–Avi) TBPH^{D23}/- background labeled similar cellular populations. Scale bar 20 µm. (B) Quantification of the number of GFP positive motoneurons present in the dorsal medial cluster of different abdominal segments at the ventral ganglion. No differences between wild type flies and TBPH mutant alleles were observed. $n = 7$ larvae.
(TIF)

Figure S3 Subcellular localization patterns and protein expression levels of different presynaptic proteins involved in NMJs formation were not affected by TBPH

depletion. (A) Confolcal images showing the distribution of the active zone marker Bruchpilot in (Ai–Aiii) wild type, (Aiv–Avi) in $TBPH^{D23}$/- and (Avii–Aix) in $TBPH^{D142}$/-. Other presynaptic terminal markers such as (Bi-Bix) Synapsin showed no difference in their localization in TBPH null alleles compared to wild type. Scale 5 µm. Western blots analysis showing no difference in the expression levels of pre-synaptic proteins (C) Fas-II, (D) Wit-C, (E) Bruchpilot and (F) Spectrin. Note that tubulin was used as a loading control in the bottom panel of each blot and its expression levels were further corroborated against actin used as a second loading control (G).
(TIF)

Figure S4 Genetic interactions between TBPH and *futsch* transheterozygous flies. Quantitative analysis of (A) number of big synaptic boutons and (B) terminal branches in muscle number 6/7 abdominal segments II and III. Heterozygous and trans heterozygous alleles of $futsch^{N94}$ and $TBPH^{D23}$ present no significant changes in the number of big synaptic boutons and synaptic branches compared to wild type larval NMJ. (C) Larval motility in the third instar larvae showing no rescue with the Tau protein expression in TBPH mutant background compared to similar rescue with endogenous TBPH expression. ($n = 40$ larvae for each genotype).
(TIF)

Figure S5 Functional comparisons between TBPH wild type protein and the RNA binding defective $TBPH^{F/L150\text{-}152}$ isoform (A) Nuclear localization of TBPH wild type protein (Ai–Aiii) and $TBPH^{F/L150–152}$ (Aiv-Avi) in the neuronal cell bodies of the dorsal medial motor neurons of ventral ganglion. Scale bar 20 µm. (B) Expression levels of TBPH full-length protein and $TBPH^{F/L150–152}$ in the fly heads expressed with *elav*-Gal4 (upper panel). Tubulin was used as a loading control (bottom panel). (C) $TBPH^{F/L150–152}$ rescues the motility defects such as larval movement, (D) defects in walking ($n = 50$) and (E) climbing ($n = 250$). (F) Real-time PCR quantifications of the *futsch* transcript levels in the heads from wild type, TBPH minus alleles and endogenous TBPH rescue with *D42*-Gal4 and *elav*-Gal4. Four independent experiments were quantified and the average is plotted in the graph.
(TIF)

Acknowledgments

We thank Bloomington Drosophila Stock Center at Indiana University for fly stocks and Developmental Hybridoma Bank at Iowa University for antibodies. This work was supported by the Agenzia di Ricerca per la Sclerosi Laterale Amiotrofica (AriSLA).

Author Contributions

Conceived and designed the experiments: MR EB FEB FF . Performed the experiments: VKG GR MR CA RK EB FF. Analyzed the data: VKG GR MR CA RK EB FEB FF. Wrote the paper: FF.

References

1. Buratti E, Baralle FE (2009) The molecular links between TDP-43 dysfunction and neurodegeneration. Adv Genet 66: 1–34.
2. Strong MJ () The evidence for altered RNA metabolism in amyotrophic lateral sclerosis (ALS). J Neurol Sci 288: 1–12.
3. Buratti E, Baralle FE (2001) Characterization and functional implications of the RNA binding properties of nuclear factor TDP-43, a novel splicing regulator of CFTR exon 9. J Biol Chem 276: 36337–36343.
4. Moisse K, Volkening K, Leystra-Lantz C, Welch I, Hill T, et al. (2009) Divergent patterns of cytosolic TDP-43 and neuronal progranulin expression following axotomy: implications for TDP-43 in the physiological response to neuronal injury. Brain Res 1249: 202–211.
5. Neumann M, Sampathu DM, Kwong LK, Truax AC, Micsenyi MC, et al. (2006) Ubiquitinated TDP-43 in frontotemporal lobar degeneration and amyotrophic lateral sclerosis. Science 314: 130–133.
6. Chen-Plotkin AS, Lee VM, Trojanowski JQ () TAR DNA-binding protein 43 in neurodegenerative disease. Nat Rev Neurol 6: 211–220.
7. Lagier-Tourenne C, Polymenidou M, Cleveland DW () TDP-43 and FUS/TLS: emerging roles in RNA processing and neurodegeneration. Hum Mol Genet 19: R46–64.
8. Feiguin F, Godena VK, Romano G, D'Ambrogio A, Klima R, et al. (2009) Depletion of TDP-43 affects Drosophila motoneurons terminal synapsis and locomotive behavior. FEBS Lett 583: 1586–1592.
9. Lu Y, Ferris J, Gao FB (2009) Frontotemporal dementia and amyotrophic lateral sclerosis-associated disease protein TDP-43 promotes dendritic branching. Mol Brain 2: 30.
10. Hanson KA, Kim SH, Wassarman DA, Tibbetts RS (2010) Ubiquilin modifies TDP-43 toxicity in a Drosophila model of amyotrophic lateral sclerosis (ALS). J Biol Chem 285: 11068–11072.
11. Li Y, Ray P, Rao EJ, Shi C, Guo W, et al. (2010) A Drosophila model for TDP-43 proteinopathy. Proc Natl Acad Sci U S A 107: 3169–3174.
12. Miguel L, Frebourg T, Campion D, Lecourtois M (2010) Both cytoplasmic and nuclear accumulations of the protein are neurotoxic in Drosophila models of TDP-43 proteinopathies. Neurobiol Dis.
13. Ritson GP, Custer SK, Freibaum BD, Guinto JB, Geffel D, et al. (2010) TDP-43 mediates degeneration in a novel Drosophila model of disease caused by mutations in VCP/p97. J Neurosci 30: 7729–7739.
14. D'Ambrogio A, Buratti E, Stuani C, Guarnaccia C, Romano M, et al. (2009) Functional mapping of the interaction between TDP-43 and hnRNP A2 in vivo. Nucleic Acids Res 37: 4116–4126.
15. Budnik V (1996) Synapse maturation and structural plasticity at Drosophila neuromuscular junctions. Curr Opin Neurobiol 6: 858–867.
16. Schuster CM, Davis GW, Fetter RD, Goodman CS (1996) Genetic dissection of structural and functional components of synaptic plasticity. I. Fasciclin II controls synaptic stabilization and growth. Neuron 17: 641–654.
17. Zito K, Parnas D, Fetter RD, Isacoff EY, Goodman CS (1999) Watching a synapse grow: noninvasive confocal imaging of synaptic growth in Drosophila. Neuron 22: 719–729.
18. Kabashi E, Lin L, Tradewell ML, Dion PA, Bercier V, et al. Gain and loss of function of ALS-related mutations of TARDBP (TDP-43) cause motor deficits in vivo. Hum Mol Genet 19: 671–683.
19. Rohrbough J, Rushton E, Woodruff E, 3rd, Fergestad T, Vigneswaran K, et al. (2007) Presynaptic establishment of the synaptic cleft extracellular matrix is required for post-synaptic differentiation. Genes Dev 21: 2607–2628.
20. Eaton BA, Fetter RD, Davis GW (2002) Dynactin is necessary for synapse stabilization. Neuron 34: 729–741.
21. Eaton BA, Davis GW (2005) LIM Kinase1 controls synaptic stability downstream of the type II BMP receptor. Neuron 47: 695–708.
22. Sanyal S (2009) Genomic mapping and expression patterns of C380, OK6 and D42 enhancer trap lines in the larval nervous system of Drosophila. Gene Expr Patterns 9: 371–380.
23. Johansen J, Halpern ME, Johansen KM, Keshishian H (1989) Stereotypic morphology of glutamatergic synapses on identified muscle cells of Drosophila larvae. J Neurosci 9: 710–725.
24. Packard M, Koo ES, Gorczyca M, Sharpe J, Cumberledge S, et al. (2002) The Drosophila Wnt, wingless, provides an essential signal for pre- and postsynaptic differentiation. Cell 111: 319–330.
25. Ruiz-Canada C, Ashley J, Moeckel-Cole S, Drier E, Yin J, et al. (2004) New synaptic bouton formation is disrupted by misregulation of microtubule stability in aPKC mutants. Neuron 42: 567–580.
26. Kittel RJ, Wichmann C, Rasse TM, Fouquet W, Schmidt M, et al. (2006) Bruchpilot promotes active zone assembly, Ca2+ channel clustering, and vesicle release. Science 312: 1051–1054.
27. Akbergenova Y, Bykhovskaia M (2007) Synapsin maintains the reserve vesicle pool and spatial segregation of the recycling pool in Drosophila presynaptic boutons. Brain Res 1178: 52–64.
28. Schuster CM, Davis GW, Fetter RD, Goodman CS (1996) Genetic dissection of structural and functional components of synaptic plasticity. II. Fasciclin II controls presynaptic structural plasticity. Neuron 17: 655–667.
29. Marques G, Bao H, Haerry TE, Shimell MJ, Duchek P, et al. (2002) The Drosophila BMP type II receptor Wishful Thinking regulates neuromuscular synapse morphology and function. Neuron 33: 529–543.
30. Pielage J, Fetter RD, Davis GW (2005) Presynaptic spectrin is essential for synapse stabilization. Curr Biol 15: 918–928.
31. Hummel T, Krukkert K, Roos J, Davis G, Klambt C (2000) Drosophila Futsch/22C10 is a MAP1B-like protein required for dendritic and axonal development. Neuron 26: 357–370.
32. Roos J, Hummel T, Ng N, Klambt C, Davis GW (2000) Drosophila Futsch regulates synaptic microtubule organization and is necessary for synaptic growth. Neuron 26: 371–382.

Figure S1.

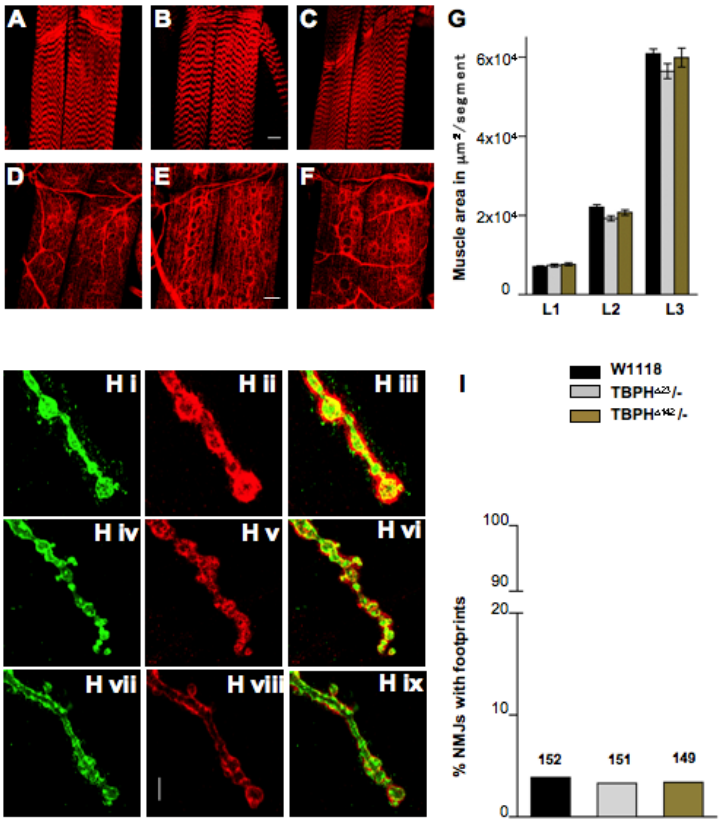

Figure S2.

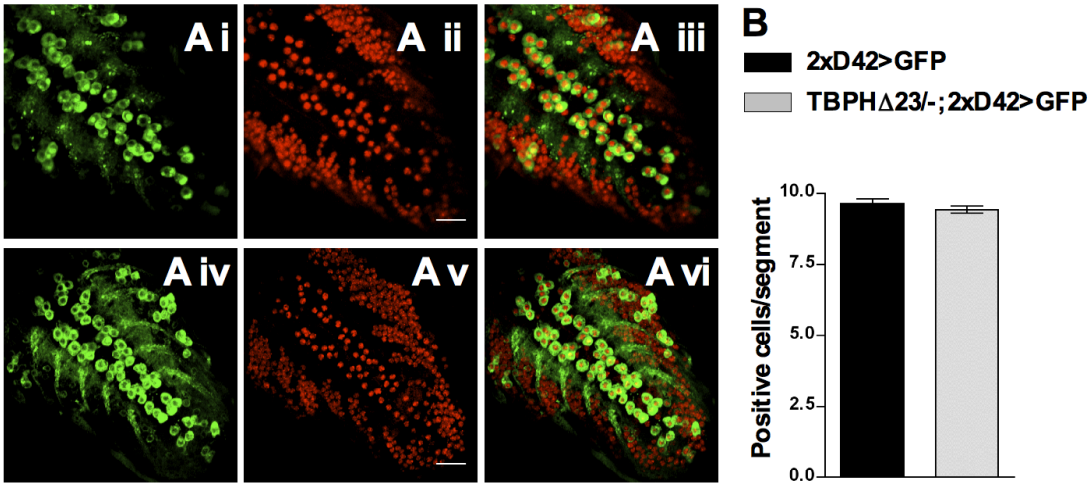

Figure S3.

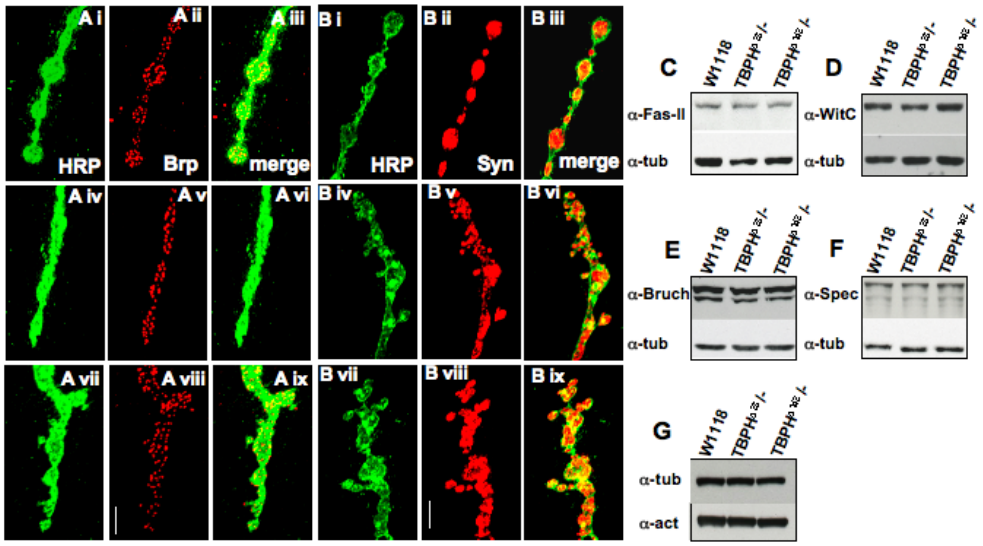

Figure S4.

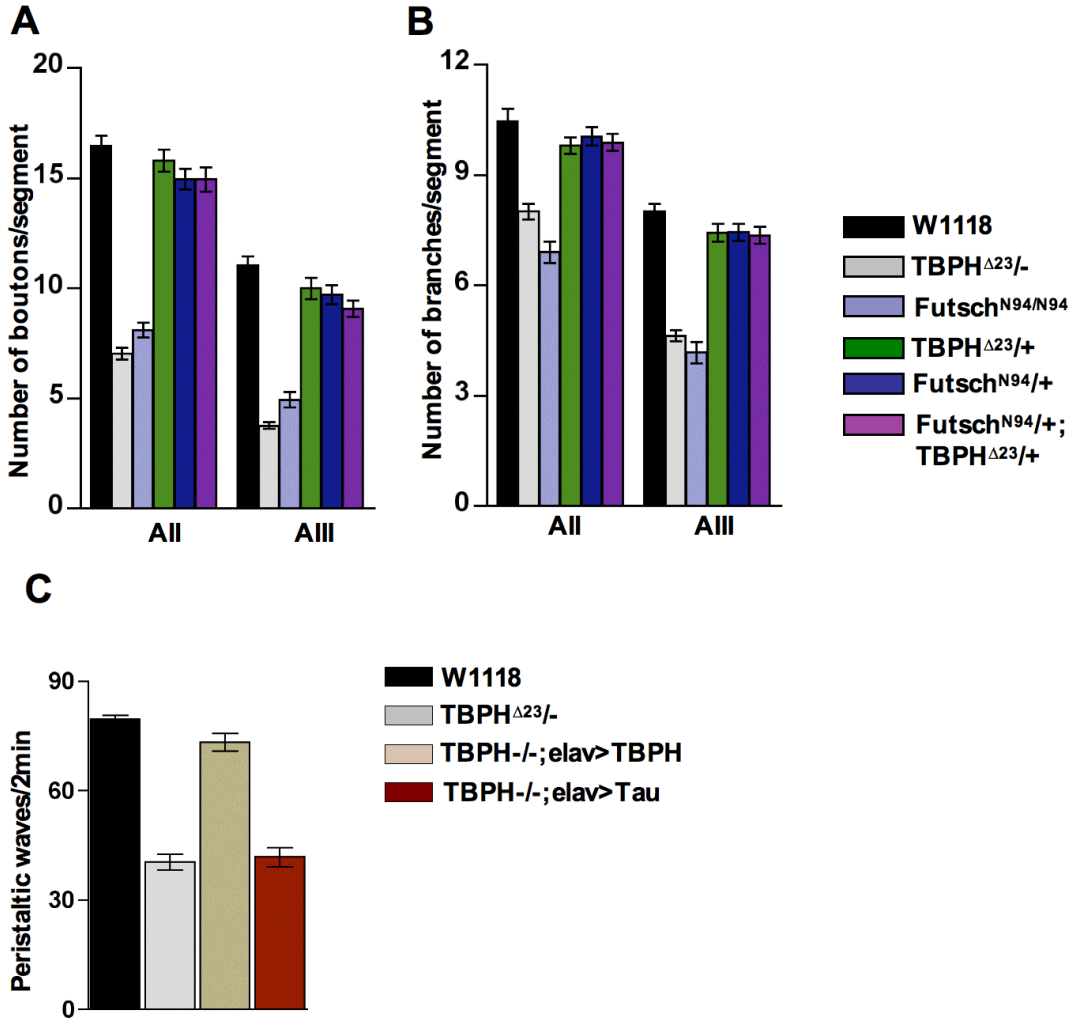

Figure S5.

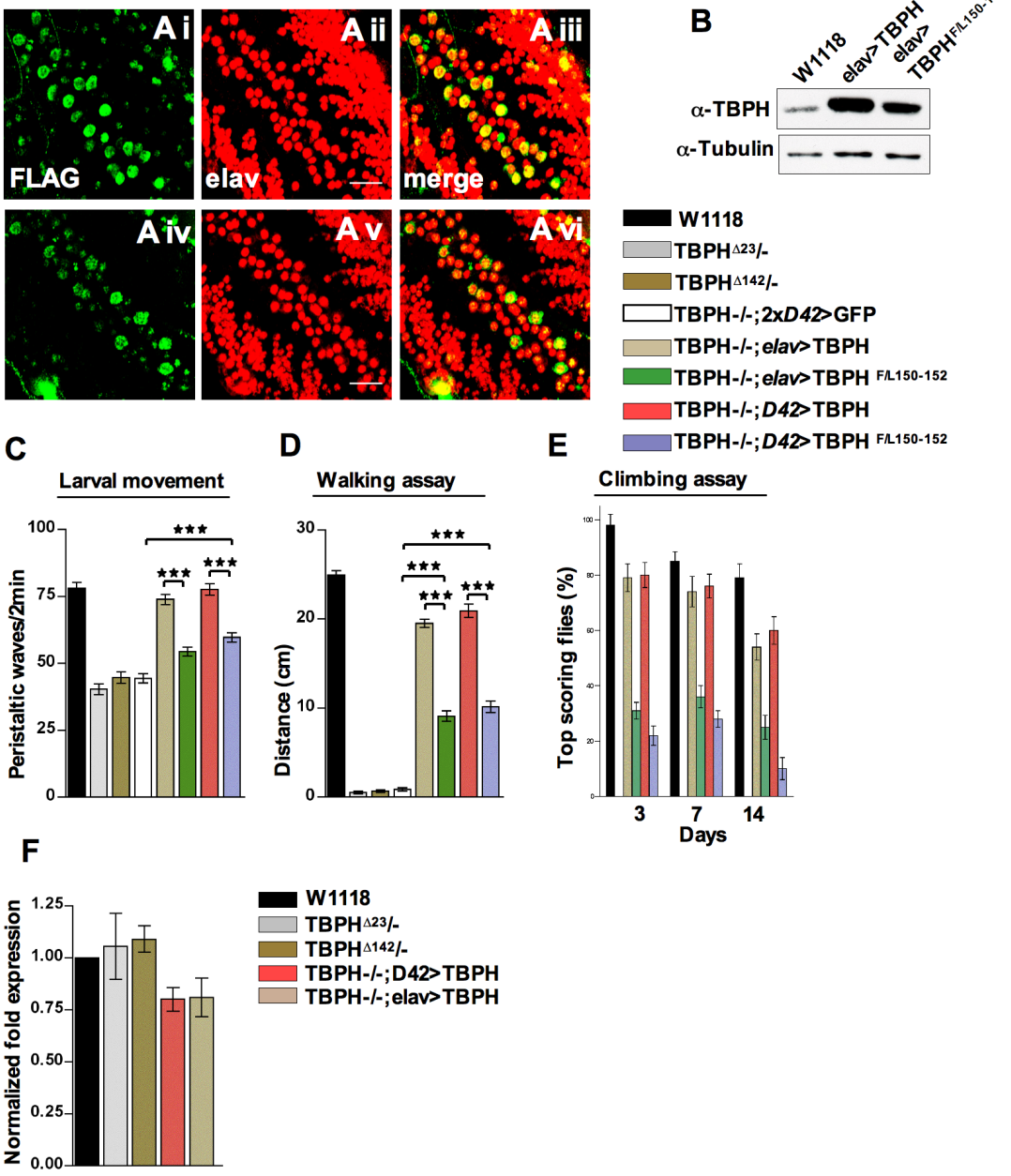
A i
A ii
A iii
A iv
A v
A vi
FLAG
elav
merge
B
W1118
elav>TBPH
elav> TBPH F/L150-152
α-TBPH
α-Tubulin
W1118
TBPH Δ23/-
TBPH Δ142/-
TBPH-/-;2xD42>GFP
TBPH-/-;elav>TBPH
TBPH-/-;elav>TBPH F/L150-152
TBPH-/-;D42>TBPH
TBPH-/-;D42>TBPH F/L150-152
C
Larval movement
Peristaltic waves/2min
D
Walking assay
Distance (cm)
E
Climbing assay
Top scoring flies (%)
3
7
14
Days
F
Normalized fold expression
W1118
TBPH Δ23/-
TBPH Δ142/-
TBPH-/-;D42>TBPH
TBPH-/-;elav>TBPH

JBC Papers in Press. Published on February 3, 2014 as Manuscript M114.548859
The latest version is at http://www.jbc.org/cgi/doi/10.1074/jbc.M114.548859

Evolutionarily-conserved hnRNP A/B proteins functionally interact with human and Drosophila TAR DNA-binding protein 43 (TDP-43).

Maurizio Romano[1]‡, Emanuele Buratti[2], Giulia Romano[2], Raffaella Klima[2], Lisa Del Bel Belluz[1], Cristiana Stuani[2] Francisco Baralle[2] and Fabian Feiguin[2].

[1] Department of Life Sciences, University of Trieste, Via A. Valerio 28, 34127, Trieste, Italy.; [2] International Centre for Genetic Engineering an Biotechnology, Padriciano 99, I-34149, Trieste, Italy

*Running Title: *Cooperation between TDP-43 and hnRNP A1/A2 orthologs.*
‡To whom correspondence should be addressed: Department of Life Sciences, University of Trieste, Via A. Valerio 28, 34127 Trieste. Tel: +39-040-3757312; Fax: +39-040-226555;
E-mail: mromano@units.it

Keywords: TDP-43, TARDBP, TBPH, hnRNP A/B, Hrp38, Hrb98DE, CG9983, mRNA splicing, RNA-binding proteins, Drosophila.

Background: TDP-43 and hnRNPA1/A2 factors are implicated in neurodegeneration.
Results: The human and fruit fly TDP-43 and hnRNPA1/A2 orthologs show physical, genetic and functional interplays.
Conclusion: The functional cooperation between TBPH/Hrp38 and TDP-43/hnRNP A/B is conserved throughout evolution.
Significance: TBPH/Hrp38 interplay can be critical for neurodegeneration and Drosophila is a model suitable to study the impact of this interaction.

ABSTRACT

Human TDP-43 represents the main component of neuronal inclusions found in patients with neurodegenerative diseases, especially FTLD and ALS. In vitro and in vivo studies have shown that the TDP-43 Drosophila ortholog (TBPH) can biochemically and functionally overlap the properties of the human factor. The recent direct implication of the human hnRNPs A2B1 and A1, known TDP-43 partners, in the pathogenesis of multisystem proteinopathy and ALS, supports the hypothesis that the physical and functional interplay between TDP-43 and hnRNP A/B orthologs might play a crucial role in the pathogenesis of neurodegenerative diseases. To test this hypothesis and further validate the fly system as a useful model to study this type of diseases, we have now characterized human TDP-43 and drosophila TBPH similarity in terms of protein-protein interaction pathways. In this work, we show that TDP-43 and TBPH share the ability to associate *in vitro* with Hrp38/Hrb98DE/CG9983, the fruit fly ortholog of the human hnRNP A1/A2 factors. Interestingly, the protein regions of TDP-43 and Hrp38 responsible for reciprocal interactions are conserved through evolution. Functionally, experiments in HeLa cells demonstrate that TDP-43 is necessary for the inhibitory activity of Hrp38 on splicing. Finally, Drosophila *in vivo* studies show that Hrp38 deficiency produces locomotive defects and life span shortening in TDP-43 +/- animals. These results suggest that hnRNP protein levels can play a modulatory role on TDP-43 functions.

INTRODUCTION

TDP-43 (43-kDa TAR DNA-binding protein, TARDBP) is a nuclear factor involved in regulation of mRNA splicing, mRNA stability and other cellular processes (1). Initially associated with the pathogenesis of monosymptomatic forms of CFTR (2-4), TDP-43 has been found in the ubiquitin-positive cytosolic aggregates of neurons from patients with Amyotrophic Lateral Sclerosis (ALS) and Frontotemporal Lobar Degeneration (FTLD-U) (5,6). More recently, pathological TDP-43 inclusions have been described also in several additional neurodegenerative diseases such as

Alzheimer's, Huntington's and Parkinson's diseases (7) and also MSP (formerly known as IB MPFD/ALS (8). Presently, however, the molecular mechanisms that link TDP-43 to neurodegeneration are not clear. Interestingly, the observation that in all patients carrying TDP-43 aggregates this region is cleaved and becomes aberrantly phosphorylated has focused particular attention on studying the C-terminus of this protein in the pathogenesis of neurodegenerative disorders (9).

At the functional level, recent studies have demonstrated that the C-terminal domain is important for TDP-43 splicing activity and is responsible for the interaction of this protein with many other cellular factors and bodies such as stress granules (10-12). In particular, the inhibitory role in pre-mRNA splicing played by TDP-43 relies on its ability to tether different members of the hnRNP A/B family in proximity of the inhibited exon, through interactions mediated by the 342-366 Q/N-rich region localized in the C-tail (13,14). In keeping with this conclusion, mutants of human and Drosophila TDP-43 without this region are unable to interfere with exon inhibition (15). Most importantly, this Q/N-rich sequence is also involved in modulating TDP-43 self-interaction and binding to polyglutamine aggregates, thus playing an important role in reducing TDP-43 natural tendency to aggregate (16,17).

One open question that still carries considerable importance towards the development of animal models of TDP-43 pathology is to clarify how much the biological interactions and function have been conserved across different species. The reason being that a high degree of similarity will facilitate the use of these models for the development of effectors capable of modulating TDP-43 functional properties in humans. Multiple protein alignment across different species of sequence from TARDBP have highlighted that this factor has been conserved throughout evolution (15,18). This very high level of conservation can also be extended to all its basic functional properties. For example, it is clear that even TDP-43s from evolutionarily distant organisms share a binding specificity for similar (UG) rich RNA sequences (15).

In particular, the functional overlap between human and Drosophila TDP-43 with regards to the splicing process was already well known following the observation that Drosophila TBPH could functionally complement the absence of human TDP-43 in HeLa cells (14).

The biological similarity between these two proteins was even more generally confirmed in a *Drosophila melanogaster* model of TDP-43 proteinopathy, where expression of the endogenous TBPH gene was abolished (19). The resulting flies showed locomotor dysfunctions and reduced life span that could be rescued by expression of the human TDP-43 factor (19). Presently, several different studies carried out in Drosophila strongly support the functional homology of the human and Drosophila TDP-43 orthologs, as recently reviewed by us (20). Altogether, therefore, most of the data collected so far promote the use of Drosophila models to investigate the molecular mechanisms underlying human neurodegenerative disorders derived from TDP-43 alterations.

In this work, we have now further extended this connection by exploring the interaction of TDP-43 and TBPH with fruit fly hnRNP proteins. Using co-immunoprecipitation experiments we have found that the Drosophila ortholog of human hnRNP A1/A2 proteins (Hrb98DE/*Hrp38)* maintains the ability to bind both to TDP-43 and TBPH. Interestingly, we found that the regions involved in this interaction have been highly conserved in all these proteins there is a functional, genetic interaction between Hrp38 and TBPH.

EXPERIMENTAL PROCEDURES

GST-overlay (Far Western) , HPLC analysis and Mass Spectrometry.

Western blots containing 150mg of HeLa nuclear (NE), HeLa cytoplasmic (S100), and Drosophila nuclear extract (L2NE) were incubated for 2 hours with either GST-TDP-43 or GST-TBPH (10 μg of protein in 20 ml of PBS, 10% (w/v) of non-fat dried milk) for 1 hour. The membrane was then washed four times with PBS plus 0.2% Tween-20 (Polyoxyethylene sorbitan monolaurate) and is then incubated for another hour with a commercial anti-GST antibody (Sigma) at a dilution of 1:2000. The blots were then washed again four times using PBS plus 0.2% tween-20 and incubated for another hour with anti-

goat HRP antibody (Dako A/S) at a dilution of 1:2000. After four final washes the western blots were developed using ECL (Amersham Pharmacia). Fractionation of nuclear extracts was performed on a HPLC Agilent 1100 Series using a Phenomenex C4 300A (250x4.6mm) Reverse Phase Column. The proteins were eluted using a solution 95% acetonitrile+0.1%TFA in a 20 to 70% linear gradient over 38 minutes. The different fractions from 35% to 43% mobile phase were first speed dried for 2 hours to reduce volume and then concentrated using YM-10 filters (Microcon). Each fraction was then divided in two and loaded on 10% SDS-PAGE gels, one to be stained with Coomassie whilst the other was blotted on Optitran Nitrocellulose BA-S 83 membrane (Schelicher&Schuell) and subjected to GST-overlay as described above. Internal sequence analysis from the Coomassie Blue-stained bands excised from the SDS-PAGE gel was performed using an electrospray ionization mass spectrometer (LCQ DECA XP, Thermo Finnigan). The bands were digested by trypsin, and the resulting peptides were extracted with water and 60% acetonitrile/1% trifluoroacetic acid. The fragments were then analyzed by mass spectrometry and the proteins were identified by analysis of the peptide MS/MS data with Turbo SEQUEST (ThermoFinnigam) and MASCOT (Matrix Science).

Plasmid construction

The generation of pFLAG TDP-43 and pFLAG TBPH constructs has been described previously (14,15,21). The Apo AII (pTB-ApoAIIm) splicing reporter minigenes has been described by Mercado and co-workers (22), respectively. The Hrp38 ORF was kindly provided by Prof. Joan Steitz. The Hrp38 ORF was amplified by PCR with the following oligos HRP38_s, 5'-tcaGAATTCaagcttATGGTGAACTCGAACCAG AACCAGAA-3'; HRP38 _as, 5'-tcaGGTACCgcggccgcctcgagTCAATATCTGCGG TTGTTGCCACCGT-3' and subsequently cloned in pFLAG-CMV2 vector for eukaryotic expression. The EGFP-TDP-43 (321–366) vector used in the co-immunoprecipitation experiments has already been described by Budini and co-workers (16).

The EGFP-Hrp38-(293-365) vector was generated by PCR amplification of the Hrp38 region spanning the residues 293-365 with the following oligos: Hrp38 C-term XhoI_s, 5'-AGATCTCGAGCGGCGGCAACAATTGGAAC AATGGTG-3'; Hrp38 C-term BamHI_as, 5'-TCCGGTGGATCCTCAATATCTGCGGTTGTT GCCACCGTT-3'. All constructs were sequenced to confirm their identity and to exclude the presence of other mutations.

Transfections and RT-PCRs

The plasmid DNA used for transfections was purified with JetStar columns (Genomed). Liposome-mediated transfections of $2.5x10^5$ human HeLa cells were performed using Effectene (Qiagen). The amount of constructs used for each transfection ranged between 0.5 and 1µg. siRNA transfections were performed in HeLa cells by using the small interfering RNA (siRNA) oligonucleotide specific for TDP-43 (GCAAAGCCAAGAUGAGCCU) and the Oligofectamine Reagent (Invitrogen), as previously described (14). At the end of transfections, the cells were harvested and the RNA was extracted with Trifast reagent (EuroGold). The cDNA was prepared with M-MLV Reverse Transcriptase (Invitrogen) and poly-dT primer, according to the manufacturer's instructions. PCRs were carried out for 35 amplification cycles (95°C for 30s, 55°C for 30s and 72°C for 30 s) and PCR products were analyzed on 1.5% agarose gels.

Co-immunoprecipitations

For co-immunoprecipitation assays, HeLa cells (60% of confluence) were transfected with 2µg of each plasmid set and Effectene reagent. The cells were collected in PBS supplemented with protease inhibitors (Roche Applied Science) and lysed by sonication. The lysates were incubated with 0.6 µg of anti-GFP antibody (Santa Cruz Biotechnology) for 3 h at 4 °C, and then 30 µl of A/G Plus agarose beads (Santa Cruz Biotechnology) were added. After overnight incubation at 4 °C, the beads were precipitated and washed three times with PBS. After SDS-PAGE, the immunoprecipitates were probed with an anti-FLAG antibody (F1804, Sigma) in Western blot analysis.

Fly Stocks.

RNAi flies against TBPH (ID38377) and Hrp38/Hrb98DE/CG9983 (#31303) were obtained from VDRC Vienna and Bloomington Stock Center, USA, respectively.

Quantitative real time PCRs.

Total RNA was extracted from the heads of wild type W^{1118}, ElavG4, $tbph^{\Delta 23}$/+; $Hrp38^{RNAi}$ and ElavG4, tbph+/+; $Hrp38^{RNAi}$ by using Trizol reagent (Invitrogen) according to the manufacturer' s protocol. cDNA was synthesized with 1 µg of RNA sample by using Superscript™-III (Invitrogen) reverse transcriptase and oligo dT primers. Specific primers were designed to amplify the *Hrb98DE/Hrp38* gene (*forward:* GTCTAGAATATGCGCAAGCTGTTCATC and *reverse:* AGAATTCCGTTTCTTGCCAGTCTCCTT) and the gene expression levels were checked by real-time PCR using SYBR green technology. Housekeeping gene Rpl-11 (forward: CCATCGGTATCTATGGTCTGGA and reverse: CATCGTATTTCTGCTGGAACCA) and Rpl-32 (forward: AAGCGGCGACGCACTCTGTT and reverse: GCCCAGCATACAGGCCCAAG) were amplified and used to normalize the results. All amplifications were performed on CFX96™, Real-time PCR detection system (Bio-Rad). The relative expression levels were calculated according to the following equation: $\Delta C_T = C_{T(Target)}-C_{T(normalized)}$. 4 PCR reactions for each genotype (2 duplicates) were performed.

Climbing Assay.

Newly eclosed flies were transferred in batches of 20-25, (1:1 male:female), to fresh vials and aged for 4 days. They were then transferred, without anaesthesia, to an empty transparent Duran 50 ml glass cylinder. The cylinder was divided into three parts (bottom, middle and top). The climbing ability was quantified as the percentage of flies that reached the top of the tube in 15 seconds. Three trials were performed and the average value was calculated. A minimum of 160 flies for each genotype were tested.

Life Span.

Adult flies were collected for two days and transferred to fresh tubes at a density of 20-25 per vial (1:1 male:female). Every third day, flies were transferred to new tubes containing fresh medium and deaths were scored. Survival rate graph was plotted with percentage of survival flies against day. All the experiments were performed in a humidified, temperature controlled incubator at 25 °C and 60% humidity on a 12-h light and 12 h dark cycle. Flies were fed with standard cornmeal (2.9%), sugar (4.2%), yeast (6.3%) fly food.

Immunohistochemistry

Drosophila adult brains were dissected in 1X PB (100mM Na_2HPO_4/NaH_2PO_4, pH 7.2) 0.3%Triton X-100 and fixed in 4% paraformaldehyde for 20 minutes. Brains were washed in PB 0.3%Triton (20 minutes for 3 times) and than were blocked in 5% Normal Goat Serum 30 minutes. Primary antibodies (anti-Elav DSHB 1:250 and anti anti-Futsch 22C10s DSHB 1:50) were incubated over night at 4°C. Secondary antibodies were incubated at room temperature for two hours (Alexa Fluor® 488 mouse, 1:500; Alexa Fluor® 555 rat 1:500). Images were captured on a Zeiss 510 Meta confocal microscope. Labelling futsch intensities normalized to anti-Elav staining / area were calculated with ImageJ.

RESULTS

Human and Drosophila TDP-43 orthologs share the same pattern of human and fruitfly nuclear interactors

In order to compare the interactors of both human and drosophila TDP-43 a GST-overlay (Far-Western) analysis was performed as previously described (13). In this experiment, equal amounts of human HeLa nuclear (NE) and cytoplasmic (s100) extracts along with S2 drosophila nuclear extract (L2NE) were blotted onto a Western blot membrane (Fig. 1A, left panel) and incubated with recombinant GST-TDP-43 (Fig. 1A, central panel) or GST-TBPH (Fig. 1A, right panel). Comparison of the signals in the NE and L2NE lanes confirmed that GST-TDP-43 and GST-TBPH shared a similar recognition pattern of interactors mostly localized in the 32.5-47.5 kDa MW range. As control, both GST-TDP-43 and GST-TBPH yielded negligible signals in the cytoplasmic extract (S100 lane).

Previous characterization of human TDP-

43 interacting factors using this kind of assay found that the strongest bands were hnRNP A1, hnRNP A2, hnRNP C1, hnRNP B1 and hnRNP A3, respectively (13). Interestingly, GST-TBPH was also observed to bind specifically to these proteins in the HeLa nuclear extract (Fig.1A, middle panel). This was also in keeping with previous reports from our lab that GST-TBPH could supershift human GST-hnRNP A2 in a band-shift experiment (14).

Most interestingly, a similar situation to the human extract recognition pattern could also be observed for the nuclear Drosophila proteins in the L2NE extract. In particular, three major bands that we named 1, 2, and 3 respectively were specifically recognized both by GST-TDP-43 and GST-TBPH (Fig.1A, middle and central panel). However, no further information was available with regards to the identity of these three bands.

Identification of the Drosophila factors interacting with TDP-43 and TBPH.

To identify these factors, the L2NE nuclear extract was fractionated by HPLC with a C4 reverse phase column (see Fig.1B, upper panel, for the elution profile). After collection, equal amounts of each fraction were loaded onto two separate SDS-polyacrylamide gels. The first was stained with Coomassie Blue (data not shown), whereas the other was blotted and incubated with GST-TDP-43 in a Far-Western assay (Fig. 1B, lower panel). By alignment of the Coomassie Blue-stained gel with the overlay signals we observed one faint and one strong band that migrated at the same height as the overlays shown in Fig.1A, right panel. These bands were excised from the Coomassie Blue-stained gel and identified by mass-spec analysis as Hrp38/ Hrb98DE/ CG9983 (P07909) (band 2) and as hnRNP Squid/Hrp40/CG16901 (Q08473) (band 1). Unfortunately, using this technique we could not discover the identity of band 3, probably because the reverse-phase fractionation of the Drosophila nuclear extract caused its denaturation. However, based on the nature and relative mobility of the two identified factors it is highly probable that band 3 may represent HRB87F/hrp36/ CG12749, another well known hnRNP A/B homologue in Drosophila.

Interestingly, both identified proteins belong to the Drosophila hnRNP A family and are orthologs of the human hnRNP A1 and hnRNP A2/B1 factors (23-25), that were previously shown to be the most efficient at interacting specifically with human TDP-43 (14). From these data, we concluded that the Drosophila hnRNP A/B family are the most efficient interactors of Drosophila TBPH in the same way that their human orthologs, hnRNP A1 and hnRNP A2/B1 factors, are of human TDP 43 (14).

The observation that Drosophila TBPH and human hnRNP proteins can cross-interact is also consistent with the substantial conservation in TBPH of the 321-366 region located within the C-tail of TDP-43 (Fig. 1C). In fact, we have already established in previous studies that the 321-366 region of TDP-43 is important for TDP-43 hnRNP A/B protein-protein interactions (14,16).

Mapping the sequences required for the interaction of TDP-43 with Drosophila Hrp38.

After the identification of Hrp38/ Hrb98DE/ CG9983 and Squid/Hrp40/CG16901 as two putative interactors of both human and Drosophila TDP-43 we focused the attention on Hrp38 because its signal in the GST-overlay using human GST-TDP-43 was much stronger than that of Hrp40, both before (Fig.1A, right panel) and after fractionation (Fig.1B, lower panel). This is in keeping with the observation that there is an extremely high sequence similarity also between Drosophila Hrp38 and human hnRNP A1 and A2 at the level of both the RRM and C-terminal sequences that are known to be mostly involved in determining RNA-protein and protein-protein interactions, respectively

First of all, therefore, we sought to validate using co-immunoprecipitation the interaction between TDP-43 and Hrp38 *in vivo*. To achieve this aim, we cloned the Hrp38 cDNA in the pFLAG eukaryotic expression vector (flag-Hrp38) and set up a co-immunoprecipitation assay by co-transfecting in HEK293 cells a GFP-TDP-43 wild type fusion protein (EGFP-TDP-43) in combination with the plasmid expressing flag-Hrp38. The results shown in Fig.2A demonstrate that flag-Hrp38 can efficiently co-immunoprecipitate EGFP-TDP-43, but not EGFP alone. As control, Western blot analysis showed that both EGFP and EGFP-TDP-43 were strongly expressed at the protein level (Fig. 2A, lower panel α-EGFP).

To perform a more precise mapping of the interacting region, recent experiments aiming at mapping the TDP-43 domain responsible of binding to the various hnRNPs demonstrated that the region spanning from residue 321 to residue 366 is responsible for the interaction with hnRNP A2 (14,16).

In this respect, the alignment of the human and fly TDP-43 C-terminal domains highlights that this area of human TDP-43 shows a very high degree of similarity within the Gly-rich domain of TBPH spanning residues 428-481 (Fig. 1C). Therefore, we repeated the co-immunoprecipitation experiments of flag-Hrp38 (Fig. 2B, upper panel, flag-Hrp38) in combination with a fusion protein consisting of EGFP carrying only the human region 321-366 (Fig. 2B, upper panel, EGFP-TDP-321-366). As shown in Figure 2B, flag-Hrp38 co-immunoprecipitated also with TDP-321-366, but not with EGFP alone.

Mapping the Hrp38 sequence required for the interaction with human TDP-43.

With regards to identifying the Hrp38 region involved in this interaction, previous studies on hnRNP A1-mediated protein interactions have shown that they mostly rely on a short region within the Gly-rich domain of the human hnRNP A1 (26). In keeping with this original observation, we have also recently shown by immunoprecipitation analysis that the region of hnRNP A2 involved in the interaction between this protein and TDP-43 must be comprised within its C-terminus region that spans residues 288-341 (16) and that the C-terminus of TBPH is required to supershift hnRNP A2 in a band-shift assay (14).

Based on these considerations, the alignment of the C-terminus regions of human hnRNPA1 and hnRNP A2 with Hrp38 showed that within the hnRNP A1, hnRNP A2, and Hrp38 sequences there is a highly conserved motif that could be responsible for this cross-interaction (Fig. 2C).

Therefore, we prepared a fusion vector of EGFP with the region of Hrp38 spanning from residue 293 to 365 (EGFP-Hrp38 (293-365)) and carried out co-transfection and co-immunoprecipitation experiments in combination with a flagged version of human TDP-43 (flag-TDP-43) or of fly TBPH. As shown in Fig. 2D and 2E, the Hrp38 region spanning these amino acids was able to specifically co-immunoprepitate both flag-TDP-43 and flag-TBPH, thus establishing this region as the one responsible for the interaction of Hrp38 with both human and fly TDP-43 orthologs.

Hrp38 supports the inhibitory role of TDP-43 for Apo AII exon 3 splicing.

After confirming the *in vivo* interaction between TDP-43 and Hrp38 and mapping the interacting sequences, it was then interesting to test whether this interaction was also functionally significant. To achieve this, we used the Hrp38 cDNA eukaryotic expression vector to test whether Hrp38 could affect the splicing of TDP-43-related reporter minigenes similarly to what had been observed for the human hnRNP A2 ortholog (14). Initially, the effects of Hrp38 overexpression in HEK293 cells were monitored by using the ApoAII splicing reporter assay (Fig. 3A) where the involvement of TDP-43 was previously well characterized (22,27). In this system, the independent overexpression of Hrp38 was able to decrease the amount of exon inclusion (Fig. 3B, lanes 3 and 4), although to a lesser extent compared to TDP-43 overexpression (Fig. 3B, lane 2).

Most importantly, in order to assess whether the activity of Hrp38 on splicing was direct or indirect (i.e., dependent on the presence of TDP-43), we repeated the experiment after endogenous TDP-43 silencing by siRNA treatment. The hypothesis behind this experiment is that if the effects of Hrp38 on ApoAII splicing were mediated by TDP-43, then the silencing of endogenous TDP-43 should abrogate the Hrp38 splicing inhibition observed in Fig.3B.

In normal conditions, the Apo AIIm minigene reporter displays approximately 35+/-5% of exon inclusion (Fig. 3C, lane 1). As expected, the RNAi with anti-TDP-43 resulted in a significant increase in the amount of the ApoAII exon 3 inclusion (Fig.3C, lane 2) whilst the overexpression of siRNA-resistant wild-type TDP-43 promoted strong ApoAII exon 3 skipping (Fig. 3C, lane 3). Unlike TDP-43, however, the overexpression of Hrp38 in the absence of endogenous TDP-43 did not modify the splicing pattern of both reporters (Fig. 3C, lane 4).

Similar results were obtained by using another well characterized splicing reporter assay

(CFTR C155T; data not shown) (3,28,29). In conclusion, these results demonstrate that Drosophila Hrp38 can interact with human TDP-43 also at the functional level.

It was therefore important to see whether Hrp38 could modulate the disease phenotype in our Drosophila models.

Hrp38 and TBPH genetically interact to prevent locomotor defects and reduced life span in a Drosophila model of Amyotrophic Lateral Sclerosis.

We have previously shown that the suppression of TBPH exclusively in neurons by RNA interference (RNAi) closely mirrored the main symptoms observed in ALS, such as drastic alterations in locomotive behaviours and shortening of life span (19,30). We now sought to investigate whether the suppression of Hrp38 in Drosophila neurons could induce similar ALS-related phenotypes *in vivo* or enhance the neurological alterations provoked by the reduction of TBPH expression. It should first of all be noted that the *in vivo* depletion of the two single genes are lethal when homozygous (19,31). For these reasons, in order to test the presence of a genetic interaction between TBPH and Hrp38 genes, *hypomorphic* alleles and heterozygous backgrounds were used for both genes.

Therefore, efficient pan-neuronal RNAi-mediated knockdown of Hrp38 was obtained using the *elav*-GAL4 driver. The reduction of Hrp38 expression in Drosophila brains (Fig. 4C) produced significant locomotor alterations, as revealed by defects in climbing assay, associated to a severe shortening of the life span, as compared to controls (Fig. 4A-B). These phenotypes closely resemble the defects observed in the TBPH-ko flies (19), and suggest that these proteins might be involved in the regulation of similar genetic traits.

Indeed, on one hand, we found that TBPH gene dose modifications in Hrp38-RNAi backgrounds strongly enhanced the above described phenotypes. This is outlined by the remarkable differences observed in climbing activity between *Elav*-GAL4, tbph+/+; $Hrp38^{RNAi}$ flies and in flies where TBPH expression levels were reduced by either removing one copy of the gene (*Elav*-GAL4, $tbph^{\Delta 23}$/+; $Hrp38^{RNAi}$) or by expression of a double RNAi against these two proteins (*ElavGAL4,* $tbph^{\Delta 23}$/+; $TBPH^{RNAi}$/$Hrp38^{RNAi}$) (Fig. 4A).

On the other hand, the observation that reduction in life span was directly proportional to the TBPH-gene copy number in the *Elav*-GAL4/$Hrp38^{RNAi}$ flies (Fig. 4B), suggested that these genes are functionally related to common metabolic pathways.

In order to determine whether the differences in locomotive behaviours and life span described above were effectively due to increased degeneration of Drosophila neurons, we used the human homolog microtubule-binding molecule MAP-1B, *futsch* in Drosophila, as maker of neuronal damage, as demonstrated by our previous studies on TBPH-dependent synaptic microtubules organization (30).

Therefore, we stained adult brains with a monoclonal antibody against *futsch* and analysed the distribution of the axons in the lamina and medulla, a highly innervated cerebral areas sited in the Drosophila optic lobes, immediately behind the retina. We observed that the neuropil of *Elav*-GAL4, $tbph^{\Delta 23}$/+; $Hrp38^{RNAi}$; or *Elav*-GAL4, $tbph^{\Delta 23}$/+; $TBPH^{RNAi}$ individually treated flies in the lamina appeared less stained and thinner compared to wild type controls with the presence of irregular holes in these structures due to the loss of innervating axons. Nevertheless, these phenotypes became drastically increased after the expression of a double RNAi against these two proteins (*Elav*-GAL4, $tbph^{\Delta 23}$/+/$Hrp38^{RNAi}$; $TBPH^{RNAi}$) (Fig. 5A). Demonstrating that these proteins are required to maintain the innervation of complex cerebral areas and indicating that the neurological defects observed in TBPH and Hrp38 supressed flies involved an enlarged neurodegenerative process.

DISCUSSION

TDP-43 is a nuclear factor highly conserved through evolution (18). A high degree of homology exists among the TDP-43 orthologs from human, rodents, *Drosophila melanogaster* and *Caenorhabditis elegans* (15). From a structural point of view, TDP-43 belongs to the hnRNP family of nuclear proteins (32) and its functions are mostly involved in the regulation of all aspects of mRNA metabolism, starting from transcriptional regulation, the control of pre-

mRNA splicing, mRNA transport/stability, microRNA expression, and probably mRNA translation (1). The central importance played by this factor to maintain cellular viability comes from knockout transgenic mice lines in which it was observed that embryonic development was severely impaired when in a homozygous state (33-35). From a human disease point of view, several studies have demonstrated that TDP-43 has a primary role in the origin and development of different neurodegenerative diseases, the exact molecular mechanism(s) mediating such an involvement is still largely unknown (36).

In order to better understand its biological role in health and disease it is obviously of the utmost importance to characterize its molecular targets and cellular partners. In fact, as with almost all members of the hnRNP family, the biological functions mostly depend on the presence of complex interaction networks that form distinct functional modules (37-39). For example, it has been long established that within the nuclear compartment hnRNP proteins are usually assembled into ribonucleoprotein particles, (40) and binary interactions have been described between several of these members: such as PTB and hnRNP L (41), hnRNP K and hnRNP A1, hnRNP A2/B1 and other nuclear proteins (42). In addition, it has been demonstrated that hnRNP A1, C1, E2, I, K, and L can form both homodimeric and heterodimeric interactions with each other (43). This behaviour has also been observed for TDP-43. This protein, in fact, has been proposed to exist as a dimer or as part of ribonucleoprotein complexes within the nuclear environment (44-47).

Considering these similarities, therefore, it is expected that knowledge of TDP-43 protein-binding network will help researchers to better understand the pathways underlying the pathogenesis of diseases, as has been previously shown to occur for several other factors involved in neurodegeneration (48-51).

In this direction, recent proteomic studies have shown that TDP-43 can associate with several factors involved in trafficking of biological membranes and transcription (52-54) as well as RNA metabolism both in the nucleus and in the cytoplasm (55,56). At present, however, the number of verified partners of TDP-43 is still limited. Nonetheless, it is now well known that among the better characterized interactors, there are several hnRNP A/B family members such as hnRNP A2/B1, A1, A3, and C2 (13,14,57,58).

In keeping with this situation, we show here that one Drosophila ortholog of the human hnRNP A/B family (Hrp38) can bind very efficiently to both TBPH and human TDP-43. Most importantly, our results show that the regions of the human and fly factors involved in this protein-protein interaction seem to be structurally conserved. In fact, TDP-43 residues 321-366 that were previously mapped as the minimal binding region required for interaction with hnRNP A2 (14) retain the ability to bind Hrp38. This conservations appears to be reciprocated by Hrp38 itself, as the cluster of amino acids implicated in this protein-protein interactions also shows a very good level of evolutionary conservation between Hrp38 and hnRNPs A1/A2, with 36% identity and 33% similarity over 33 residues.

Most importantly, the high degree of conservation of these interactions can be carried over at the functional level, as Hrp38 can modulate the splicing of two model exons only in presence of TDP-43. Even at a more general level, *in vivo* studies carried out in Drosophila also support this view. In particular, the locomotor deficit and reduction in life span, as well as the level of neuropil degeneration caused by the simultaneous decrease in expression of both factors were higher than that expected by an additive effect of reduction in the level of the two single factor.

Taken together, these observations support the hypothesis that the functional cooperation between TBPH/Hrp38 and TDP-43/hnRNP A/B are fundamental also *in vivo* and are extremely well conserved throughout evolution, despite the observation that the general structural conservation of the human and Drosophila TDP-43 C-terminal domains is low.

This is a particularly important conclusion, considering the recent criticism that research focused on neurodegeneration based on classic lab-animal models can lead to potentially misleading results if not sufficient care is taken to establish whether the chosen model is sufficiently similar to the human disease under study (59). What these results mean, therefore, is that the Drosophila system should be considered quite

adequate to study ways that modulate the interaction of TDP-43 and other hnRNP factors.

Most importantly, it has recently been found that mutations in hnRNPA2/B1 and hnRNPA1 can also lead to multisystem proteinopathy and ALS (60). Interestingly, the position of these mutations D290V/D302V in hnRNP A2B1 and D262V/D314V are in the region that is involved with the binding to TDP-43. The expression of these mutant forms of human hnRNPA2 and hnRNPA1, as well as of mutant forms of the fly homologue Hrp38 in transgenic Drosophila led to severe muscle degeneration and enhanced formation of fibrils by the mutated proteins, due to the fact that these missense substitutions are localized in a prion-like domain (60). For these reasons, therefore, a better characterization of this interaction could be quite important to provide us with additional insights on disease mechanisms and the factors which can potentially affect its origin and severity.

REFERENCES

1. Buratti, E., and Baralle, F. E. (2008) Multiple roles of TDP-43 in gene expression, splicing regulation, and human disease. *Front Biosci* **13**, 867-878
2. Buratti, E., and Baralle, F. E. (2001) Characterization and functional implications of the RNA binding properties of nuclear factor TDP-43, a novel splicing regulator of CFTR exon 9. *J Biol Chem* **276**, 36337-36343
3. Buratti, E., Dork, T., Zuccato, E., Pagani, F., Romano, M., and Baralle, F. E. (2001) Nuclear factor TDP-43 and SR proteins promote in vitro and in vivo CFTR exon 9 skipping. *EMBO J* **20**, 1774-1784
4. Buratti, E., Brindisi, A., Pagani, F., and Baralle, F. E. (2004) Nuclear factor TDP-43 binds to the polymorphic TG repeats in CFTR intron 8 and causes skipping of exon 9: a functional link with disease penetrance. *Am J Hum Genet* **74**, 1322-1325
5. Neumann, M., Sampathu, D. M., Kwong, L. K., Truax, A. C., Micsenyi, M. C., Chou, T. T., Bruce, J., Schuck, T., Grossman, M., Clark, C. M., McCluskey, L. F., Miller, B. L., Masliah, E., Mackenzie, I. R., Feldman, H., Feiden, W., Kretzschmar, H. A., Trojanowski, J. Q., and Lee, V. M. (2006) Ubiquitinated TDP-43 in frontotemporal lobar degeneration and amyotrophic lateral sclerosis. *Science* **314**, 130-133
6. Arai, T., Hasegawa, M., Akiyama, H., Ikeda, K., Nonaka, T., Mori, H., Mann, D., Tsuchiya, K., Yoshida, M., Hashizume, Y., and Oda, T. (2006) TDP-43 is a component of ubiquitin-positive tau-negative inclusions in frontotemporal lobar degeneration and amyotrophic lateral sclerosis. *Biochem Biophys Res Commun* **351**, 602-611
7. Baloh, R. H. (2011) TDP-43: the relationship between protein aggregation and neurodegeneration in amyotrophic lateral sclerosis and frontotemporal lobar degeneration. *The FEBS journal* **278**, 3539-3549
8. Greenberg, S. A. (2011) Inclusion body myositis. *Curr Opin Rheumatol* **23**, 574-578
9. Banks, G. T., Kuta, A., Isaacs, A. M., and Fisher, E. M. (2008) TDP-43 is a culprit in human neurodegeneration, and not just an innocent bystander. *Mammalian genome : official journal of the International Mammalian Genome Society* **19**, 299-305

10. Bentmann, E., Neumann, M., Tahirovic, S., Rodde, R., Dormann, D., and Haass, C. (2012) Requirements for stress granule recruitment of fused in sarcoma (FUS) and TAR DNA-binding protein of 43 kDa (TDP-43). *J Biol Chem* **287**, 23079-23094
11. Colombrita, C., Zennaro, E., Fallini, C., Weber, M., Sommacal, A., Buratti, E., Silani, V., and Ratti, A. (2009) TDP-43 is recruited to stress granules in conditions of oxidative insult. *J Neurochem* **111**, 1051-1061
12. Kawahara, Y., and Mieda-Sato, A. (2012) TDP-43 promotes microRNA biogenesis as a component of the Drosha and Dicer complexes. *Proc Natl Acad Sci U S A* **109**, 3347-3352
13. Buratti, E., Brindisi, A., Giombi, M., Tisminetzky, S., Ayala, Y. M., and Baralle, F. E. (2005) TDP-43 binds heterogeneous nuclear ribonucleoprotein A/B through its C-terminal tail: an important region for the inhibition of cystic fibrosis transmembrane conductance regulator exon 9 splicing. *J Biol Chem* **280**, 37572-37584
14. D'Ambrogio, A., Buratti, E., Stuani, C., Guarnaccia, C., Romano, M., Ayala, Y. M., and Baralle, F. E. (2009) Functional mapping of the interaction between TDP-43 and hnRNP A2 in vivo. *Nucleic Acids Res* **37**, 4116-4126
15. Ayala, Y. M., Pantano, S., D'Ambrogio, A., Buratti, E., Brindisi, A., Marchetti, C., Romano, M., and Baralle, F. E. (2005) Human, Drosophila, and C.elegans TDP43: nucleic acid binding properties and splicing regulatory function. *J Mol Biol* **348**, 575-588
16. Budini, M., Buratti, E., Stuani, C., Guarnaccia, C., Romano, V., De Conti, L., and Baralle, F. E. (2012) Cellular model of TAR DNA-binding protein 43 (TDP-43) aggregation based on its C-terminal Gln/Asn-rich region. *J Biol Chem* **287**, 7512-7525
17. Fuentealba, R. A., Udan, M., Bell, S., Wegorzewska, I., Shao, J., Diamond, M. I., Weihl, C. C., and Baloh, R. H. (2010) Interaction with polyglutamine aggregates reveals a Q/N-rich domain in TDP-43. *J Biol Chem* **285**, 26304-26314
18. Wang, H. Y., Wang, I. F., Bose, J., and Shen, C. K. (2004) Structural diversity and functional implications of the eukaryotic TDP gene family. *Genomics* **83**, 130-139
19. Feiguin, F., Godena, V. K., Romano, G., D'Ambrogio, A., Klima, R., and Baralle, F. E. (2009) Depletion of TDP-43 affects Drosophila motoneurons terminal synapsis and locomotive behavior. *FEBS Lett* **583**, 1586-1592
20. Romano, M., Feiguin, F., and Buratti, E. (2012) Drosophila Answers to TDP-43 Proteinopathies. *Journal of amino acids* **2012**, 356081
21. Ayala, Y. M., Zago, P., D'Ambrogio, A., Xu, Y. F., Petrucelli, L., Buratti, E., and Baralle, F. E. (2008) Structural determinants of the cellular localization and shuttling of TDP-43. *J Cell Sci* **121**, 3778-3785
22. Mercado, P. A., Ayala, Y. M., Romano, M., Buratti, E., and Baralle, F. E. (2005) Depletion of TDP 43 overrides the need for exonic and intronic splicing enhancers in the human apoA-II gene. *Nucleic Acids Res* **33**, 6000-6010
23. Matunis, M. J., Matunis, E. L., and Dreyfuss, G. (1992) Isolation of hnRNP complexes from Drosophila melanogaster. *J Cell Biol* **116**, 245-255
24. Matunis, E. L., Matunis, M. J., and Dreyfuss, G. (1992) Characterization of the major hnRNP proteins from Drosophila melanogaster. *J Cell Biol* **116**, 257-269
25. Zu, K., Sikes, M. L., Haynes, S. R., and Beyer, A. L. (1996) Altered levels of the Drosophila HRB87F/hrp36 hnRNP protein have limited effects on alternative splicing in vivo. *Mol Biol Cell* **7**, 1059-1073

26. Cartegni, L., Maconi, M., Morandi, E., Cobianchi, F., Riva, S., and Biamonti, G. (1996) hnRNP A1 selectively interacts through its Gly-rich domain with different RNA-binding proteins. *J Mol Biol* **259**, 337-348
27. Arrisi-Mercado, P., Romano, M., Muro, A. F., and Baralle, F. E. (2004) An exonic splicing enhancer offsets the atypical GU-rich 3' splice site of human apolipoprotein A-II exon 3. *J Biol Chem* **279**, 39331-39339
28. Niksic, M., Romano, M., Buratti, E., Pagani, F., and Baralle, F. E. (1999) Functional analysis of cis-acting elements regulating the alternative splicing of human CFTR exon 9. *Hum Mol Genet* **8**, 2339-2349
29. Pagani, F., Buratti, E., Stuani, C., Romano, M., Zuccato, E., Niksic, M., Giglio, L., Faraguna, D., and Baralle, F. E. (2000) Splicing factors induce cystic fibrosis transmembrane regulator exon 9 skipping through a nonevolutionary conserved intronic element. *J Biol Chem* **275**, 21041-21047
30. Godena, V. K., Romano, G., Romano, M., Appocher, C., Klima, R., Buratti, E., Baralle, F. E., and Feiguin, F. (2011) TDP-43 Regulates Drosophila Neuromuscular Junctions Growth by Modulating Futsch/MAP1B Levels and Synaptic Microtubules Organization. *PLoS One* **6**, e17808
31. Ji, Y., and Tulin, A. V. (2012) Poly(ADP-ribose) controls DE-cadherin-dependent stem cell maintenance and oocyte localization. *Nature communications* **3**, 760
32. Dreyfuss, G., Kim, V. N., and Kataoka, N. (2002) Messenger-RNA-binding proteins and the messages they carry. *Nature reviews. Molecular cell biology* **3**, 195-205
33. Sephton, C. F., Good, S. K., Atkin, S., Dewey, C. M., Mayer, P., 3rd, Herz, J., and Yu, G. (2010) TDP-43 is a developmentally regulated protein essential for early embryonic development. *J Biol Chem* **285**, 6826-6834
34. Wu, L. S., Cheng, W. C., Hou, S. C., Yan, Y. T., Jiang, S. T., and Shen, C. K. (2010) TDP-43, a neuro-pathosignature factor, is essential for early mouse embryogenesis. *Genesis* **48**, 56-62
35. Kraemer, B. C., Schuck, T., Wheeler, J. M., Robinson, L. C., Trojanowski, J. Q., Lee, V. M., and Schellenberg, G. D. (2010) Loss of murine TDP-43 disrupts motor function and plays an essential role in embryogenesis. *Acta Neuropathol* **119**, 409-419
36. Buratti, E., and Baralle, F. E. (2012) TDP-43: gumming up neurons through protein-protein and protein-RNA interactions. *Trends Biochem Sci* **37**, 237-247
37. Hartwell, L. H., Hopfield, J. J., Leibler, S., and Murray, A. W. (1999) From molecular to modular cell biology. *Nature* **402**, C47-52
38. Oltvai, Z. N., and Barabasi, A. L. (2002) Systems biology. Life's complexity pyramid. *Science* **298**, 763-764
39. Shen-Orr, S. S., Milo, R., Mangan, S., and Alon, U. (2002) Network motifs in the transcriptional regulation network of Escherichia coli. *Nat Genet* **31**, 64-68
40. Pinol-Roma, S., Choi, Y. D., Matunis, M. J., and Dreyfuss, G. (1988) Immunopurification of heterogeneous nuclear ribonucleoprotein particles reveals an assortment of RNA-binding proteins. *Genes & development* **2**, 215-227
41. Hahm, B., Cho, O. H., Kim, J. E., Kim, Y. K., Kim, J. H., Oh, Y. L., and Jang, S. K. (1998) Polypyrimidine tract-binding protein interacts with HnRNP L. *FEBS Lett* **425**, 401-406

42. Mikula, M., Dzwonek, A., Karczmarski, J., Rubel, T., Dadlez, M., Wyrwicz, L. S., Bomsztyk, K., and Ostrowski, J. (2006) Landscape of the hnRNP K protein-protein interactome. *Proteomics* **6**, 2395-2406
43. Kim, J. H., Hahm, B., Kim, Y. K., Choi, M., and Jang, S. K. (2000) Protein-protein interaction among hnRNPs shuttling between nucleus and cytoplasm. *J Mol Biol* **298**, 395-405
44. Kuo, P. H., Doudeva, L. G., Wang, Y. T., Shen, C. K., and Yuan, H. S. (2009) Structural insights into TDP-43 in nucleic-acid binding and domain interactions. *Nucleic Acids Res* **37**, 1799-1808
45. Shiina, Y., Arima, K., Tabunoki, H., and Satoh, J. (2010) TDP-43 dimerizes in human cells in culture. *Cell Mol Neurobiol* **30**, 641-652
46. Sephton, C. F., Cenik, C., Kucukural, A., Dammer, E. B., Cenik, B., Han, Y., Dewey, C. M., Roth, F. P., Herz, J., Peng, J., Moore, M. J., and Yu, G. (2011) Identification of neuronal RNA targets of TDP-43-containing ribonucleoprotein complexes. *The Journal of biological chemistry* **286**, 1204-1215
47. Tollervey, J. R., Curk, T., Rogelj, B., Briese, M., Cereda, M., Kayikci, M., Konig, J., Hortobagyi, T., Nishimura, A. L., Zupunski, V., Patani, R., Chandran, S., Rot, G., Zupan, B., Shaw, C. E., and Ule, J. (2011) Characterizing the RNA targets and position-dependent splicing regulation by TDP-43. *Nat Neurosci* **14**, 452-458
48. Chen, H. K., Fernandez-Funez, P., Acevedo, S. F., Lam, Y. C., Kaytor, M. D., Fernandez, M. H., Aitken, A., Skoulakis, E. M., Orr, H. T., Botas, J., and Zoghbi, H. Y. (2003) Interaction of Akt-phosphorylated ataxin-1 with 14-3-3 mediates neurodegeneration in spinocerebellar ataxia type 1. *Cell* **113**, 457-468
49. Goehler, H., Lalowski, M., Stelzl, U., Waelter, S., Stroedicke, M., Worm, U., Droege, A., Lindenberg, K. S., Knoblich, M., Haenig, C., Herbst, M., Suopanki, J., Scherzinger, E., Abraham, C., Bauer, B., Hasenbank, R., Fritzsche, A., Ludewig, A. H., Bussow, K., Coleman, S. H., Gutekunst, C. A., Landwehrmeyer, B. G., Lehrach, H., and Wanker, E. E. (2004) A protein interaction network links GIT1, an enhancer of huntingtin aggregation, to Huntington's disease. *Molecular cell* **15**, 853-865
50. Ravikumar, B., Vacher, C., Berger, Z., Davies, J. E., Luo, S., Oroz, L. G., Scaravilli, F., Easton, D. F., Duden, R., O'Kane, C. J., and Rubinsztein, D. C. (2004) Inhibition of mTOR induces autophagy and reduces toxicity of polyglutamine expansions in fly and mouse models of Huntington disease. *Nat Genet* **36**, 585-595
51. Tsuda, H., Jafar-Nejad, H., Patel, A. J., Sun, Y., Chen, H. K., Rose, M. F., Venken, K. J., Botas, J., Orr, H. T., Bellen, H. J., and Zoghbi, H. Y. (2005) The AXH domain of Ataxin-1 mediates neurodegeneration through its interaction with Gfi-1/Senseless proteins. *Cell* **122**, 633-644
52. Lehner, B., and Sanderson, C. M. (2004) A protein interaction framework for human mRNA degradation. *Genome Res* **14**, 1315-1323
53. Sato, S., Tomomori-Sato, C., Parmely, T. J., Florens, L., Zybailov, B., Swanson, S. K., Banks, C. A., Jin, J., Cai, Y., Washburn, M. P., Conaway, J. W., and Conaway, R. C. (2004) A set of consensus mammalian mediator subunits identified by multidimensional protein identification technology. *Molecular cell* **14**, 685-691
54. Stelzl, U., Worm, U., Lalowski, M., Haenig, C., Brembeck, F. H., Goehler, H., Stroedicke, M., Zenkner, M., Schoenherr, A., Koeppen, S., Timm, J., Mintzlaff, S., Abraham, C., Bock, N., Kietzmann, S., Goedde, A., Toksoz, E., Droege, A., Krobitsch,

S., Korn, B., Birchmeier, W., Lehrach, H., and Wanker, E. E. (2005) A human protein-protein interaction network: a resource for annotating the proteome. *Cell* **122**, 957-968
55. Freibaum, B. D., Chitta, R. K., High, A. A., and Taylor, J. P. (2010) Global analysis of TDP-43 interacting proteins reveals strong association with RNA splicing and translation machinery. *J Proteome Res* **9**, 1104-1120
56. Ling, S. C., Albuquerque, C. P., Han, J. S., Lagier-Tourenne, C., Tokunaga, S., Zhou, H., and Cleveland, D. W. (2010) ALS-associated mutations in TDP-43 increase its stability and promote TDP-43 complexes with FUS/TLS. *Proc Natl Acad Sci U S A* **107**, 13318-13323
57. Zhang, Y. J., Xu, Y. F., Cook, C., Gendron, T. F., Roettges, P., Link, C. D., Lin, W. L., Tong, J., Castanedes-Casey, M., Ash, P., Gass, J., Rangachari, V., Buratti, E., Baralle, F., Golde, T. E., Dickson, D. W., and Petrucelli, L. (2009) Aberrant cleavage of TDP-43 enhances aggregation and cellular toxicity. *Proc Natl Acad Sci U S A* **106**, 7607-7612
58. Budini, M., Romano, V., Avendano-Vazquez, S. E., Bembich, S., Buratti, E., and Baralle, F. E. (2012) Role of selected mutations in the Q/N rich region of TDP-43 in EGFP-12xQ/N-induced aggregate formation. *Brain Res* **1462**, 139-150
59. Bolker, J. (2012) Model organisms: There's more to life than rats and flies. *Nature* **491**, 31-33
60. Kim, H. J., Kim, N. C., Wang, Y. D., Scarborough, E. A., Moore, J., Diaz, Z., MacLea, K. S., Freibaum, B., Li, S., Molliex, A., Kanagaraj, A. P., Carter, R., Boylan, K. B., Wojtas, A. M., Rademakers, R., Pinkus, J. L., Greenberg, S. A., Trojanowski, J. Q., Traynor, B. J., Smith, B. N., Topp, S., Gkazi, A. S., Miller, J., Shaw, C. E., Kottlors, M., Kirschner, J., Pestronk, A., Li, Y. R., Ford, A. F., Gitler, A. D., Benatar, M., King, O. D., Kimonis, V. E., Ross, E. D., Weihl, C. C., Shorter, J., and Taylor, J. P. (2013) Mutations in prion-like domains in hnRNPA2B1 and hnRNPA1 cause multisystem proteinopathy and ALS. *Nature* **495**, 467-473
61. Edgar, R. C. (2004) MUSCLE: multiple sequence alignment with high accuracy and high throughput. *Nucleic Acids Res* **32**, 1792-1797

ACKNOWLEDGEMENTS

This work was supported by AriSLA (TARMA to FB) and (ALSMNDTDP-43 to FF), Thierry Latran Foundation (REHNPALS to EB and FF) and University of Trieste - Finanziamento per Ricercatori di Ateneo. The Hrp-38 ORF was kindly provided by Prof. Joan Steitz.

FIGURES LEGENDS

Figure 1. Identification of TDP-43 and TBPH interactors by GST-overlay and reverse-phase chromatography methods.
A) Staining (Red Ponceau) and GST-overlays (TBPH and TDP-43) of human HeLa cytoplasmic (S100), HeLa nuclear (NE), and drosophila second instar larva nuclear extracts (L2NE). Molecular weights (kDa) are shown on the left. The assays were carried out using recombinant GST-TDP-43 or GST-TBPH as probes. B) reverse-phase chromatography (upper panel) and GST-overlay (lower panel) of Drosophila L2NE fractionated nuclear extract. Mass spec analysis of the drosophila TDP-interactors has permitted to identify at least two factors, Squid/Hrp40 (1) and HRB98/Hrp38 (2). C) Amino acid alignment of the C-terminal domains from TDP-43 and TBPH. The region of TDP-43 spanning residues 321-366 is underlined. Symbols below the alignment indicate: identity (asterisk), close similarity (colon), more distant similarity (period).

Figure 2. Hrp38 co-precipitates with TDP-43.
A) Co-immunoprecipitation of Hrp38 with TDP-43. HEK293 cells were cotransfected with flag-Hrp38 and EGFP-TDP43 or EGFP-empty constructs and subjected to immunoprecipitation with polyclonal anti-EGFP (IP α-EGFP) followed by immunoblotting with antibodies as indicated. A non specific band (*), probably derived from a cleavage in the TDP 43 portion as it is not seen in EGFP alone, was also detected by anti-EGFP antibody.
B) Co-immunoprecipitation of Hrp38 with the region of TDP-43 spanning residues 321-366. HEK293 cells were cotransfected with flag-Hrp38 and EGFP-TDP43 (321-366) or EGFP-empty constructs and subjected to immunoprecipitation with polyclonal anti-EGFP (IP α-EGFP) followed by immunoblotting with antibodies as indicated.
C) Amino acid alignment of the Gly-rich tract of Hrp38 (ROA1_DROME) with the regions from the human hnRNP A1 (ROA1_HUMAN) hnRNP A2 (ROA2_HUMAN) critical for protein-protein interaction according to the mapping previously performed (26). Symbols below the alignment indicate: identity (asterisk), close similarity (colon), more distant similarity (period). MUSCLE program was used for alignment (61).
D) Co-immunoprecipitation of TDP-43 with the region of Hrp38 spanning residues 293-365. HEK293 cells were cotransfected with flag-TDP-43 and EGFP-Hrp38 (293-365) or EGFP-empty constructs and subjected to immunoprecipitation with polyclonal anti-EGFP (IP α-EGFP) followed by immunoblotting with antibodies as indicated.
E) Co-immunoprecipitation of TBPH with the region of Hrp38 spanning residues 293-365. HEK293 cells were cotransfected with flag-TBPH and EGFP-Hrp38 (293-365) or EGFP-empty constructs and subjected to immunoprecipitation with polyclonal anti-EGFP (IP α-EGFP) followed by immunoblotting with antibodies as indicated.

Figure 3. Hrp38 factor inhibits splicing of the ApoAII exon 3 in a TDP-43-dependent manner.
(A) Schematic representation of the minigene ApoAII-ISEm used in the splicing assay. The human ApoA-II exon 3 and its flanking introns were cloned in the α-globin/fibronectin reporter system (pTB). α-globin, fibronectin EDB exons and human ApoA-II exon 3 are indicated in grey, black and white boxes, respectively. Solid lines indicate Apo AII IVS2 and IVS3. The black circle indicates the $(GT)_{16}$ tract. Dashed lines indicate splicing options. (B) Hrp38 overexpression has an inhibitory effect on splicing of ApoAII-ISEm (lane 4). The RT–PCRs

show the increasing splicing inhibitory activity of Hrp38 with respect to the controls (lane 1, -). The percentages of exon inclusion along with SEMs obtained in three independent transfection experiments are reported. Western blots against the FLAG peptide and tubulin are shown below to show equal transgene expression. The overexpression of TDP-43 was used as a control of splicing inhibition (lane 3). (C) The inhibitory effect of Hrp38 on the splicing of ApoAII-ISEm is lost after TDP-43 silencing. The percentages of exon inclusion along with SEMs obtained in three independent transfection experiments are reported. Western blots against TDP-43, tubulin and FLAG peptide are shown below to show silencing efficiency (anti-TDP-43), transgene overexpression (anti-FLAG) and comparable protein load (anti-tubulin). The overexpression of TDP-43 was used as a control of splicing inhibition (lane 3).

Figure 4. Hrp38 and TBPH genetically interact to regulate flies locomotion and life span.
(A) Climbing ability analysis of Hrp38 silenced flies demonstrates the existence of a genetic interaction between TBPH and Hrp38. The phenotype of Hrp38 neuronal silencing becomes significantly stronger if one copy of TBPH is removed, as compared to the silencing in a wild type background (Elav-GAL4, tbph$^{\Delta 23}$/+; Hrp38^{RNAi} versus Elav-GAL4, tbph+/+; Hrp38^{RNAi}, p<0,01). The results of Hrp38 silencing in a TBPH sensible background further support this genetic interaction. In fact, Hrp38 silencing exacerbated the phenotype caused by TBPH silencing (Elav-GAL4, tbph$^{\Delta 23}$/+; TBPH^{RNAi} versus Elav-GAL4, tbph$^{\Delta 23}$/+; TBPH^{RNAi}/Hrp38^{RNAi}, p<0,001). n = 200 flies for genotype, error bars indicate SEM. Statistics were performed using GraphPad Prism. One-way ANOVA was performed using Bonferroni's multiple comparison test to compare the genotypes (** indicates p<0,01 and *** p<0,001). (B) Percentage of flies survivors during aging. Median lifespan are: 49 days for wild type (n=208), 44 days for tbph$^{\Delta 23}$/+ (n=126), 33 days for Elav-GAL4, tbph$^{\Delta 23}$/+; TBPH^{RNAi} (n=150), 14 days for Elav-GAL4, tbph$^{\Delta 23}$/+; TBPH^{RNAi}/Hrp38^{RNAi} (n=138), 51 days for Elav-GAL4, tbph$^{\Delta 23}$/+; GFP (n=159), 32 days for Elav-GAL4, tbph$^{\Delta 23}$/+; Hrp38^{RNAi} (n=312) and 36 days for Elav-GAL4, tbph+/+; Hrp38^{RNAi} (n=235). Log rank test and p-value: wild type versus tbph$^{\Delta 23}$/+ (p=ns), wild type versus Elav-GAL4, tbph$^{\Delta 23}$/+; TBPH^{RNAi} (p<0.0001), wild type versus Elav-GAL4, tbph$^{\Delta 23}$/+; TBPH^{RNAi} /Hrp38^{RNAi} (p<0.0001), wild type versus Elav-GAL4, tbph$^{\Delta 23}$/+; GFP (p=ns), wild type versus Elav-GAL4, tbph$^{\Delta 23}$/+; Hrp38^{RNAi} (p<0,0001), wild type versus Elav-GAL4, tbph+/+; Hrp38^{RNAi} (p<0.0001), Elav-GAL4, tbph$^{\Delta 23}$/+; TBPH^{RNAi} versus Elav-GAL4, tbph$^{\Delta 23}$/+; TBPH^{RNAi} /Hrp38^{RNAi} (p<0.0001) and Elav-GAL4, tbph+/+; Hrp38^{RNAi} versus Elav-GAL4, tbph$^{\Delta 23}$/+; Hrp38^{RNAi} (p<0.0001) . Statistics were performed using GraphPad Prism. Logrank test was performed to compare survival distribution of the genotypes (*** indicates p<0.001). (C) RNAi treatment against Hrp38, reduced mRNA expression levels in Drosophila heads, as compared to control untreated flies.

Figure 5. Increased neuropil degeneration in RNAi treated adult flies.
(A) Confocal images of optic lobe of adult brains stained with anti-Elav (in red) and anti-22C10 (futsch) (in green) antibodies in 1/2 days old flies, reveals strong defects in the innervation of the lamina and medulla regions in control brains (i-iii) compared to Elav-GAL4,tbph$^{\Delta 23}$/+; TBPH^{RNAi} (iv-vi), Elav-GAL4,tbph$^{\Delta 23}$/+; TBPH^{RNAi} /Hrp38^{RNAi} (vii-ix) and Elav-GAL4, tbph$^{\Delta 23}$/+; Hrp38^{RNAi} (x-xii). Scale bar 30 μm (B) Quantification of *futsch* intensity in lamina and medulla regions indicated that the density of axons in these regions became dramatically reduced after RNAi treatments. n=5.

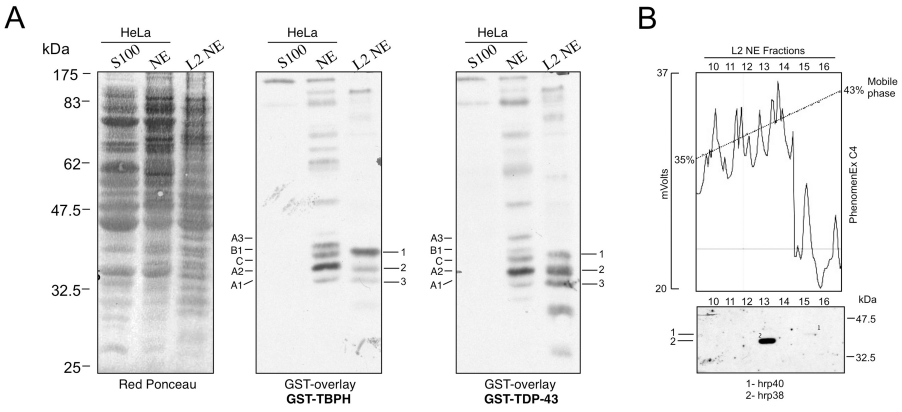

Fig.1

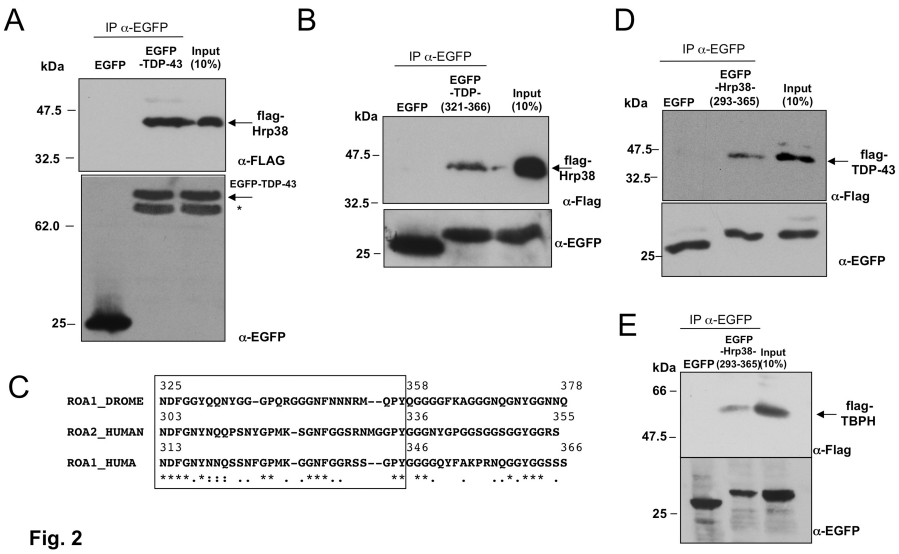

Fig. 2

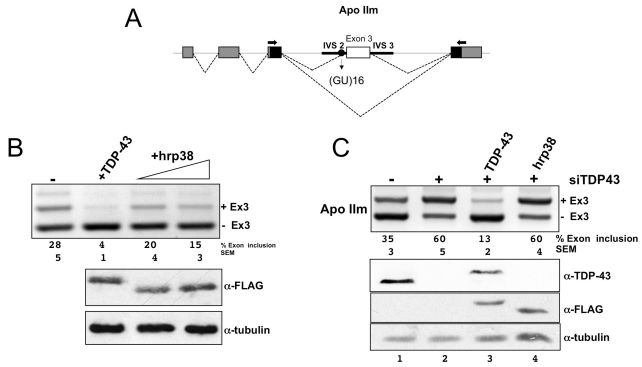

Fig. 3

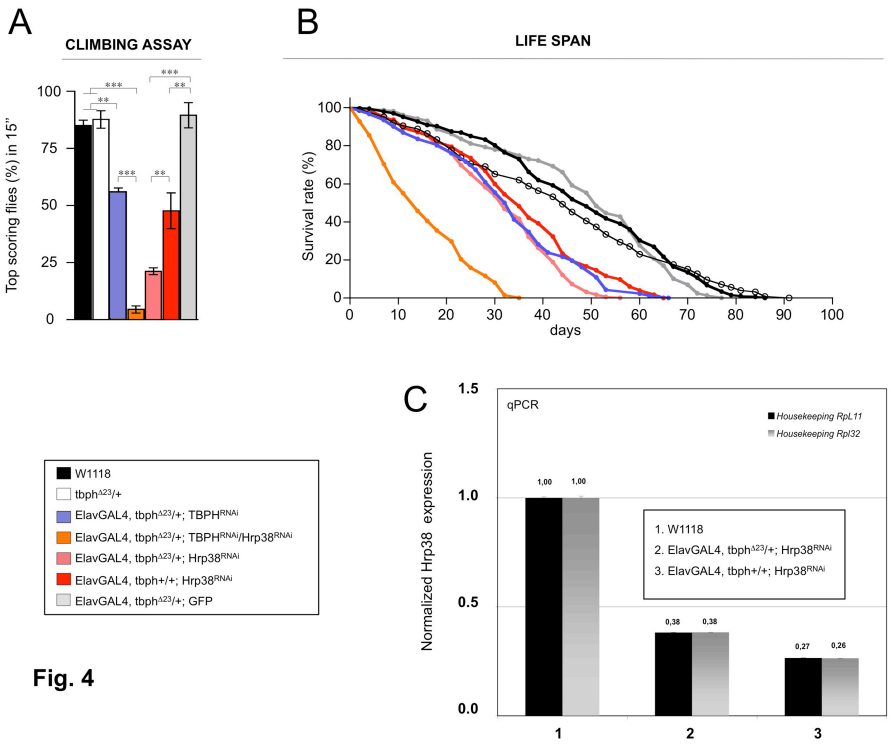

Fig. 4

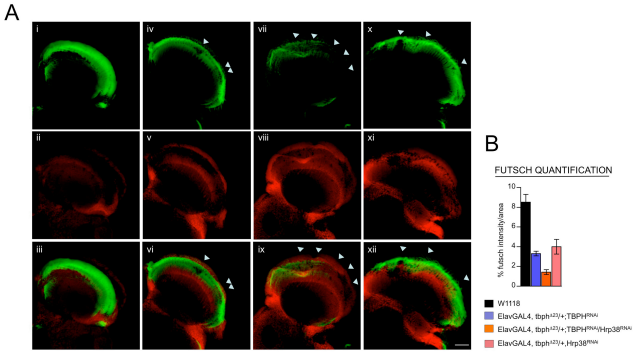

Fig. 5

References

Abhyankar MM, Urekar C & Reddi PP (2007) A novel CpG-free vertebrate insulator silences the testis-specific SP-10 gene in somatic tissues: role for TDP-43 in insulator function. *J. Biol. Chem.* **282:** 36143–36154

Amador-Ortiz C, Lin W-L, Ahmed Z, Personett D, Davies P, Duara R, Graff-Radford NR, Hutton ML & Dickson DW (2007) TDP-43 immunoreactivity in hippocampal sclerosis and Alzheimer's disease. *Ann. Neurol.* **61:** 435–445

Ambegaokar SS, Roy B & Jackson GR (2010) Neurodegenerative models in Drosophila: polyglutamine disorders, Parkinson disease, and amyotrophic lateral sclerosis. *Neurobiol. Dis.* **40:** 29–39

Ankö M-L, Morales L, Henry I, Beyer A & Neugebauer KM (2010) Global analysis reveals SRp20- and SRp75-specific mRNPs in cycling and neural cells. *Nat. Struct. Mol. Biol.* **17:** 962–970

Antic D & Keene JD (1997) Embryonic lethal abnormal visual RNA-binding proteins involved in growth, differentiation, and posttranscriptional gene expression. *Am. J. Hum. Genet.* **61:** 273–278

Arai T, Hasegawa M, Akiyama H, Ikeda K, Nonaka T, Mori H, Mann D, Tsuchiya K, Yoshida M, Hashizume Y & Oda T (2006) TDP-43 is a component of ubiquitin-positive tau-negative inclusions in frontotemporal lobar degeneration and amyotrophic lateral sclerosis. *Biochem. Biophys. Res. Commun.* **351:** 602–611

Arnold ES, Ling S-C, Huelga SC, Lagier-Tourenne C, Polymenidou M, Ditsworth D, Kordasiewicz HB, McAlonis-Downes M, Platoshyn O, Parone PA, Da Cruz S, Clutario KM, Swing D, Tessarollo L, Marsala M, Shaw CE, Yeo GW & Cleveland DW (2013) ALS-linked TDP-43 mutations produce aberrant RNA splicing and adult-onset motor neuron disease without aggregation or loss of nuclear TDP-43. *Proc. Natl. Acad. Sci. U. S. A.* **110:** E736–745

Ash PEA, Zhang Y-J, Roberts CM, Saldi T, Hutter H, Buratti E, Petrucelli L & Link CD (2010) Neurotoxic effects of TDP-43 overexpression in C. elegans. *Hum. Mol. Genet.* **19:** 3206–3218

Avendaño-Vázquez SE, Dhir A, Bembich S, Buratti E, Proudfoot N & Baralle FE (2012) Autoregulation of TDP-43 mRNA levels involves interplay between transcription, splicing, and alternative polyA site selection. *Genes Dev.* **26:** 1679–1684

Ayala YM, De Conti L, Avendaño-Vázquez SE, Dhir A, Romano M, D'Ambrogio A, Tollervey J, Ule J, Baralle M, Buratti E & Baralle FE (2011) TDP-43 regulates its mRNA levels through a negative feedback loop. *EMBO J.* **30:** 277–288

Ayala YM, Misteli T & Baralle FE (2008a) TDP-43 regulates retinoblastoma protein phosphorylation through the repression of cyclin-dependent kinase 6 expression. *Proc. Natl. Acad. Sci. U. S. A.* **105:** 3785–3789

Ayala YM, Pagani F & Baralle FE (2006) TDP43 depletion rescues aberrant CFTR exon 9 skipping. *FEBS Lett.* **580:** 1339–1344

Ayala YM, Pantano S, D'Ambrogio A, Buratti E, Brindisi A, Marchetti C, Romano M & Baralle FE (2005) Human, Drosophila, and C.elegans TDP43: nucleic acid binding properties and splicing regulatory function. *J. Mol. Biol.* **348:** 575–588

Ayala YM, Zago P, D'Ambrogio A, Xu Y-F, Petrucelli L, Buratti E & Baralle FE (2008b) Structural determinants of the cellular localization and shuttling of TDP-43. *J. Cell Sci.* **121:** 3778–3785

Baetz NW & Goldenring JR (2013) Rab11-family interacting proteins define spatially and temporally distinct regions within the dynamic Rab11a-dependent recycling system. *Mol. Biol. Cell* **24:** 643–658

Banks GT, Kuta A, Isaacs AM & Fisher EMC (2008) TDP-43 is a culprit in human neurodegeneration, and not just an innocent bystander. *Mamm. Genome Off. J. Int. Mamm. Genome Soc.* **19:** 299–305

Benzer S (1967) BEHAVIORAL MUTANTS OF Drosophila ISOLATED BY COUNTERCURRENT DISTRIBUTION. *Proc. Natl. Acad. Sci. U. S. A.* **58:** 1112–1119

Bettencourt da Cruz A, Schwärzel M, Schulze S, Niyyati M, Heisenberg M & Kretzschmar D (2005) Disruption of the MAP1B-related protein FUTSCH leads to changes in the neuronal cytoskeleton, axonal transport defects, and progressive neurodegeneration in Drosophila. *Mol.*

Biol. Cell **16:** 2433–2442

Bier E (2005) Drosophila, the golden bug, emerges as a tool for human genetics. *Nat. Rev. Genet.* **6:** 9–23

Bischof J, Maeda RK, Hediger M, Karch F & Basler K (2007) An optimized transgenesis system for Drosophila using germ-line-specific phiC31 integrases. *Proc. Natl. Acad. Sci. U. S. A.* **104:** 3312–3317

Van Blitterswijk M, DeJesus-Hernandez M & Rademakers R (2012) How do C9ORF72 repeat expansions cause amyotrophic lateral sclerosis and frontotemporal dementia: can we learn from other noncoding repeat expansion disorders? *Curr. Opin. Neurol.* **25:** 689–700

Bloch RJ & Pumplin DW (1988) Molecular events in synaptogenesis: nerve-muscle adhesion and postsynaptic differentiation. *Am. J. Physiol. - Cell Physiol.* **254:** C345–C364

Bose JK, Wang I-F, Hung L, Tarn W-Y & Shen C-KJ (2008) TDP-43 overexpression enhances exon 7 inclusion during the survival of motor neuron pre-mRNA splicing. *J. Biol. Chem.* **283:** 28852–28859

Brand AH & Perrimon N (1993a) Targeted gene expression as a means of altering cell fates and generating dominant phenotypes. *Dev. Camb. Engl.* **118:** 401–415

Brand AH & Perrimon N (1993b) Targeted gene expression as a means of altering cell fates and generating dominant phenotypes. *Dev. Camb. Engl.* **118:** 401–415

Broadie K & Bate M (1993) Activity-dependent development of the neuromuscular synapse during Drosophila embryogenesis. *Neuron* **11:** 607–619

Budini M, Baralle FE & Buratti E (2011) Regulation of gene expression by TDP-43 and FUS/TLS in frontotemporal lobar degeneration. *Curr. Alzheimer Res.* **8:** 237–245

Budnik V, Koh YH, Guan B, Hartmann B, Hough C, Woods D & Gorczyca M (1996) Regulation of synapse structure and function by the Drosophila tumor suppressor gene dlg. *Neuron* **17:** 627–640

Buratti E & Baralle FE (2001) Characterization and functional implications of the RNA binding properties of nuclear factor TDP-43, a novel splicing regulator of CFTR exon 9. *J. Biol. Chem.* **276:** 36337–36343

Buratti E & Baralle FE (2008) Multiple roles of TDP-43 in gene expression, splicing regulation, and human disease. *Front. Biosci. J. Virtual Libr.* **13:** 867–878

Buratti E & Baralle FE (2009) The molecular links between TDP-43 dysfunction and neurodegeneration. *Adv. Genet.* **66:** 1–34

Buratti E & Baralle FE (2010) The multiple roles of TDP-43 in pre-mRNA processing and gene expression regulation. *RNA Biol.* **7:** 420–429

Buratti E, Brindisi A, Giombi M, Tisminetzky S, Ayala YM & Baralle FE (2005) TDP-43 binds heterogeneous nuclear ribonucleoprotein A/B through its C-terminal tail: an important region for the inhibition of cystic fibrosis transmembrane conductance regulator exon 9 splicing. *J. Biol. Chem.* **280:** 37572–37584

Buratti E, De Conti L, Stuani C, Romano M, Baralle M & Baralle F (2010) Nuclear factor TDP-43 can affect selected microRNA levels. *FEBS J.* **277:** 2268–2281

Buratti E, Dörk T, Zuccato E, Pagani F, Romano M & Baralle FE (2001) Nuclear factor TDP-43 and SR proteins promote in vitro and in vivo CFTR exon 9 skipping. *EMBO J.* **20:** 1774–1784

Campos-Melo D, Droppelmann CA, He Z, Volkening K & Strong MJ (2013) Altered microRNA expression profile in Amyotrophic Lateral Sclerosis: a role in the regulation of NFL mRNA levels. *Mol. Brain* **6:** 26

Casadio A, Martin KC, Giustetto M, Zhu H, Chen M, Bartsch D, Bailey CH & Kandel ER (1999) A transient, neuron-wide form of CREB-mediated long-term facilitation can be stabilized at specific synapses by local protein synthesis. *Cell* **99:** 221–237

Castello A, Fischer B, Hentze MW & Preiss T (2013) RNA-binding proteins in Mendelian disease. *Trends Genet. TIG* **29:** 318–327

Cerezo JR, Jiménez F & Moya F (1995) Characterization and gene cloning of Drosophila syntaxin 1 (Dsynt1): the fruit fly homologue of rat syntaxin 1. *Brain Res. Mol. Brain Res.* **29:** 245–252

Chang K-Y & Ramos A (2005) The double-stranded RNA-binding motif, a versatile macromolecular docking platform. *FEBS J.* **272:** 2109–2117

Chen K & Featherstone DE (2005) Discs-large (DLG) is clustered by presynaptic innervation and regulates postsynaptic glutamate receptor

subunit composition in Drosophila. *BMC Biol.* **3:** 1

Chen YA & Scheller RH (2001) SNARE-mediated membrane fusion. *Nat. Rev. Mol. Cell Biol.* **2:** 98–106

Childers M, Eckel G, Himmel A & Caldwell J (2007) A new model of cystic fibrosis pathology: lack of transport of glutathione and its thiocyanate conjugates. *Med. Hypotheses* **68:** 101–112

Chiò A, Calvo A, Mazzini L, Cantello R, Mora G, Moglia C, Corrado L, D'Alfonso S, Majounie E, Renton A, Pisano F, Ossola I, Brunetti M, Traynor BJ, Restagno G & PARALS (2012) Extensive genetics of ALS: a population-based study in Italy. *Neurology* **79:** 1983–1989

Christoforidis S, McBride HM, Burgoyne RD & Zerial M (1999) The Rab5 effector EEA1 is a core component of endosome docking. *Nature* **397:** 621–625

Cléry A & Allain FH-T (2000) From Structure to Function of RNA Binding Domains. Available at: http://www.ncbi.nlm.nih.gov/books/NBK63528/?report=printable [Accessed June 18, 2014]

Collins CA & DiAntonio A (2007) Synaptic development: insights from Drosophila. *Curr. Opin. Neurobiol.* **17:** 35–42

Colombrita C, Onesto E, Megiorni F, Pizzuti A, Baralle FE, Buratti E, Silani V & Ratti A (2012) TDP-43 and FUS RNA-binding proteins bind distinct sets of cytoplasmic messenger RNAs and differently regulate their post-transcriptional fate in motoneuron-like cells. *J. Biol. Chem.* **287:** 15635–15647

Cooper TA, Wan L & Dreyfuss G (2009) RNA and disease. *Cell* **136:** 777–793

D'Ambrogio A, Buratti E, Stuani C, Guarnaccia C, Romano M, Ayala YM & Baralle FE (2009) Functional mapping of the interaction between TDP-43 and hnRNP A2 in vivo. *Nucleic Acids Res.* **37:** 4116–4126

Danckwardt S, Gantzert A-S, Macher-Goeppinger S, Probst HC, Gentzel M, Wilm M, Gröne H-J, Schirmacher P, Hentze MW & Kulozik AE (2011) p38 MAPK controls prothrombin expression by regulated RNA 3' end processing. *Mol. Cell* **41:** 298–310

Darnell RB (2010) RNA regulation in neurologic disease and cancer.

Cancer Res. Treat. Off. J. Korean Cancer Assoc. **42:** 125–129

Dawson-Scully K, Lin Y, Imad M, Zhang J, Marin L, Horne JA, Meinertzhagen IA, Karunanithi S, Zinsmaier KE & Atwood HL (2007) Morphological and functional effects of altered cysteine string protein at the Drosophila larval neuromuscular junction. *Synap. N. Y. N* **61:** 1–16

Van Deerlin VM, Leverenz JB, Bekris LM, Bird TD, Yuan W, Elman LB, Clay D, Wood EM, Chen-Plotkin AS, Martinez-Lage M, Steinbart E, McCluskey L, Grossman M, Neumann M, Wu I-L, Yang W-S, Kalb R, Galasko DR, Montine TJ, Trojanowski JQ, et al (2008) TARDBP mutations in amyotrophic lateral sclerosis with TDP-43 neuropathology: a genetic and histopathological analysis. *Lancet Neurol.* **7:** 409–416

DeJesus-Hernandez M, Mackenzie IR, Boeve BF, Boxer AL, Baker M, Rutherford NJ, Nicholson AM, Finch NA, Flynn H, Adamson J, Kouri N, Wojtas A, Sengdy P, Hsiung G-YR, Karydas A, Seeley WW, Josephs KA, Coppola G, Geschwind DH, Wszolek ZK, et al (2011) Expanded GGGGCC hexanucleotide repeat in noncoding region of C9ORF72 causes chromosome 9p-linked FTD and ALS. *Neuron* **72:** 245–256

Delaney SJ, Rich DP, Thomson SA, Hargrave MR, Lovelock PK, Welsh MJ & Wainwright BJ (1993) Cystic fibrosis transmembrane conductance regulator splice variants are not conserved and fail to produce chloride channels. *Nat. Genet.* **4:** 426–431

DiAntonio A, Petersen SA, Heckmann M & Goodman CS (1999) Glutamate receptor expression regulates quantal size and quantal content at the Drosophila neuromuscular junction. *J. Neurosci. Off. J. Soc. Neurosci.* **19:** 3023–3032

Diaper DC, Adachi Y, Sutcliffe B, Humphrey DM, Elliott CJH, Stepto A, Ludlow ZN, Vanden Broeck L, Callaerts P, Dermaut B, Al-Chalabi A, Shaw CE, Robinson IM & Hirth F (2013) Loss and gain of Drosophila TDP-43 impair synaptic efficacy and motor control leading to age-related neurodegeneration by loss-of-function phenotypes. *Hum. Mol. Genet.* **22:** 1539–1557

Dietzl G, Chen D, Schnorrer F, Su K-C, Barinova Y, Fellner M, Gasser B, Kinsey K, Oppel S, Scheiblauer S, Couto A, Marra V, Keleman K & Dickson BJ (2007) A genome-wide transgenic RNAi library for conditional

gene inactivation in Drosophila. *Nature* **448:** 151–156

Dresbach T, Qualmann B, Kessels MM, Garner CC & Gundelfinger ED (2001) The presynaptic cytomatrix of brain synapses. *Cell. Mol. Life Sci. CMLS* **58:** 94–116

Dreyfuss G, Kim VN & Kataoka N (2002) Messenger-RNA-binding proteins and the messages they carry. *Nat. Rev. Mol. Cell Biol.* **3:** 195–205

Eaton BA, Fetter RD & Davis GW (2002) Dynactin is necessary for synapse stabilization. *Neuron* **34:** 729–741

Fasshauer D, Sutton RB, Brunger AT & Jahn R (1998) Conserved structural features of the synaptic fusion complex: SNARE proteins reclassified as Q- and R-SNAREs. *Proc. Natl. Acad. Sci. U. S. A.* **95:** 15781–15786

Featherstone DE, Rushton E & Broadie K (2002) Developmental regulation of glutamate receptor field size by nonvesicular glutamate release. *Nat. Neurosci.* **5:** 141–146

Feiguin F, Godena VK, Romano G, D'Ambrogio A, Klima R & Baralle FE (2009) Depletion of TDP-43 affects Drosophila motoneurons terminal synapsis and locomotive behavior. *FEBS Lett.* **583:** 1586–1592

Fiesel FC & Kahle PJ (2011) TDP-43 and FUS/TLS: cellular functions and implications for neurodegeneration. *FEBS J.* **278:** 3550–3568

Fiesel FC, Voigt A, Weber SS, Van den Haute C, Waldenmaier A, Görner K, Walter M, Anderson ML, Kern JV, Rasse TM, Schmidt T, Springer W, Kirchner R, Bonin M, Neumann M, Baekelandt V, Alunni-Fabbroni M, Schulz JB & Kahle PJ (2010) Knockdown of transactive response DNA-binding protein (TDP-43) downregulates histone deacetylase 6. *EMBO J.* **29:** 209–221

Filimonenko M, Stuffers S, Raiborg C, Yamamoto A, Malerød L, Fisher EMC, Isaacs A, Brech A, Stenmark H & Simonsen A (2007) Functional multivesicular bodies are required for autophagic clearance of protein aggregates associated with neurodegenerative disease. *J. Cell Biol.* **179:** 485–500

Forman MS, Trojanowski JQ & Lee VM-Y (2007) TDP-43: a novel neurodegenerative proteinopathy. *Curr. Opin. Neurobiol.* **17:** 548–555

Fortini ME, Skupski MP, Boguski MS & Hariharan IK (2000) A survey

of human disease gene counterparts in the Drosophila genome. *J. Cell Biol.* **150:** F23–30

Gabanella F, Butchbach MER, Saieva L, Carissimi C, Burghes AHM & Pellizzoni L (2007) Ribonucleoprotein Assembly Defects Correlate with Spinal Muscular Atrophy Severity and Preferentially Affect a Subset of Spliceosomal snRNPs. *PLoS ONE* **2:** Available at: http://www.ncbi.nlm.nih.gov/pmc/articles/PMC1976558/ [Accessed June 6, 2014]

Geser F, Martinez-Lage M, Kwong LK, Lee VM-Y & Trojanowski JQ (2009) Amyotrophic lateral sclerosis, frontotemporal dementia and beyond: the TDP-43 diseases. *J. Neurol.* **256:** 1205–1214

Godena VK, Romano G, Romano M, Appocher C, Klima R, Buratti E, Baralle FE & Feiguin F (2011) TDP-43 Regulates Drosophila Neuromuscular Junctions Growth by Modulating Futsch/MAP1B Levels and Synaptic Microtubules Organization. *PLOS ONE* **6:** e17808

Goellner B & Aberle H (2012) The synaptic cytoskeleton in development and disease. *Dev. Neurobiol.* **72:** 111–125

Gorczyca M, Augart C & Budnik V (1993) Insulin-like receptor and insulin-like peptide are localized at neuromuscular junctions in Drosophila. *J. Neurosci. Off. J. Soc. Neurosci.* **13:** 3692–3704

Graf ER, Heerssen HM, Wright CM, Davis GW & DiAntonio A (2011) Stathmin is required for stability of the Drosophila neuromuscular junction. *J. Neurosci. Off. J. Soc. Neurosci.* **31:** 15026–15034

Gramates LS & Budnik V (1999) Assembly and maturation of the Drosophila larval neuromuscular junction. *Int. Rev. Neurobiol.* **43:** 93–117

Gregory RI, Yan K-P, Amuthan G, Chendrimada T, Doratotaj B, Cooch N & Shiekhattar R (2004) The Microprocessor complex mediates the genesis of microRNAs. *Nature* **432:** 235–240

Grishin NV (2001) KH domain: one motif, two folds. *Nucleic Acids Res.* **29:** 638–643

Groth AC, Fish M, Nusse R & Calos MP (2004) Construction of transgenic Drosophila by using the site-specific integrase from phage phiC31. *Genetics* **166:** 1775–1782

Gupta GD, M. G. S, Kumari S, Lakshminarayan R, Dey G & Mayor S

(2009) Analysis of Endocytic Pathways in Drosophila Cells Reveals a Conserved Role for GBF1 in Internalization via GEECs. *PLoS ONE* **4:** e6768

Gurney ME (1994) Transgenic-mouse model of amyotrophic lateral sclerosis. *N. Engl. J. Med.* **331:** 1721–1722

Hadano S, Hand CK, Osuga H, Yanagisawa Y, Otomo A, Devon RS, Miyamoto N, Showguchi-Miyata J, Okada Y, Singaraja R, Figlewicz DA, Kwiatkowski T, Hosler BA, Sagie T, Skaug J, Nasir J, Brown RH Jr, Scherer SW, Rouleau GA, Hayden MR, et al (2001) A gene encoding a putative GTPase regulator is mutated in familial amyotrophic lateral sclerosis 2. *Nat. Genet.* **29:** 166–173

Halpern ME, Chiba A, Johansen J & Keshishian H (1991) Growth cone behavior underlying the development of stereotypic synaptic connections in Drosophila embryos. *J. Neurosci. Off. J. Soc. Neurosci.* **11:** 3227–3238

Hasegawa M, Arai T, Nonaka T, Kametani F, Yoshida M, Hashizume Y, Beach TG, Morita M, Nakano I, Oda T, Tsuchiya K & Akiyama H (2008) [Significance of the TDP-43 deposition in FTLD-U and ALS]. *Rinshō Shinkeigaku Clin. Neurol.* **48:** 994–997

Hasegawa M, Arai T, Nonaka T, Tsuji H, Yamashita M, Hosokawa M, Kametani F, Tamaoka A & Akiyama H (2010) [Molecular dissection of TDP-43 in ALS and FTLD]. *Rinshō Shinkeigaku Clin. Neurol.* **50:** 937–939

Hazelett DJ, Chang J-C, Lakeland DL & Morton DB (2012) Comparison of parallel high-throughput RNA sequencing between knockout of TDP-43 and its overexpression reveals primarily nonreciprocal and nonoverlapping gene expression changes in the central nervous system of Drosophila. *G3 Bethesda Md* **2:** 789–802

Hilfiker S, Pieribone VA, Czernik AJ, Kao H-T, Augustine GJ & Greengard P (1999) Synapsins as regulators of neurotransmitter release. *Philos. Trans. R. Soc. Lond. B. Biol. Sci.* **354:** 269–279

Hoang B & Chiba A (2001) Single-Cell Analysis of Drosophila Larval Neuromuscular Synapses. *Dev. Biol.* **229:** 55–70

Hoell JI, Larsson E, Runge S, Nusbaum JD, Duggimpudi S, Farazi TA, Hafner M, Borkhardt A, Sander C & Tuschl T (2011) RNA targets of wild-type and mutant FET family proteins. *Nat. Struct. Mol. Biol.* **18:** 1428–1431

Hogan DJ, Riordan DP, Gerber AP, Herschlag D & Brown PO (2008) Diverse RNA-binding proteins interact with functionally related sets of RNAs, suggesting an extensive regulatory system. *PLoS Biol.* **6:** e255

Holtmaat A, Randall J & Cane M (2013) Optical imaging of structural and functional synaptic plasticity in vivo. *Eur. J. Pharmacol.*

Hoopmann P, Punge A, Barysch SV, Westphal V, Bückers J, Opazo F, Bethani I, Lauterbach MA, Hell SW & Rizzoli SO (2010) Endosomal sorting of readily releasable synaptic vesicles. *Proc. Natl. Acad. Sci.***:** 201007037

Horgan CP & McCaffrey MW (2011) Rab GTPases and microtubule motors. *Biochem. Soc. Trans.* **39:** 1202–1206

Huey ED, Ferrari R, Moreno JH, Jensen C, Morris CM, Potocnik F, Kalaria RN, Tierney M, Wassermann EM, Hardy J, Grafman J & Momeni P (2012) FUS and TDP43 genetic variability in FTD and CBS. *Neurobiol. Aging* **33:** 1016.e9–17

Hummel T, Krukkert K, Roos J, Davis G & Klämbt C (2000) Drosophila Futsch/22C10 is a MAP1B-like protein required for dendritic and axonal development. *Neuron* **26:** 357–370

Igaz LM, Kwong LK, Chen-Plotkin A, Winton MJ, Unger TL, Xu Y, Neumann M, Trojanowski JQ & Lee VM-Y (2009) Expression of TDP-43 C-terminal Fragments in Vitro Recapitulates Pathological Features of TDP-43 Proteinopathies. *J. Biol. Chem.* **284:** 8516–8524

Imran M & Mahmood S (2011) An overview of human prion diseases. *Virol. J.* **8:** 559

Ishida M, Ohbayashi N, Maruta Y, Ebata Y & Fukuda M (2012) Functional involvement of Rab1A in microtubule-dependent anterograde melanosome transport in melanocytes. *J. Cell Sci.* **125:** 5177–5187

Jahn R, Lang T & Südhof TC (2003) Membrane fusion. *Cell* **112:** 519–533

Jan LY & Jan YN (1976) L-glutamate as an excitatory transmitter at the Drosophila larval neuromuscular junction. *J. Physiol.* **262:** 215–236

Jan LY & Jan YN (1982) Antibodies to horseradish peroxidase as specific neuronal markers in Drosophila and in grasshopper embryos. *Proc. Natl. Acad. Sci. U. S. A.* **79:** 2700–2704

Johansen J, Halpern ME & Keshishian H (1989) Axonal guidance and the development of muscle fiber-specific innervation in Drosophila embryos. *J. Neurosci. Off. J. Soc. Neurosci.* **9:** 4318–4332

Johnson JO, Mandrioli J, Benatar M, Abramzon Y, Van Deerlin VM, Trojanowski JQ, Gibbs JR, Brunetti M, Gronka S, Wuu J, Ding J, McCluskey L, Martinez-Lage M, Falcone D, Hernandez DG, Arepalli S, Chong S, Schymick JC, Rothstein J, Landi F, et al (2010) Exome sequencing reveals VCP mutations as a cause of familial ALS. *Neuron* **68:** 857–864

Kabashi E, Lin L, Tradewell ML, Dion PA, Bercier V, Bourgouin P, Rochefort D, Bel Hadj S, Durham HD, Vande Velde C, Rouleau GA & Drapeau P (2010) Gain and loss of function of ALS-related mutations of TARDBP (TDP-43) cause motor deficits in vivo. *Hum. Mol. Genet.* **19:** 671–683

Kawahara Y & Mieda-Sato A (2012) TDP-43 promotes microRNA biogenesis as a component of the Drosha and Dicer complexes. *Proc. Natl. Acad. Sci. U. S. A.* **109:** 3347–3352

Kazemi-Esfarjani P & Benzer S (2000) Genetic suppression of polyglutamine toxicity in Drosophila. *Science* **287:** 1837–1840

Keshishian H, Broadie K, Chiba A & Bate M (1996) The drosophila neuromuscular junction: a model system for studying synaptic development and function. *Annu. Rev. Neurosci.* **19:** 545–575

Keshishian H & Chiba A (1993) Neuromuscular development in Drosophila: insights from single neurons and single genes. *Trends Neurosci.* **16:** 278–283

Khuong TM, Habets RLP, Kuenen S, Witkowska A, Kasprowicz J, Swerts J, Jahn R, van den Bogaart G & Verstreken P (2013) Synaptic PI(3,4,5)P3 is required for Syntaxin1A clustering and neurotransmitter release. *Neuron* **77:** 1097–1108

Kidokoro Y (2003) Roles of SNARE proteins and synaptotagmin I in synaptic transmission: studies at the Drosophila neuromuscular synapse. *Neurosignals* **12:** 13–30

Kim HJ, Kim NC, Wang Y-D, Scarborough EA, Moore J, Diaz Z, MacLea KS, Freibaum B, Li S, Molliex A, Kanagaraj AP, Carter R, Boylan KB, Wojtas AM, Rademakers R, Pinkus JL, Greenberg SA, Trojanowski JQ,

Traynor BJ, Smith BN, et al (2013) Mutations in prion-like domains in hnRNPA2B1 and hnRNPA1 cause multisystem proteinopathy and ALS. *Nature* **495:** 467–473

King OD, Gitler AD & Shorter J (2012) The tip of the iceberg: RNA-binding proteins with prion-like domains in neurodegenerative disease. *Brain Res.* **1462:** 61–80

Koh YH, Gramates LS & Budnik V (2000) Drosophila larval neuromuscular junction: molecular components and mechanisms underlying synaptic plasticity. *Microsc. Res. Tech.* **49:** 14–25

Koh YH, Popova E, Thomas U, Griffith LC & Budnik V (1999) Regulation of DLG Localization at Synapses by CaMKII-Dependent Phosphorylation. *Cell* **98:** 353–363

Kraemer BC, Schuck T, Wheeler JM, Robinson LC, Trojanowski JQ, Lee VMY & Schellenberg GD (2010) Loss of murine TDP-43 disrupts motor function and plays an essential role in embryogenesis. *Acta Neuropathol. (Berl.)* **119:** 409–419

Kwiatkowski TJ Jr, Bosco DA, Leclerc AL, Tamrazian E, Vanderburg CR, Russ C, Davis A, Gilchrist J, Kasarskis EJ, Munsat T, Valdmanis P, Rouleau GA, Hosler BA, Cortelli P, de Jong PJ, Yoshinaga Y, Haines JL, Pericak-Vance MA, Yan J, Ticozzi N, et al (2009) Mutations in the FUS/TLS gene on chromosome 16 cause familial amyotrophic lateral sclerosis. *Science* **323:** 1205–1208

Lagier-Tourenne C, Polymenidou M, Hutt KR, Vu AQ, Baughn M, Huelga SC, Clutario KM, Ling S-C, Liang TY, Mazur C, Wancewicz E, Kim AS, Watt A, Freier S, Hicks GG, Donohue JP, Shiue L, Bennett CF, Ravits J, Cleveland DW, et al (2012) Divergent roles of ALS-linked proteins FUS/TLS and TDP-43 intersect in processing long pre-mRNAs. *Nat. Neurosci.* **15:** 1488–1497

Lagow RD, Bao H, Cohen EN, Daniels RW, Zuzek A, Williams WH, Macleod GT, Sutton RB & Zhang B (2007) Modification of a hydrophobic layer by a point mutation in syntaxin 1A regulates the rate of synaptic vesicle fusion. *PLoS Biol.* **5:** e72

Lee J-Y, Bhatt D, Bhatt D, Chung W-Y & Cooper RL (2009) Furthering pharmacological and physiological assessment of the glutamatergic

receptors at the Drosophila neuromuscular junction. *Comp. Biochem. Physiol. Toxicol. Pharmacol. CBP* **150:** 546–557

Lee T & Luo L (1999) Mosaic analysis with a repressible cell marker for studies of gene function in neuronal morphogenesis. *Neuron* **22:** 451–461

Leigh PN, Whitwell H, Garofalo O, Buller J, Swash M, Martin JE, Gallo JM, Weller RO & Anderton BH (1991) Ubiquitin-immunoreactive intraneuronal inclusions in amyotrophic lateral sclerosis. Morphology, distribution, and specificity. *Brain J. Neurol.* **114 (Pt 2):** 775–788

Li Y, Ray P, Rao EJ, Shi C, Guo W, Chen X, Woodruff EA 3rd, Fushimi K & Wu JY (2010) A Drosophila model for TDP-43 proteinopathy. *Proc. Natl. Acad. Sci. U. S. A.* **107:** 3169–3174

Lin M-J, Cheng C-W & Shen C-KJ (2011) Neuronal Function and Dysfunction of Drosophila dTDP. *PLoS ONE* **6:** e20371

Littleton JT (2000) A genomic analysis of membrane trafficking and neurotransmitter release in Drosophila. *J. Cell Biol.* **150:** F77–82

Lue NF, Chasman DI, Buchman AR & Kornberg RD (1987) Interaction of GAL4 and GAL80 gene regulatory proteins in vitro. *Mol. Cell. Biol.* **7:** 3446–3451

Lukong KE, Chang K, Khandjian EW & Richard S (2008) RNA-binding proteins in human genetic disease. *Trends Genet. TIG* **24:** 416–425

Luzio JP, Gray SR & Bright NA (2010) Endosome-lysosome fusion. *Biochem. Soc. Trans.* **38:** 1413–1416

Mackenzie IRA (2007) The neuropathology of FTD associated With ALS. *Alzheimer Dis. Assoc. Disord.* **21:** S44–49

Magazanik LG & Vyskocil F (1979) Spontaneous junctional currents in Drosophila muscle fibres: effects of temperature, membrane potential and ethanol. *Experientia* **35:** 213–214

Mahoney TR, Liu Q, Itoh T, Luo S, Hadwiger G, Vincent R, Wang Z-W, Fukuda M & Nonet ML (2006) Regulation of Synaptic Transmission by RAB-3 and RAB-27 in Caenorhabditis elegans. *Mol. Biol. Cell* **17:** 2617–2625

Majounie E, Renton AE, Mok K, Dopper EGP, Waite A, Rollinson S, Chiò A, Restagno G, Nicolaou N, Simon-Sanchez J, van Swieten JC, Abramzon Y, Johnson JO, Sendtner M, Pamphlett R, Orrell RW, Mead S, Sidle KC, Houlden H, Rohrer JD, et al (2012) Frequency of the C9orf72

hexanucleotide repeat expansion in patients with amyotrophic lateral sclerosis and frontotemporal dementia: a cross-sectional study. *Lancet Neurol.* **11:** 323–330

Majumder R & Krishnan KS (2010) Synaptic vesicle recycling: genetic and cell biological studies. *J. Neurogenet.* **24:** 146–157

Maris C, Dominguez C & Allain FH-T (2005) The RNA recognition motif, a plastic RNA-binding platform to regulate post-transcriptional gene expression. *FEBS J.* **272:** 2118–2131

Maruyama H, Morino H, Ito H, Izumi Y, Kato H, Watanabe Y, Kinoshita Y, Kamada M, Nodera H, Suzuki H, Komure O, Matsuura S, Kobatake K, Morimoto N, Abe K, Suzuki N, Aoki M, Kawata A, Hirai T, Kato T, et al (2010) Mutations of optineurin in amyotrophic lateral sclerosis. *Nature* **465:** 223–226

Matsumoto K, Toh-e A & Oshima Y (1978) Genetic control of galactokinase synthesis in Saccharomyces cerevisiae: evidence for constitutive expression of the positive regulatory gene gal4. *J. Bacteriol.* **134:** 446–457

Maya-Vetencourt JF (2013) Activity-Dependent NPAS4 Expression and the Regulation of Gene Programs Underlying Plasticity in the Central Nervous System. *Neural Plast.* **2013:** 683909

Mayr C & Bartel DP (2009) Widespread shortening of 3'UTRs by alternative cleavage and polyadenylation activates oncogenes in cancer cells. *Cell* **138:** 673–684

McGuire SE, Le PT, Osborn AJ, Matsumoto K & Davis RL (2003) Spatiotemporal rescue of memory dysfunction in Drosophila. *Science* **302:** 1765–1768

McGuire SE, Mao Z & Davis RL (2004) Spatiotemporal gene expression targeting with the TARGET and gene-switch systems in Drosophila. *Sci. STKE Signal Transduct. Knowl. Environ.* **2004:** pl6

McMahon HT & Gallop JL (2005) Membrane curvature and mechanisms of dynamic cell membrane remodelling. *Nature* **438:** 590–596

Mercado PA, Ayala YM, Romano M, Buratti E & Baralle FE (2005) Depletion of TDP 43 overrides the need for exonic and intronic splicing enhancers in the human apoA-II gene. *Nucleic Acids Res.* **33:** 6000–6010

Miech C, Pauer H-U, He X & Schwarz TL (2008) Presynaptic local

signaling by a canonical wingless pathway regulates development of the Drosophila neuromuscular junction. *J. Neurosci. Off. J. Soc. Neurosci.* **28:** 10875–10884

Monastirioti M, Gorczyca M, Rapus J, Eckert M, White K & Budnik V (1995) Octopamine immunoreactivity in the fruit fly Drosophila melanogaster. *J. Comp. Neurol.* **356:** 275–287

Mukhopadhyay R, Kumar S & Hoh JH (2004) Molecular mechanisms for organizing the neuronal cytoskeleton. *BioEssays News Rev. Mol. Cell. Dev. Biol.* **26:** 1017–1025

Muqit MMK & Feany MB (2002) Modelling neurodegenerative diseases in Drosophila: a fruitful approach? *Nat. Rev. Neurosci.* **3:** 237–243

Murayama S (2010) [Clinical and pathological characteristics of FUS/TLS-associated amyotrophic lateral sclerosis (ALS)]. *Rinshō Shinkeigaku Clin. Neurol.* **50:** 948–950

Murray ME, DeJesus-Hernandez M, Rutherford NJ, Baker M, Duara R, Graff-Radford NR, Wszolek ZK, Ferman TJ, Josephs KA, Boylan KB, Rademakers R & Dickson DW (2011) Clinical and neuropathologic heterogeneity of c9FTD/ALS associated with hexanucleotide repeat expansion in C9ORF72. *Acta Neuropathol. (Berl.)* **122:** 673–690

Narayanan RK, Mangelsdorf M, Panwar A, Butler TJ, Noakes PG & Wallace RH (2013) Identification of RNA bound to the TDP-43 ribonucleoprotein complex in the adult mouse brain. *Amyotroph. Lateral Scler. Front. Degener.* **14:** 252–260

Neuenkirchen N, Chari A & Fischer U (2008) Deciphering the assembly pathway of Sm-class U snRNPs. *FEBS Lett.* **582:** 1997–2003

Neumann M, Sampathu DM, Kwong LK, Truax AC, Micsenyi MC, Chou TT, Bruce J, Schuck T, Grossman M, Clark CM, McCluskey LF, Miller BL, Masliah E, Mackenzie IR, Feldman H, Feiden W, Kretzschmar HA, Trojanowski JQ & Lee VM-Y (2006) Ubiquitinated TDP-43 in frontotemporal lobar degeneration and amyotrophic lateral sclerosis. *Science* **314:** 130–133

Nicholson L, Singh GK, Osterwalder T, Roman GW, Davis RL & Keshishian H (2008) Spatial and temporal control of gene expression in Drosophila using the inducible GeneSwitch GAL4 system. I. Screen for larval nervous system drivers. *Genetics* **178:** 215–234

Osterwalder T, Yoon KS, White BH & Keshishian H (2001) A conditional tissue-specific transgene expression system using inducible GAL4. *Proc. Natl. Acad. Sci. U. S. A.* **98:** 12596–12601

Ou SH, Wu F, Harrich D, García-Martínez LF & Gaynor RB (1995) Cloning and characterization of a novel cellular protein, TDP-43, that binds to human immunodeficiency virus type 1 TAR DNA sequence motifs. *J. Virol.* **69:** 3584–3596

Packard M, Koo ES, Gorczyca M, Sharpe J, Cumberledge S & Budnik V (2002) The Drosophila Wnt, wingless, provides an essential signal for pre- and postsynaptic differentiation. *Cell* **111:** 319–330

Pagani F, Buratti E, Stuani C, Romano M, Zuccato E, Niksic M, Giglio L, Faraguna D & Baralle FE (2000) Splicing factors induce cystic fibrosis transmembrane regulator exon 9 skipping through a nonevolutionary conserved intronic element. *J. Biol. Chem.* **275:** 21041–21047

Pasinelli P & Brown RH (2006) Molecular biology of amyotrophic lateral sclerosis: insights from genetics. *Nat. Rev. Neurosci.* **7:** 710–723

Pesiridis GS, Lee VM-Y & Trojanowski JQ (2009) Mutations in TDP-43 link glycine-rich domain functions to amyotrophic lateral sclerosis. *Hum. Mol. Genet.* **18:** R156–R162

Phukan J, Pender NP & Hardiman O (2007) Cognitive impairment in amyotrophic lateral sclerosis. *Lancet Neurol.* **6:** 994–1003

Poirier L, Shane A, Zheng J & Seroude L (2008) Characterization of the Drosophila gene-switch system in aging studies: a cautionary tale. *Aging Cell* **7:** 758–770

Polymenidou M, Lagier-Tourenne C, Hutt KR, Huelga SC, Moran J, Liang TY, Ling S-C, Sun E, Wancewicz E, Mazur C, Kordasiewicz H, Sedaghat Y, Donohue JP, Shiue L, Bennett CF, Yeo GW & Cleveland DW (2011) Long pre-mRNA depletion and RNA missplicing contribute to neuronal vulnerability from loss of TDP-43. *Nat. Neurosci.* **14:** 459–468

Raiborg C & Stenmark H (2009) The ESCRT machinery in endosomal sorting of ubiquitylated membrane proteins. *Nature* **458:** 445–452

Reddi PP, Flickinger CJ & Herr JC (1999) Round spermatid-specific transcription of the mouse SP-10 gene is mediated by a 294-base pair proximal promoter. *Biol. Reprod.* **61:** 1256–1266

Richmond JE & Broadie KS (2002) The synaptic vesicle cycle: exocytosis and endocytosis in Drosophila and C. elegans. *Curr. Opin. Neurobiol.* **12:** 499–507

Rodriguez Moncalvo VG & Campos AR (2009) Role of serotonergic neurons in the Drosophila larval response to light. *BMC Neurosci.* **10:** 66

Rohn TT & Head E (2009) Caspases as therapeutic targets in Alzheimer's disease: is it time to 'cut' to the chase? *Int. J. Clin. Exp. Pathol.* **2:** 108–118

Roman G, Endo K, Zong L & Davis RL (2001) P[Switch], a system for spatial and temporal control of gene expression in Drosophila melanogaster. *Proc. Natl. Acad. Sci. U. S. A.* **98:** 12602–12607

Romano M, Buratti E, Romano G, Klima R, Belluz LDB, Stuani C, Baralle F & Feiguin F (2014) Evolutionarily-conserved hnRNP A/B proteins functionally interact with human and Drosophila TAR DNA-binding protein 43 (TDP-43). *J. Biol. Chem.***:** jbc.M114.548859

Roos J, Hummel T, Ng N, Klämbt C & Davis GW (2000) Drosophila Futsch regulates synaptic microtubule organization and is necessary for synaptic growth. *Neuron* **26:** 371–382

Rosen DR (1993) Mutations in Cu/Zn superoxide dismutase gene are associated with familial amyotrophic lateral sclerosis. *Nature* **364:** 362

Rothman JE (1994) Mechanisms of intracellular protein transport. *Nature* **372:** 55–63

Rowland LP & Shneider NA (2001) Amyotrophic Lateral Sclerosis. *N. Engl. J. Med.* **344:** 1688–1700

Ruddy DM, Parton MJ, Al-Chalabi A, Lewis CM, Vance C, Smith BN, Leigh PN, Powell JF, Siddique T, Meyjes EP, Baas F, de Jong V & Shaw CE (2003) Two families with familial amyotrophic lateral sclerosis are linked to a novel locus on chromosome 16q. *Am. J. Hum. Genet.* **73:** 390–396

Saitoe M, Schwarz TL, Umbach JA, Gundersen CB & Kidokoro Y (2001) Absence of Junctional Glutamate Receptor Clusters in Drosophila Mutants Lacking Spontaneous Transmitter Release. *Science* **293:** 514–517

Sanelli T, Xiao S, Horne P, Bilbao J, Zinman L & Robertson J (2007) Evidence that TDP-43 is not the major ubiquitinated target within the pathological inclusions of amyotrophic lateral sclerosis. *J. Neuropathol. Exp.*

Neurol. **66:** 1147–1153

Sanyal S (2009) Genomic mapping and expression patterns of C380, OK6 and D42 enhancer trap lines in the larval nervous system of Drosophila. *Gene Expr. Patterns GEP* **9:** 371–380

Sapp PC, Hosler BA, McKenna-Yasek D, Chin W, Gann A, Genise H, Gorenstein J, Huang M, Sailer W, Scheffler M, Valesky M, Haines JL, Pericak-Vance M, Siddique T, Horvitz HR & Brown RH Jr (2003) Identification of two novel loci for dominantly inherited familial amyotrophic lateral sclerosis. *Am. J. Hum. Genet.* **73:** 397–403

Schmid A, Qin G, Wichmann C, Kittel RJ, Mertel S, Fouquet W, Schmidt M, Heckmann M & Sigrist SJ (2006) Non-NMDA-type glutamate receptors are essential for maturation but not for initial assembly of synapses at Drosophila neuromuscular junctions. *J. Neurosci. Off. J. Soc. Neurosci.* **26:** 11267–11277

Schneider I (1972) Cell lines derived from late embryonic stages of Drosophila melanogaster. *J. Embryol. Exp. Morphol.* **27:** 353–365

Schuster CM, Ultsch A, Schloss P, Cox JA, Schmitt B & Betz H (1991) Molecular cloning of an invertebrate glutamate receptor subunit expressed in Drosophila muscle. *Science* **254:** 112–114

Sephton CF, Cenik C, Kucukural A, Dammer EB, Cenik B, Han Y, Dewey CM, Roth FP, Herz J, Peng J, Moore MJ & Yu G (2011) Identification of neuronal RNA targets of TDP-43-containing ribonucleoprotein complexes. *J. Biol. Chem.* **286:** 1204–1215

Sephton CF, Good SK, Atkin S, Dewey CM, Mayer P, Herz J & Yu G (2010) TDP-43 is a developmentally regulated protein essential for early embryonic development. *J. Biol. Chem.* **285:** 6826–6834

Shaw CE, al-Chalabi A & Leigh N (2001) Progress in the pathogenesis of amyotrophic lateral sclerosis. *Curr. Neurol. Neurosci. Rep.* **1:** 69–76

Simonsen A, Lippé R, Christoforidis S, Gaullier JM, Brech A, Callaghan J, Toh BH, Murphy C, Zerial M & Stenmark H (1998) EEA1 links PI(3)K function to Rab5 regulation of endosome fusion. *Nature* **394:** 494–498

Sørensen JB, Wiederhold K, Müller EM, Milosevic I, Nagy G, de Groot BL, Grubmüller H & Fasshauer D (2006) Sequential N- to C-terminal SNARE complex assembly drives priming and fusion of secretory vesicles. *EMBO J.*

25: 955–966

Sreedharan J, Blair IP, Tripathi VB, Hu X, Vance C, Rogelj B, Ackerley S, Durnall JC, Williams KL, Buratti E, Baralle F, de Belleroche J, Mitchell JD, Leigh PN, Al-Chalabi A, Miller CC, Nicholson G & Shaw CE (2008) TDP-43 mutations in familial and sporadic amyotrophic lateral sclerosis. *Science* **319:** 1668–1672

Stepto A, Gallo J-M, Shaw CE & Hirth F (2014) Modelling C9ORF72 hexanucleotide repeat expansion in amyotrophic lateral sclerosis and frontotemporal dementia. *Acta Neuropathol. (Berl.)* **127:** 377–389

Strong MJ, Volkening K, Hammond R, Yang W, Strong W, Leystra-Lantz C & Shoesmith C (2007) TDP43 is a human low molecular weight neurofilament (hNFL) mRNA-binding protein. *Mol. Cell. Neurosci.* **35:** 320–327

Strong MJ & Yang W (2011) The frontotemporal syndromes of ALS. Clinicopathological correlates. *J. Mol. Neurosci. MN* **45:** 648–655

Strong TV, Wilkinson DJ, Mansoura MK, Devor DC, Henze K, Yang Y, Wilson JM, Cohn JA, Dawson DC & Frizzell RA (1993) Expression of an abundant alternatively spliced form of the cystic fibrosis transmembrane conductance regulator (CFTR) gene is not associated with a cAMP-activated chloride conductance. *Hum. Mol. Genet.* **2:** 225–230

Sudhof TC (2004) The synaptic vesicle cycle. *Annu. Rev. Neurosci.* **27:** 509–547

Teplova M & Patel DJ (2008) Structural insights into RNA recognition by the alternative-splicing regulator muscleblind-like MBNL1. *Nat. Struct. Mol. Biol.* **15:** 1343–1351

Thomas U, Kim E, Kuhlendahl S, Koh YH, Gundelfinger ED, Sheng M, Garner CC & Budnik V (1997) Synaptic clustering of the cell adhesion molecule fasciclin II by discs-large and its role in the regulation of presynaptic structure. *Neuron* **19:** 787–799

Tsai K-J, Yang C-H, Fang Y-H, Cho K-H, Chien W-L, Wang W-T, Wu T-W, Lin C-P, Fu W-M & Shen C-KJ (2010) Elevated expression of TDP-43 in the forebrain of mice is sufficient to cause neurological and pathological phenotypes mimicking FTLD-U. *J. Exp. Med.* **207:** 1661–1673

Vance C, Rogelj B, Hortobágyi T, De Vos KJ, Nishimura AL,

Sreedharan J, Hu X, Smith B, Ruddy D, Wright P, Ganesalingam J, Williams KL, Tripathi V, Al-Saraj S, Al-Chalabi A, Leigh PN, Blair IP, Nicholson G, de Belleroche J, Gallo J-M, et al (2009) Mutations in FUS, an RNA processing protein, cause familial amyotrophic lateral sclerosis type 6. *Science* **323:** 1208–1211

Voigt A, Herholz D, Fiesel FC, Kaur K, Müller D, Karsten P, Weber SS, Kahle PJ, Marquardt T & Schulz JB (2010) TDP-43-mediated neuron loss in vivo requires RNA-binding activity. *PloS One* **5:** e12247

Wagh DA, Rasse TM, Asan E, Hofbauer A, Schwenkert I, Dürrbeck H, Buchner S, Dabauvalle M-C, Schmidt M, Qin G, Wichmann C, Kittel R, Sigrist SJ & Buchner E (2006) Bruchpilot, a Protein with Homology to ELKS/CAST, Is Required for Structural Integrity and Function of Synaptic Active Zones in Drosophila. *Neuron* **49:** 833–844

Wang ET, Sandberg R, Luo S, Khrebtukova I, Zhang L, Mayr C, Kingsmore SF, Schroth GP & Burge CB (2008) Alternative isoform regulation in human tissue transcriptomes. *Nature* **456:** 470–476

Wang H-Y, Wang I-F, Bose J & Shen C-KJ (2004) Structural diversity and functional implications of the eukaryotic TDP gene family. *Genomics* **83:** 130–139

Watanabe S, Kaneko K & Yamanaka K (2013) Accelerated disease onset with stabilized familial amyotrophic lateral sclerosis (ALS)-linked mutant TDP-43 proteins. *J. Biol. Chem.* **288:** 3641–3654

Wegorzewska I, Bell S, Cairns NJ, Miller TM & Baloh RH (2009) TDP-43 mutant transgenic mice develop features of ALS and frontotemporal lobar degeneration. *Proc. Natl. Acad. Sci. U. S. A.* **106:** 18809–18814

Wernig A, Pécot-Dechavassine M & Stover H (1980) Sprouting and regression of the nerve at the frog neuromuscular junction in normal conditions and after prolonged paralysis with curare. *J. Neurocytol.* **9:** 278–303

Wichmann C, Fouquet W, Mertel S, Owald D, Dyba M, Eimer S & Sigrist SJ (2008) The Drosophila active zone architecture: combining confocal, STED and transmission electron microscopy. In *EMC 2008 14th European Microscopy Congress 1–5 September 2008, Aachen, Germany*, Aretz A Hermanns-Sachweh B & Mayer PDJ (eds) pp 331–332. Springer

Berlin Heidelberg Available at: http://link.springer.com/chapter/10.1007/978-3-540-85228-5_166 [Accessed November 10, 2013]

Wigby S, Slack C, Grönke S, Martinez P, Calboli FCF, Chapman T & Partridge L (2011) Insulin signalling regulates remating in female Drosophila. *Proc. Biol. Sci.* **278:** 424–431

Wils H, Kleinberger G, Janssens J, Pereson S, Joris G, Cuijt I, Smits V, Ceuterick-de Groote C, Van Broeckhoven C & Kumar-Singh S (2010) TDP-43 transgenic mice develop spastic paralysis and neuronal inclusions characteristic of ALS and frontotemporal lobar degeneration. *Proc. Natl. Acad. Sci. U. S. A.* **107:** 3858–3863

Worms PM (2001) The epidemiology of motor neuron diseases: a review of recent studies. *J. Neurol. Sci.* **191:** 3–9

Wu JS & Luo L (2006) A protocol for dissecting Drosophila melanogaster brains for live imaging or immunostaining. *Nat. Protoc.* **1:** 2110–2115

Wu L-S, Cheng W-C, Hou S-C, Yan Y-T, Jiang S-T & Shen C-KJ (2010) TDP-43, a neuro-pathosignature factor, is essential for early mouse embryogenesis. *Genes. N. Y. N 2000* **48:** 56–62

Wu MN, Fergestad T, Lloyd TE, He Y, Broadie K & Bellen HJ (1999) Syntaxin 1A Interacts with Multiple Exocytic Proteins to Regulate Neurotransmitter Release In Vivo. *Neuron* **23:** 593–605

Wu Y, Reece RJ & Ptashne M (1996) Quantitation of putative activator-target affinities predicts transcriptional activating potentials. *EMBO J.* **15:** 3951–3963

Xu Y-F, Gendron TF, Zhang Y-J, Lin W-L, D'Alton S, Sheng H, Casey MC, Tong J, Knight J, Yu X, Rademakers R, Boylan K, Hutton M, McGowan E, Dickson DW, Lewis J & Petrucelli L (2010) Wild-type human TDP-43 expression causes TDP-43 phosphorylation, mitochondrial aggregation, motor deficits, and early mortality in transgenic mice. *J. Neurosci. Off. J. Soc. Neurosci.* **30:** 10851–10859

Van der Zee J, Gijselinck I, Pirici D, Kumar-Singh S, Cruts M & Van Broeckhoven C (2007) Frontotemporal lobar degeneration with ubiquitin-positive inclusions: a molecular genetic update. *Neurodegener. Dis.* **4:** 227–235

Ziff EB (1997) Enlightening the postsynaptic density. *Neuron* **19:** 1163–1174

Zito K, Parnas D, Fetter RD, Isacoff EY & Goodman CS (1999) Watching a synapse grow: noninvasive confocal imaging of synaptic growth in Drosophila. *Neuron* **22:** 719–729

Zoccolella S, Beghi E, Palagano G, Fraddosio A, Guerra V, Samarelli V, Lepore V, Simone IL, Lamberti P, Serlenga L, Logroscino G & SLAP Registry (2008) Analysis of survival and prognostic factors in amyotrophic lateral sclerosis: a population based study. *J. Neurol. Neurosurg. Psychiatry* **79:** 33–37

Zou B, Yan H, Kawasaki F & Ordway RW (2008) MAP1 structural organization in Drosophila: in vivo analysis of FUTSCH reveals heavy- and light-chain subunits generated by proteolytic processing at a conserved cleavage site. *Biochem. J.* **414:** 63–71